Chemical Constituents from the Sponge *Pachastrissa nux*

Thanchanok Sirirak

A Thesis Submitted in Partial Fulfillment of the Requirements for the Degree of

Doctor of Philosophy in Pharmaceutical Sciences

Prince of Songkla University

2012

Thesis Title	Chemical constituents from the sponge *Pachastrissa nux*
Author	Miss Thanchanok Sirirak
Major Program	Pharmaceutical Sciences

Major Advisor:

…….

(Asst. Prof. Dr. Anuchit Plubrukarn)

Examination Committee:

……..Chairperson

(Dr. Khanit Suwanborirux)

…….Committee

(Asst. Prof. Dr. Anuchit Plubrukarn)

…….Committee

(Assoc. Prof. Dr. Suchana Chavanich)

…….Committee

(Assoc. Prof. Dr. Lothar Brecker)

…….Committee

(Assoc. Prof. Dr. Suchada Chantrapromma)

The Graduate School, Prince of Songkla University, has approved this thesis as partial fulfillment of the requirements for the Degree of Doctor of Philosophy in Pharmaceutical Sciences

…….....

(Prof. Dr. Amornrat Phongdara)

Dean of Graduate School

ชื่อวิทยานิพนธ์ องค์ประกอบทางเคมีของฟองน้ำ *Pachastrissa nux*
ผู้เขียน นางสาว ธันย์ชนก ศิริรักษ์
สาขาวิชา เภสัชศาสตร์
ปีการศึกษา 2554

บทคัดย่อ

จากการศึกษานำร่องสารสกัดเมธานอลของฟองน้ำ *Pachastrissa nux* (de Laubenfels, 1954) จากเกาะเต่า จังหวัดสุราษฎร์ธานี พบว่ามีฤทธิ์ต้านมาลาเรียเมื่อทดสอบด้วยเชื้อ *Plasmodium falciparum* สายพันธุ์ K1 (IC_{50} 13.3 μg/mL) จากสกัดแยกด้วยเทคนิคทางโครมาโต-กราฟีทำให้ได้อนุพันธ์ทริสออกซาโซลมาโครไลด์ชนิดใหม่ 3 ชนิดได้แก่ คาบิราไมด์ J, K และ L กับสารที่มีรายงานแล้ว 5 ชนิด ได้แก่ คาบิราไมด์ B, C, D, G และ I สารใหม่ทั้ง 3 ชนิดข้างต้นเป็นสารคาบิราไมด์กลุ่มใหม่ที่มีหมู่ 30-α,β-enone บนโซ่กิ่งและเป็นกลุ่มสารที่มีรายงานการสกัดแยกจากฟองน้ำ *P. nux* เท่านั้น สารที่สกัดแยกได้ทั้งหมดมีฤทธิ์ความเป็นพิษต่อเซลล์ไฟโบรบลาสต์และเซลล์มะเร็งเต้านมโดยมีค่า IC_{50} อยู่ในช่วง 0.50-7.59 μM และ 0.02-2.00 μM ตามลำดับ และยังมีฤทธิ์ต้านมาลาเรียต่อเชื้อ *P. falciparum* K1 ค่า IC_{50} อยู่ในช่วง 0.31-4.79 μM

เมื่อวิเคราะห์การกระจายตัวของอนุพันธ์ทริสออกซาโซลมาโครไลด์ในแต่ละโคโลนีของฟองน้ำ *P. nux* พบว่า ฟองน้ำ *P. nux* สามารถจัดสรรอนุพันธ์คาบิราไมด์ไปยังส่วนแคปิตัมซึ่งเป็นส่วนที่เจริญยื่นขึ้นมาจากส่วนฐานที่มีรูปร่างไม่สม่ำเสมอได้อย่างจำเพาะเจาะจงเมื่อสารคาบิราไมด์ C และ G เป็นสารอ้างอิง พบว่าฟองน้ำมีการจัดสรรให้สารกลุ่มคาบิราไมด์ทั้ง 2 ชนิด ไปยังส่วนแคปิตัมในสัดส่วนที่มากกว่าไปยังส่วนฐานอย่างมีนัยสำคัญ และชี้ให้เห็นว่า ฟองน้ำ *P. nux* อาจใช้ประโยชน์จากสารกลุ่มนี้เพื่อเป็นกลไกการปกป้องตนเองจากผู้ล่าหรือป้องกันการลงเกาะของสิ่งมีชีวิตชนิดอื่น

Thesis Title	Chemical constituents from the sponge *Pachastrissa nux*
Author	Miss Thanchanok Sirirak
Major Program	Pharmaceutical Sciences
Academic year	2011

ABSTRACT

Preliminary study of the MeOH-extract from the sponge *Pachastrissa nux* (de Laubenfels, 1954) from Koh Tao, Surat-Thani Province, showed strong antimalarial activity (IC_{50} 13.3 μg/mL) against *Plasmodium falciparum* K1. Further investigation using chromatographic techniques led to the isolation of three new trisoxazole macrolides, kabiramides J, K, and L, along with a series of known kabiramide analogs, kabiramides B, C, D, G, and I. The three new kabiramides belong to a new class of trisoxazole macrolides possessing 30-α,β-enone moiety, which have been found solely associated with the *P. nux* sponge. All the isolated compounds showed cytotoxic activity against both normal human fibroblast and MCF-7 breast adenocarcinoma cell lines (IC_{50}s 0.50-7.59 μM and 0.02-2.00 μM, respectively) and antimalarial activity against *P. falciparum* K1 (IC_{50}s 0.31-4.79 μM).

In addition, *P. nux* possessed an ability to allocate the kabiramides specifically towards the capitum part, the growth form protruding over the irregular-shape base. Choosing kabiramides C and G as chemical markers, specific allocation of the macrolides towards the capitum suggested the utilization of kabiramides as a defense mechanism against predators and/or settlement of other fouling species in the *P. nux* sponge.

ACKNOWLEDGEMENTS

First and foremost, I would like to express my gratitude to my supervisor, Asst. Prof. Dr. Anuchit Plubrukarn, for his guidance and suggestion throughout my study. Thank you for his encourage that leads me to have a good academic performance.

Besides my advisor, I would like to thank Asst. Prof. Dr. Supreeya Yuenyong-sawad, for cytotoxic activity test, Dr. Sireewan Kaewsuwan for protein content determination, and Mrs Niwan Intaraksa for structural content determination.

I thank Dr. Khanit Suwanborirux, Department of Pharmacognosy and Pharmaceutical Botany, Faculty of Pharmaceutical Sciences, Chulalongkorn University for his crucial suggestion on my thesis and Pharmaceutical Research Equipment Center, Faculty of Pharmaceutical Sciences, Chulalongkorn University, for support in optical rotation.

My sincere gratitude also goes to Prof. Dr. Vatcharin Rukachaisirikul and Dr. Yaowapa Sukpondma, Department of Chemistry, Faculty of Science, Prince of Songkla University; and to Mrs Roosanee Kulvijitra, Scientific Equipment Center, Prince of Songkla University for NMR experiments.

I would like to thank Dr. Sumaitt Putchakarn, Institute of Marine Science, Burapha University, for his help in sponge identification.

It is my pleasure to thank Assoc. Prof. Dr. Supa Hannongbua, Department of Chemistry, Faculty of Science, Kasetsart University, for her kind suggestions, Prof. Dr. Peter Wolschann, Institute of Theoretical Chemistry, University of Vienna, for his suggestions and support during my stay in Vienna, and Assoc. Prof. Dr. Lothar Brecker, Department of Organic Chemistry, University of Vienna, for his kind support in NMR experiments.

I would like to thank Miss Siriporn Kittiwisut, for her help in cytotoxic activity determination and Miss Chittrawan Janma, for her assistance in the batch isolation of kabiramides. Thank to all my colleagues in Marine Natural Product Research Unit and all staff of Department of Pharmacognosy and Pharmaceutical Botany, Faculty of Pharmaceutical Sciences, Prince of Songkla University, for their encouragement and support throughout my thesis work.

This thesis would not have been possible unless financial support from Academic Excellence Enhancing Program in Pharmaceutical Sciences, Prince of Songkla

University; Graduate School, Prince of Songkla University; Marine Natural Products Research Unit, Faculty of Pharmaceutical Sciences, Prince of Songkla University; Biodiversity Research and Training Program (BRT T653014); and Center of Bioactive Natural Products from Marine Orgaisms and Endophytic Fungi (BNPME) under Commission on Higher Education.

Finally I would like to express my grateful thank to my family, for their encouragement, understanding, and support during my study.

Thanchanok Sirirak

CONTENTS

CONTENTS (cont.)

CONTENTS (cont.)

LIST OF TABLES

LIST OF FIGURES

LIST OF FIGURES (cont.)

LIST OF SCHEMES

LIST OF ABBREVIATIONS AND SYMBOLS

$[\alpha]_D$	specific rotation
δ	chemical shift in ppm
ε	molar extinction coefficient
λ_{max}	maximum wavelength
ν_{max}	wave number
2D NMR	two-dimentional nuclear magnetic resonance
br	broad (for IR and NMR signals)
c	concentration
COSY	correlation spectroscopy
d	doublet (for NMR signals)
EMEM	Eagle's minimal essential medium
ESIMS	electrospray ionization mass spectroscopy
FABMS	fast-atom bombardment mass spectroscopy
HMBC	heteronuclear multiple bond coherence
HMQC	heteronuclear multiple-quantum coherence
HRESIMS	high-resolution electrospray ionization mass spectroscopy
HRFABMS	high-resolution fast-atom bombardment mass spectroscopy
IC_{50}	inhibitory concentration at 50% of test subject
IC_{99}	inhibitory concentration at 99% of test subject
J	coupling constant
J-MOD	J-Modulated spin-echo
LC_{50}	lethal concentration at 50% of test subject
m	multiplet (for NMR signals)
m/z	mass-over-charge ratio
NOE	nuclear Overhauser effect
NOEDS	nuclear Overhauser enhanced differential spectroscopy
NOESY	nuclear Overhauser effect spectroscopy
ppm	part per million

LIST OF ABBREVIATIONS AND SYMBOLS (cont.)

q	quartet (for NMR signals)
RPMI	Roswell Park Memorial Institute medium
s	singlet (for NMR signals)
TOCSY	total correlation spectroscopy
t	triplet (for NMR signals)
t_R	retention time

CHAPTER 1

INTRODUCTION

1.1 General introduction

Herbal medicines, or drugs from nature, are among areas that have revolved around the history of mankind. Whereas addressed as "herbal", herbal medicines in fact extend their meaning to include all drugs from nature whether they come from plants, animals, or mineral and salts. Tracing back into the ancient records, men have employed surrounding resources for the medical, and sometime spiritual, purposes to the great extent.

The evolution of modern technology has led to the isolation of active ingredients from these herbal medicines, and allows them to be used more effectively with less adverse and undesired reactions. To date, it has been estimated that up to 46% of currently used medicines come directly from their natural sources, and additional 24% are from synthetic analogs inspired by the chemical structures of the "lead" compounds (Newman and Cragg, 2007; Blunt et al., 2011). Such inspiration is among primary reasons for natural product chemists and scientists in related areas to keep searching for new and fascinating chemicals from natural resources.

Similar to the terrestrial counterparts, marine organisms have been known to be sources of various classes of natural products, most of which are unprecedented in terrestrial organisms. The origin of marine natural products stemmed back in the 1950's when a series of arabinonucleosides and ribo-pentosyl nucleosides were isolated from *Cryptotethia crypta* (Bergmann and Freeney, 1951; Bergmann and Burke, 1956; Bergmann and Stempien, 1957). The discovery led to the development and commercialization of anticancer drugs, cytarabine (Ara-C), and antiviral drug, vidarabine (Ara-A). Since then, the unique and complex structures of marine-derived molecules have been an inspiring and driving force for the search of new molecules in drug discovery. To date, six marine-derived compounds have been approved to be used clinically. These included ziconotide (Prialt®), a synthetic form of ω-conotoxin from the cone

snail *Conus magus*. Ziconotide is registered as an intrathecal analgesic for systemic analgesics, adjunctive therapies, or IT morphine-intolerant chronic pain in 2004 (U.S. FDA/CDER, 2012). Another approved drug is antitumor trabectedin (Yondelis®, formerly ecteinascidin 743) from the tunicate *Ecteinascidia turbinata* (European Medicine Agency, 2012). The drug was approved by European Union for soft tissue sarcoma and relapsed platinum-sensitive ovarian cancer in 2007, and is now in phase III trials for the approval to be used in the USA (U.S. National Institute of Health, 2012).

Marine-derived eribulin mesylate (Halaven™), a synthetic analog of halichondrin B from the sponge *Halichondria okadai*, was approved in 2010 for the intravenous treatment of metastasis breast cancer, particularly in the patients who have received at least two prior chemotherapy regimens for late-stage disease (U.S. FDA, 2012). In August 2011, U.S. FDA/CDER (2012) approved brentuximab vedotin (Adcetris™), a derivative of dolastatin 10 originally isolated from the sea hare *Dolabella auricularia*, for Hodgkin's lymphoma and systemic anaplastic large cell lymphoma treatment. The extended list of marine-derived drugs in various phases of clinical trial are excerpted in Table 1.

Table 1. Current clinical pipeline of marine-derived compounds

Compound name	Source	Disease area
Approved		
cytarabine, Ara-C (Cytosar-U®)	*Cryptotethia crypta* (sponge)	cancer
vidarabine, Ara-A (Vira-A®)	*C. crypta* (sponge)	viral infection
ziconotide (Prialt®)	*Conus magus* (cone snail)	chronic pain
trabectedin (Yondelis®)	*Ecteinascidia turbinata* (tunicate)	cancer
(EU registered only)		
eribulin mesylate (Halaven™)	*Halichondria okadai* (sponge)	cancer
brentuximab vedotin	*Dolabella auricularia* (sea hare;	cancer
(Adcetris™)	synthetic derivative of dolastatin-10)	

Table 1. (cont.)

Compound name	Source	Disease area
Phase III		
trabectedin (Yondelis®) (U.S. registered only)	*E. turbinata* (tunicate)	cancer
soblidotin (Auristatin PE)	*Symploca* sp. (cyanobacteria; synthetic derivative of dolastatin-10)	cancer
Phase II		
DMXBA	*Amphiporus angulatus* (marine worm)	schizophrenia
plitidepsin (Aplidin®)	*Aplidium albicans* (tunicate)	cancer
elisidepsin (Irvalec®)	*Elysia rufescens* (nudibranch)	cancer
PM1004 (Zalypsis®)	*Jorunna funebris* (nudibranch)	cancer
plinabulin	*Halimeda lacrimosa* (green algae)	cancer
tasidotin, synthadotin	*Dolabella auricularia* (sea hare; synthetic of dolastatin-15)	cancer
pseudopterosins	*Pseudopterogorgia elisabethae* (soft coral)	inflammation
Phase I		
bryostatin 1	*Bugula neritina* (bryozoan)	cancer
hemiasterlin	*Hemiasterella minor* (sponge)	cancer
marizomib (salinosporamide A)	*Salinispora tropica* (obligate marine bacterium)	cancer

Note: Modified from Mayer et al. (2010) and from http://www.accessdata.fda.gov; access January, 2012.

Over the past two decades the rate in discovery of new structural entities and novel activities of natural products from marine organisms has accelerated. This is in part due to the accessibility of SCUBA diving equipments, which allows researchers to probes the areas never been explored, and the state-of-the-art isolation and structure elucidation technology.

Expanding the areas of marine natural products also allow an extensive research not only toward

the compounds that may be used in medical and pharmaceutical purposes but also toward the relationship within and between marine species, thereby leading to the sustainable exploitation of marine bioresources.

1.2 Chemical constituents from the sponge *Pachastrissa nux*

The sponge *P. nux* belongs to the family Calthropellidae, order Astrophorida, class Demospongiae. Underwater, the sponge has two different growth forms; a grayish-black capitum, and branching, irregular-shaped base covering with dense algae or other sponges. On the surface, the exterior of the sponge was grayish-black, and the firm interior was whitish brown with black margin.

Chemically, the sponge *P. nux* has not been widely studied. In fact, to date, only three reports on the chemical constituents from the genus *Pachastrissa* have been published. Fernández et al. (1999) reported eleven bengazoles, five bengamides, and a "lactone" from the sponge *Pachastrissa* sp. Bengazoles 1-10 were active against *Candida albicans* (MICs 0.8-1.5 µg/mL). Later, Kuroda et al. (2002) reported the isolation of pachastrissamine from *Pachastrissa* sp. The alkaloid was cytotoxic against P388, A549, and MEL28 cell lines (IC_{50} 0.01 µg/mL).

Recently, a Thai specimen of the sponge *P. nux* from Sichang Island was investigated, and four new cytotoxic trisoxazole macrolides (kabiramides F-I) were isolated along with three known kabiramides B-D (Petchprayoon et al., 2006). All but kabiramide H showed cytotoxic activity against A549, HT29, KB, BC, and/or NCI-H187 cell lines (IC_{50}s 0.03-0.18 µg/mL).

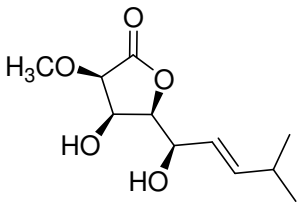

lactone

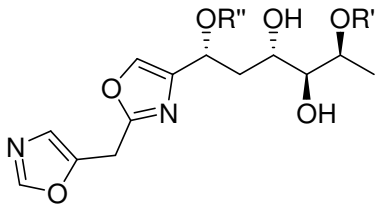

	R'	R"
bengazole 1;	$CO(CH_2)_{14}CH_3$	H
bengazole 2;	H	$CO(CH_2)_{14}CH_3$
bengazole 3;	$CO(CH_2)_{12}CH(CH_3)_2$	H
bengazole 4;	H	$CO(CH_2)_{12}CH(CH_3)_2$
bengazole 5;	$CO(CH_2)_{13}CH_3$	H
bengazole 6;	H	$CO(CH_2)_{13}CH_3$
bengazole 7;	$CO(CH_2)_{11}CH(CH_3)_2$	H
bengazole 8;	H	$CO(CH_2)_{11}CH(CH_3)_2$
bengazole 9;	$CO(CH_2)_{12}CH_3$	H
bengazole 10;	H	$CO(CH_2)_{12}CH_3$
bengazole 11;	H	H

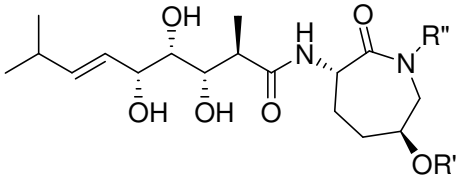

	R'	R"
bengamide A;	$CO(CH_2)_{12}CH_3$	H
bengamide B;	$CO(CH_2)_{12}CH_3$	CH_3
bengamide E;	H	H
bengamide F;	H	CH_3
bengamide L;	$CO(CH_2)_{11}CH(CH_3)_2$	H

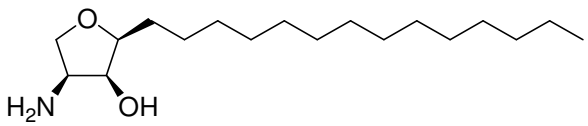

pachastrissamine

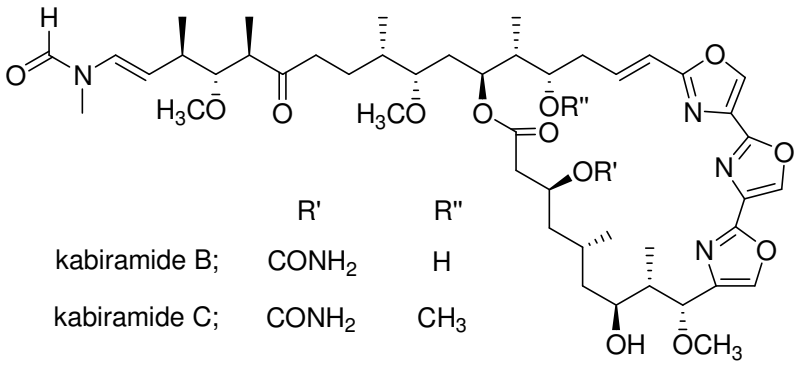

	R'	R''
kabiramide B;	$CONH_2$	H
kabiramide C;	$CONH_2$	CH_3
kabiramide D;	H	CH_3
kabiramide F;	H	H

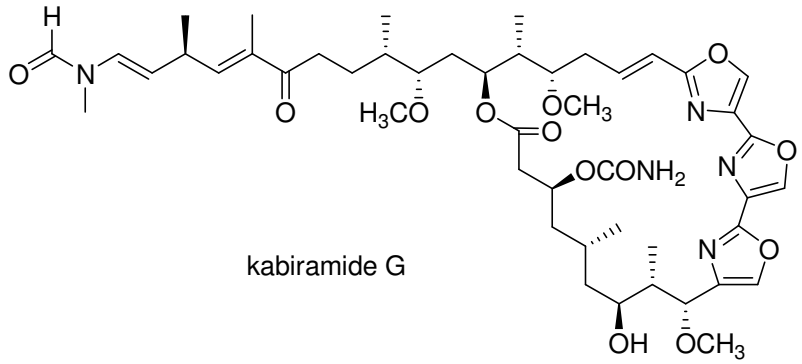

kabiramide G

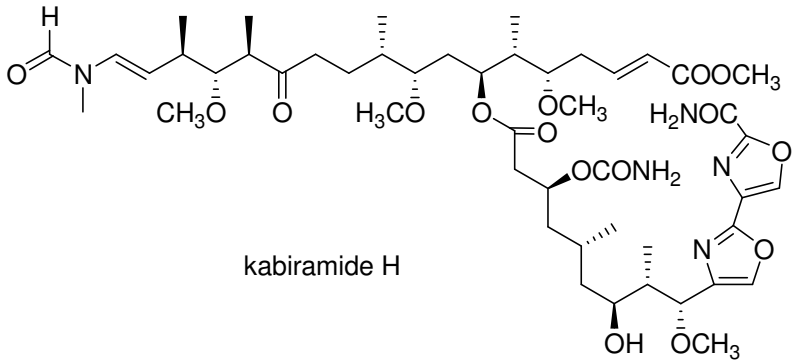

kabiramide H

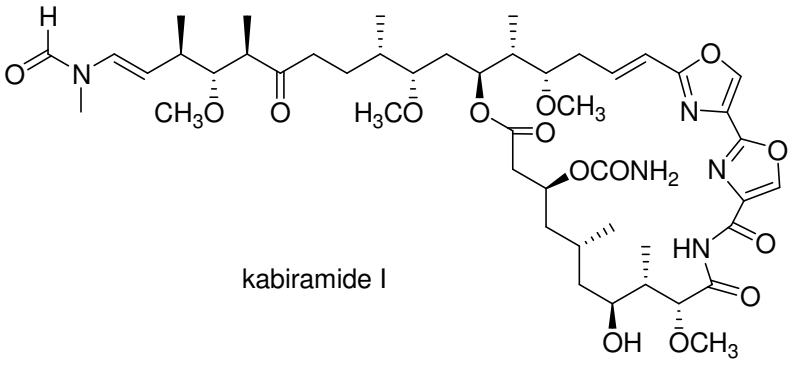

kabiramide I

1.3 Trisoxazole macrolides

Trisoxazole macrolides is a class of polyketide-serine derived macrolides that are solely found in marine organisms. The primary sources were sponges of the genera *Halichondria*, *Mycale*, *Jaspis*, *Chondrosia*, and *Pachastrissa* (Table 2). Other famous sources were the nudibranch *Hexabranchus sanguineus* and its egg masses. The discovery of accumulation of trisoxazole macrolides in the mantle of the nudibranch in fact was among the first evidences of dietary transfer of compounds from the sponge prey to the nudibranch as for the defensive benefit in the slug (Pawlik et al., 1988).

The trisoxazole macrolide analogs were structurally characterized by a 25-membered macrocyclic lactone containing three consecutive oxazole rings and attached to an 11-carbon panhandle side chain with an *N*-formyl terminal. The core skeleton of trisoxazole macrolides are highly conserved with only limited variation in substitution pattern. Out of 36 carbon atoms on their core skeleton, the macrolides normally contained 10-13 chiral centers. The determination of the configuration, however, has been reported to be quite problematic due to their wax-like nature and highly flexible structures that forbade crystallization and NOE-related experiments. The absolute configuration of trisoxazole macrolides was first determined through X-ray crystallography of actin complex with ulapaulide A (Allingham et al., 2004).

Biologically, trisoxazole macrolides were strongly cytotoxic. This was attributed to the actin binding mechanism (Saito et al., 1994; Klenchin et al., 2003; Tanaka et al., 2003; Allingham et al., 2004). The trisoxazole macrolide bound to G(+)-ending capping domain of actin with high affinity and specificity. The interfering of normal actin filament dynamics, which was fundamental of eukaryotic cell functions, leads to cell death and has been presumed as primary mechanisms of several reported biological activity of trisoxazole macrolides, i.e., cytotoxic, antifungal, and proteasome-inhibiting activities.

To date, there have been 43 trisoxazole macrolides reported. Shown in Table 2 are naturally occurring trisoxazole macrolide analogs with their biological activities. The list was organized due to similarity among each subclass of the macrolides, particularly based on the substitution pattern at C4-C7 and C30-C33.

1.4 Organ- and tissue-specific accumulations of secondary metabolites

The accumulations of the secondary metabolites in different parts of living organisms have been proposed as the allocation of functional molecules towards crucial parts with specific purposes. The chemical distributions have long been observed widely in terrestrial plants. Early example included the distribution of plant hormone auxins as observed by Darwin since 1880 and documented by Went in 1926, in which auxins regulation was described to play a role in promoting cell growth. The auxins were allocated to growing parts, i.e., shoot apex, root, and auxiliary bud, in higher level than that in mature tissues. Secondary metabolites, on the other hand, are well known for their defensive functions against predators (Leyser, 2010). The proposed ecological role of secondary metabolites usually involved a plant-herbivore interaction, in which plants adapted and allocated unpalatable toxic metabolites, e.g., phenolic compounds and volatile oils, to the highly vulnerable parts.

Similar to their terrestrial counterparts, allocation of secondary metabolites for defense was proposed in marine organisms. For example, green algae in order Caulerpales produced toxic metabolites in young growing parts and reproductive structures at a higher concentration than in mature tissues. Determination of inter-specimen variation also showed that the algae collected from the areas with high herbivory pressure shown higher variation both qualitatively and quantitatively than in the other less hostile areas (Paul and Fenicals, 1986). The inter-specimen allocation was supported by spatial-variation-in-consumers model (McClintock and Baker, 2001). For defensive allocation in the sponges, the study of Becerro et al. (1998) was the first that introduced intra-colonial variation, in which the contents of two sesterterpenes, scalaradial, and desacetylscalaradial, in the sponge *Cacospongia* sp. were found in higher concentration in the tips than in the bases of the sponges. The defensive function of these two metabolites was proposed to be related to feeding behavior of the nudibranch *Glossodoris pallida*, which prefers to feed on the base parts than on the tips of the sponge. Another evidence was the intra-specimen variation of kuanoniamines C and D in unusual growth forms of the sponge *Oceanapia* sp. The concentrations of the metabolites increased sharply from the buried base to the protruding capitum (Schupp et al., 1999). Fish feeding deterrent activity of kuanoniamines C

and D suggested that such allocation related to defense mechanism. Extended list of chemical allocation in marine organisms is shown in Table 3.

Table 3. Chemical variation in marine organisms

Organisms	Accumulated metabolites	Types of allocation	References
algae			
Emiliania huxleyi (unicellular algae)	dimethylsulphoniopropio-nate, dimethyl sulphide	intra-specimen (activated defense)	Wolfe et al., 1997
Caulerpa sertularioides, *C. racemosa*, *C. cupressoides* (green algae)	caulerpin, caulerpenyne	intra-specimen	Meyer and Paul, 1992
Caulerpa taxifolia (green algae)	caulerpenyne	inter-specimen (seasonal variation)	Amade and Lemée, 1998
Caulerpales sp (green algae)	dihydrorhipocephalin, aldehyde, udoteal, pehodi, dihydroudoteal, rhipo-cephalin, habmedatrial, halimeda tetraacetate, chlorodesmin, caulerpenyne	intra- and inter-specimen	Paul and Fenical, 1986
Halimeda sp. (green algae)	halimedatrial, halimeda-tetraacetate, epihali-medatrial	intra- (activated defense) and inter-specimen (geographic variation)	Paul and Fenical, 1986; Paul and Van Alstyne, 1988, 1992
Stypopodium zonale (brown algae)	polycyclic terpene, prenylated hydroquinones	inter-specimen (geographic variation)	Gerwick et al., 1985; Soares et al., 2003

Table 3. (cont.)

Organisms	Accumulated metabolites	Types of allocation	References
Dictyota bartayresii, *D. cervicornis*, *Padina tenuis*, *Hydroclathrus clathratus*, *Sargassum polycystum*, *Sargassum cristaefolium*, *Sagrassum muticum*, *Turbinaria ornata* (Agat), *Turbinaria ornata* (Pago), *Cystoseira osmundacea*, *Fucus distichus*, *Halidrys dioica*, *Pelvetiopsis limitata*, *Agarum fimbriatum*, *Alaria marginata*, *Costaria costata*, *Egregia menziesii*, *Hedophyllum sessile*, *Laminaria dentigera*, *Nereocystis luetkeana* (brown algae)	polyphenolic compounds	inter-specimen (species variation)	Van Alstyne and Paul, 1990

Table 3. (cont.)

Organisms	Accumulated metabolites	Types of allocation	References
Postelsia palmaeformis, *Sargassum polyceratium*, *Dictyota* sp. *Petalonia fascia*, *Dictyota ciliolata*, *D. menstrualis, Scytosiphon lomentaria*, *Zoaria tournefortii* (brown algae), *Acetabularia calyculus, Halimeda incrassata, H. opuntia*, *H. tuna*, *Rhipocephalus phoenix* (green algae), *Digenea simplex*, *Laurencia poiteaui* (red algae)	NA[a]	intra-specimen (activated defense)	Cetrulo and Hay, 2000
Delisea pulchra (red algae)	halogenated furanones	inter-specimen (geographic variation)	de Nys et al., 1996; Wright et al., 2000
Laurencia obtusa (red algae)	elatol	intra-specimen	Sudatti et al., 2006
sponge			
Amphimedon sp.	Diisocyanoadociane, $\Delta^{5,7}$-sterol	intra-specimen	Garson et al., 1992

Table 3. (cont.)

Organisms	Accumulated metabolites	Types of allocation	References
Agelas conifera	oroidin, sceptrin, bromosceptrin, dibromosceptrin, ageliferin, bromoageliferin, dibromoageliferin	intra- (cellular localization) and inter-specimen (geographic variation)	Assmann et al., 2000; Richelle-Maurer et al., 2003
Agelas wiedenmayeri	4,5-dibromopyrrole-2-carboxylic acid, oroidin, bromoageliferin	intra- and inter-specimen (geographic variation)	Assmann et al., 2000
Aplysina aerophoba	aerophobin-2, aplysinamisin-1, isofistularin-3	intra-specimen (activated defense, cell localization, symbiosis)	Ebel et al., 1997; Turon et al., 2000; Sacristán-Soriano et al., 2011a, 2011b
Aplysina fulva	2-(3',5'-dibromo-4'-hydroxyphenyl)acetamide, aplysinafulvin, 2-(3,5-dibromo-1-hydroxy-4,4-dimethoxycyclohexa-2,5-dienyl)acetamide, 2-(3,5-dibromo-4-ethoxy-1-hydroxy-4-methoxy-cyclohexa-2,5-dienyl) acetamide, subereatensin, oxazolidinone	intra-(structural variation) and inter-specimen (geographic variation)	Nuñez et al., 2008; Freeman and Gleason, 2010, 2011
Aplysilla glacialis	manoöl, cholesterol endoperoxide	intra-specimen	Bobzin and Faulkner, 1992

Table 3. (cont.)

Organisms	Accumulated metabolites	Types of allocation	References
Aplysina fistularis (= *Verongia thiona*)	areothionine, homoaerothionine	intra- (cell localization) and inter-specimen (season variation)	Thompson et al., 1983; Betancourt-Lozano et al., 1998
Cacospongia sp.	scalaradial, desacetyl-scalaradial	inter-specimen (geographic variation)	Becerro et al., 1998
Chondrilla nucula	cerebroside	inter-specimen (geographic variation)	Schmitz and McDonald, 1974; Swearingen and Pawlik, 1998
Clathrina clathrus	clathridimine	intra-specimen (cell localization)	Roué et al., 2010
Crambe crambe	crambines A, B, C1, C2, crambescidins 800, 816, 830, 844	intra- (cell localization) and inter-specimen (size structure and geo graphic variation)	Becerro et al., 1995, 1997; Turon et al., 1996; Uriz et al., 1996b
Dysidea avara	averol	intra- (cell localization) and inter-specimen (geographic variation)	Müller et al., 1986; Uriz et al., 1996a; Martí et al., 2003
Ectyoplasia ferox	ectyoplasides A-B, feroxosides A-B	intra-specimen	Kubanek et al., 2002
Erylus formosus	formaside, formaside B, terpene glycosides	intra-specimen	Kubanek et al., 2000, 2002

Table 3. (cont.)

Organisms	Accumulated metabolites	Types of allocation	References
Haliclona sp.	salicylihalamide A	inter-specimen (color and geographic variations)	Abdo et al., 2007
Ircinia felix, I. campana	furanosesterterpene tetronic acid	intra-specimen	Freeman and Gleason, 2010, 2011
Ircinia variabilis	palinurin	inter-specimen (geographic variation)	Martí et al., 2003
Latrunculia sp.	discorhabdins A-D, G	intra- and inter-specimen (species variation)	Yang and Baker, 1995; Miller et al., 2001; Furrow et al., 2003
Melophlus sarassinorum	melophins A-B, D-E, G-I, O, Q-S	intra-specimen	Aoki et al., 2000; Xu et al., 2006; Rohde and Schupp, 2011
Mycale hentscheli	mycalamide A, pateamine, peloruside A	inter-specimen (geographic variations)	Page et al., 2005
Negombata magnifica	latrunculin B	intra-specimen (cell localization)	Gillor et al., 2000
Oceanapia sp.	kuanoniamines C-D, *N*-deacetyl-kuanoniamine D	intra-specimen	Eder et al., 1998; Schupp et al., 1999
Rhopaloeides odorabile	spongiadiol, spongiadiol diacetate, spongiatriol, spongiatriol acetate	inter-specimen (geographic variation)	Thompson et al., 1987

Table 3. (cont.)

Organisms	Accumulated metabolites	Types of allocation	References
Spongia lamella	ergosteryl myristate, nitenin, isonitenin, dihydronitenin, 12-episcalarin, 12-epideoxoscalarin, 12-episcalaradial, 12,18-iepisclalaradial	inter-specimen (geographic variation)	Noyer et al., 2011
Theonella swinhoei	swinholide A, P 951	intra-specimen (symbiosis)	Bewley et al., 1996
gorgonian			
Annella mollis, A. reticulata	NA[a]	inter-specimen (geographic variation)	Puglisi et al., 2000
Briareum asbestinum	briaranes, asbestinanes	inter-specimen	Harvell et al., 1993
Gorgonia ventalina, *G. flabellum*	furano-germacrene, julieannafuran, phospholipid fatty acids carotenoids, 5,10-epoxy-muurolane, 12,13-epoxy-α-santalene, isosericenine	intra- (size structure and infected disease) and inter-specimen (geographic variations)	Cronin et al., 1995; Slattery, 1999; Kim et al., 2000; Dube et al., 2002; Roussis et al., 2001
Pseudopterogorgia acerosa, *P. rigida*	pseudopterolide, curcuhydroquinone	intra-specimen	Harvell and Fenical, 1989
soft coral			
Parerythropodium fulvum fulvum	fulfulvene, 5-hydroxy-8-methoxy-calamenene, 5-hydroxy-8-methoxy-calamenene-6-al	inter-specimen (geographic variation)	Kelman et al., 2000

Table 3. (cont.)

Organisms	Accumulated metabolites	Types of allocation	References
Sinularia flexibilis	flexibilide, dihydro-flexibilide, sinulariolide	inter-specimen (size structure and geo-graphic variations)	Maida et al., 1993
bryozoan			
Flustra foliacea	benzaldehyde, 6-methyl-5-heptene-2-one, rosefuran, linalool, citronellal, rosefuran epoxide, nerol, geraniol, geranial, 1,4,5-trimethyl-6-(3-methyl-2-butenyl)-5-(4-methyl-3-pentanyl)-1,3-cyclohexa-diene, 4,6-bis(4-methyl-pent-3-en-1-yl)-6-methyl-cyclohexa1,3-diene-carbaldehyde, dihydro-flustramine C, flustraminols A-B, flustramines A-D, 6-bromo-2(1,1-dimethyl-2-propenyl)-1H-indole-3-carbaldehyde, deformyl-flustrabromine B, deformyl-flustrabromin; (3a*R**, 8a*S**)-6-bromo-3a[(2*E*)-3,7-dimethyl-2,6-octadienyl]-1,2,3,3a,8, 8a-	intra- and inter-specimen (age and geographic variations)	Peters et al., 2004

Table 3. (cont.)

Organisms	Accumulated metabolites	Types of allocation	References
	hexahydro pyrrolo[2,3-*b*]indol-7-ol, flustrabromine, *N*-(2-[6-bromo-2-(1,1-dimethyl-2-propenyl)-1H-indol-3-yl]ethyl)-*N*-methyl methane-sulfonamide		
sea slug			
Aplysia parvula (sea hare)	halogenated furanones	intra-specimen (organ-specific variation)	de Nys et al., 1996
Cadlina luteomarginata (nudibranch)	furodysinin, idiadione, pallescensis A, isonitriles, isothiocyanates	intra-specimen (organ-specific variation)	Thompson et al., 1982
Chromodoris funerea (nudibranch)	12-*epi*-scalarin, deoxoscalarin, luffairiellin-C, luffairiellin-D, ketodeoxoscalarin	inter-specimen (geographic variation)	Kernan et al., 1988a
brachiopod			
Liothyrella uva	NA[a]	intra-specimen (tissue-specific variation)	Mahon et al., 2003
ascidian			
Cystodytes sp.	ascididemin, 11-hydroxyascididemin, shermilamine B, deacetyl-shermilamine B, kuano-niamine D, deacetylkuano-niamine D	intra- and inter-specimen (color variation)	López-Legentil et al., 2005, 2006

Table 3. (cont.)

Organisms	Accumulated metabolites	Types of allocation	References
Distaplia cylindrica	organic acid	intra-specimen	McClintock et al., 2004
echinoderm			
Astropecten articulatus, Tethyaster grandis, Echinaster sp., *Henricia downeyae, Anthenoides piercei, Goniaster tessellatus, Tosia parva, Luidia clathrata, Chaetaster nodosus, Linkia nodosa, Narcissia trigonaria, Tamaria halperni, Oreaster reticulaus, Astrocyclus caecilia, Astroporpa annulata, Astrophyton muricatum, Holothuria lentigenosa, H. thomasi, Isostichopus badionotus, Comactinia meridionalis*	NA[a]	intra-specimen (specific tissue)	Bryan et al., 1996

Note: [a]Data is not available.

1.5 Rationales and objectives

The sponge *P. nux* is one of abundant benthic species in coral reefs along the Gulf of Thailand. Preliminary screening showed that its methanolic extract had a good antimalarial activity (IC_{50} 13.3 μg/mL) and cytotoxicity (>80% inhibition against MCF-7, HeLa, KB, and HT-29 cancer cell lines at 25 μg/mL). In addition, the careful examination suggested that such activities distributed unevenly between two growth forms of the sponge specimens, implying different chemical compositions in each part. It is of interest to investigate whether the localization of such compounds, along with the production and deposition of biologically active compounds, could be accounted for their roles in survival of the sponge and configure the importance of the bioactive metabolites in sponge as one of chemical defenses. The aims of this work are;

i) To isolate and elucidate the structures of the chemical constituents from the sponge *Pachastrissa nux*.

ii) To determine the biological activities, including the antimalarial activity and cytotoxicity, of the isolated compounds.

iii) To evaluate the distribution of chemical constituents among various growth forms of the sponge specimens.

CHAPTER 2

EXPERIMENTAL

2.1 General experimental procedures

Unless stated otherwise, all chemicals and chromatographic packing materials were used as purchased. The solvent used for general purposed were commercial grade and were re-distilled prior to use. All HPLC solvents were HPLC grade, and were filtered through a 0.45 μm membrane filter and degassed in ultrasonic bath (30 min). Analytical TLC was performed on silica gel 60 F_{254} (0.02 mm layer thickness; Merck®) and silica gel RP-18 F_{254S} (0.02 mm layer thickness; Merck®). The visualization was done under UV light (254 nm), and with iodine vapor.

The vacuum and flash chromatographies were carried out on silica gel 60 (particle size 0.04-0.06 mm; Scharlau®). The size exclusion chromatography was conducted on Sephadex™ LH-20 (GE Healthcare®), which was saturated in eluting solvents as stated for 24 h before using. Semi-preparative HPLC was performed either on a Waters 600E System Controller equipped with a Rheodyne 7125 injector port, a Waters 484 tunable absorbance detector, and a Jasco 807-IT integrator, or on a Thermo Finnigan Spectra system controller SCM 1000 equipped with P 4000 quaternary pump, Rheodyne 7725i injector port, and UV 6000 LP diode array detector, operated with ChromQuest 4.2.34 (3.1.6) software.

Optical rotations were measured on a Perkin Elmer Polarimeter 341 (Pharmaceutical Research Equipment Center, Faculty of Pharmaceutical Sciences, Chulalongkorn University). UV spectra were obtained either from a Hewlett Packard 8452A diode array (Department of Pharmaceutical Chemistry, Faculty of Pharmaceutical Sciences, Prince of Songkla University), a Shimadsu UV-160A UV-visible recording spectrophotometer (Pharmaceutical Research Equipment Center, Faculty of Pharmaceutical Sciences, Chulalongkorn University), or a Thermo The Spectronic™ GENESYS™ 6 UV-visible (Department of

Pharmacognosy and Pharmaceutical Botany, Faculty of Pharmaceutical Sciences, Prince of Songkla University). IR spectra were recorded on a Jasco 810 IR spectrophotometer (Department of Pharmacognosy and Pharmaceutical Botany, Faculty of Pharmaceutical Sciences, Prince of Songkla University). Mass spectra were measured either on a Micromass LCT spectrometer (Scientific Equipment Center, Prince of Songkla University), or on a maXis Bruker Daltonics (Department of Organic Chemistry, University of Vienna) for ESIMS spectra, and on a Thermo FinniganMAT 95 XL mass spectrometer for FABMS (Scientific Equipment Center, Prince of Songkla University). NMR spectra were recorded either on a Varian Unity Inova 500 MHz NMR spectrometer (500 MHz for ^{1}H, 125 MHz for ^{13}C; Scientific Equipment Center, Prince of Songkla University) or on a Bruker DRX-600 AVANCE spectrometer (600 MHz for ^{1}H; 150 MHz for ^{13}C; Department of Organic Chemistry, University of Vienna). The operating solvents were benzene-d_6 (7.15 ppm of residual C_6HD_5 for ^{1}H and 128.0 ppm for ^{13}C NMR) and chloroform-*d (*7.24 ppm of residual $CHCl_3$ for ^{1}H and 77.0 ppm for ^{13}C NMR). The spectra were all referred to solvent signals stated accordingly as internal standards.

The HPLC-UV based quantitative analysis was performed on a Shimadzu SCL-10A solvent delivering system with an LC-10AD pump. This was equipped with an SPD-10A UV diode array detector and an SIL-10AD autosampler. Chromatographic systems and chromatogram management were operated with a CLASSVP 6.13 PS1 software.

2.2 Chemical constituents of the sponge *P. nux*

2.2.1 Animal material

The specimens of the sponge *P. nux* were collected from three different expeditions; two from Koh Tao, Surat-Thani Province (10° 6.058' N, 99° 51.238' E), in April 2004 and April 2006, and one from Chumphon Islands National Park, Chumphon Province (10° 29.468' N, 99° 25.132' E), in April 2008, all at the depth of 15-20 m. The specimens were procured in an ice chest (0°C) upon surfacing and at -20°C once arrived at the laboratory until extraction. The sponge was identified to be *Pachastrissa nux* (de Laubenfels, 1954) (family

Calthropellidae) by Dr. Sumaitt Putchakarn, Institute of Marine Science, Burapha University. The sponge has two fundamental growth forms, a grayish-black branched capitum randomly protruding from an irregular-shape grayish-black base covering underwater substratum (Figure 1). A voucher specimen (AP04-002-01) was deposited at the Department of Pharmacognosy and Pharmaceutical Botany, Faculty of Pharmaceutical Sciences, Prince of Songkla University.

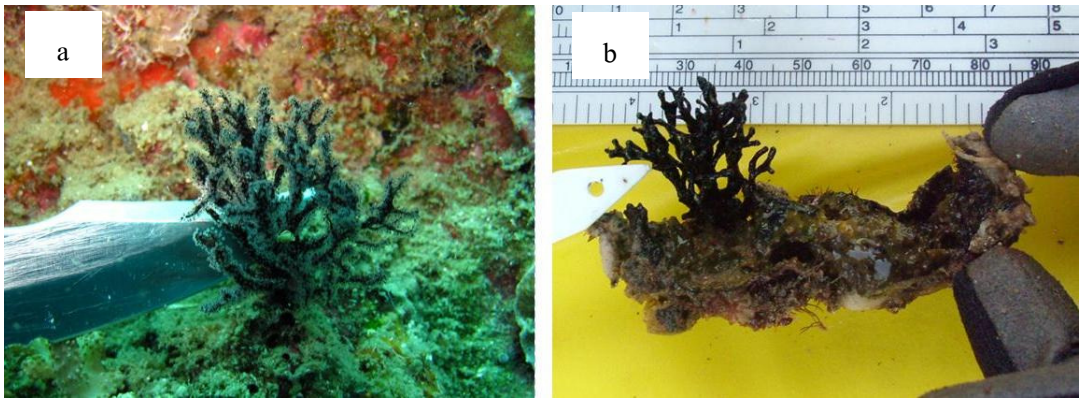

Figure 1. The sponge *Pachastrissa nux*: underwater (a) and upon surfacing (b).

2.2.2 Extraction and isolation

The chemical investigation of the sponge specimens from three collecting expeditions was carried out separately and independently. The freeze-dried specimens from the 2004- and 2006-expeditions (517 g, total), were pooled and macerated in CH_3OH (5 × 700 mL). The dried CH_3OH-extract was partitioned with a series of solvents to yield hexane-, CH_2Cl_2-, and *n*-BuOH-extracts (9, 4, and 36 g, respectively). The CH_2Cl_2-extract (IC_{50} 0.7 µg/mL against *Plasmodium falciparum* K1) was selected for further purification. The extract was fractionated with two consecutive SiO_2 columns, (5% CH_3OH in CH_2Cl_2; and gradient CH_3OH/hexane/CH_2Cl_2 from 2.5:1:96.5 to 30:1:69) to yield two major fractions. An aliquot (213 mg) of the first fraction was chromatographed over Sephadex™ LH-20 (CH_3OH), then with HPLC RP-C8 column (Supelco® Ascentis™, 10 µm, 250 × 10 mm; 40% H_2O in CH_3CN, flow rate 3.0 ml/min) to yield kabiramides B (**1**, 9 mg), C (**2**, 13 mg), G (**3**, 8 mg), J (**4**, 3 mg), and a pooled fraction (101 mg).

This pooled fraction was further fractionated using HPLC RP-C8 column (Supelco®Ascentis™, 10 μm, 250 × 10 mm; 50% H_2O in CH_3CN, flow rate 3.3 mL/min), then HPLC RP-C18 column (Vertical VertiSep™ GES, 5 μm, 150 × 4.6 mm, 35% H_2O in CH_3OH, flow rate 1.5 mL/min), and kabiramide I (**5**, 2 mg) was obtained (Scheme 1). Additional amounts of **1**, **2**, and **3** were later obtained from the remaining aliquot (223 mg) using HPLC RP-C18 column (Phenomenex®, 10 μm, 250 × 10 mm, 35% H_2O in CH_3CN flow rate 3.5 mL/min). The total yields for **1**-**3** were 23, 40, and 25 mg, respectively.

The second fraction (290 mg) was purified using an HPLC RP-C18 column (Phenomenex®, 10 μm, 250 × 10 mm, 35% H_2O in CH_3CN flow rate 3.5 mL/min) to yield **2** (23 mg) and a pooled fraction. This was further separated using an HPLC RP-C18 column (Phenomenex®, 10 μm, 250 × 10 mm, 35% H_2O in CH_3CN flow rate 3.5 mL/min), and kabiramide D (**6**, 3 mg) was obtained (Scheme 1).

The specimen from the 2008 expedition was freeze-dried (790 g) and extracted in the same manner as previously described to yield hexane-, CH_2Cl_2-, and *n*-BuOH-extracts (14, 7, and 4 g, respectively). The CH_2Cl_2-extract was isolated with consecutive chromatographies as followed; SiO_2 column (5% CH_3OH in CH_2Cl_2), SiO_2 column (0.5% CH_3OH in EtOAc), Sephadex™ LH-20 column (CH_3OH), and HPLC RP-C8 column (Phenomenex®, 10 μm, 250 × 10 mm, 50% H_2O in CH_3CN, flow rate 8.0 mL/min). Along with additional amounts of **1** (86 mg), **2** (232 mg), and **3** (111 mg), two fractions were obtained. The first fraction (12 mg) was purified using a HPLC RP-C8 column (Supelco®Ascentis™, 10 μm, 250 × 10 mm; 22% H_2O in MeOH, flow rate 3.5 mL/min) to yield kabiramide K (**7**, 6 mg), and the second fraction (21 mg) was purified with a HPLC RP-C8 column (Supelco®Ascentis™, 10 μm, 250 × 10 mm; 25% H_2O in MeOH, flow rate 3.5 mL/min) to yield **4** (12 mg) with a fraction which was further purified with a HPLC RP-C18 column (Vertical VertiSep™ GES, 5 μm, 150 × 4.6 mm, 30% H_2O in CH_3OH, flow rate 1.5 mL/min) to obtain kabiramide L (**8**, 2 mg) (Scheme 2).

Kabiramide B (1); white solid; $[\alpha]_D$ +4 (*c* 0.6 $CHCl_3$); UV (CH_3OH) λ_{max} (log ε) 252 (5.19), 212 (5.10) nm; IR (thin film) ν_{max} 3600-3250 (br), 3450, 3350, 3150, 2960, 2925, 1730, 1718, 1690, 1659 cm^{-1}; ^1H and ^{13}C NMR see Table 8; ESIMS *m/z* (% relative intensity) 950.0 ($[M+Na]^+$, 100).

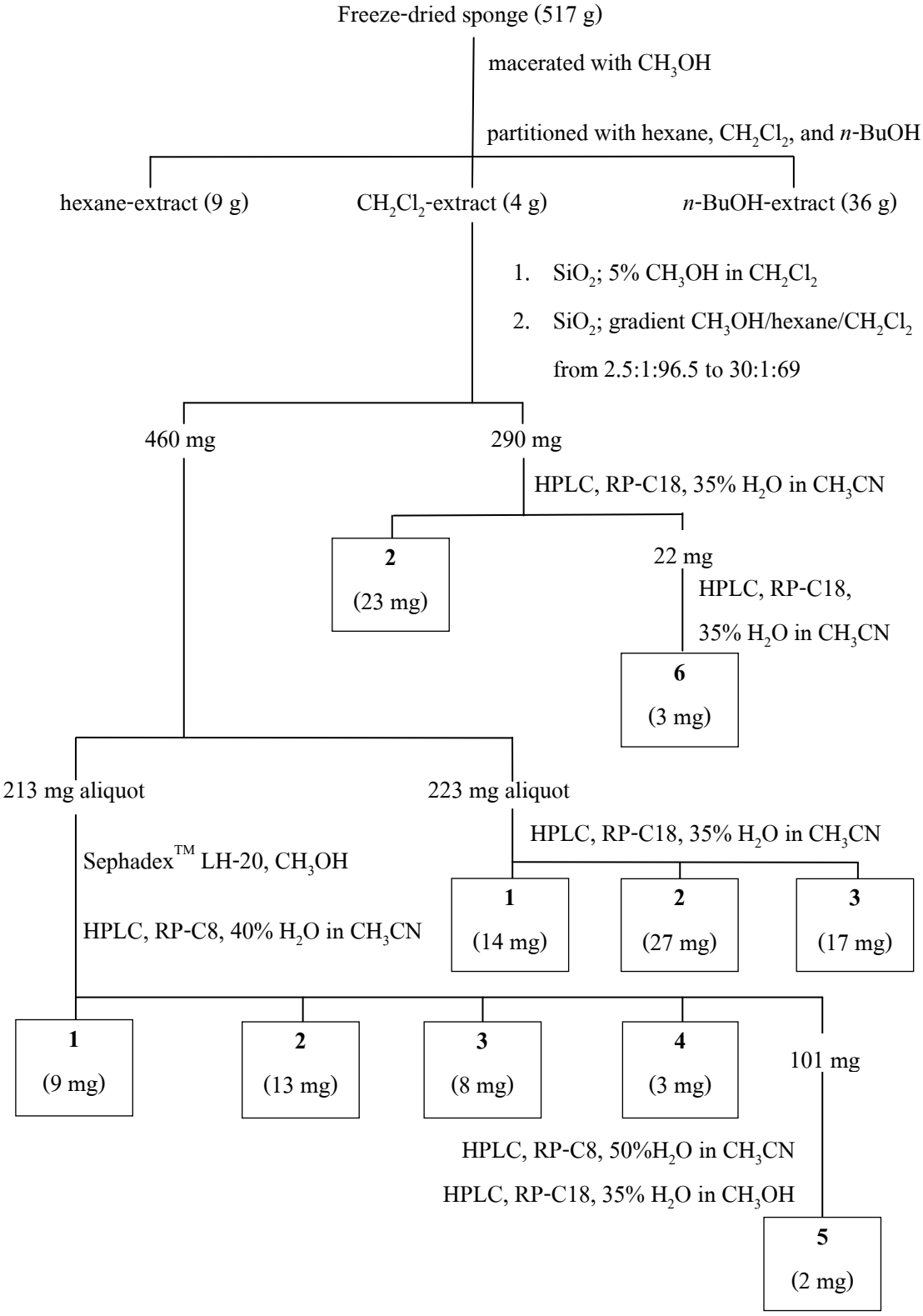

Scheme 1. Isolation scheme of the sponge *P. nux* (2004 and 2006 specimens).

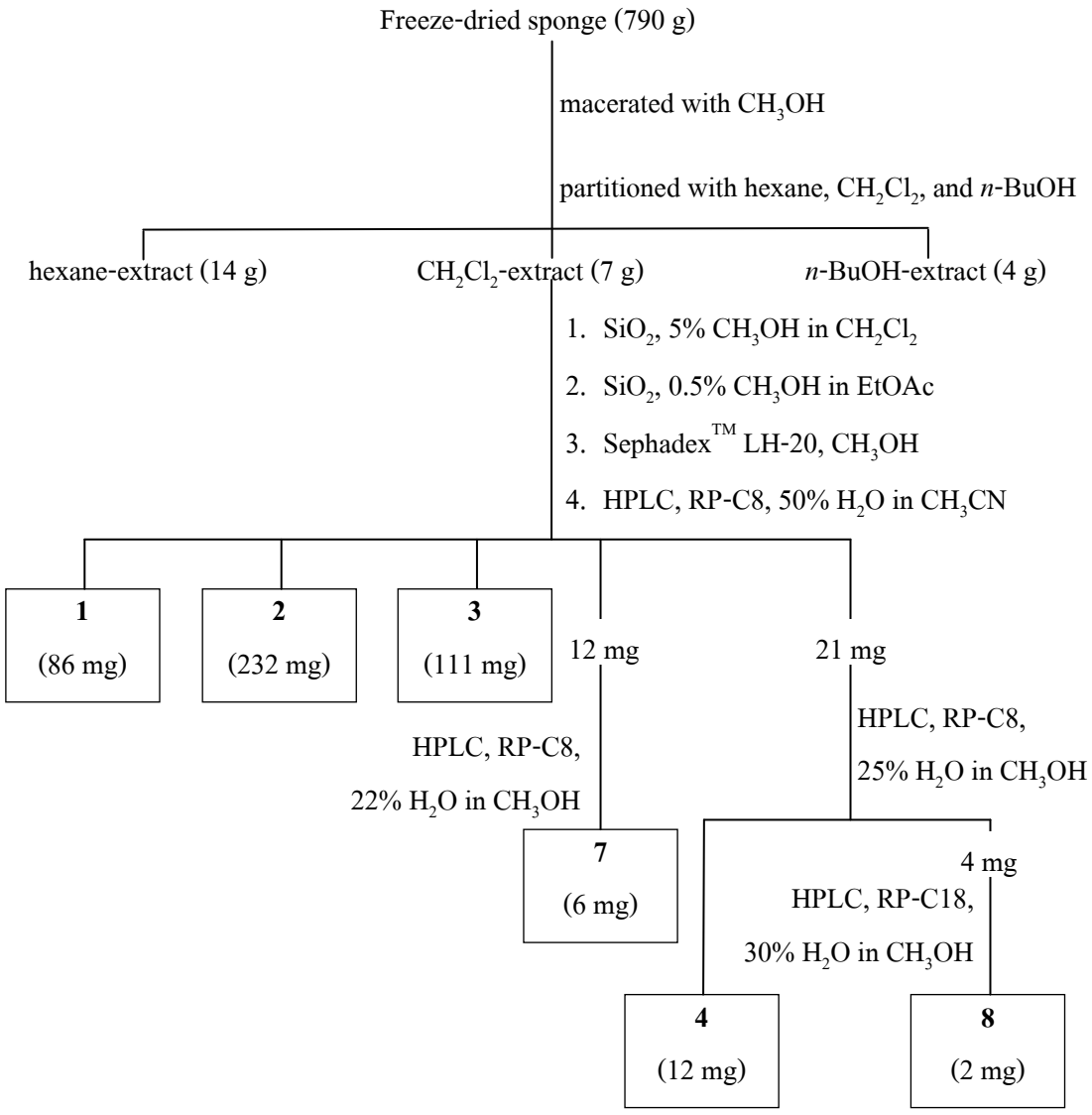

Scheme 2. Isolation scheme of the sponge *P. nux* (2008 specimen).

Kabiramide C (2); white solid; $[\alpha]_D$ +10 (*c* 0.6 $CHCl_3$); UV (CH_3OH) λ_{max} (log ε) 252 (5.20), 210 (5.11) nm; IR (thin film) ν_{max} 3600-3250 (br), 3450, 3350, 3150, 2960, 2925, 1725, 1720, 1698, 1650 cm^{-1}; ^1H and ^{13}C NMR see Table 9; ESIMS *m/z* (% relative intensity) 963.9 ($[M+Na]^+$, 100).

Kabiramide G (3); white solid; $[\alpha]_D$ +27 (*c* 0.3 $CHCl_3$); UV (CH_3OH) λ_{max} (log ε) 236 (5.31), 212 (5.26) nm; IR (thin film) ν_{max} 3600-3250 (br), 3460, 3350, 3150, 2960, 2925, 1725, 1720,

1690, 1659 cm^{-1}; ^{1}H and ^{13}C NMR see Table 10; ESIMS *m/z* (% relative intensity) 931.9 ($[M+Na]^+$, 100).

Kabiramide J (4); white solid; $[\alpha]_D$ +6 (*c* 0.8 CH_3OH); UV (CH_3OH) λ_{max} (log ε) 248 (4.55) nm; IR (thin film) ν_{max} 3600-3250 (br), 3460, 3375, 3175, 2960, 2925, 1735, 1720, 1690, 1659 cm^{-1}; ^{1}H and ^{13}C NMR see Table 4; ESIMS *m/z* (% relative intensity) 918.5 ($[M+Na]^+$, 100); HRESIMS *m/z* 918.4463 (calcd for $C_{46}H_{65}N_5O_{13}Na$ 918.4476).

Kabiramide I (5); white solid; $[\alpha]_D$ -8 (*c* 0.04 $CHCl_3$); UV (CH_3OH) λ_{max} (log ε) 248 (4.65) nm; IR (thin film) ν_{max} 3600-3200 (br), 3450, 3350, 2955, 2925, 1730, 1720, 1710, 1680, 1670, 1650 cm^{-1}; ^{1}H and ^{13}C NMR see Table 11; ESIMS *m/z* (% relative intensity) 968.6 ($[M+Na]^+$, 100), 984.6 ($[M+K]^+$, 15).

Kabiramide D (6); white solid; $[\alpha]_D$ -11 (*c* 0.2 $CHCl_3$); UV (CH_3OH) λ_{max} (log ε) 236 (6.49) nm; IR (thin film) ν_{max} 3600-3250 (br), 3175, 2960, 2925, 1735, 1690, 1659 cm^{-1}; ^{1}H and ^{13}C NMR see Table 12; ESIMS *m/z* (% relative intensity) 921.5 ($[M+Na]^+$, 100).

Kabiramide K (7); white solid; $[\alpha]_D$ +9 (*c* 0.3 CH_3OH); UV (CH_3OH) λ_{max} (log ε) 246 (4.55) nm; IR (thin film) ν_{max} 3600-3250 (br), 3175, 2960, 2925, 1735, 1690, 1659 cm^{-1}; ^{1}H and ^{13}C NMR see Table 5; FABMS *m/z* (% relative intensity) 867.5 ($[MH]^+$, 3), 563.5 (2), 282.3 (100), 256.3 (18); HRFABMS *m/z* 867.4713 (calcd for $C_{46}H_{67}N_4O_{12}$ 867.4755).

Kabiramide L (8); white solid; $[\alpha]_D$ +2 (*c* 0.2 CH_3OH); UV (CH_3OH) λ_{max} (log ε) 231 (4.73), 217 (4.71), 207 (4.71) nm; IR (thin film) ν_{max} 3600-3250 (br), 2960, 2925, 2850, 1720, 1680, 1675, 1659 cm^{-1}; ^{1}H and ^{13}C NMR see Table 6; ESIMS *m/z* (% relative intensity) 875.5 ($[M+Na]^+$, 100), 891.5 ($[M+K]^+$, 15); HRESIMS *m/z* 875.4429 (calcd for $C_{45}H_{64}N_4O_{12}Na$ 875.4415), 891.4176 (calcd for $C_{45}H_{64}N_4O_{12}K$ 891.4141).

2.2.3 Biological activities

2.2.3.1 Antimalarial activity

The assay for antimalarial activity was serviced by Bioassay Laboratory (BIOTEC central research unit, BIOTEC, Thailand). The targeted parasite was *Plasmodium*

falciparum (K1 multidrug resistant strain), which was maintained in RPMI 1640 medium containing 20 mM HEPES (*N*-2-hydroxyethylpiperazine-*N*′2-ethanesulfonic acid), 32 mM $NaHCO_3$, and 10% heat activated human serum (Trager and Jensen, 1976). The assay was performed according to microculture radioisotope technique (Desjadins et al., 1979; Jongrungruangchok et al., 2004). In brief, a 200 µL mixture of 1.5% of erythrocytes with 1% parasitemia at an early ring state was exposed to 25 µL of RPMI medium containing tested sample in a serial dilution (doped with DMSO, 0.1% final concentration). This was inoculated at 37°C under a 5%-CO_2 atmosphere for 24 h. A 25 µL of [^{3}H]hypoxanthine in the RPMI medium (10 µCi) was added to each well and the plate was incubated for additional 24 h addition. Detection of incorporated [^{3}H]hypoxanthine was performed on a TopCount microplate scintillation counter. The activity was reported in IC_{50} scale, using dihydroartemisinin as the standard reference (IC_{50}s 1.1-4.4 nM).

2.2.3.2 Cytotoxic activity

The cytotoxic activity determination based on sulphorrhodamine B method (Skehan et al., 1990) was supported by Asst. Prof. Dr. Supreeya Yuenyongsawad, Department of Pharmacognosy and Pharmaceutical Botany, Faculty of Pharmaceutical Sciences, Prince of Songkla University. The breast cancer (MCF-7) and normal (human fibroblast) cell lines were targeted. In brief, the monolayer culture of each targeted cell line in a 96-well micro-liter plate was exposed to a serial dilution of tested samples in an EMEM medium doped with 2 mM glutamine, 10% heat-inactivated new born calf serum, 50 IU/mL penicillin G sodium, 50 µg/mL streptomycin sulphate, and 0.125 µg/mL amphotericin B. The plate was incubated at 37°C (5% CO_2, 95% humidity) for 6 days, at the middle of which time the medium was refreshed. Cells were fixed with 100 µL of iced-cold 40% trichloroacetic acid. The fixed cells are washed and stained with 0.4% SRB in 1% acetic acid. The excess dye was removed and the plate is allowed to dry for an overnight. Stained dye was dissolved with Tris base for the measurements. The survival percentage of the cells was determined on a microplate reader (Biotek PowerWaveX) at 492 nm using camptothecin as the reference standard.

2.3 Quantification of kabiramide contents

2.3.1 Animal material

The specimens of the sponge *P. nux* were separately collected on a single colony basis from Koh Tao, Surat-Thani Province (10° 7.140' N, 99° 50.948' E), in April 2007. The sponge was identified and authenticated as described in 2.2.1. The sponge was immediately stored in ice chest (0°C) upon surfacing, then at -20°C once arrived at the laboratory until investigation.

2.3.2 Sample preparations

Each sponge specimen was cut into three parts; capitum, stalk, and base (Figure 2). The stalks, approximately 1-cm long, were dismissed from this investigation to avoid the complication from contamination and chemical communication between two other parts. All fouling organisms were removed, and each specimen was separately freeze-dried on an individual basis. Each sample was separately refluxed in THF (15 mL, 1 h). The extract was collected, and the sponge residue was washed with THF (3 × 5 mL). The combined extract and the washing were evaporated to dryness, and stored at -20°C until the quantification. Each extract was dispersed in CH_3CN and diluted also with CH_3CN to achieve a 500 μg/mL sample solution. This was filtered through a 0.45 μm membrane filter, and subjected to the quantification without further pre-chromatographic treatment.

2.3.3 Standard preparations

Kabiramides C and G were selected to be chemical markers throughout this investigation due to the chromatographic clarity and availability. The reference standards were obtained in-house according to the isolation described in 2.2.2, and were authenticated based on spectroscopic data (Huizing et al., 1995; Charlet et al., 2002; Zhou et al., 2008). The purity of

both references were referred to the NMR spectra, in which no significant impurity was observed. The stock solution of each reference standard was prepared by dissolving accurately weighed standard in CH_3CN to 500 µg/mL. Standard preparations were prepared by diluting the stock solution quantitatively with CH_3CN to appropriate concentrations.

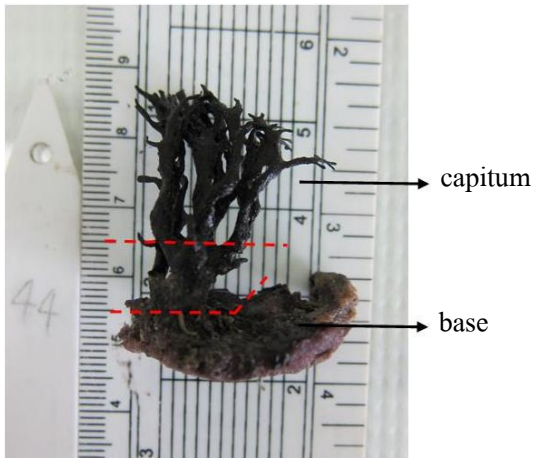

Figure 2. Surface appearance of the sponge *P. nux* showing capitum and base parts. The dashed lines indicate the cutting lines for the sponge parts to be investigated.

2.3.4 Quantification of kabiramide contents

The HPLC-UV based quantification was performed on a Vertical VertoSep^{TM}GES RP-C18 column (5 µm, 150 × 4.6 mm). The chromatographic conditions were as followed; 1% v/v aqueous AcOH/CH_3CN 37:63, flow rate 1.0 mL/min, 45°C, 20-µL injecting volume, UV 254 nm detection. Determination of kabiramide C content was referred to the peak area (t_R 8.7 min) obtained directly from each chromatogram. As for kabiramide G, of which peak was overlapped with the unknown impurities, determination of the height of positive peak from first-derivative chromatogram (t_R 9.9 min) was employed. Each sample preparation (2.3.2) was subjected to the devised chromatographic condition (all in triplicate). The concentration was calculated from the calibration plots, and the contents were calculated on the basis of the extract dry weight.

2.3.5 Validation of the devised HPLC-UV based quantification protocol

Prior to the quantification, the devised analytical method was validated for the linearity, precision, accuracy, limit of detection (LOD), and limit of quantification (LOQ) according to the guideline by the International Conference on Harmonization (ICH, 2005).

2.3.5.1 Linearity

The standard solutions of kabiramides C and G were diluted with CH_3CN to a series of appropriate concentrations (from LOQ to 100 μg/mL). Each standard solution was subjected to the devised chromatographic condition (all in triplicate). The linearity of peak area- or positive peak height-concentration plot was determined by means of linear regression.

2.3.5.2 Precision

Standard solutions of kabiramides C and G (1, 5, and 10 μg/mL), all in triplicate, were subjected to the devised chromatographic conditions to determine intra-day robustness, and the determination was repeated in three consecutive days for the inter-day precision. Relative standard deviation (RSD) of retention time, peak area (for kabiramide C), and peak height in first-derivative chromatogram (for kabiramide G) were determined.

2.3.5.3 Accuracy

Sample solutions, spiked with standard solutions (10, 20, and 30 μg/mL), were subjected to the devised analytical protocol (all in triplicate). Recovery percentages of the standards over the background concentration in the sample solution were determined.

2.3.5.4 Limit of detection (LOD) and limit of quantification (LOQ)

The concentrations at LOD and LOQ were achieved based on extrapolation from peak height of analyzed peak and noise that give signal-to-noise ratios of 3 and 10, respectively. All extrapolated LOD and LOQ concentrations were confirmed on standard solutions prepared at the calculated concentration.

2.3.6 Determination of structural components

Determination of the structural components was referred to those described by Schupp et al. (1999). Ash content determination was kindly carried out by Mrs Niwan Intaraksa, Department of Pharmacognosy and Pharmaceutical Botany, Faculty of Pharmaceutical Sciences, Prince of Songkla University. Each specimen was cut and dried in the same manner as described in 2.3.2. Each freeze-dried specimen (n = 7) was soaked in 3% v/v H_2O_2/30% v/v NH_4OH (75:25) for 7 days. The specimen was removed and dried to constant weight of sponge structural materials (mg/sponge dry weight). Each dried specimen was then pre-burned on a Bunsen burner, and put in a muffle furnace (Neytech 85P) at 450°C for 24-36 h to obtain ash at a constant weight. Ash content percentages were calculated on a basis of per sponge dry weight.

Determination of soluble proteins was carried out by Asst. Prof. Dr. Supreeya Yuenyongsawad and Dr. Sireewan Kaewsuwan, Department of Pharmacognosy and Pharmaceutical Botany, Faculty of Pharmaceutical Sciences, Prince of Songkla University, as described in Bradford method (Bradford, 1976). The specimens (n = 5), prepared as described in 2.3.2, were extracted for soluble proteins using an extraction protocol described by Ericsson et al. (2007). Each chilled specimen was extracted using an appropriate volume (10 times sponge dry weight) of 2% sodium dodecyl sulfate buffer (pH 6.8). The resulting mixtures were shaken (1400 rpm, 70°C, 10 min) and centrifuged (13.2×10^3 g, RT, 5 min). To a 0.1 mL of clear supernatants were added and mixed well (2 min) with Coomassie Brilliant Blue solution (USB corporation, 0.01% w/v). The resulting bright blue solutions were determined for soluble protein content at

595 nm. The calculation was referred to a calibration plot using bovine serum albumin as standard, and was reported on a w/w percentage of dry sponge basis.

2.3.7 Data analysis

The normal distribution of all data was determined before analysis (SPSS 15.0). The Wilcoxon sign-ranked test (SPSS 15.0) was used to determine the variation in the contents of kabiramides C and G in either parts of the sponge, and Pearson's correlation coefficient was for correlations among the contents of each marker in each part (Microsoft Excel 2003). Paired *t*-test (Microsoft Excel 2003) was used to compare structural materials between each part.

CHAPTER 3

RESULTS AND DISCUSSION

The chemical investigation of the sponge *P. nux* reported in this thesis is composed of two independent, but related projects. The first part is the isolation and structure determination of the chemical constituents from the sponge *P. nux*. The major components reported here are trisoxazole macrolides in the kabiramide family, among which three new compounds are reported here. The biological activities, namely antimalarial and cytotoxic activities, are also reported. The second part is referred to the observation of the different growth forms of the sponge *P. nux* and the implication in the specific chemical allocation in each growth form. The relation between the chemical allocation and structural materials, implying optimal defense mechanism, is also discussed.

3.1 Chemical constituents of the sponge *P. nux*

In the chemical investigation of the sponge *P. nux*, the CH_2Cl_2-extract, showing a potent antimalarial activity (IC_{50} 0.7 µg/mL against *P. falciparum* K1) was chosen. The investigation led to the isolation of three new and five known trisoxazole macrolides in the kabiramide series. All the isolated compounds were subjected to antimalarial activity and cytotoxicity assays to show that most are strongly active against *P. falciparum* K1, and all are cytotoxic against breast cancer (MCF-7) and human fibroblast cell lines.

3.1.1 Isolation of chemical constituents from the sponge *P. nux*

The sponge *P. nux* was collected from three separated expeditions in April 2004, April 2006, and April 2008. The combined specimens from 2004 and 2006 expeditions were freeze-dried (517 g), and macerated in CH_3OH to yield a crude extract. Solvent partitioning yielded hexane-, CH_2Cl_2-, and *n*-BuOH-extracts. The active CH_2Cl_2-extract (IC_{50} 0.7 µg/mL

against *P. falciparum*) was fractionated chromatographically to yield compounds **1**-**6** (23, 63, 25, 3, 2, and 3 mg, respectively). The specimen from 2008 expedition (790 g, dry weight) was extracted in a similar fashion. The CH_2Cl_2-extract was chromatographed to yield two additional new derivatives, **7** (6 mg) and **8** (2 mg) together with **4** (12 mg).

3.1.2 The structure elucidation of the isolated compounds

In the discussion on structure elucidation in this thesis, the structures of three new compounds, **4**, **7**, and **8**, are to be discussed first, followed by the identification of five remaining known compounds.

3.1.2.1 Kabiramide J (4)

Compound **4** was obtained as a white solid (15 mg, 1.1% w/w dry sponge). The molecular formula of compound **4** was deduced to be $C_{46}H_{65}N_5O_{13}$ according to a pseudomolecular peak in the ESIMS mass spectrum at *m/z* 918.5 ($[M+Na]^+$). This was confirmed by the HRESI mass at *m/z* 918.4463 (calcd for $C_{46}H_{65}N_5O_{13}Na$ 918.4476). The purposed molecular formula required an unsaturation degree of 17. This included six olefins, and seven carbonyl/imine system, based on the ^{13}C NMR spectrum; therefore four rings were required. The UV spectrum with a λ_{max} at 248 nm (log ε 4.55) corresponded with the presence of the oxazole ring. The IR absorption bands at ν_{max} 3460, 3375, and 1720 cm^{-1} and a resonance at δ_C 158.4 in the ^{13}C NMR spectrum (3-O*C*ONH_2) were characteristic to a primary carbamate moiety. The presences of lactone, enone, and formamide carbonyls were respectively indicated by the characteristic IR absorption bands at ν_{max} 1735, 1690, and 1659 cm^{-1}, and by the ^{13}C NMR signals at δ_C 171.6 (C-1), 201.0 (C-30), and 161.7 (35-N*C*HO), respectively.

The ^1H and ^{13}C NMR spectra of **4** (500 MHz for ^1H, benzene-d_6, Figures 3 and 4) showed the resonances of a 1:2 mixture of two inseparable conformers, caused by restricted rotation about an *N*-methyl-formamide bond. The ^1H NMR spectrum of **4** showed the signals of

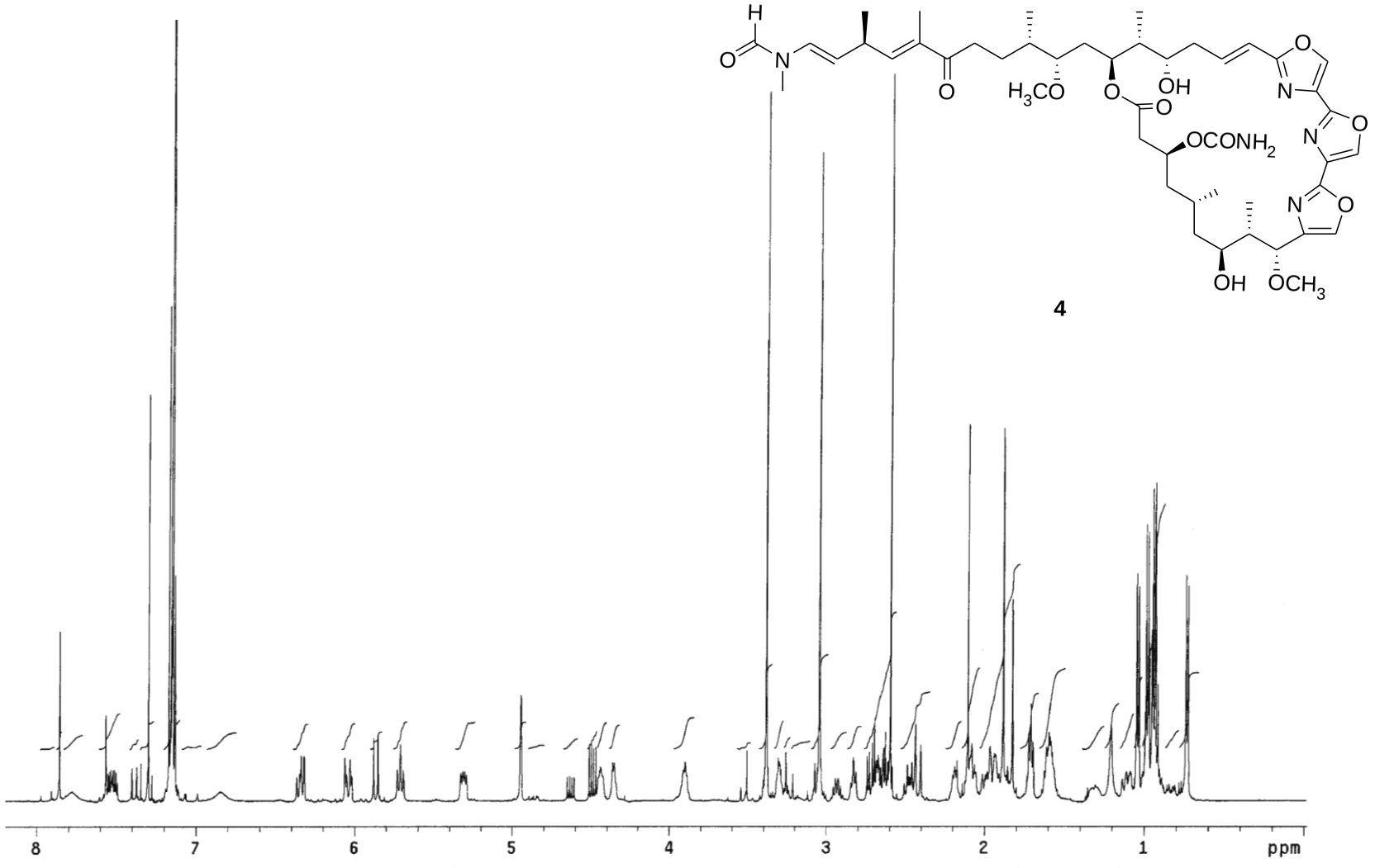

Figure 3. ^{1}H NMR spectrum of kabiramide J (**4**) (500 MHz, C_6D_6).

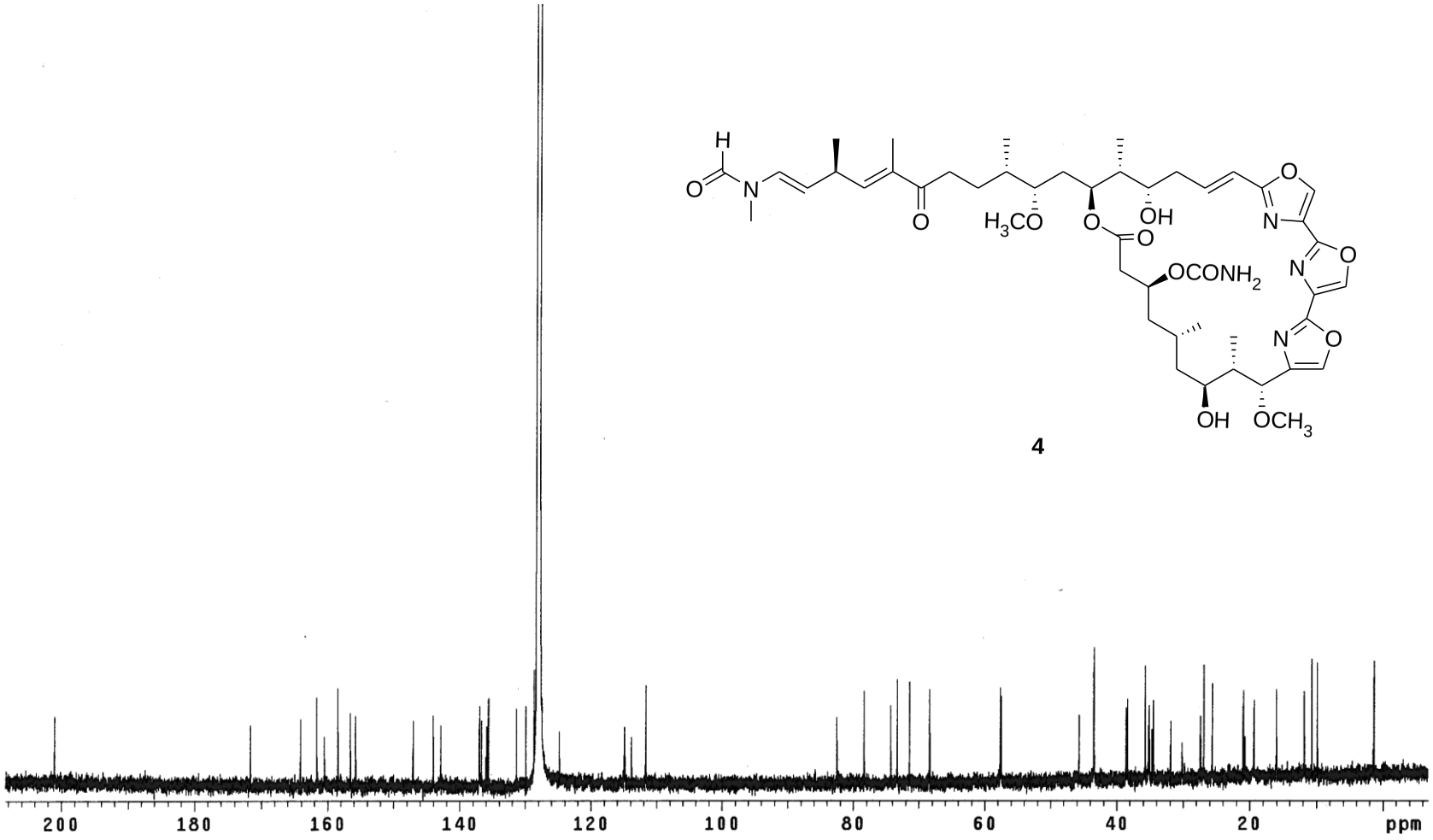

Figure 4. ^{13}C NMR spectrum of kabiramide J (**4**) (125 MHz, C_6D_6).

nine methyls, seven methylenes, and twenty methines. Included among these were five olefins, three oxazoles, and one formamide moiety. The complexity of the spectrum required an extensive use of ^{1}H-^{1}H COSY and HMBC experiments to construct all the structural frameworks. Five substructures were proposed according to ^{1}H-^{1}H COSY spectrum (Figure 5). These included a spin system of C-2 – C-9, on which 3-OCONH$_2$ (δ_H 7.78, br s; 6.85, br s; δ_C 158.4), 5-CH$_3$ (δ_H 0.73, d, J = 6.6 Hz; δ_C 19.3), 7-OH (δ_H 2.82, d, J = 6.5 Hz), 8-CH$_3$ (δ_H 0.98, d, J = 7.8 Hz; δ_C 10.7), and 9-OCH$_3$ (δ_H 3.04, s; δ_C 57.5) groups substituted. The second spin system was composed of C-19 – C-35. Although this was fragmented through the ^{1}H-^{1}H COSY spectrum, consecutive HMBC correlations from 23-CH_3 (δ 1.60, overlapped) to C-22 (δ 68.3) and C-24 (δ 74.2); 27-CH_3 (δ 0.93, d, J = 7.1 Hz) to C-26 (δ 82.5) and C-28 (δ 27.4); H-29 (δ 2.67, m; δ 2.64, m), 31-CH_3 (δ 1.88, d, J = 1.3 Hz), and H-32 (δ 6.32, dq, J = 9.3, 1.2 Hz) to C-30 (δ 201.0) allowed the thorough connection. HMBC experiments also allowed the connection of both spin systems through a correlation from H-24 (δ 5.71, td, J = 10.3, <1.0 Hz) to C-1 (δ 171.6) and also helped terminating the side chain with an *N*-methyl formamide (δ_H 2.60, s; 7.86, s; δ_C 161.7).

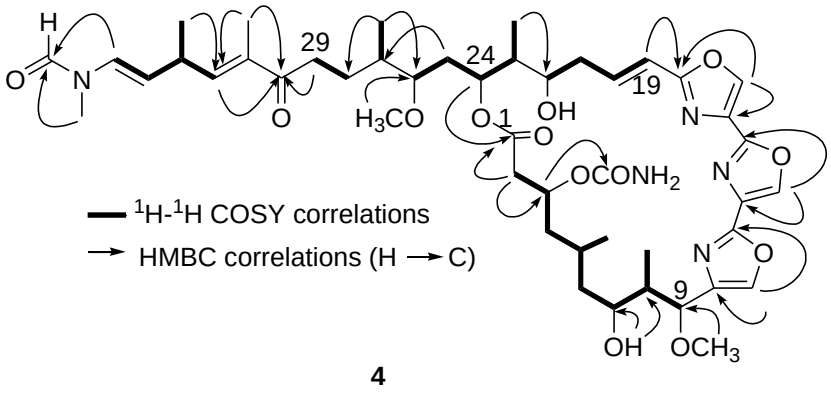

4

Figure 5. ^{1}H-^{1}H COSY and key HMBC correlations of kabiramide J (**4**).

Three consecutive oxazoles (C-10 – C-18) were proposed according to the characteristic signals at δ_H 7.13 (s), 7.17 (s), and 7.30 (s). The orientation of all three rings were placed as suggested by conventional oxazole biogenesis (Ishibashi et al., 1986; Shinha et al., 1999; Ichino et al., 2006) and also referred to previous reports (Roesener and Scheuer, 1986;

Matsunaga et al., 1986; Petchprayoon et al., 2006; Dalisay et al., 2009). Connection of the trisoxazole moiety onto the aliphatic moieties was relied on HMBC correlations from H-9 (δ 4.95, d, J = 1.0 Hz) and H-11 (δ 7.13, s) to C-10 (δ 142.8); H-17 (δ 7.17, s) and H-19 (δ 6.06, dd, J = 16.1, 1.0 Hz) to C-18 (δ 164.1), therefore furnishing the structure of **4** as a new trisoxazole macrolide in the kabiramide family, named kabiramide J.

In order to determine the configurations of **4**, a series of NOEDS and NOESY experiments were attempted, however with no usable information obtained. Here, the relative configurations were proposed according to comparable chemical shifts and coupling constants to other known kabiramide analogs (Matsunaga et al., 1986; Petchprayoon et al., 2006; Dalisay et al., 2009). Special attentions were paid on the geometry of 30-enone and the configuration on C-9. Δ^{31} was assigned as *E* due to characteristically upfield chemical shift of 31-CH_3 (δ 11.8; Petchprayoon et al., 2006). On the other hand, configuration at C-9, which is the only chiral center reported in both configurations, was proposed to be α-OCH_3 according to the coupling constant of H-9 (δ 4.95, d, J = 1.0 Hz; Dalisay et al., 2009).

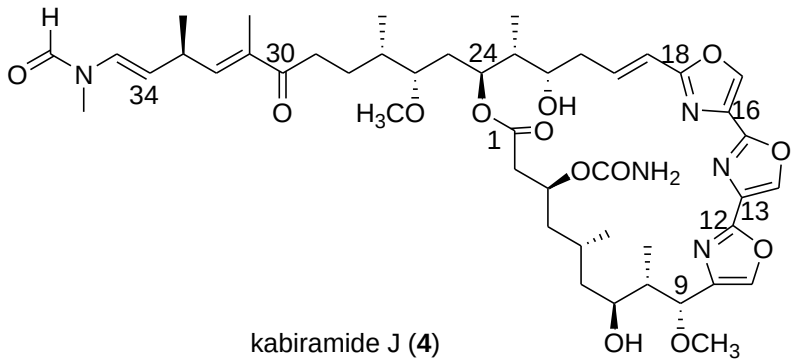

kabiramide J (**4**)

Table 4. ^{1}H and ^{13}C NMR data of kabiramide J (**4**) (500 MHz for ^{1}H and 125 MHz for ^{13}C, C_6D_6)[a]

Position	δ_C	δ_H (J in Hz)[b]
1	171.6, C	-
2	43.4, CH_2	2.71, dd (16.1, 6.6); 2.42, dd (16.1, 1.2)
3	71.3, CH	5.31, br dd (12.1, 6.6)

Table 4. (cont.)

Position	δ_C	δ_H (J in Hz)[b]
4	45.7, CH_2	2.07, m; 1.11, m
5	25.6, CH	1.92, overlapped
6	43.4, CH_2	1.71, m
7	73.3, CH	3.90, br dd (6.1, 5.5)[c]
8	38.6, CH	2.19, m
9	78.3, CH	4.95, d (1.0)
10	142.8, C	-
11	135.6, CH	7.13, s
12	155.7, C	-
13	131.4, C	-
14	137.0, CH	7.30, s
15	156.5, C	-
16	130.0, C	-
17	136.7, CH	7.17, s
18	164.1, C	-
19	114.9 [114.8], CH	6.06 [6.03], dd (16.1, 1.0)
20	147.0, CH	7.53, ddd (16.1, 9.4, 3.4)
21	38.4, CH_2	2.48, ddd (14.8, 9.4, 8.9); 1.97, overlapped
22	68.3, CH	4.44, br dd (9.0, 7.7)[c]
23	43.39, CH	1.60, overlapped
24	74.2, CH	5.71, td (10.3, <1.0)
25	35.1, CH_2	2.00, overlapped; 1.57, overlapped
26	82.5 [82.4], CH	3.30, m
27	35.2, CH	1.85, overlapped
28	27.4 [27.3], CH_2	2.09, overlapped; 1.62, overlapped
29	35.7, CH_2	2.67, m; 2.64, m
30	201.0, C	-

Table 4. (cont.)

Position	δ_C	δ_H (J in Hz)[b]
31	136.0, C	-
32	144.0, CH	6.32 [6.35], dq (9.3, 1.2)
33	34.5 [34.7], CH	2.93 [3.02], m
34	111.7 [113.8], CH	4.49 [4.63], dd (14.0, 7.3)
35	128.6 [124.8], CH	5.86 [7.38], d (14.0)
3-$CONH_2$	158.4, C	7.78, br s; 6.85, br s
5-CH_3	19.3, CH_3	0.73, d (6.6; 3H)
7-OH	-	2.82, d (6.5)
8-CH_3	10.7, CH_3	0.98, d (7.8; 3H)
9-OCH_3	57.5 [57.51], CH_3	3.04 [3.05], s, 3H
22-OH	-	4.35, br d (7.7)
23-CH_3	9.9, CH_3	1.04, d (6.8; 3H)
26-OCH_3	57.6 [57.63], CH_3	3.39 [3.38], s 3H
27-CH_3	16.0 [15.9], CH_3	0.93 [0.92], d (7.1; 3H)
31-CH_3	11.8 [11.7], CH_3	1.88 [1.83], d (1.2; 3H)
33-CH_3	20.9 [20.7], CH_3	0.94 [0.95], d (7.2; 3H)
35-NCH_3	26.9 [31.9], CH_3	2.60 [2.11], s, 3H
35-NCHO	161.7[160.5], CH	7.86 [7.57], s

Note: [a]Chemical shifts of the minor conformers are presented in brackets. [b]Unless stated otherwise, each proton signal was integrated as 1 proton. [c]The coupling constants were calculated according to the D_2O-exchanged spectrum.

3.1.2.2 Kabiramide K (7)

Compound **7** was obtained as a white solid (6 mg, 0.8% w/w dry sponge). The molecular formula of **7** was purposed to be $C_{46}H_{66}N_4O_{12}$ according to the pseudomolecular peak $[MH]^+$ at *m/z* 867.5 in the FAB mass spectrum, and was confirmed by the HRFAB mass

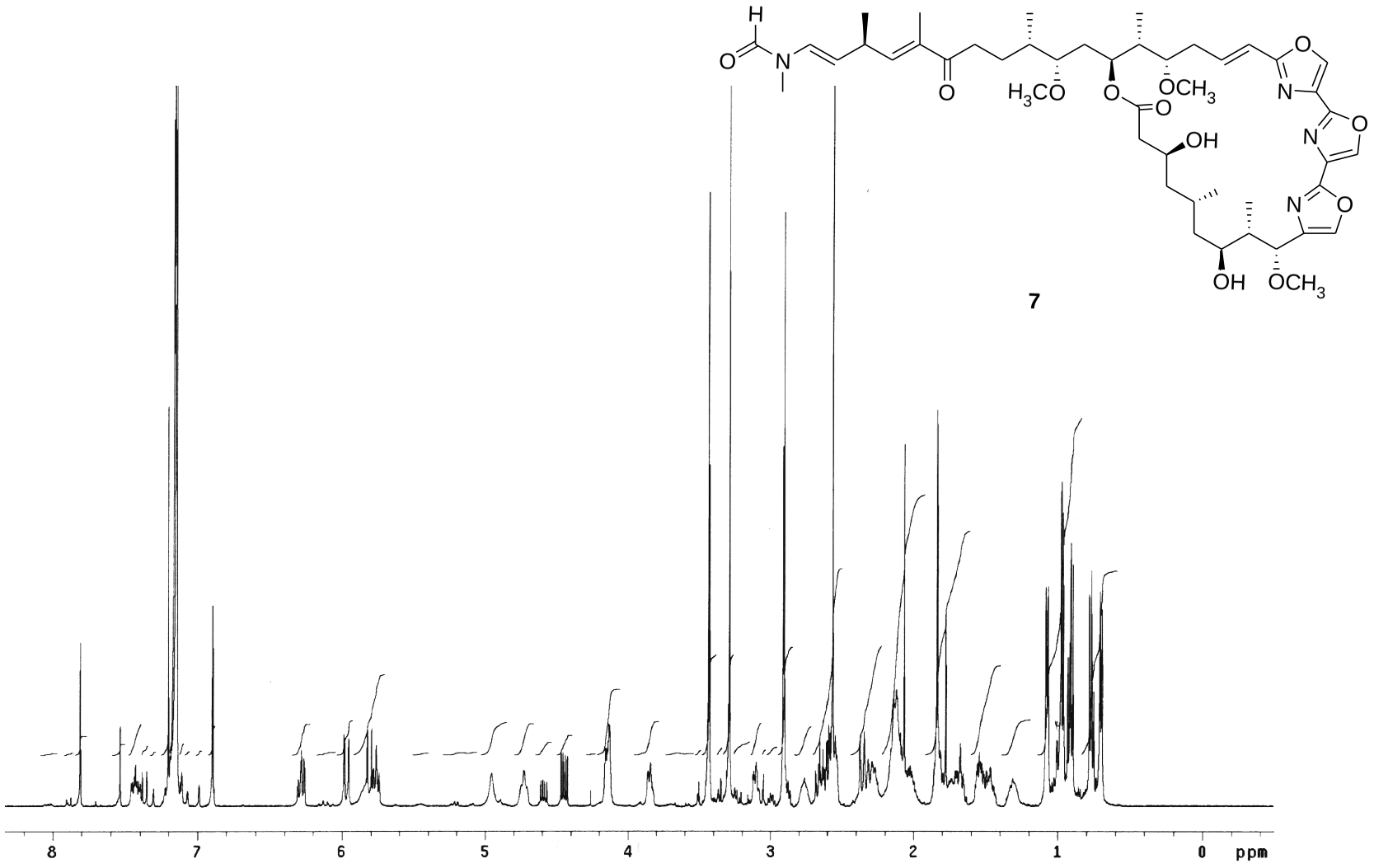

Figure 6. ^{1}H NMR spectrum of kabiramide K (**7**) (500 MHz, C_6D_6).

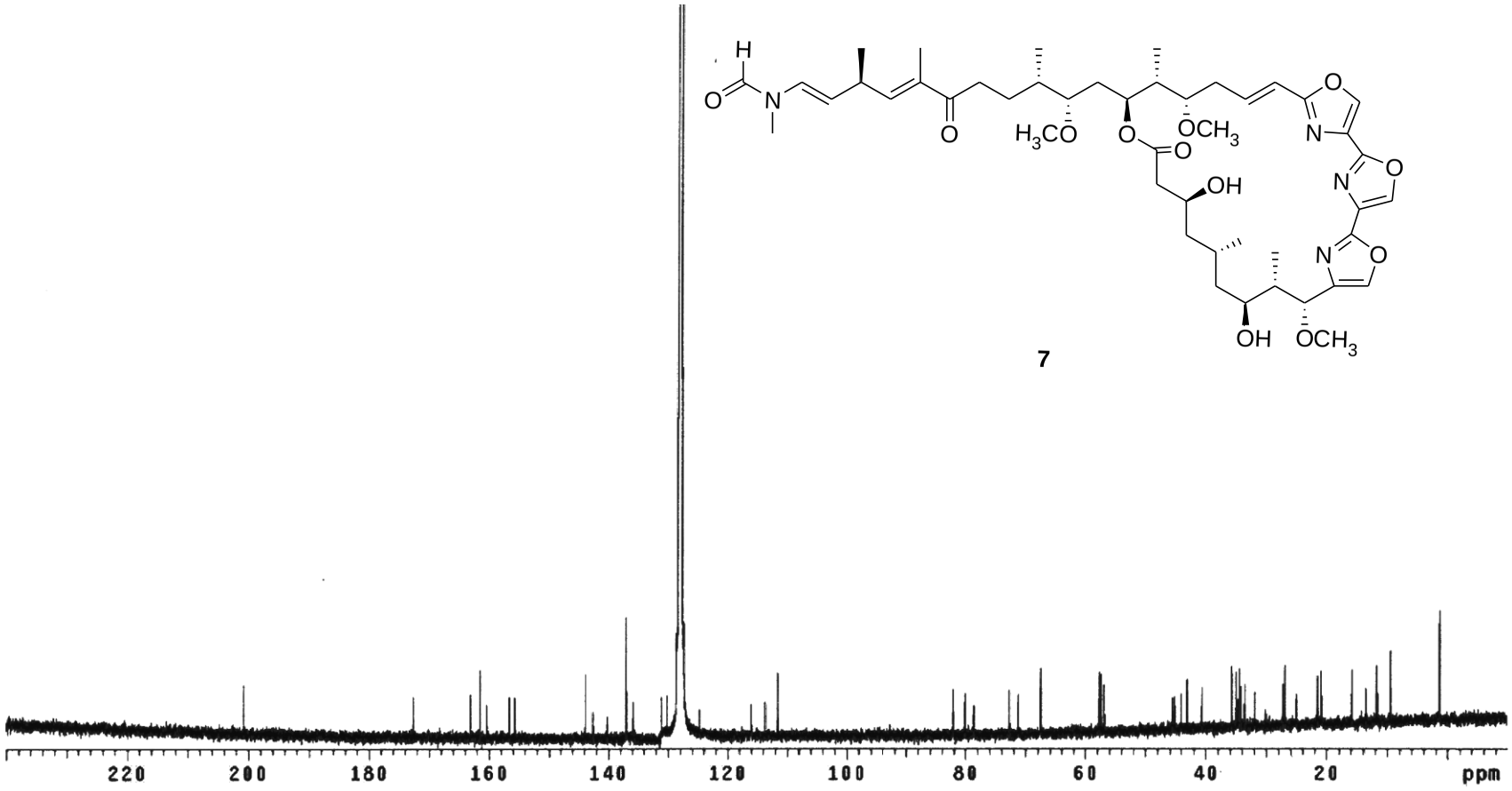

Figure 7. ^{13}C NMR spectrum of kabiramide K (**7**) (125 MHz, C_6D_6).

spectrum, which showed an $[MH]^+$ peak at *m/z* 867.4713 (calcd for $C_{46}H_{67}N_4O_{12}$ 867.4755). The molecular formula of **7** required unsaturation degree of 16, analyzed to be six olefinic double bonds, six carbonyl/imine bonds, and four ring systems. Absorption band in the UV spectrum at λ_{max} 246 nm (log ε4.55) also suggested trisoxazole part similar to that of **4**. The IR spectrum of **7** showed specific absorption bands at ν_{max} 3600-3250, 1735, 1690, and 1659 cm^{-1}, indicating hydroxy, lactone, enone, and formamide functionalities, respectively. Similarity in the ^1H and ^{13}C NMR spectra (500 MHz for ^1H, benzene-d_6, Figures 6 and 7) between **7** and **4** indicated that the two compounds shared a similar core skeleton. This included the characteristic signals in a 1:2 ratio of two rotamers, and the presence of trisoxazole macrolide part possessing the unique 30-enone moiety. The major differences among the two compounds were the presence of an additional methoxy group on C-22 (δ_H 3.43, s), and the absence of the carbamate on C-3 (δ 67.5), which was replaced by a hydroxyl group (δ 4.96, br s). This was strongly confirmed based on the complete analyses of the ^1H-^1H COSY and HMBC spectra (Figure 8). The structure of **7** was therefore proposed to be another new kabiramide derivative, named kabiramide K. Chemical shifts of all protons and carbons are summarized in Table 5.

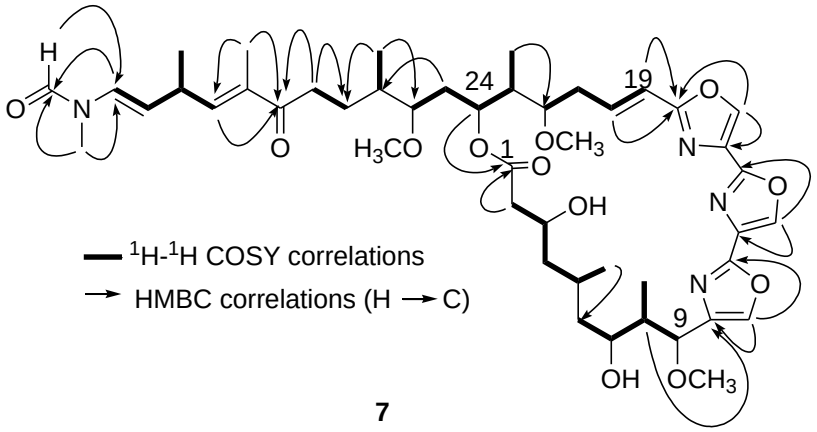

Figure 8. ^1H-^1H COSY and key HMBC correlations of kabiramide K (**7**).

Also similar to **4** was the configuration of **7**. All the asymmetric carbons were proposed to possess the relative configuration as referred to other related trisoxazole macrolides (Matsunaga et al., 1986; Petchprayoon et al., 2006; Dalisay et al., 2009). The geometry at Δ^{31} and orientation of H-9 were determined according to the same argument as given for **4**.

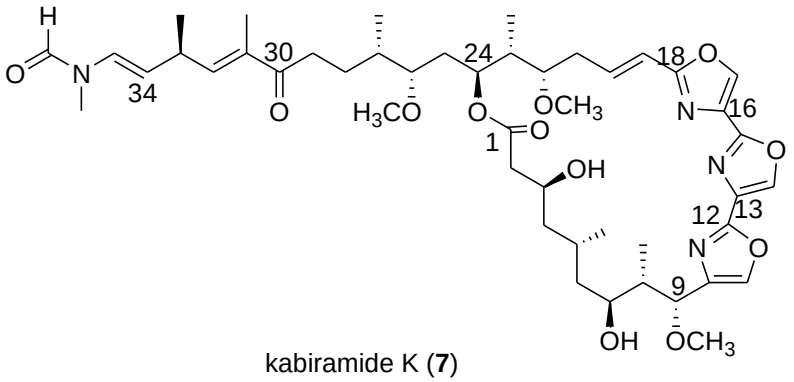

kabiramide K (**7**)

Table 5. ^{1}H and ^{13}C NMR data of kabiramide K (**7**) (500 MHz for ^{1}H and 125 MHz for ^{13}C, C_6D_6)[a]

Position	δ_C	δ_H (*J* in Hz)[b]
1	172.7, C	-
2	45.5, CH_2	2.65, dd (14.3. 3.2); 2.35, br d (14.3)
3	67.5, CH	4.73, br dd (10.6, 10.6)
4	44.0, CH_2	2.30, m; 1.00, br dd (10.6, 10.6)
5	25.0, CH	2.76, m
6	45.1, CH_2	1.67, ddd (13.0, 11.0, 3.2); 1.55, m
7	71.2 [71.3], CH	4.14, overlapped
8	43.1, CH	2.25, overlapped
9	80.1[80.09], CH	4.12, overlapped
10	140.2, C	-
11	137.0, CH	6.90, s
12	155.8, C	-
13	131.2, C[c]	-
14	137.0, CH	7.20, s
15	156.5, C	-
16	131.1, C[c]	-
17	137.0, CH	7.16, s
18	163.1, C	-

Table 5. (cont.)

Position	δ_C	δ_H (J in Hz)[b]
19	116.0, CH	5.95, dd (15.5, 1.7)
20	142.6, CH	7.43, ddd (15.5, 10.7, 4.6)
21	34.1, CH_2	2.55, overlapped; 2.15, overlapped
22	78.6, CH	3.84, m
23	40.6, CH	1.79, overlapped
24	72.7, CH	5.76, td (9.7, 1.0)
25	33.6, CH_2	1.82, overlapped; 1.45, m
26	82.11 [82.10], CH	3.11 [3.09], m
27	35.0, CH	1.75, overlapped
28	27.2 [27.1], CH_2	2.02 [1.99], overlapped; 1.51 [1.44], overlapped
29	35.7, CH_2	2.63, m; 2.60, m
30	200.8, C	-
31	135.9 [136.0], C	-
32	143.8 [142.5], CH	6.27 [6.30], dq (9.5, 1.2)
33	34.7 [34.5], CH	2.88 [3.00], overlapped
34	111.6 [113.7], CH	4.45 [4.59], dd (14.0, 7.3)
35	130.2 [124.8], CH	5.80 [7.36], d (14.0)
3-OH	-	4.96, br s[d]
5-CH_3	21.5, CH_3	1.08 [1.07], d (6.6; 3H)
7-OH	-	5.84, br s[d]
8-CH_3	13.6 [13.5], CH_3	0.70 [0.71], d (6.8; 3H)
9-OCH_3	56.8 [56.9], CH_3	2.90 [2.91], s, 3H
22-OCH_3	57.4 [57.3], CH_3	3.43 [3.42], s, 3H
23-CH_3	9.5, CH_3	0.97, d (7.1; 3H)
26-OCH_3	57.7 [57.8], CH_3	3.29, s, 3H
27-CH_3	15.9 [15.8], CH_3	0.77 [0.75], d (7.1; 3H)
31-CH_3	11.8 [11.7], CH_3	1.83 [1.77], d (1.2; 3H)

Table 5. (cont.)

Position	δ_C	δ_H (J in Hz)[b]
33-CH_3	20.9 [20.7], CH_3	0.91 [0.92], d (6.8; 3H)
35-NCH_3	26.8 [31.8], CH_3	2.56 [2.07], s, 3H
35-NCHO	161.7[160.4], CH	7.81 [7.54], s

Note: [a]Chemical shifts of the minor conformers are presented in brackets. [b]Unless stated otherwise, each proton signal was integrated as 1 proton. [c, d]The chemical shifts are interchangeable.

3.1.2.3 Kabiramide L (8)

Compound **8** was obtained as a white solid (2 mg, 0.3% w/w dry sponge). The molecular formula of **8** was purposed to be $C_{45}H_{64}N_4O_{12}$ based on the $[M+Na]^+$ peak in the ESI mass spectrum at *m/z* 875.5. This agreed well with the HRESI mass spectrum, in which the $[M+Na]^+$ peak was observed at *m/z* 875.4429 (calc for $C_{45}H_{64}N_4O_{12}Na$ 875.4418). The purposed structure required 16 unsaturated units, composed of six olefinic double bonds, six carbonyl/imine bonds, and four ring systems. The IR absorption at ν_{max} 3600-3250 cm^{-1} (br) indicated the presence of a hydroxy group. The presence of ester, enone, and formamide moieties were identified from the absorption bands at ν_{max} 1720, 1680, and 1659 cm^{-1}, respectively.

Also similar to **4** and **7**, the ^1H and ^{13}C NMR spectra of **8** (600 MHz for ^1H, benzene-d_6; Figures 9 and 10) were characteristic to trisoxazole macrolides, composing of two rotamers in a 1:2 ratio, with three consecutive oxazole rings and an *N*-methyl formamide terminal. Fourteen mass unit less than of **7** indicated that **8** is a demethyl analog of **7**. In order to elucidate the structure of **8**, ^1H-^1H COSY and HMBC experiments were attempted. The ^1H-^1H COSY spectra yielded three structural fragments (Figure 11), and indicated the similarity among **4**, **7**, and **8**. Close observation also suggested the substitution of a hydroxy group on C-22 (δ 69.1) as the major difference between **7** and **8**. However, the limited amount of **8** prohibited an extensive and thorough analysis of the HMBC spectrum, including the correlations necessary to connect

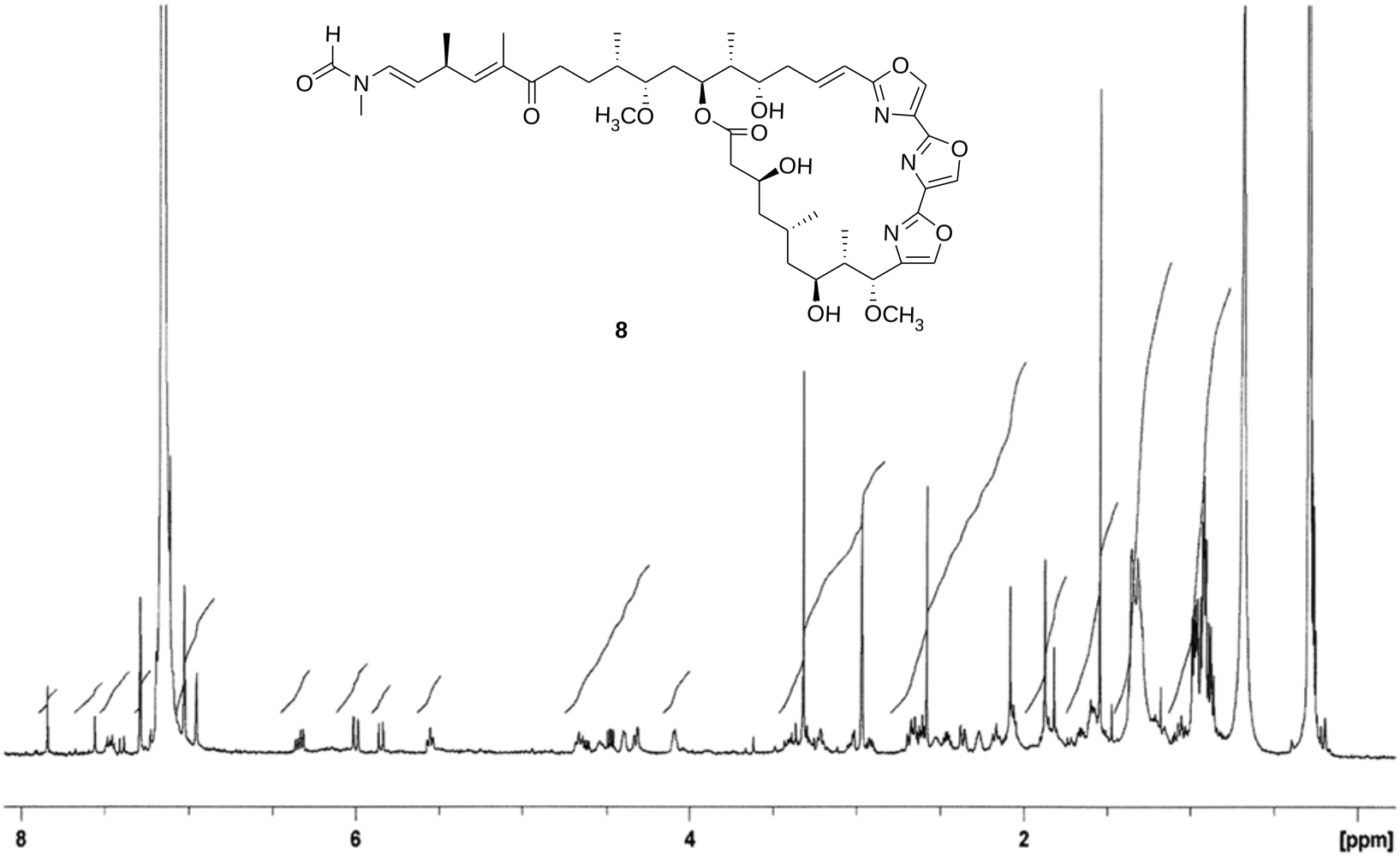

Figure 9. ^{1}H NMR spectrum of kabiramide L (**8**) (600 MHz, C_6D_6).

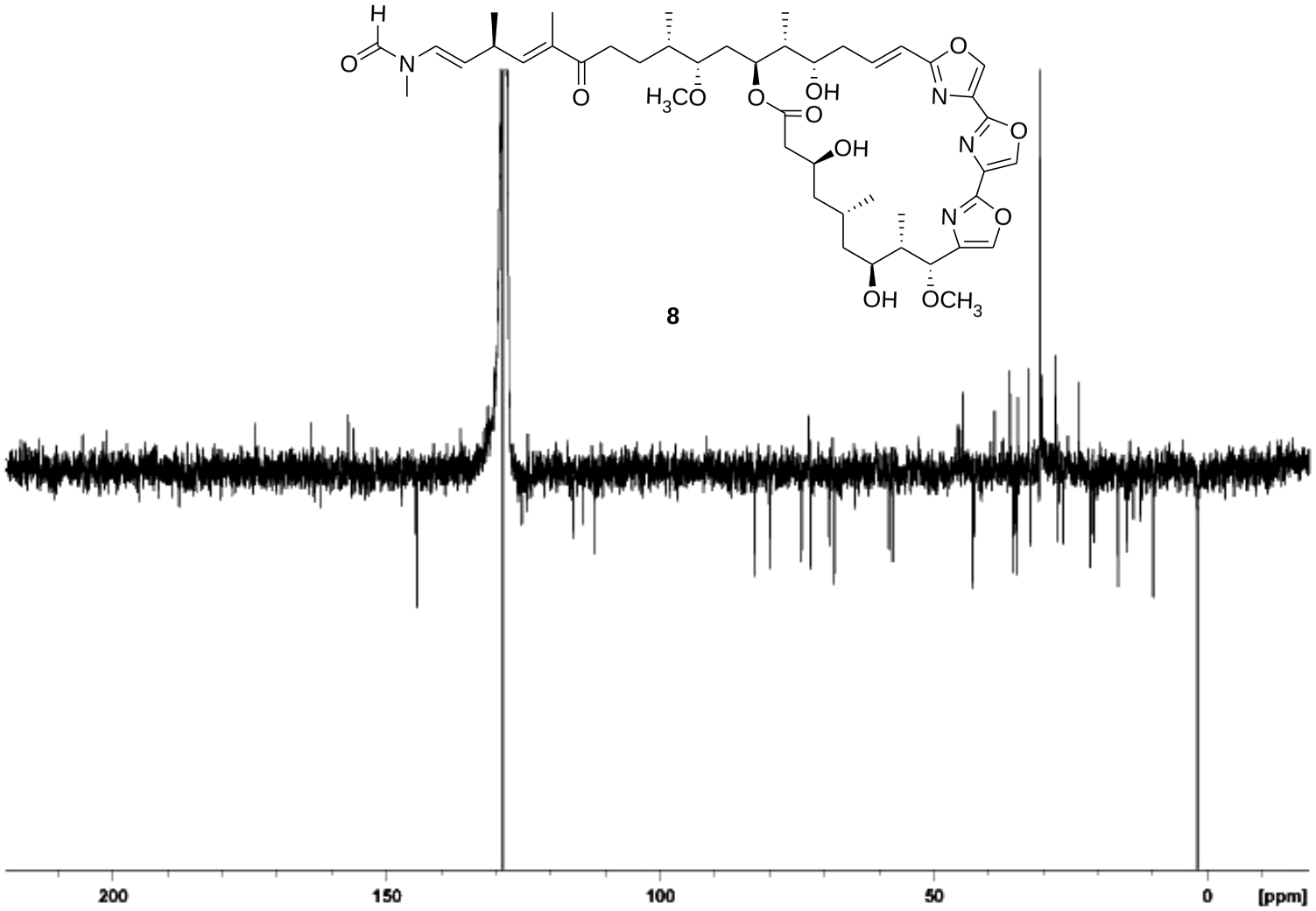

Figure 10. J-MOD NMR spectrum of kabiramide L (**8**) (150 MHz, C_6D_6); CH_3 and CH (negative); CH_2 and C (positive).

the lactone linkage and to attach the oxazole moieties onto the macrolide (Figure 11). Here, a direct comparison of the chemical shifts from ^{13}C NMR spectrum of trisoxazole macrolides obtained in this investigation, i.e., kabiramide G (**3**), **4**, and **7**, were employed (Table 7). The prominent resemblance between **7** and **8** was evident with the primary deviations locating solely at C-20 – C-24. The major difference at C-22 (δ 69.3) was affirmative to the proposed substitution of the hydroxyl group. **8** was therefore proposed to be a new member of kabiramide family, designated as kabiramide L.

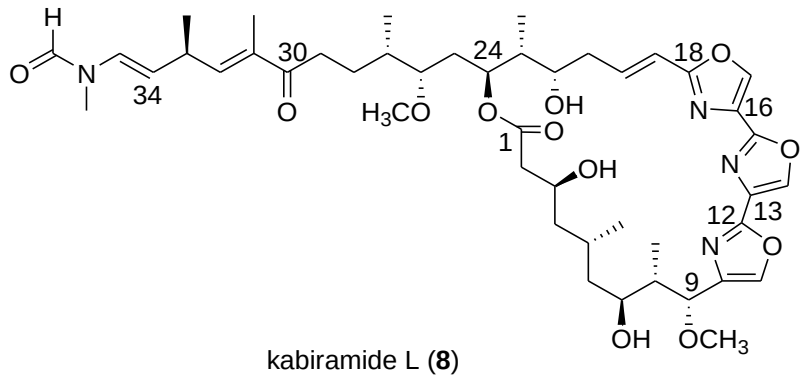

kabiramide L (**8**)

Table 6. ^{1}H and ^{13}C NMR data of kabiramide L (**8**) (600 MHz for ^{1}H and 150 MHz for ^{13}C, C_6D_6)[a]

Position	δ_C	δ_H (*J* in Hz)[b]
1	174.2, C	-
2	45.9, CH_2	2.68, m; 2.36, br d (14.3)
3	68.1, CH	4.66, br dd (13.0, 11.1)
4	45.5, CH_2	2.16, ddd (13.5, 13.0, 2.2);
		1.08, ddd (13.5, 11.1, 1.9)
5	26.4, CH	2.53, m
6	44.6, CH_2	1.86, overlapped; 1.66, ddd (13.2, 6.0, 2.3)
7	72.5, CH	4.09, m
8	42.4, CH	2.27, m
9	80.0, CH	4.31 [4.33], d (2.6)

Table 6. (cont.)

Position	δ_C	δ_H (J in Hz)[b]
10	141.3, C	-
11	135.7, CH	6.95, s
12	156.1, C	-
13	131.5, C	-
14	137.3, CH	7.19, s
15	157.0, C	-
16	129.1, C	-
17	134.8, CH	7.11, s
18	163.9, C	-
19	115.8, CH	6.00, d (15.6)
20	139.3, CH	7.46, ddd (15.6, 7.5, 4.5)
21	38.9, CH_2	2.46, ddd (13.7, 13.7, 7.5); 2.05, overlapped
22	69.1, CH	4.40, m
23	42.9, CH	1.60, overlapped
24	74.1, CH	5.55, td (9.1, 1.6)
25	34.6, CH_2	1.87, overlapped; 1.57, overlapped
26	82.6, CH	3.21, m
27	35.5, CH	1.80 [1.73], overlapped
28	27.6, CH_2	2.06, overlapped; 1.59, overlapped
29	36.1, CH_2	2.63, m; 2.60, m
30	201.2, C	-
31	136.5 [136.4], C	-
32	144.3 [144.7], CH	6.32 [6.35], dq (9.4, 1.5)
33	34.9 [35.1], CH	2.91 [3.02], m
34	111.9 [114.1], CH	4.48 [4.62], dd (14.1, 7.2)
35	128.7 [125.2], CH	5.84 [7.40], d (14.1)
5-CH_3	20.6, CH_3	0.99 [0.98], d (6.6; 3H)

Table 6. (cont.)

Position	δ_C	δ_H (*J* in Hz)[b]
8-CH_3	12.8 [12.75], CH_3	0.91 [0.92], d (6.9; 3H)
9-OCH_3	57.4, CH_3	2.96 [2.97], s, 3H
23-CH_3	9.9, CH_3	0.97 [0.95], d (6.6; 3H)
26-OCH_3	58.2, CH_3	3.31, s, 3H
27-CH_3	16.3, CH_3	0.88 [0.87], d (6.9; 3H)
31-CH_3	12.2 [12.19], CH_3	1.82 [1.88], d (1.5; 3H)
33-CH_3	21.3 [21.1], CH_3	0.93 [0.96], d (6.8; 3H)
35-NCH_3	27.3 [32.3], CH_3	2.58 [2.08], s, 3H
35-NCHO	161.5 [160.6], CH	7.84 [7.56], s

Note: [a]Chemical shifts of the minor conformers are presented in brackets. [b]Unless stated otherwise, each proton signal was integrated as 1 proton.

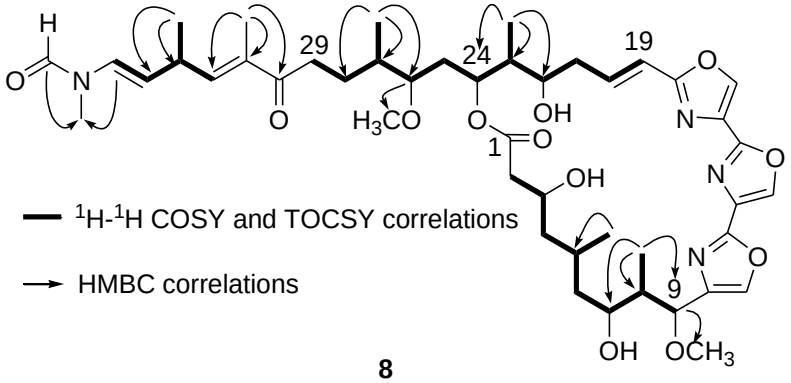

8

Figure 11. ^{1}H-^{1}H COSY, TOCSY, and HMBC correlations of kabiramide L (**8**).

Table 7. ^{13}C chemical shifts of kabiramide G (**3**), J (**4**), K (**7**), and L (**8**)

Position	δ_C[a]			
	3	**4**	**7**	**8**
1	171.7	171.6	172.7	174.2
2	43.7	43.4	45.5	45.9
3	70.0	71.3	67.5	68.1

Table 7. (cont.)

Position	δ_C [a]			
	3	**4**	**7**	**8**
4	45.4	45.7	44.0	45.5
5	25.3	25.6	25.0	26.4
6	43.9	43.4	45.1	44.6
7	73.2	73.3	71.2	72.5
8	38.5	38.6	43.1	42.4
9	78.6	78.3	80.1	80.0
10	142.7	142.8	140.2	141.3
11	135.6	135.6	137.0	135.7
12	155.7	155.7	155.8	156.1
13	131.4	131.4	131.2	131.5
14	136.6	137.0	137.0	137.3
15	156.4	156.5	156.5	157.0
16	130.1	130.0	131.1	129.1
17	136.9	136.7	137.0	134.8
18	163.5	164.1	163.1	163.9
19	114.8	114.9	116.0	115.8
20	143.9	147.0	142.6	139.3
21	34.7	38.4	34.1	38.9
22	78.7	68.3	78.6	69.1
23	41.5	43.39	40.6	42.9
24	74.1	74.2	72.7	74.1
25	33.7	35.1	33.6	34.6
26	82.4	82.5	82.11	82.6
27	35.0	35.2	35.0	35.5
28	27.4	27.4	27.2	27.6
29	35.7	35.7	35.7	36.1

Table 7. (cont.)

Position	δ_C [a]			
	3	**4**	**7**	**8**
30	200.9	201.0	200.8	201.2
31	135.9	136.0	135.9	136.5
32	144.1	144.0	143.8	144.3
33	34.5	34.5	34.7	34.9
34	111.7	111.7	111.6	111.9
35	128.6	128.6	130.2	128.7

Note: [a]Only the chemical shifts of major conformers were compared.

The identical ^{1}H and ^{13}C NMR spectra between **7** and **8** also allowed the configuration of **8** to be proposed in the same manner to that for **7**. The same magnitude in the coupling constants, suggested that **8** possessed the same configurations as that of **7**.

3.1.2.4 Kabiramide B (1)

Compound **1** was obtained as a white solid (99 mg, 7.6% w/w dry sponge). Suggested by the $[M+Na]^+$ peak in ESI mass spectrum at *m/z* 950.0, the molecular formula was purposed to be $C_{47}H_{69}N_5O_{14}$. The resulting unsaturation degree of 16 was identified to be five olefins, seven carbonyl/imines, and four rings. The UV spectrum with λ_{max} 252 nm (log ε 5.19) indicated the oxazole structure common to **4**, **7**, and **8**. The IR absorption bands at ν_{max} 3600-3250 (br) indicated the hydroxy group and the bands for carbonyls did the carbamate (ν_{max} 3450, 3350, and 1718 cm^{-1}), lactone (ν_{max} 1730 cm^{-1}), ketone (ν_{max} 1690 cm^{-1}), and formamide (ν_{max} 1659 cm^{-1}) functionalities.

The ^{1}H and ^{13}C NMR spectra of **1** (Figures 12 and 13, Table 8) were almost identical to **4**, indicating that both possessed similar core skeleton. Thirty-two mass unit difference between **1** and **4** was coherent with the absence of the 30-enone formerly observed in **4**

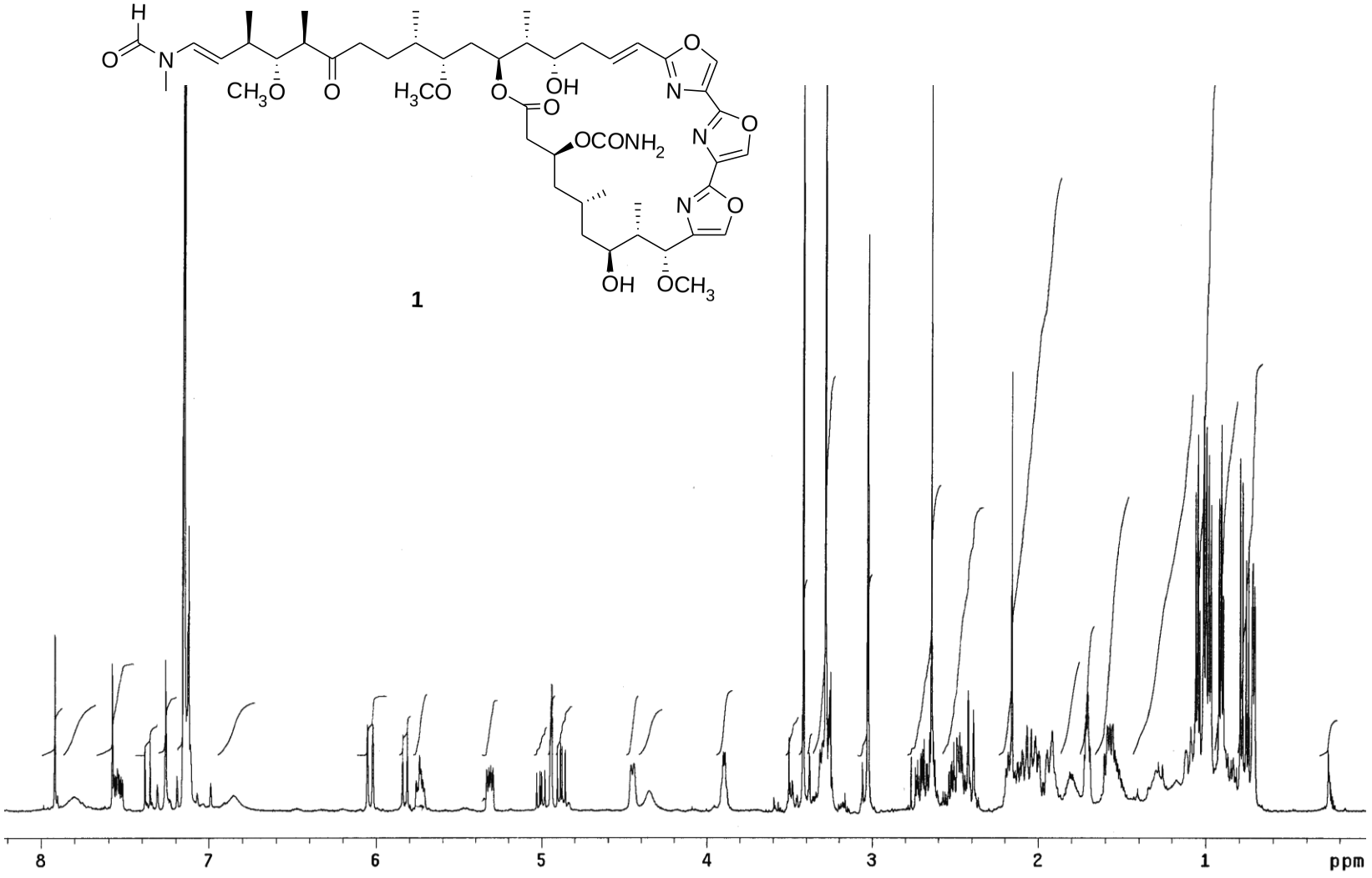

Figure 12. ^{1}H NMR spectrum of kabiramide B (**1**) (500 MHz, C_6D_6).

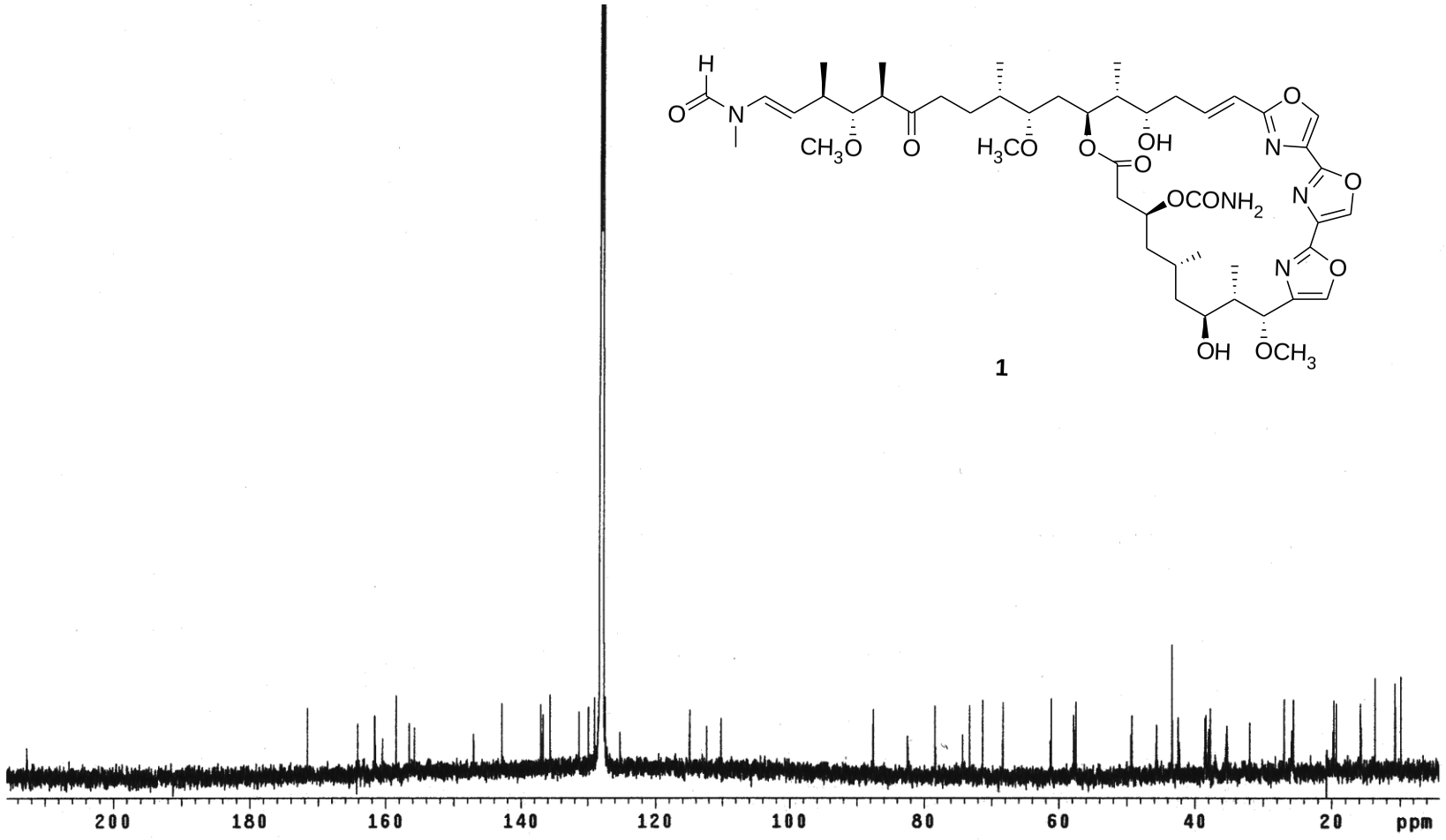

Figure 13. ^{13}C NMR spectrum of kabiramide B (**1**) (125 MHz, C_6D_6).

and the presence of methoxy group (δ_H 3.28, s; δ_C 61.0, 32-OCH_3) proposed to substitute on C-32 (δ 87.6). Based on the analyses of the ^{1}H-^{1}H COSY and HMBC correlations (Figure 14), **1** is proposed to be the known kabiramide B. This was confirmed by a comparison with reported data (Matsunaga et al., 1989), in which the comparable optical rotation ($[\alpha]_D$ +4 *c* 0.6, $CHCl_3$; lit. ($[\alpha]_D$ +8 *c* 0.1, $CHCl_3$) also indicated the same configuration as to that reported therein.

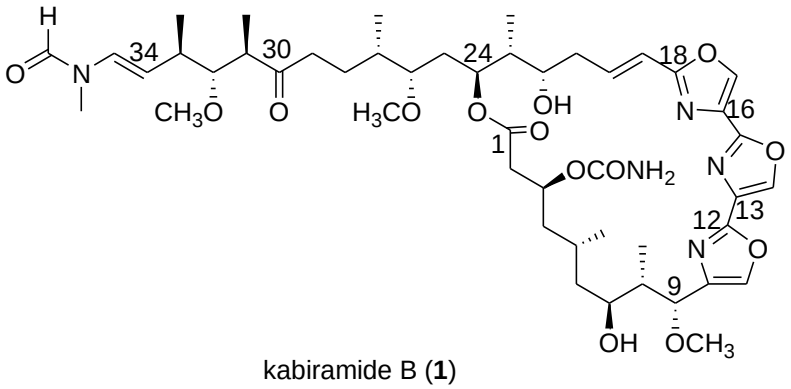

kabiramide B (**1**)

Table 8. ^{1}H and ^{13}C NMR data of kabiramide C (**1**) (500 MHz for ^{1}H and 125 MHz for ^{13}C, C_6D_6)[a]

Position	δ_C	δ_H (*J* in Hz)[b]
1	171.6, C	-
2	43.4, CH_2	2.73, m; 2.47, dd (6.0, 2.0)
3	71.3, CH	5.31, br dd (12.0, 6.5)
4	45.7, CH_2	2.07, m; 1.11, m
5	25.6, CH	1.92, m
6	43.4, CH_2	1.70, m, 2H
7	73.3, CH	3.89, d (5.5)
8	38.5, CH	2.18, dd (6.5, 6.0)
9	78.3, CH	4.94, br s
10	142.8, C	-
11	135.6, CH	7.12, s
12	155.7, C	-
13	131.4, C	-

Table 8. (cont.)

Position	δ_C	δ_H (J in Hz)[b]
14	137.0, CH	7.26, s
15	156.5, C	-
16	129.9, C	-
17	136.7, CH	7.14, s
18	164.1, C	-
19	114.9, CH	6.02, d (16.5)
20	147.0, CH	7.55, ddd (15.5, 10.0, 5.5)
21	38.4, CH_2	2.45, ddd (6.5, 6.0, 2.5); 1.94, m
22	68.3, CH	4.50, br d (9.0)
23	43.3, CH	1.50, m
24	74.3, CH	5.74, ddd (10.0, 10.0, 4.5)
25	35.3, CH_2	2.00, ddd (9.5, 2.5, 2.5);
		1.57, ddd (8.6, 6. 7, 2.3)
26	82.4, CH	3.30, dd (6.0, 3.0)
27	35.3, CH	1.80, m
28	25.7, CH_2	2.11, m; 1.53, m
29	42.3, CH_2	2.50, m; 2.42, m
30	212.9, C	-
31	49.1 [49.2], C	2.67, dd (9.0, 7.0)
32	87.6, CH	3.31, dd (9.0, 3.0)
33	37.7 [38.0], CH	2.04 [2.13], m
34	110.2 [112.4], CH	4.87 [5.00], dd (14.1, 9.5)
35	129.1 [125.3], CH	5.82 [7.36], d (14.1)
3-$OCONH_2$	158.5, C	-
5-CH_3	19.3, CH_3	0.71, d (6.0, 3H)
8-CH_3	10.7, CH_3	0.97, d (7.1; 3H)
9-OCH_3	57.4, CH_3	3.02, s, 3H

Table 8. (cont.)

Position	δ_C	δ_H (J in Hz)[b]
23-CH_3	9.9, CH_3	1.05, d (7.1; 3H)
26-OCH_3	57.8, CH_3	3.42, s, 3H
27-CH_3	15.8 [15.7], CH_3	0.91, d (6.5; 3H)
31-CH_3	13.7, CH_3	0.78 [0.75], d (7.0; 3H)
32-OCH_3	61.0, CH_3	3.28 [3.29], s, 3H
33-CH_3	19.7 [19.8], CH_3	1.01 [1.02], d (6.8; 3H)
35-NCH_3	26.9 [32.0], CH_3	2.64 [2.16], s, 3H
35-NCHO	161.6[160.5], CH	7.92 [7.58], s

Note: [a]Chemical shifts of the minor conformers are presented in brackets. [b]Unless stated otherwise, each proton signal was integrated as 1 proton.

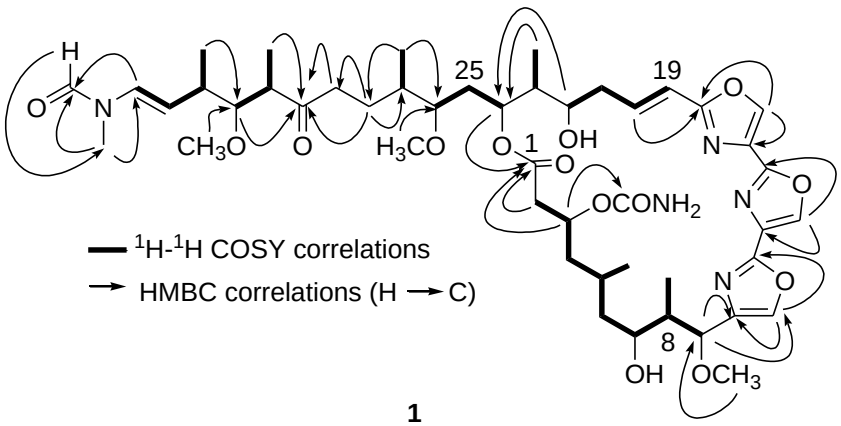

1

Figure 14. ^{1}H-^{1}H COSY and key HMBC correlations of kabiramide B (**1**).

3.1.2.5 Kabiramide C (2)

Compound **2** was isolated as white solid (295 mg, 22.6% w/w dry sponge). Molecular formula of compound **2** was established as $C_{48}H_{71}N_5O_{14}$ on the basis of $[M+Na]^+$ peak at *m/z* 963.9 in the ESI mass spectrum. The unsaturation degree of 16 was deduced to be five olefins, seven carbonyls/imines, and four rings similar to **1**. Also similar to **1** were the presences

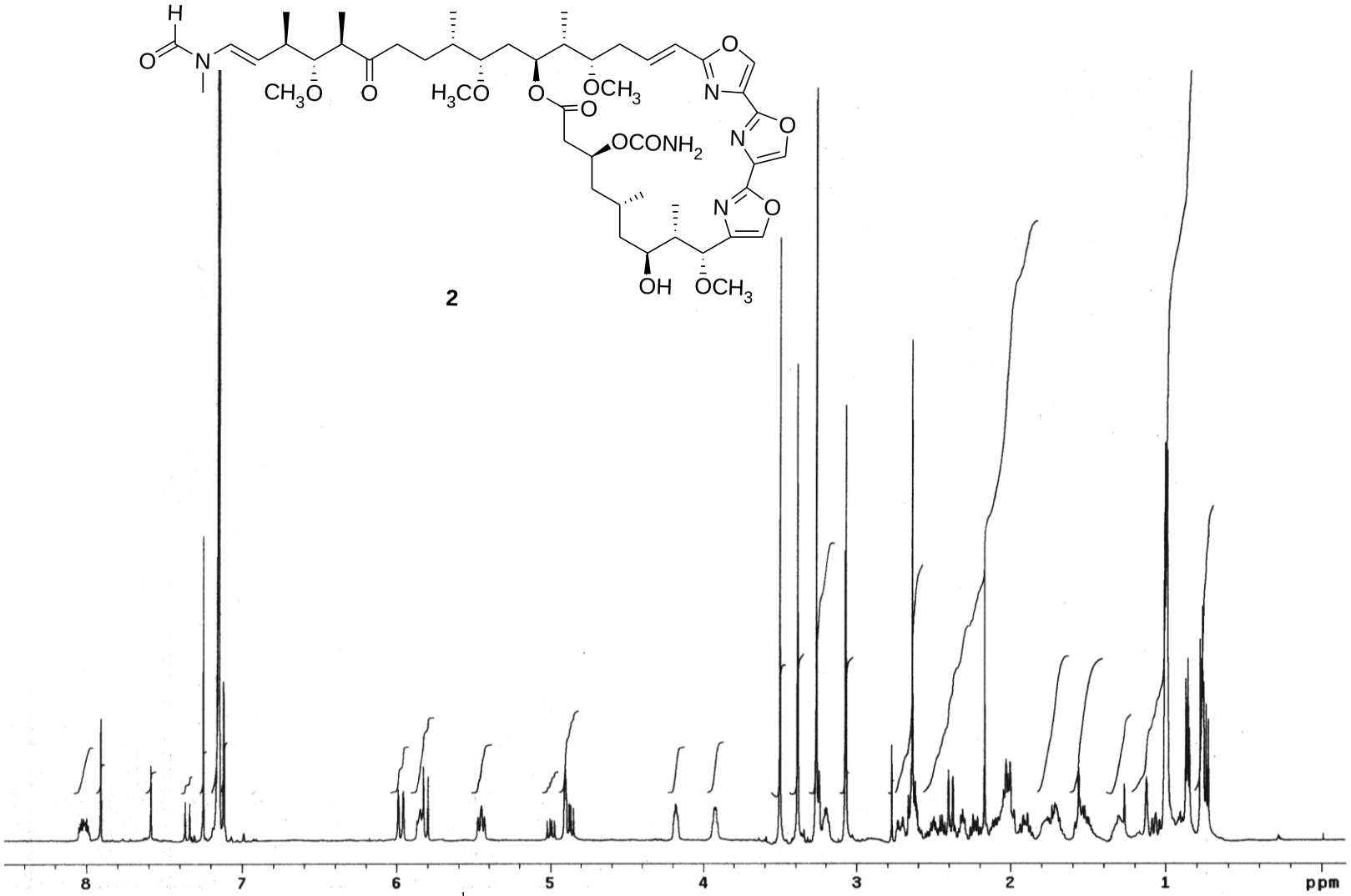

Figure 15. ^{1}H NMR spectrum of kabiamide C (**2**) (500 MHz, C_6D_6).

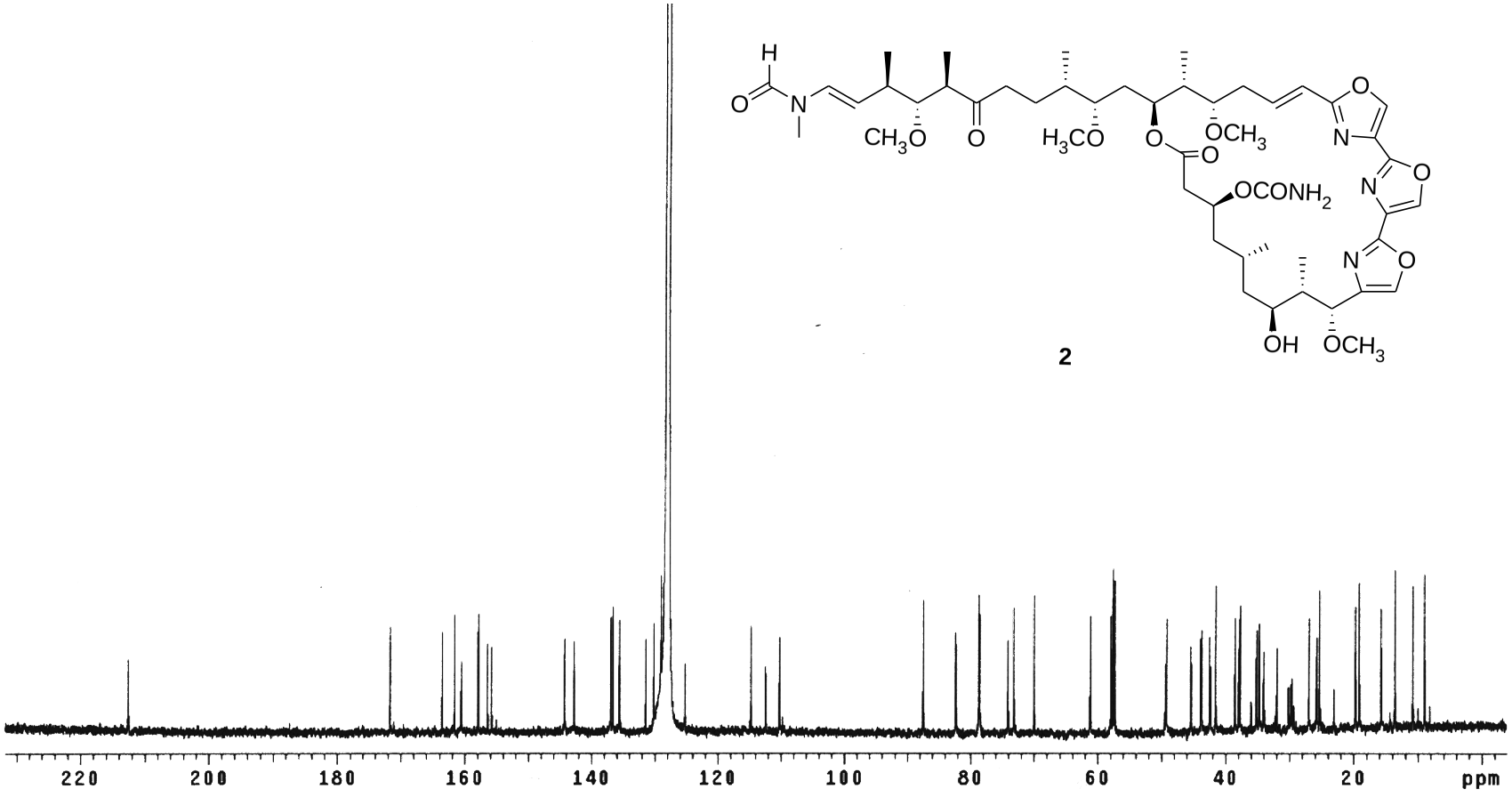

Figure 16. ^{1}H NMR spectrum of kabiramide C (**2**) (125 MHz, C_6D_6).

of the carbamate (ν_{max} 3450, 3350, 1720 cm^{-1}), hydroxy (3600-3250 cm^{-1}), lactone (1725 cm^{-1}), ketone (1698 cm^{-1}), and formamide (1650 cm^{-1}) functional groups as indicated by IR absorption bands. The presence of trisoxazole moiety was supported by UV absorption at λ_{max} 252 nm (log ε 5.02).

The ^{1}H and ^{13}C NMR spectra of **2** (Figures 15 and 16) were almost identical to that of **1** except for an additional methoxy group as indicated by the signal at δ_H 3.50 (s). This methoxy group was proposed to replace 22-OH in **1**, according to HMBC correlations from 22-OCH_3 to C-22 (δ 78.7). The remaining parts in the chemical structure of **2** were furnished according to the ^{1}H-^{1}H COSY and HMBC spectral analyses (Figure 17), and to the comparison with published report. **2** was therefore proposed to be a known kabiramide analog, kabiramide C (Matsunaga et al., 1986, 1989). The configuration of **2** as shown was confirmed by the comparable specific rotation to that reported by Matsunaga et al. (1986) ($[\alpha]_D$ +10 *c* 0.6, $CHCl_3$; lit. $[\alpha]_D$ +20 *c* 0.1, $CHCl_3$).

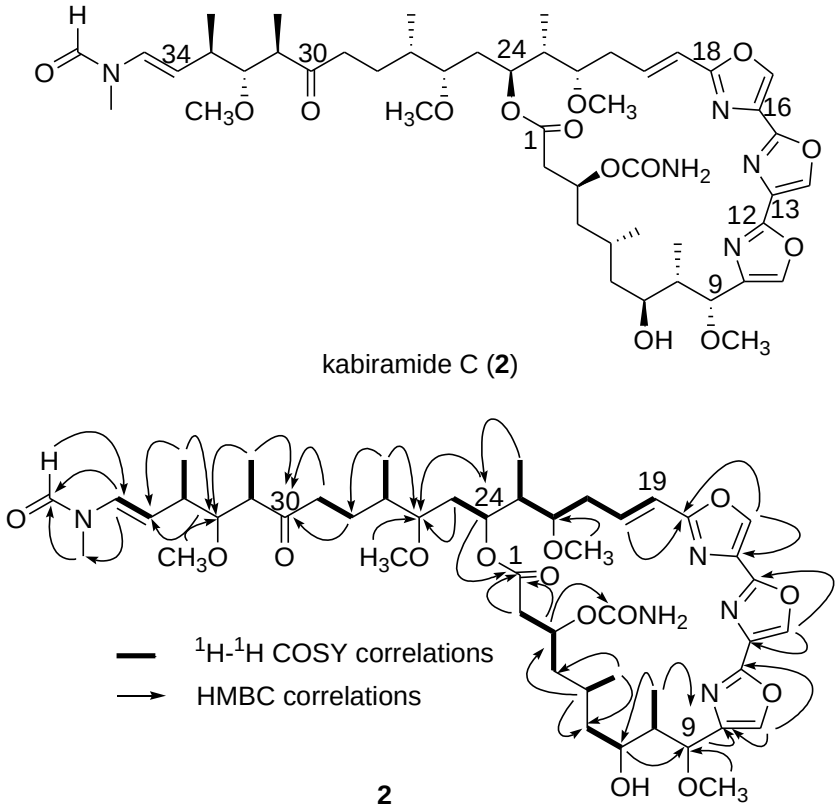

Figure 17. ^{1}H-^{1}H COSY and key HMBC correlations of kabiramide C (**2**).

Table 9. ^{1}H and ^{13}C NMR data of kabiramide C (**2**) (500 MHz for ^{1}H and 125 MHz for ^{13}C, C_6D_6)[a]

Position	δ_C	δ_H (*J* in Hz)[b]
1	171.7, C	-
2	43.8, CH_2	2.63, overlapped; 2.39, br d (14.5)
3	70.0, CH	5.45, br dd (10.0, 10.0)
4	45.4, CH_2	1.99, overlapped; 1.06, dd (11.7, 10.0)
5	25.3, CH	2.11, overlapped
6	43.7, CH_2	1.72, overlapped; 1.70, overlapped
7	73.2, CH	3.93, dt (7.5, 3.5)
8	38.5, CH	2.32, overlapped
9	78.6, CH	4.90, br s
10	142.8, C	-
11	135.6, CH	7.12, s
12	156.4, C	-
13	130.1, C	-
14	136.9, CH	7.25, s
15	157.9, C	-
16	129.0, C	-
17	136.5, CH	7.15, s
18	163.5, C	-
19	114.8, CH	5.96, d (16.0)
20	144.2, CH	8.01, ddd (16.0, 9.1, 5.1)
21	34.7, CH_2	2.71, dddd (15.9, 5.1, 4.9, 2.4);
		2.23, ddd (15.9, 9.6, 9.1)
22	78.7, CH	4.18, ddd (9.6, 4.9. 2.9)
23	41.5, CH	2.10, overlapped
24	74.1, CH	5.85, m
25	33.9, CH_2	1.91, ddd (12.5, 9.3. <1.0); 1.56, br d (12.5)

Table 9. (cont.)

Position	δ_C	δ_H (J in Hz)[b]
26	82.3, CH	3.20, ddd (9.0, 6.0, 2.5)
27	35.2, CH	1.77, m
28	25.7, CH_2	2.00, overlapped; 1.50, m
29	42.8, CH_2	2.50, ddd (19.3, 9.3, 2.9);
		2.45, ddd (19.3, 9.3, 2.9)
30	212.6, C	-
31	49.1, C	2.62 [2.65], overlapped
32	87.6 [87.5], CH	3.24, dd (9.1, 2.4)
33	37.7 [38.0], CH	2.02 [2.12], overlapped
34	110.2 [112.4], CH	4.87 [5.00], dd (14.5, 10.0)
35	129.0 [125.2], CH	5.80 [7.34], d (14.5)
3-$OCONH_2$	157.9, C	-
5-CH_3	19.1, CH_3	0.77, d (6.3; 3H)
8-CH_3	10.8, CH_3	1.00, d (6.8; 3H)
9-OCH_3	57.6, CH_3	3.07 [3.08], s, 3H
22-OCH_3	57.3, CH_3	3.50, s
23-CH_3	8.9, CH_3	0.99, d (6.2; 3H)
26-OCH_3	57.8 [57.9], CH_3	3.39 [3.38], s, 3H
27-CH_3	15.8 [15.7], CH_3	0.86 [0.87], d (6.8; 3H)
31-CH_3	13.6, CH_3	0.78 [0.73], d (6.8; 3H)
32-OCH_3	61.1 [61.2], CH_3	3.26, s, 3H
33-CH_3	19.7 [19.8], CH_3	1.01 [0.99], d (7.6; 3H)
35-NCH_3	26.9 [32.0], CH_3	2.64 [2.17], s, 3H
35-NCHO	161.6 [160.5], CH	7.91 [7.59], s

Note: [a]Chemical shifts of the minor conformers are presented in brackets. [b]Unless stated otherwise, each proton signal was integrated as 1 proton.

3.1.2.6 Kabiramide G (3)

Compound **3** was obtained as a white solid (136 mg, 10.4% w/w dry sponge). The ESIMS spectrum of **3** exhibited an $[M+Na]^+$ peak at *m/z* 931.9 indicating a molecular formula of $C_{47}H_{67}N_5O_{13}$. An unsaturation degree of 17 were deduced to be six olefinic double bonds, seven carbonyls/imines, and four rings. Absorption band in the UV spectrum at λ_{max} 236 nm (log ε 5.31) also suggested trisoxazole part. The presences of lactone, enone, and formamide functionalities were respectively indicated by the characteristic IR absorption bands at ν_{max} 1725, 1690, and 1659 cm^{-1}.

The ^1H and ^{13}C NMR spectra (Figures 18 and 19, Table 10) of **3** were comparable to those of other trisoxazole macrolides reported here, indicating a similar core skeleton. The NMR spectra of **3** were in fact the most resembled to those of **4** as a trisoxazole macrolide with a carbamate on C-2 (δ 43.7) and an enone on C-31 (δ 135.9). The major difference between **4** and **3** was the additional methoxy (δ_H 3.49, s; δ_C 57.3) group substituted on C-22 (δ 78.7) of **3**. The analysis of ^1H-^1H COSY and HMBC spectra (Figure 20) led to the proposed structure of **3** as kabiramide G, originally reported by Petchprayoon et al (2006). The configurations as shown were deduced in the same manner to those for **1**, **2**, **4**, **7**, and **8**; i.e., $[\alpha]_D$ of **3** was +27 (*c* 0.3, $CHCl_3$), lit +38 (*c* 0.4, $CHCl_3$) (Petchprayoon et al., 2006).

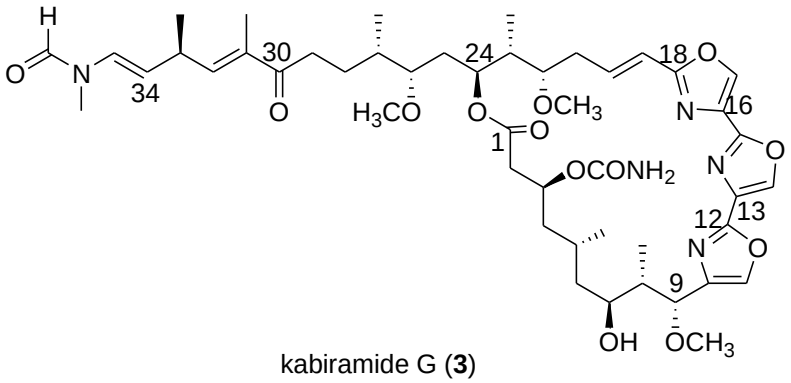

kabiramide G (**3**)

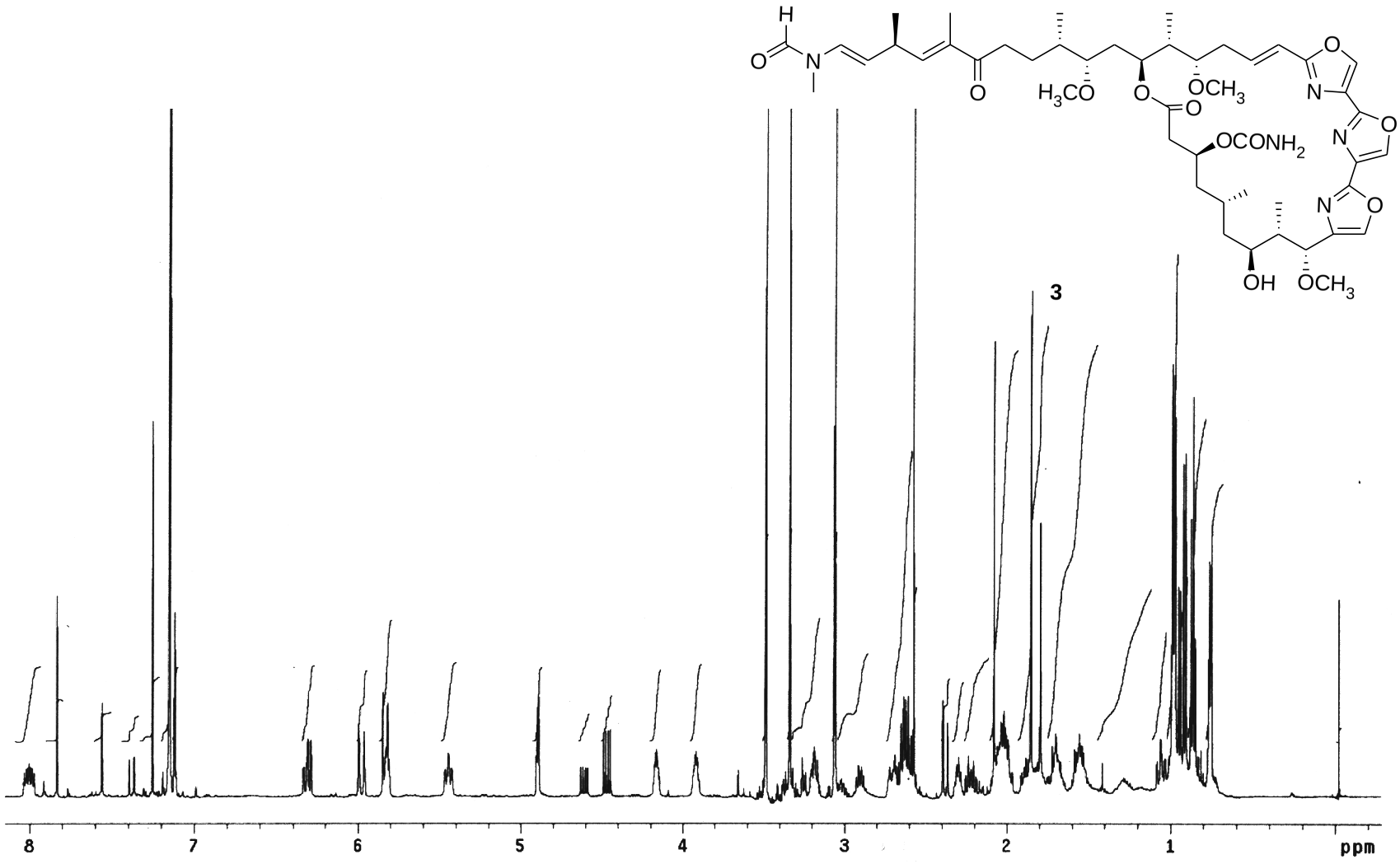

Figure 18. ^{1}H NMR spectrum of kabiramide G (**3**) (500 MHz, C_6D_6).

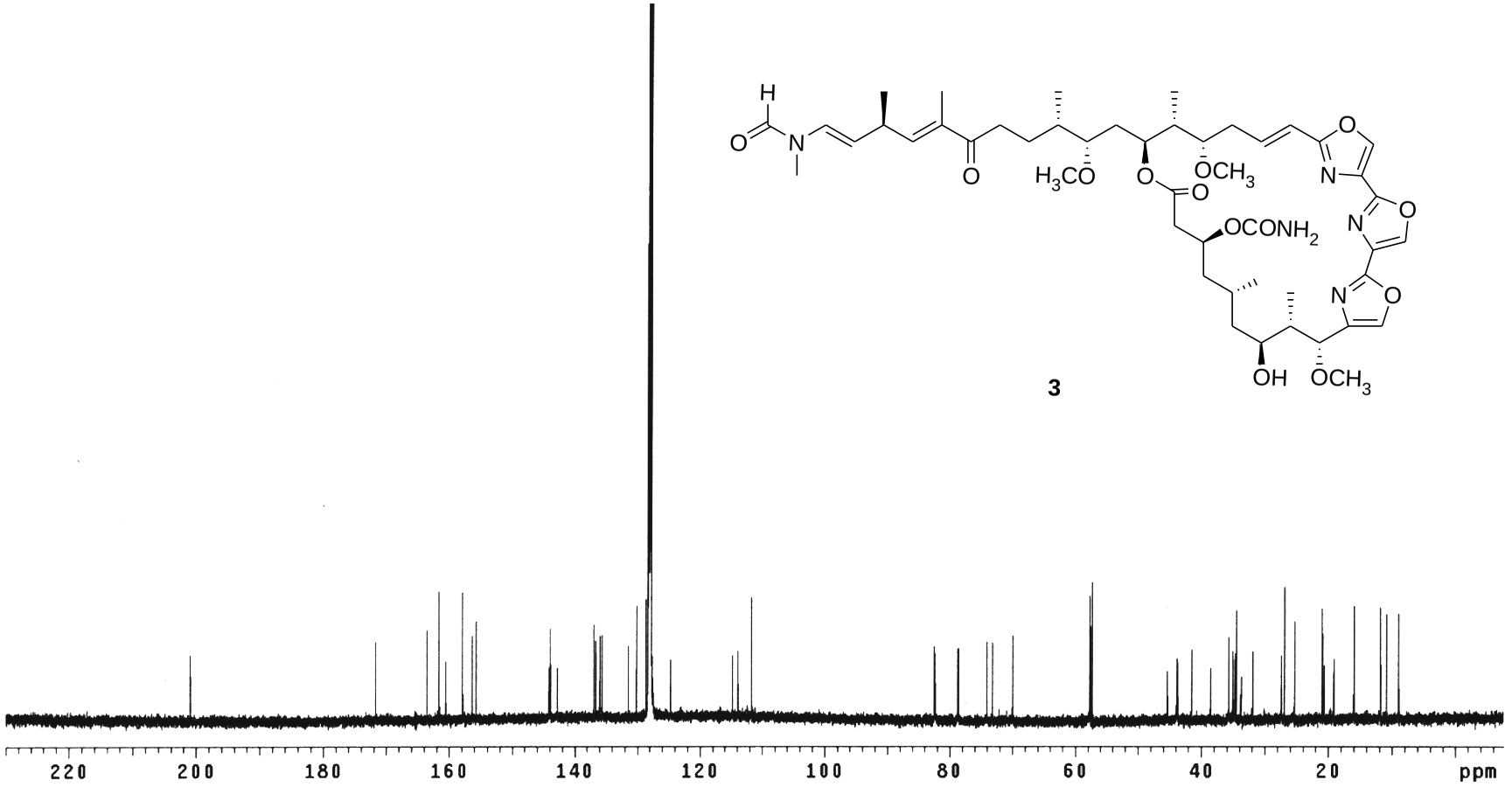

Figure 19. ^{13}C NMR spectrum of kabiramide G (**3**) (125 MHz, C_6D_6).

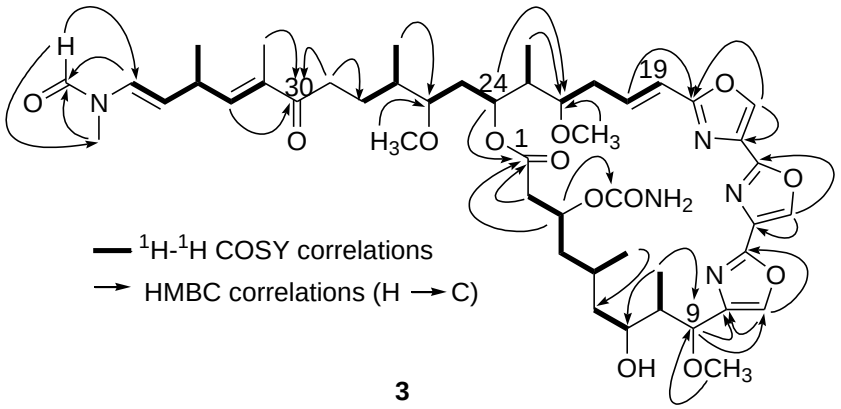

3

Figure 20. ^{1}H-^{1}H COSY and key HMBC correlations of kabiramide G (**3**).

Table 10. ^{1}H and ^{13}C NMR data of kabiramide G (**3**) (500 MHz for ^{1}H and 125 MHz for ^{13}C, C_6D_6)[a]

Position	δ_C	δ_H (*J* in Hz)[b]
1	171.7, C	-
2	43.7, CH_2	2.62, br d (14.0); 2.37, br d (14.0)
3	70.0, CH	5.45, br dd (9.6, 9.6)
4	45.4, CH_2	2.00, br d (12.8); 1.06, ddd (12.8, 9.6, 1.8)
5	25.3, CH	2.03, dd (7.0, 1.5)
6	43.9, CH_2	1.71, br dd (8.7, 4.6); 1.68, ddd (8.7, 5.9, 4.6)
7	73.2, CH	3.92, ddd (12.4, 4.6, 4.6)
8	38.5, CH	2.30, dqd (12.4, 6.2, 1.3)
9	78.6, CH	4.89 [4.90], d (1.3)
10	142.7, C	-
11	135.6, CH	7.12, s
12	155.7, C	-
13	131.4, C	-
14	136.6, CH	7.25, s
15	156.4, C	-
16	130.1, C	-

Table 10. (cont.)

Position	δ_C	δ_H (J in Hz)[b]
17	136.9, CH	7.15, s
18	163.5, C	-
19	114.8, CH	5.98, br d (16.0)
20	143.9, CH	8.00, dddd (16.0, 9.2, 5.5, 2.3)
21	34.7, CH_2	2.70, ddd (15.3, 5.5, 1.8); 2.22, ddd (15.3, 10.1, 9.2)
22	78.7, CH	4.16, ddd (10.1, 4.6, 2.8)
23	41.5, CH	2.02, br d (7.3, 3.0)
24	74.1, CH	5.82, ddd (9.4, 4.8, 1.8)
25	33.7, CH_2	1.89, ddd (15.3, 9.4, 1.8); 1.58, br dd (15.3, 4.8)
26	82.4, CH	3.19, m
27	35.0, CH	2.60, br d (8.7)
28	27.4, CH_2	1.82, m; 1.54, m
29	35.7, CH_2	2.65, dd (8.0, 7.3); 2.59, dd (8.7, 8.0)
30	200.9, C	-
31	135.9, C	-
32	144.1 [144.2], CH	6.30 [6.32], dq (8.1, 1.4)
33	34.5 [34.6], CH	2.90 [3.01], ddq (8.1, 7.2, 6.6)
34	111.7 [113.9], CH	4.46 [4.60], dd (14.4, 7.2)
35	128.6 [124.7], CH	5.83 [7.38], d (14.4)
3-$OCONH_2$	157.9, C	-
5-CH_3	19.1, CH_3	0.76 [0.77], d (6.7; 3H)
8-CH_3	10.9, CH_3	0.99, d (6.2; 3H)
9-OCH_3	57.6, CH_3	3.06 [3.07], s; 3H
22-OCH_3	57.3, CH_3	3.49, s
23-CH_3	9.0, CH_3	0.98, d (7.3; 3H)
26-OCH_3	57.7, CH_3	3.34, s, 3H
27-CH_3	16.0, CH_3	0.87 [0.86], d (7.0; 3H)

Table 10. (cont.)

Position	δ_C	δ_H (J in Hz)[b]
31-CH_3	11.8 [11.7], CH_3	1.85 [1.79], d (1.4, 3H)
33-CH_3	20.9 [20.6], CH_3	0.91 [0.95], d (6.6, 3H)
35-NCH_3	26.9 [33.7], CH_3	2.57 [2.08], s, 3H
35-NCHO	161.7 [160.5], CH	7.83 [7.56], s

Note: [a]Chemical shifts of the minor conformers are presented in brackets. [b]Unless stated otherwise, each proton signal was integrated as 1 proton.

3.1.2.7 Kabiramide I (5)

Compound **5** was obtained as a white solid (2 mg, 0.4% w/w dry sponge). The pseudomolecular masses $[M+Na]^+$ and $[M+K]^+$ in ESI mass spectrum at *m/z* 968.6 and 984.6 respectively indicated a molecular formula of $C_{47}H_{71}N_5O_{15}$. An unsaturation degree of 15 were deduced to be four olefinic double bonds, eight carbonyls/imines, and three rings. The UV absorption band at 248 nm (log ε1.67) indicated oxazole moiety. The cluster carbonyl functional groups were clarified as lactone (ν_{max} 1730 cm^{-1}), carbamate (ν_{max} 3450, 3350, and 1720 cm^{-1}), imide (ν_{max} 1710, 1680 cm^{-1}), and formamide (ν_{max} 1670 cm^{-1}) moieties according to the IR spectrum.

Due to the limited amount of **5**, only ^1H and ^{13}C NMR spectra of **5** were obtained (500 MHz for ^1H, $CDCl_3$; 150 MHz for ^{13}C, C_6D_6; Figures 21 and 22). Extended 2D NMR experiments were attempted; however no analyzable correlations were detected. The identification of **5** was carried out here based on the ^1H NMR spectral analysis. Among ^1H NMR spectra of all macrolides reported earlier, the spectrum of **5** was closely related that of **2** except for one missing signal of oxazole. An additional imide moiety was proposed to connected C-9 and C-13. Directly comparison to imide-containing trisoxazole macrolide, ^1H chemical shifts and coupling constants of **5** agree well with the reported kabiramide I (Table 11; Petchprayoon et al., 2006). Therefore, structure of **5** was proposed as kabiramide I with similar relative configuration according to ^1H-^1H coupling constants.

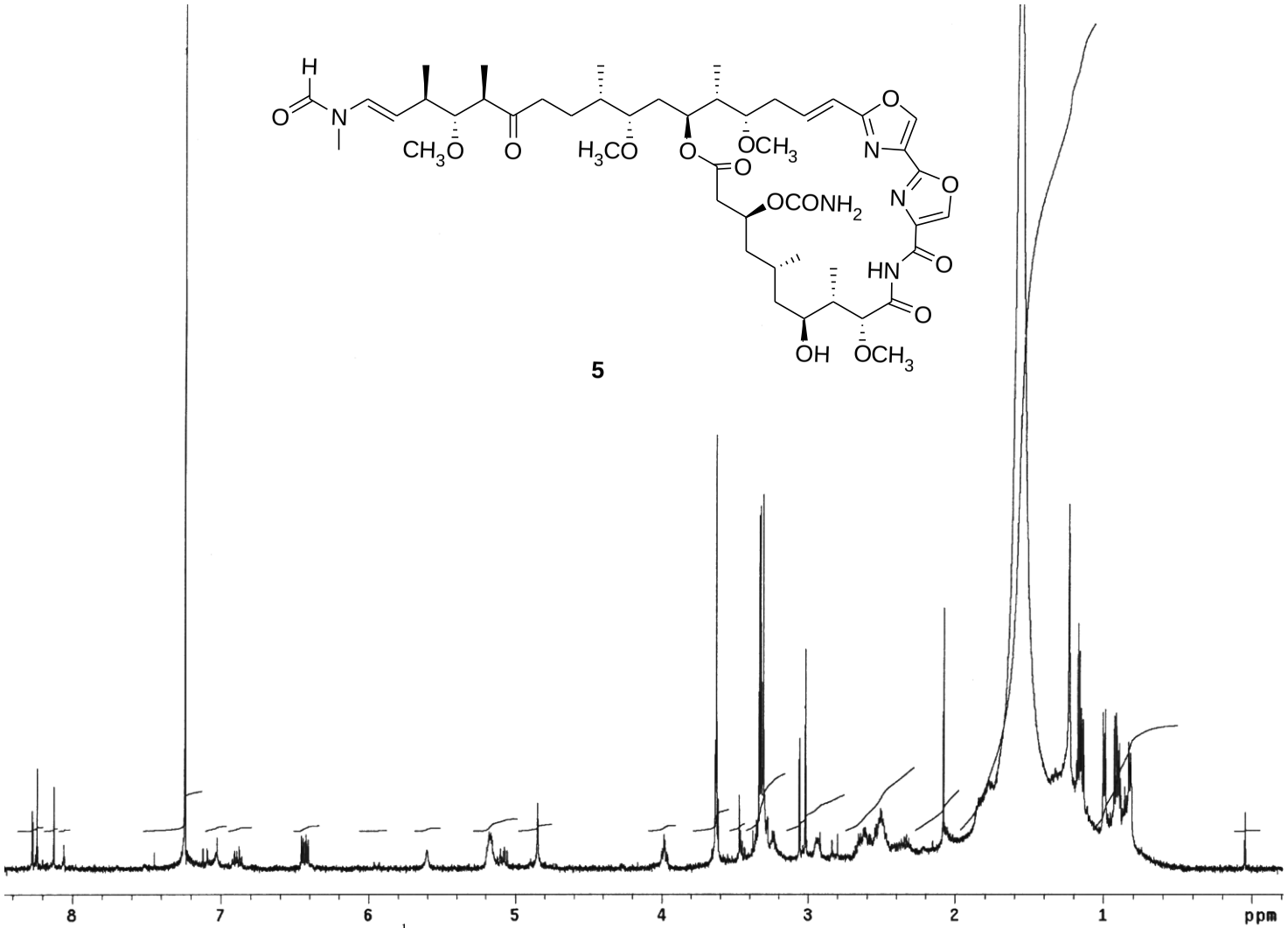

Figure 21. ^{1}H NMR spectrum of kabiramide I (**5**) (500 MHz, $CDCl_3$).

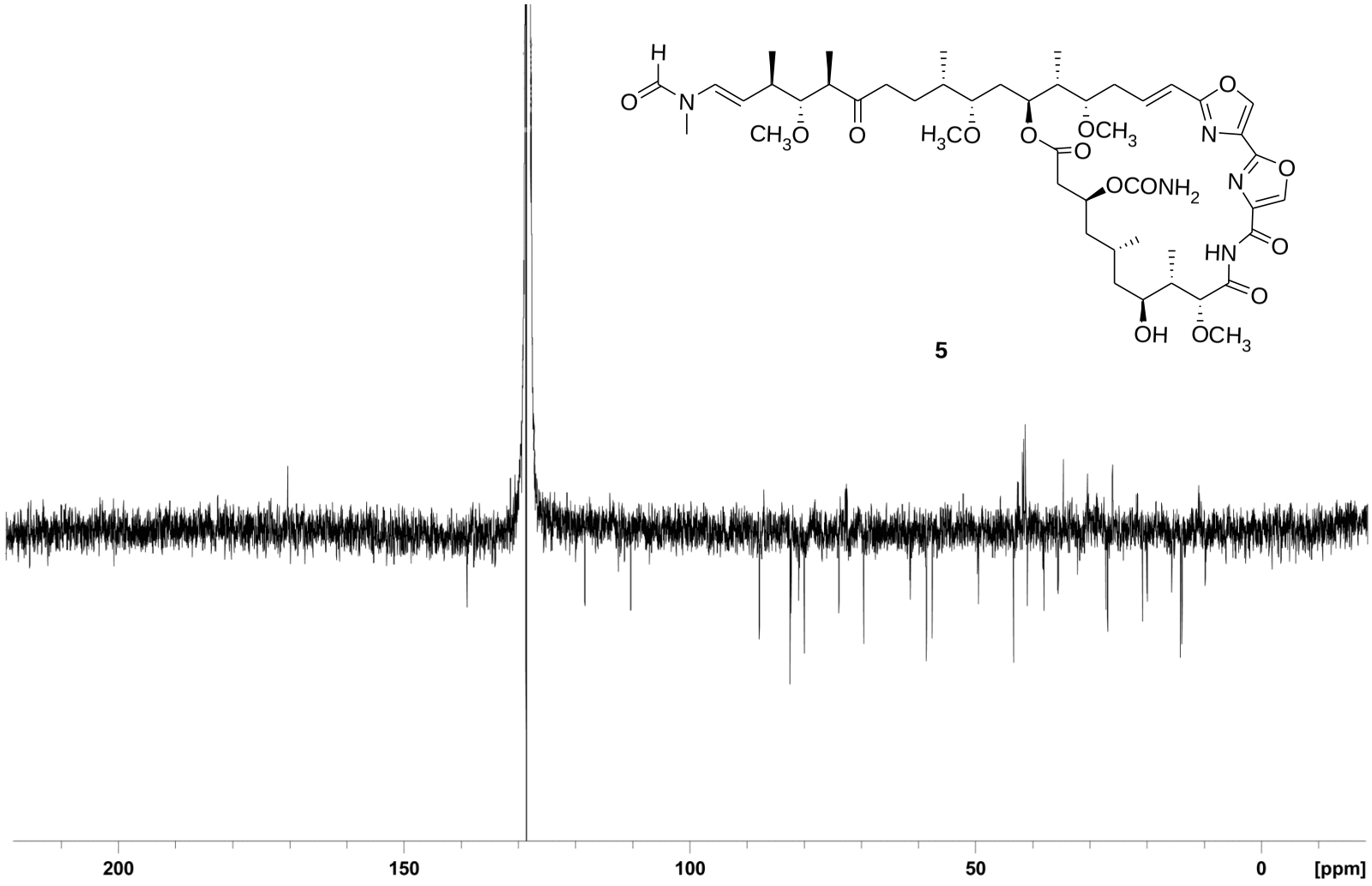

Figure 22. J-MOD NMR spectrum of kabiramide I (**5**) (150 MHz, C_6D_6); CH_3 and CH (negative); CH_2 and C (positive).

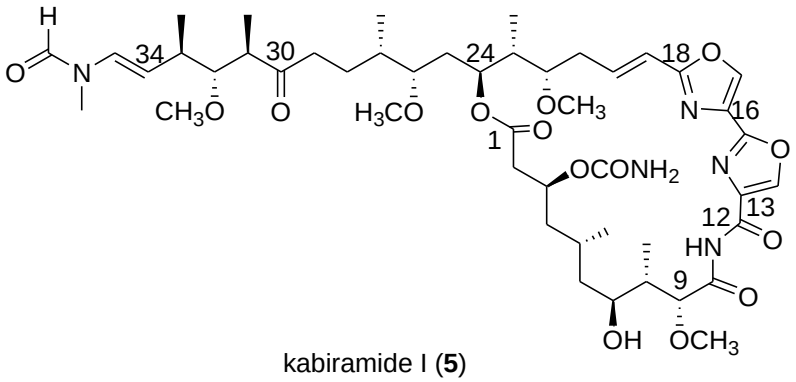

kabiramide I (**5**)

Table 11. ^{1}H and ^{13}C NMR data of kabiramide I (**5**) (500 MHz for ^{1}H, $CDCl_3$ and 150 MHz for ^{13}C, C_6D_6)[a]

Position	δ_C	δ_H (*J* in Hz)[b]
1	170.0, C	-
2	41.1, CH_2	2.58, overlapped;
		2.65, overlapped
3	69.3, CH	5.18, overlapped
4	41.3, CH_2	1.35, overlapped;
		1.80, overlapped
5	26.6, CH	1.78, overlapped
6	41.5, CH_2	1.55, overlapped;
		1.65, overlapped
7	79.7, CH	3.98, td (9.0, 2.5)
8	43.1, CH	2.07, m
9	82.2, CH	3.62, d (11.0)
10	174.2, C	-
11	-	-
12	162.1 C	-
13	136.6, C	-
14	141.5, CH	8.24, s
15	156.3, C	-

Table 11. (cont.)

Position	δ_C	δ_H (J in Hz)[b]
16	131.1, C	-
17	138.6, CH	8.12, s
18	162.3, C	-
19	118.0 CH	6.42 , d (16.3)
20	138.7, CH	6.89, dt (16.3, 7.5)
21	34.4, CH_2	2.51, overlapped;
		2.61, overlapped
22	80.7, CH	3.23, br d (5.5)
23	40.7, CH	1.85, overlapped
24	73.7, CH	5.16, overlapped
25	32.8, CH_2	1.35, overlapped;
		1.57, overlapped
26	82.0, CH	2.95, m
27	35.3, CH	1.71, overlapped
28	25.8, CH_2	1.25, overlapped;
		1.78, overlapped
29	42.3, CH_2	2.54, m, 2H
30	212.9, C	-
31	49.2 [49.4], C	2.66, overlapped
32	87.5 [87.6], CH	3.30, overlapped
33	37.8 [37.9], CH	2.35 [2.36], m
34	110.0 [112.3], CH	5.08 [5.10], dd (13.7, 9.5)
35	129.1 [125.2], CH	7.10 [6.43], d (13.7)
3-$OCONH_2$	159.0, C	-
5-CH_3	20.5, CH_3	1.00, d (6.5; 3H)
8-CH_3	13.9, CH_3	1.17, d (5.5; 3H)
9-OCH_3	58.4, CH_3	3.63, s, 3H

Table 11. (cont.)

Position	δ_C	δ_H (*J* in Hz)[b]
22-OCH_3	57.4, CH_3	3.33, s, 3H
23-CH_3	9.6, CH_3	0.92, d (7.0; 3H)
26-OCH_3	58.3, CH_3	3.31, s, 3H
27-CH_3	15.5, CH_3	0.82, d (7.0; 3H)
31-CH_3	13.7, CH_3	0.90, d (4.0; 3H)
32-OCH_3	61.1 [61.2], CH_3	3.32, s, 3H
33-CH_3	19.7 [19.8]	1.14, d (7.0; 3H)
35-NCH_3	26.9 [31.9], CH_3	3.02 [3.06], s,3H
35-NCHO	161.0 [160.6], CH	8.05 [8.26], s

Note: [a]Chemical shifts of the minor conformers are presented in brackets. [b]Unless stated otherwise, each proton signal was integrated as 1 proton.

3.1.2.8 Kabiramide D (6)

Compound **6** was obtained as a white solid (3 mg, 0.6% w/w dry sponge). A molecular formula of $C_{47}H_{70}N_4O_{13}$ was proposed on the basis of the ESI mass spectrum *m/z* 921.5 ($[M+Na]^+$). The molecular formula yielded an unsaturation degree of 15, accounted for five olefinic double bonds, six carbonyls/imines, and four rings. The carbonyl carbons were deduced to be lactone, ketone, and formamide moieties according to IR absorption bands at ν_{max} 1735, 1690, and 1659 cm^{-1}, respectively.

The identical ^1H and ^{13}C NMR spectra of **6** (Figures 23 and 24, Table 12) to those of **1**-**5**, **7**, and **8** are again prominent. Specifically, **6** was the most closely related to **7**, as trisoxazole macrolide derivatives with an hydroxy group on C-3 (δ 67.5) and methoxy (δ 3.44, s) on C-22 (δ 78.9). The major differences between **6** and **7** were the lack of the enone moiety and the presence of a methoxy (δ_H 3.23, s; δ_C 61.1) on C-32 (δ 87.5). The thorough analysis of the ^1H-^1H COSY and HMBC spectra (Figure 25) indicated that **6** was another member of kabiramide, kabiramide D. The compound was previously reported by Matsunaga et al (1989).

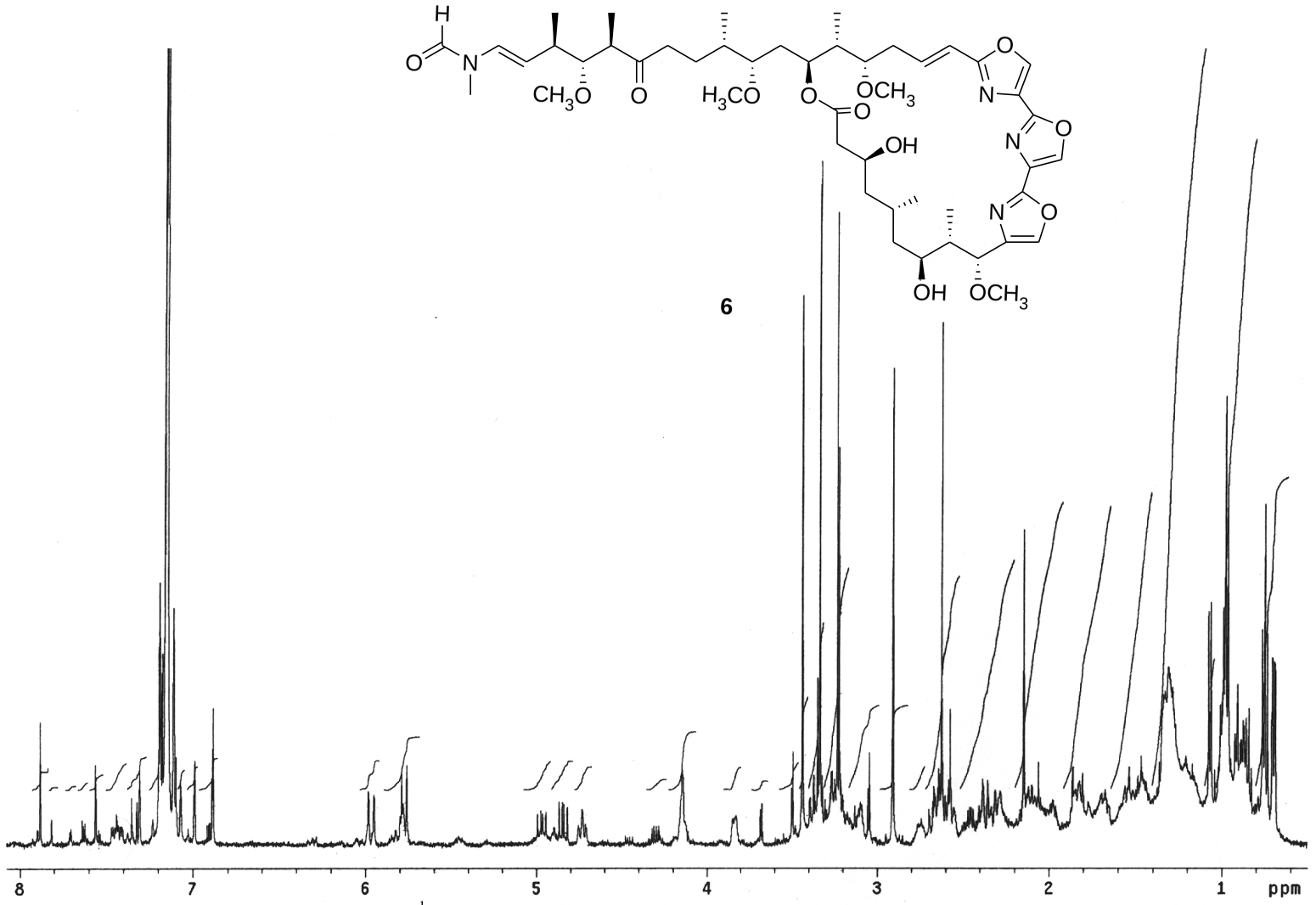

Figure 23. ^{1}H NMR spectrum of kabiramide D (**6**) (500 MHz, C_6D_6).

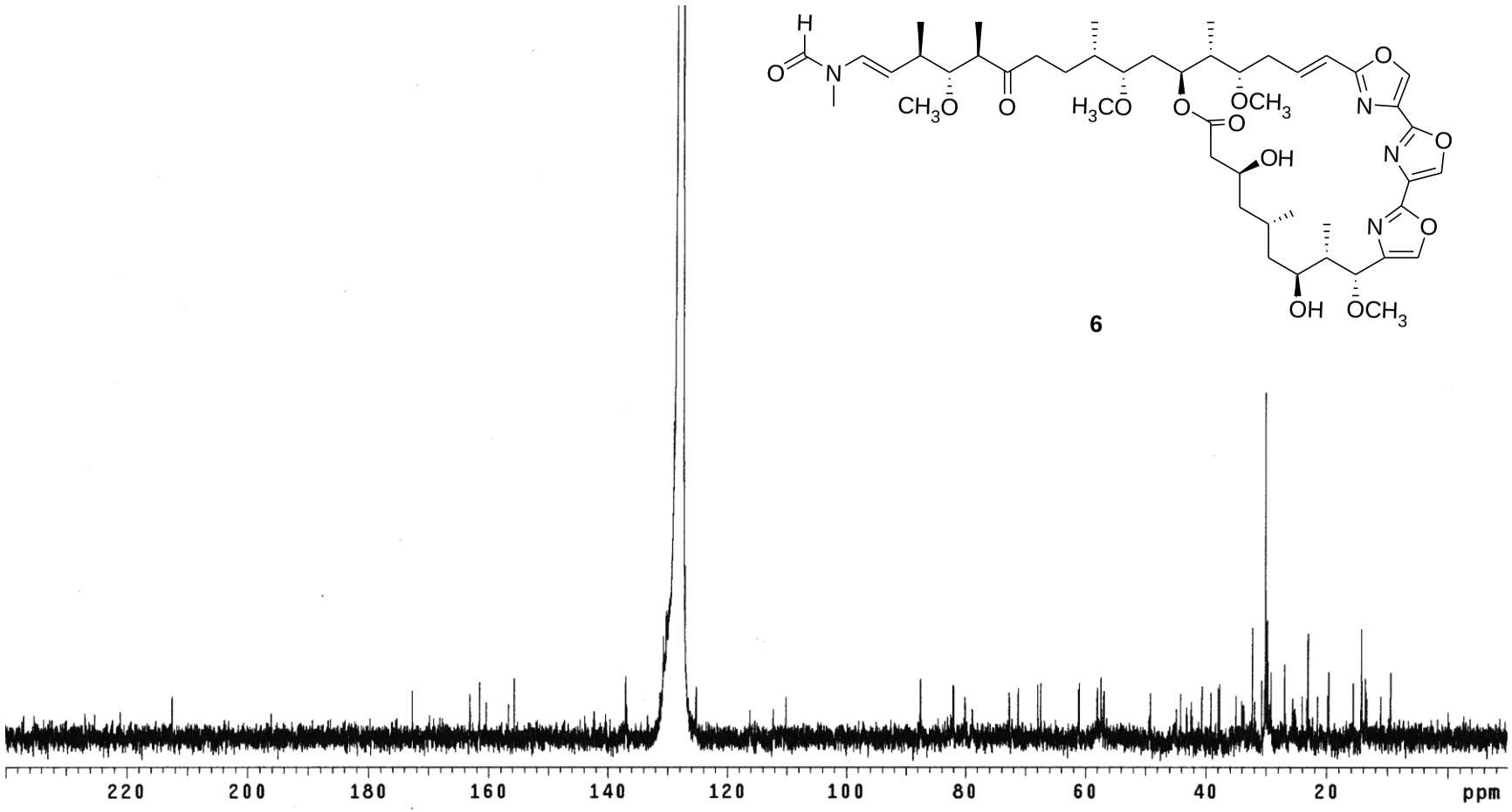

Figure 24. ^{13}C NMR spectrum of kabiramide D (**6**) (125 MHz, C_6D_6).

The configuration of **6** was proposed to be as shown due to the comparable specific rotation ($[\alpha]_D$ -11 *c* 0.2, $CHCl_3$; lit. $[\alpha]_D$ -5 *c* 0.1, $CHCl_3$).

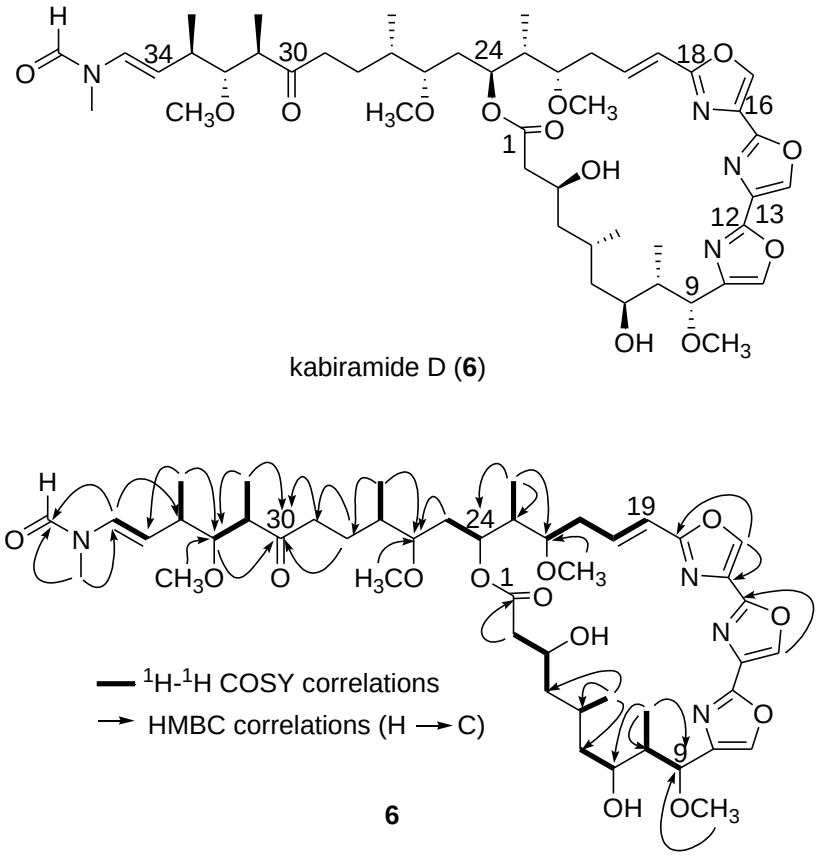

Figure 25. ^{1}H-^{1}H COSY and key HMBC correlations of kabiramide D (**6**).

Table 12. ^{1}H and ^{13}C NMR data of kabiramide D (**6**) (500 MHz for ^{1}H and 125 MHz for ^{13}C, C_6D_6)[a]

Position	δ_C	δ_H (*J* in Hz)[b]
1	172.6, C	-
2	42.4, CH_2	2.40, br d (14.0); 2.28, m
3	67.5, CH	4.73, br dd (11.0, 11.0)
4	44.8, CH_2	2.66, ddd (14.0, 11.0, 3.0); 2.33, m
5	25.2, CH	2.75, overlapped
6	44.1, CH_2	1.68, overlapped; 1.56, overlapped

Table 12. (cont.)

Position	δ_C	δ_H (J in Hz)[b]
7	71.2, CH	4.14, br s
8	43.2, CH	2.30, m
9	80.1, CH	4.15, br s
10	140.3, C	-
11	137.0, CH	7.10, s
12	155.7, C	-
13	131.0, C	-
14	137.0, CH	7.19, s
15	156.7, C	-
16	130.4, C	-
17	137.1, CH	7.15, s
18	163.1, C	-
19	116.2, CH	5.97, d (16.0)
20	142.2, CH	7.44, ddd (16.0, 10.0, 5.0)
21	34.1, CH_2	2.56, br d (10.3); 2.10, br d (10.3)
22	78.9, CH	3.83, br d (7.0)
23	39.1, CH	1.80, d (1.5)
24	72.6, CH	5.78, m
25	33.7, CH_2	1.82, overlapped; 1.43, overlapped
26	82.1, CH	3.10, m
27	35.0, CH	1.69, overlapped
28	25.5, CH_2	2.00, overlapped; 1.50, overlapped
29	43.1, CH_2	2.37, br d (14.0); 2.30, br d (14.0)
30	212.5, C	-
31	49.1, C	2.58, qd (7.2, 2.0)
32	87.5 [87.6], CH	3.21, m
33	37.7 [38.0], CH	1.98, m

Table 12. (cont.)

Position	δ_C	δ_H (J in Hz)[b]
34	110.1 [125.2], CH	4.84 [4.97], dd (14.5, 9.5)
35	128.9 [129.0], CH	5.77 [7.33], d (14.5)
5-CH_3	21.5, CH_3	1.06, d (6.5; 3H)
8-CH_3	13.4, CH_3	0.70, d (7.0; 3H)
9-OCH_3	56.9, CH_3	2.91, s, 3H
22-OCH_3	57.4, CH_3	3.44, s
23-CH_3	9.5, CH_3	0.97, d (7.0; 3H)
26-OCH_3	58.0, CH_3	3.34, s, 3H
27-CH_3	15.7, CH_3	0.75, d (6.5; 3H)
31-CH_3	15.6, CH_3	0.73, d (7.2; 3H)
32-OCH_3	61.1 [61.2], CH_3	3.23 [3.22], s, 3H
33-CH_3	19.7, CH_3	0.96, d (7.0; 3H)
35-NCH_3	26.9 [31.9], CH_3	2.62 [2.15], s, 3H
35-NCHO	161.5[160.4], CH	7.88 [7.56], s

Note: [a]Chemical shifts of the minor conformers are presented in brackets. [b]Unless stated otherwise, each proton signal was integrated as 1 proton.

3.2 Biological activities

All the isolated compounds were assessed for the antimalarial activity against *P. falciparum* K1 and cytotoxicity against MCF-7 and human fibroblast cell (Table 13). All trisoxazole macrolides showed antimalarial activity in micromolar range except for **3**, which was virtually inactive at 10 μg/mL. This is the first report on the antimalarial activity of trisoxazole macrolides, albeit the activity is far less than that of standard dihydroartemisinin. The cytotoxicity of all trisoxazole macrolides was potent; most exhibited a micromolar range stronger than standard camptothecin against MCF-7. This is in fact not surprising as all trisoxazole

macrolides were proposed to possess actin binding activity, which may disrupt the crucial cellular functions that involve actin of most living cells (Klenchin et al., 2003).

Table 13. The antimalarial and cytotoxic activities of the isolated compounds

Compound	Antimalarial activity (IC_{50}; μM)	Cytotoxic activity (IC_{50}; μM)	
		MCF-7	Human fibroblast
kabiramide B (**1**)	1.67	0.45	0.95
kabiramide C (**2**)	4.79	0.47	7.59
kabiramide G (**3**)	inactive[a]	0.02	2.37
kabiramide J (**4**)	0.31	0.02	2.84
kabiramide I (**5**)	4.48	2.00	ND[b]
kabiramide D (**6**)	1.87	0.02	0.50
kabiramide K (**7**)	0.39	0.07	ND[b]
kabiramide L (**8**)	2.64	0.03	ND[b]
dihydroartimistinine	1.1×10^{-3}-4.4×10^{-3}	-	-
camptothecin	-	1.60×10^{-3}-3.30×10^{-3}	459.30×10^{-3}

Note: [a] The compound showed no calculable inhibition against targeted microbe at the highest concentration of 10 μg/mL. [b] The activity was not determined.

3.3 Allocation of kabiramides in the sponge *P. nux*

As mentioned earlier, the sponge *P. nux* possesses two different growth forms, a protruding capitum on a substratum-attached base. The preliminary screening of both growth forms showed the stronger biological activities in the extract from capitum part. Such contrasting potency was presumed to reflect different chemicals profiles, either in production or accumulation of bioactive secondary metabolites between the two growth forms. In order to prove the hypothesis, the HPLC-UV-based quantification of chemical constituents in each part was developed using kabiramides C and G as chemical markers.

3.3.1 Quantification of kabiramides

Kabiramide contents in the sponge extracts were determined with an HPLC-UV based analytical protocol. The targeted analytes were kabiramides C and G, selected specifically according to the clarity in the HPLC chromatogram and the availability of the compounds as standard chemical markers. The chromatographic conditions were a C18 reverse phase with acidic mobile phase and elevated temperature (1% aqueous AcOH:MeCN 37:63, 45°C, λ 254 nm). The raised temperature improved efficiency by means of reduced theoretical plates and increased diffusion coefficient of the analytes, therefore sharpening the shape of each analytes (Figure 26). The increased diffusion coefficients also increase mass transfer between mobile and stationary phases, therefore reducing retention time of analytes. In addition, at higher temperatures, the rotation about nitrogen-carbon bond of formamide moiety, as mention in 1.3 and 3.1.2.1, is faster, thus narrowing the peaks of analytes (Moriyasu et al., 1983). The devised conditions yielded an acceptable resolution that allowed an immediate determination of kabiramide C (Figure 26).

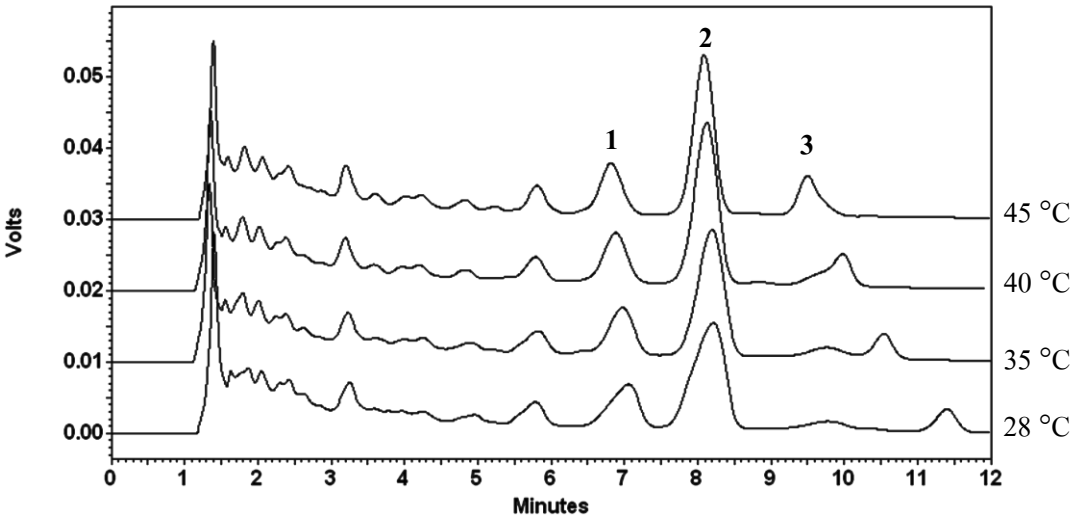

Figure 26. Effect of raised temperatures on the HPLC chromatograms of the sponge *P. nux* extracts; **1**, **2**, and **3** denoted the peaks of kabiramides B, C, and G, respectively.

The overlapping peak of kabiramide G with unknown impurities, however, was not able to be resolved immediately based on this condition. The first derivative chromatogram was therefore applied. Determination of kabiramide G content was based on the height of positive peak (t_R 8.60 min; Figure 27). This allowed a simultaneous determination of both standard markers without prechromatographic treatment.

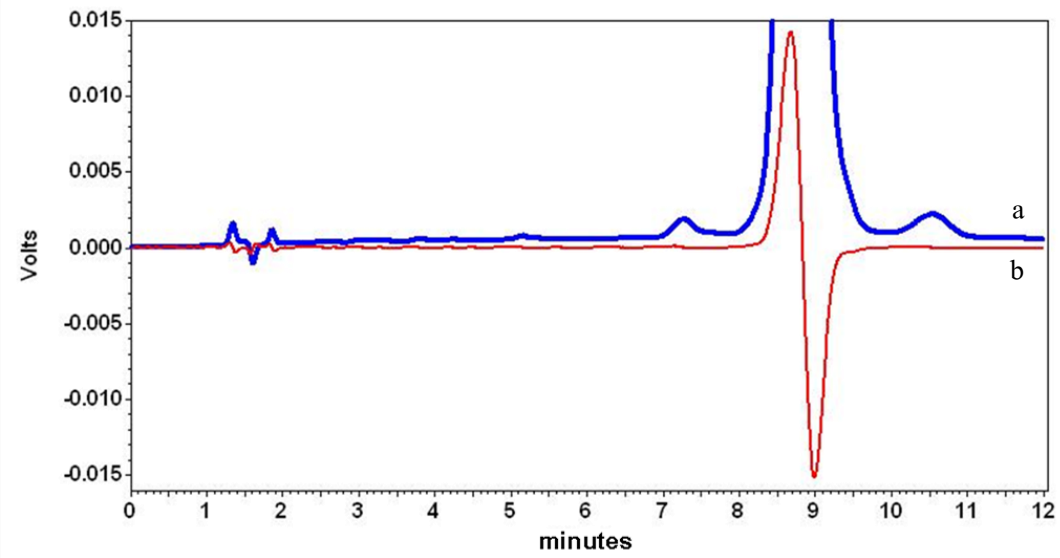

Figure 27. HPLC chromatogram of kabiramide G; (a) reference and (b) first derivative chromatograms.

The determination of both chemical markers was validated according to ICH guideline (2005). LODs of kabiramides C and G (S/N = 3) were 0.02 and 0.01 µg/mL, respectively, whereas LOQs (S/N = 10) were 0.06 and 0.04 µg/mL. Linearity, constructed based on the resulting LOQ of each compound, was met in a range of 0.06-100 µg/mL (r^2 = 0.9998; n = 7) for kabiramide C and 0.04-100 µg/mL (r^2 = 0.9993; n = 7) for kabiramide G. Intra-day precisions (n = 3) for the retention time and peak areas of kabiramide C were achieved with RSD in a range of 0.04-0.05 and 2.17-3.10, and those for the inter-day (n = 3) ones were in a range of 4.22-4.26 and 2.63-5.00, respectively. As for kabiramide G, the RSD of intra-day precision (n = 3) for retention time and first-derivative peak height were 0.03-0.20 and 1.82-2.70, and those of inter-day (n = 3) were 1.90-2.63 and 2.67-4.95, respectively. The accuracy, determined as recovery percentages of the spiked standards, was in a range of 97.7-105.3% (Table 14).

Table 14. Recovery percentage of kabiramides C and G

Spiked standard (µg/mL)	% Recovery±SD	
	kabiramide C	**kabiramide G**
Intra-day (n=3)		
10	101.5±0.1	98.88±1.6
20	104.9±0.4	96.92±1.9
30	105.3±0.1	100.5±2.0
Inter-day (n=9)		
10	100.2±1.4	97.8±0.9
20	104.3±1.5	97.7±2.5
30	104.6±1.2	100.3±2.0

3.3.2 Determination of kabiramide contents in the capitum and base parts of the sponge *P. nux*

The assessment of intra-colonial allocation of kabiramide analogs in two growth forms of the sponge *P. nux* was based on the determination of the contents of kabiramides C and G using devised chromatographic conditions described in 2.3.4. Nineteen specimens were collected in a selective manners, i.e., only colonies with protruding capita were collected with appropriated masses of attached bases. Freeze-dried capita and bases after removal of fouling organisms was weighed 50-640 mg and 380-2,820 mg, respectively. Extract yields of capitum and base of each colony were 3.04±0.56 and 1.42±0.33% w/w, respectively.

Subjecting each extract to the devised analytical protocol showed that, in most specimens, the contents of either standard kabiramide markers, or both, were higher in the capitum part (for examples, colonies 4, 8, and 13, Figure 28a , b, and d), nevertheless with some exception, e.g., colony 12 (Figure 28c), in which the base contained higher level of kabiramide analogs. The contents of kabiramides C were determined to range 0–8.85 mg/g and 0–0.44 mg/g for capitum and base parts, and that of kabiramide G at 0.05–1.72 mg/g and 0–0.24 mg/g in each part, respectively (Figure 29). Throughout the collected population, the sponge tends to allocate

either or both kabiramide analogs in higher proportion toward the capitum part (p = 0.001 for kabiramide C alone, and for both kabiramides C and G combined; 0.01 for kabiramide G). However, within either part, the contents of kabiramides C and G were not statistically different (p = 0.122 for capitum and p = 0.260 for base). Pearson's correlation matrix (Table 15) also showed that two compounds had weak correlations between the content of each marker in each part, indicating that the allocation of each compounds in each part had neither inductive nor suppressive influences onto each other. In another word, the sponge allocates the toxic kabiramides in an independent manner. The chemical variation among different parts in one colony has been known to be influenced by environmental factors, e.g., symbiotic organisms, salinity, depth, and light (Hay, 1996). As for the sponge *P. nux*, personal observation suggests the possible antifouling effect as the bases are found densely covered by other fouling setters.

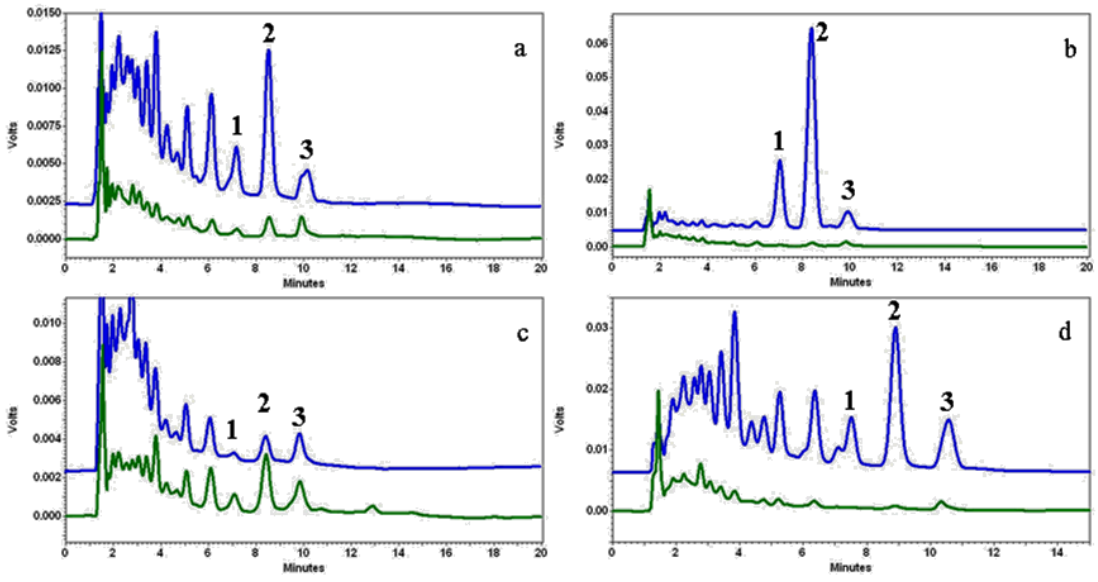

Figure 28. Selected HPLC chromatograms of capitum (blue) and base (green) extracts obtained from colonies 4 (a), 8 (b), 12 (c), and 13 (d). Peaks denoted with **1**, **2**, and **3** correspond to kabiramides B, C, and G, respectively.

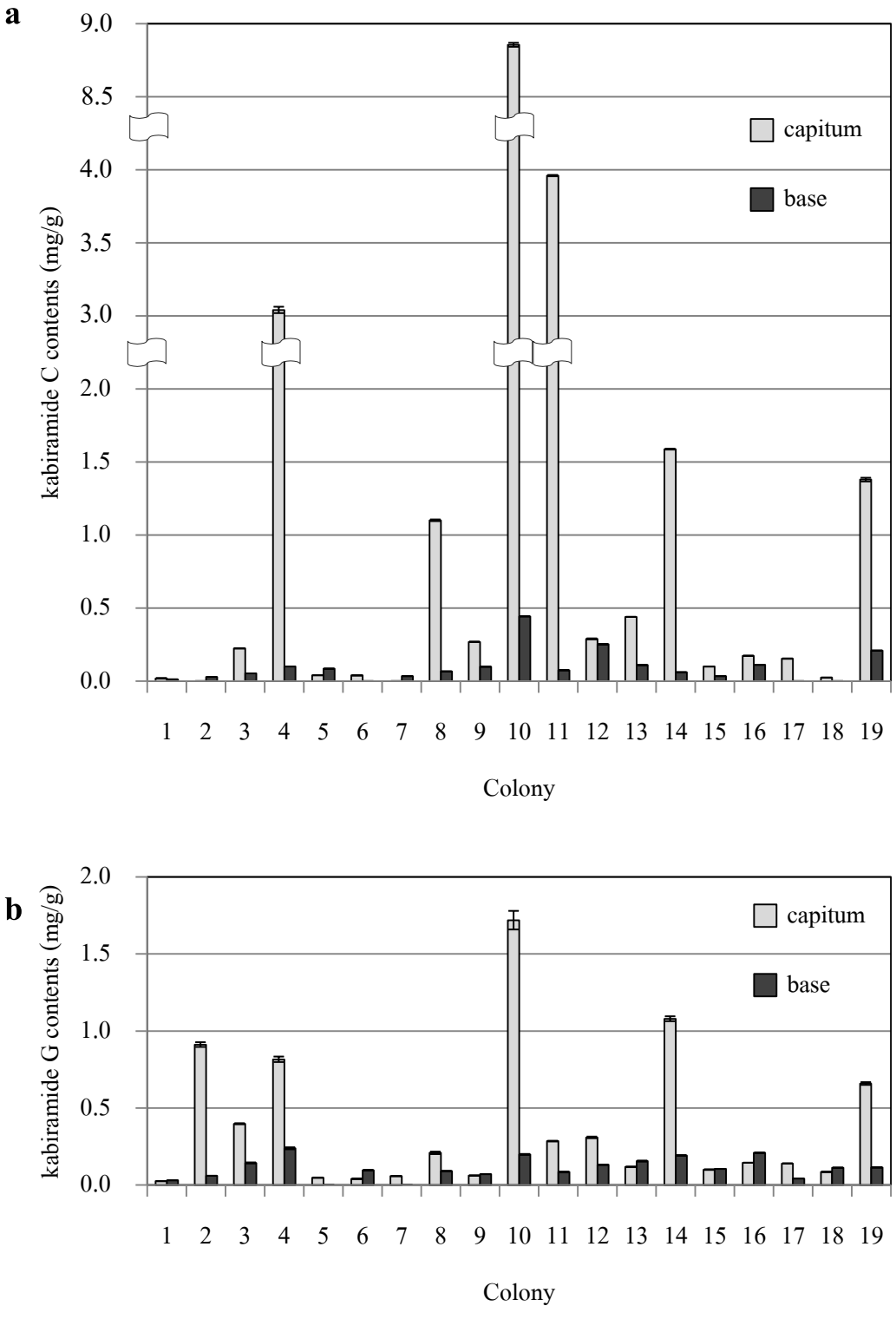

Figure 29. Contents of kabiramides C (a) and G (b) in collected specimens of the sponge *P. nux*. Notice the axis breaks in 28a at 2.0-3.0 and at 4.0-8.5 mg/g.

Table 15. Pearson's correlations (r^2) of kabiramides C (KC) and G (KG) contents in capitum and base parts

	KC (capitum)	KG (capitum)	KC (base)	KG (base)
KC (capitum)	1.000			
KG (capitum)	0.7472	1.000		
KC (base)	0.7695	0.6513	1.000	
KG (base)	0.4582	0.4481	0.5481	1.000

The organ-specific allocations of toxic kabiramides raised a question whether there were any correlations between chemical accumulation and physical structures. Determinations of three structural materials, including structural components, ash contents, and soluble protein contents were carried out. Structural components and ash contents were found in a higher proportion in the base parts ($p = 0.002$, $t = -5.098$; and $p = 0.007$, $t = -3.99$, respectively), whereas soluble protein contents in the capitum parts were otherwise higher ($p = 0.014$, $t = 4.147$) (Figure 30). On the other hand, fiber contents, calculated as a subtraction of ash contents from structural components, showed no statistical difference between the two parts ($p = 0.125$, $t = 1.830$). As structural component and ash contents are direct indicators for physical strength in

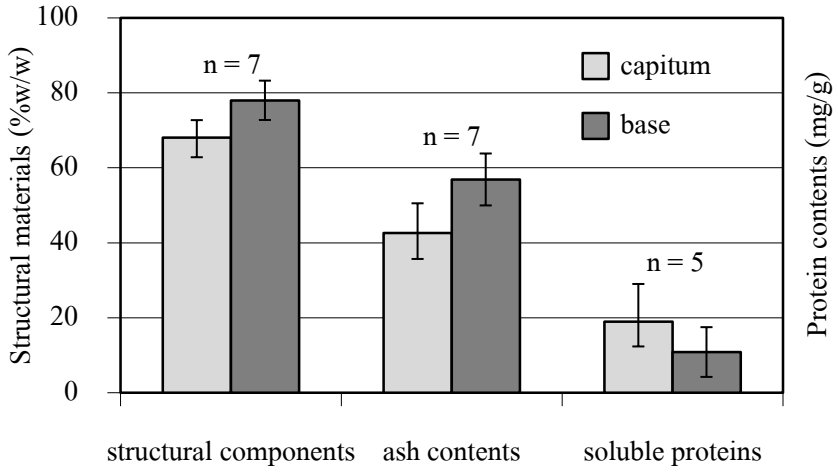

Figure 30. Structural components, ash content, and soluble protein contents in the capita and bases of the sponge *P. nux*.

sponge, the results clearly showed that there was a trade-off between chemical composition and structural materials in two growth forms of the sponge *P. nux*.

Whereas the contents of kabiramide analogs were evidentially accumulated in a higher portion in the capitum part, Figure 29 showed on the other hand high degree of content variation of kabiramide contents among each colony, ranging from non-detectable to as high as 9 mg/g sponge dry weight. Although it is not clearly accountable what may contribute to such variation, the consistent amount of extracts from each part suggested that such variation was resulted from genuinely intrinsic factors within each sponge colony, and not from experimental defects.

CHAPTER 4

CONCLUSION

The chemical investigation of the sponge *Pachastrissa nux* (de Laubenfels, 1954) using bioassay-guided fractionation led to the isolation of eight trisoxazole macrolides, all of which are in kabiramide series. Three new trisoxazole macrolides, kabiramides J, K, and L (**4**, **7**, and **8**, respectively), were reported here for, along with five known kabiramide analogs, kabiramides B (**1**), C (**2**), D (**6**), G (**3**), and I (**5**). The three new kabiramides belong to a new class of trisoxazole macrolide possessing 30-α,β-enone moiety, which found solely associated with the sponge *P. nux*. All the isolated compounds showed potent cytotoxic activity to both normal and MCF-7 breast cancer cell lines (IC_{50}s 0.50-7.59 μM and 0.02-2.00 μM, respectively), and antimalarial activity in a good range (IC_{50}s 0.31-4.79 μM). The toxicity of trisoxazole macrolides to all eukaryotic cells clearly forbids the further development of the macrolides towards plausible clinical uses. However, as a class of irreversible G-actin binding agents with a specific binding site, this opens up an opportunity to consider trisoxazole macrolides as a research tool in biomedical sciences probing the molecular events that involve actin dynamics. In fact, as reported by Petchprayoon et al. (2005), derivatization of kabiramide C a toward fluorescent probe demonstrated the possibility of the compounds for the biomedical applications.

The sponge *P. nux* possesses an ability to allocate the toxic kabiramides analogs specifically towards the capitum part, the growth form that protrudes over the foundation of irregular-shaped base. Such specific allocations of the macrolides towards the capitum suggested the utilization of toxic components as a possible chemical defense against predator or as an antifouling agent against fouling species over vulnerable part of each colony. As discussed earlier, the variation in chemical allocation within a single sponge species could be affected by environmental factors, both biological and physical once. Field observation suspected the class interconnection between fouling species and the accumulated toxins in the *P. nux* sponge. An extensive determination on ecological impact is now underway.

Marine natural products have long been recognized among promising resources of bioactive compounds with highly diverse and unique chemical structures and modes of biological activities. Milestones such as ziconotide and trabectedin, and other compounds in the clinical trials and pre-clinical studies are among the best examples for such statements. Extending the use of such bioactive compounds for biomedical applications toward ecological areas as a marker for the production and accumulation of secondary metabolites in marine organisms reflects the close inter-species relationship in marine habitats. Exemplified by the results described in this dissertation, the studies in marine natural products have broadened the scope of secondary metabolites in marine organisms that may allow the sustainable management of marine bioresources utilization.

REFERENCES

Abdo, D. A.; Motti, C. A.; Battershill, C. N.; Harvey, E. S. Temperature and spatiotemporal variability of salicylihalamide A in the sponge *Halichondria* sp. *J. Chem. Ecol*. **2007**, *33*, 1635-1645.

Allingham, J. S.; Tanaka, J.; Marriott, G.; Rayment, I. Absolute stereochemistry of ulapaulide A. *Org. Lett*. **2004**, *6*, 597-599.

Amade, P.; Lemée, R. Chemical defense of the Mediterranean alga *Caulerpa taxifolia*: variations in caulerpenyne production. *Aquat. Toxicol*. **1998**, *43*, 287-300.

Aoki, S.; Higuchi, K.; Ye, Y.; Satari, R.; Kobayashi, M. Melophlins A and B, novel tetramic acids reversing the phenotype of *ras*-transformed cells, from the marine sponge *Melophlus sarassinorum*. *Tetrahedron*. **2000**, *56*, 1833-1836.

Assmann, M.; Lichte, E.; Pawlik, J. R.; Köck, M. Chemical defenses of the Caribbean sponges *Agelas wiedenmayeri* and *Agelas conifera*. *Mar. Ecol. Prog. Ser*. **2000**, *207*, 255-262.

Becerro, M. A.; Paul, V. J.; Starmer, J. Intracolonial variation in chemical defenses of the sponge *Cacospongia* sp. and its consequences on generalist fish predators and the specialist nudibranch predator *Glossodoris pallida*. *Mar. Ecol. Prog. Ser*. **1998**, *168*, 187-196.

Becerro, M. A.; Turon, X.; Uriz, M. J. Natural variation of toxicity in encrusting sponge *Crambe crambe* (Schmith) in relation to size and environment. *J. Chem. Ecol.* **1995**, *21*, 1931-1946.

Becerro, M. A.; Uriz, M. J.; Turon, X. Chemically-mediated interaction in benthic organisms: the chemical ecology of *Crambe crambe* (Porifera, Poecilosclerida). *Hydrobiologia*. **1997**, *356*, 77-89.

Bergmann, W.; Burke, D. C. Contributions to the study of marine products. XXXIX. The nucleosides of sponges. III. Spongothymidine and spongouridine. *J. Org. Chem*. **1956**, *22*, 226-228.

Bergmann, W.; Feeney, R. J. Contributions to the study of marine products. XXXII. The nucleosides of sponges. I. *J. Org. Chem*. **1951**, *16*, 981-987.

Bergmann, W.; Stempien, M. F. Contributions to the study of marine products. XLIII. The nucleosides of sponges. V. The synthesis of spongosine. *J. Org. Chem*. **1957**, *22*, 1575-1557.

Betancourt-Lozano, M.; González-Farias, F.; González-Acosta, B.; García-Gasca, A.; Bastida-Zavala, J. R. Variation of antimicrobial activity of the sponge *Aplysina fistularis* (Pallas, 1766) and its relation to associated fauna. *J. Exp. Mar. Biol. Ecol*. **1998**, *223*, 1-18.

Bewley, C. A.; Holland, N. D.; Faulkner, D. J. Two classes of metabolites from *Theonella swinhoei* are localized in distinct populations of bacterial symbionts. *Experientia*. **1996**, *52*, 716-722.

Blunt, J. W.; Copp, B. R.; Munro, M. H. G.; Northcote, P. T.; Prinsep, M. R. Marine natural products. *Nat. Prod. Rep*. **2011**, *28*, 196-268.

Bobzin, S. C.; Faulkner, D. J. Chemistry and chemical ecology of the Bahamian sponge *Aplysilla glacialis*. *J. Chem. Ecol*. **1992**, *18*, 309-332.

Bradford, M. M. A rapid and sensitive method for the quantification of microgram quantities of protein utilizing the principle of protein-dye binding. *Anal. Biochem*. **1976**, *72*, 248-254.

Bryan, P. J.; Rittschof, D.; McClintock, J. B. Bioactivity of echinoderm ethanolic body-wall extracts: an assessment of marine bacterial attachment and macroinvertebrate larval settlement. *J. Exp. Mar. Biol. Ecol.* **1996**, *196*, 79–96.

Cetrulo, G. L.; Hay, M. E. Activated chemical defenses in tropical versus temperate seaweeds. *Mar. Ecol. Prog. Ser*. **2000**, *207*, 243-253.

Charlet, S.; Bensaddek, L.; Raynaud, S.; Gillet, F.; Mesnard, F.; Fliniaux, M. An HPLC procedure for the quantification of anhydrosecoisolariciresinol. Application to the evaluation of flax lignin content. *Plant Physiol. Biochem*. **2002**, *40*, 225-229.

Cronin, G.; Hay, M. E.; Fenical, W.; Lindquist, N. Distribution, density, and sequestration of host chemical defenses by the specialist nudibranch *Tritonia hamnerorum* found at high densities on the sea fan *Gorgonia ventalina*. *Mar. Ecol. Prog. Ser*. **1995**, *119*, 177-189.

Dalisay, D. S.; Rogers, E. W.; Edison, A. S.; Molinski, T. F. Structure elucidation at the nanomole scale. 1. Trisoxazole macrolides and thiazole-containing cyclic peptides from the nudibranch *Hexabranchus sanguineus*. *J. Nat. Prod*. **2009**, *72*, 732-738.

de Nys, R.; Steinberg, P. D.; Rogers, C. N.; Charlton, T. S.; Duncan, M. W. Quantitative variation of secondary metabolites in the sea hare *Aplysia parvula* and its host plant, *Delisea pulchra*. *Mar. Ecol. Prog. Ser*. **1996**, *130*, 135-146.

Desjadins, R. E.; Canfield, C. L.; Haynes, J. D.; Chula, J. D. Quantitative assessment of antimalarial activity in vitro by a semi-automated microdilution technique. *Antimicrob. Agents Chemother*. **1979**, *16*, 710-718.

Dube, D.; Kim, K.; Alker, A. P.; Harvell, D. Size structure and geographic variation in chemical resistance of sea fan corals *Gorgonia ventalina* to a fungal pathogen. *Mar. Ecol. Prog. Ser.* **2002**, *231*, 139-150.

Ebel, R.; Brenzinger M.; Kunze, A.; Gross, H. J.; Proksch P. Wound activation of protoxins in marine sponge *Aplysina aerophoba*. *J. Chem. Ecol*. **1997**, *23*, 1451-1462.

Eder, C.; Schupp, P.; Proksch, P.; Wray, V.; Steube, K.; Müller, C. E.; Frobenius, W.; Herderich, M.; van Soest, R. W. M. Bioactive pyridoacridine alkaloids from the Micronesian sponge *Oceanapia* sp. *J. Nat. Prod*. **1998**, *61*, 301-305.

Ericsson, C.; Peredo, I.; Nistér, M. Optimized protein extraction from cryopreserved brain tissue samples. *Acta. Oncologica*. **2007**, *46*, 10-20.

European Medicines Agency. European Medicines Agency: Science Medicines Health Home Page. http://www.ema.europa.eu/ema/index.jsp?curl=pages/medicines/human/medicines/000773/human_med_001165.jsp&jsenabled=true (January 14, 2012).

Fernández, R.; Dherbomez, M.; Letourneux, Y.; Nabil, M.; Verbist, J. F.; Biard, J. F. Antifungal metabolites from the marine sponge *Pachastrissa* sp.: new bengamide and bengazole derivatives. *J. Nat. Prod*. **1999**, *62*, 678-680.

Freeman, C. J.; Gleason, D. F. Chemical defense, nutritional quality, and structural components in three sponge species: *Ircinia felix*, *I. campana*, and *Aplysina fulva*. *Mar. Biol*. **2010**, *157*, 1083-1093.

Freeman, C. J.; Gleason, D. F. Does concentrating chemical defense within specific regions of marine sponges result in enhanced protection from predators? *Hydrobiologia*. [Online early access]. DOI 10.1007/s10750-0. Published online: June 22, 2011. http://www.springerlink.com/content/p1tu7j844551w753/ (accessed January 14, 2012).

Furrow, B. F.; Amsler, C. D.; McClintock, J. B.; Baker, B. J. Surface sesquestration of chemical feeding deterrents in the Antarctic sponge *Latrunculia apicalis* as an optimal defense against sea star spongivory. *Mar. Biol*. **2003**, *143*, 443-449.

Fusetani, N.; Sugawara, T.; Matsunaga, S. Cytotoxic metabolites of the marine sponge *Mycale adhaerens* Lambe. *J. Org. Chem*. **1991**, *56*, 4971-4974.

Fusetani, N.; Yasumuro, K.; Matsunaga, S.; Hashimoto, K. Mycalolides A-C, hybrid macrolides of ulapaulides and halichondramide, from a sponge of the genus *Mycale*. *Tetrahedron Lett*. **1989**, *30*, 2809-2812.

Garson, M. J.; Thompson, J. E.; Larsen, R. M.; Battershill, C. N.; Murphy, P. T.; Bergquist, P. R. Terpenes in sponge cell membranes: cell separation and membrane fractionation studies with the tropical marine sponge *Amphimedon* sp. *Lipids*. **1992**, *27*, 378-388.

Gerwick, W. H.; Fenical, W.; Norrist, J. N. Chemical variation in the tropical seaweed *Stypopodium zonale* (Dictyotaceae). *Phytochemistry*. **1985**, *24*, 1279-1283.

Gillor, O.; Carmeli, S.; Rahamin Y.; Fishelson, Z.; Ilan M. Immunolocalization of the toxin latrunculin B within the red sea sponge *Negombata magnifica*. *Mar. Biotechnol*. **2000**, *2*, 213-223.

Harvell, C. D.; Fenical, W. Chemical and structural defense of Caribbean gorgonians (*Pseudopterogorgia* spp.): intracolony localization of defense. *Limnol. Oceanogr*. **1989**, *34*, 382-389.

Harvell, C. D.; Fenical, W.; Roussis, V.; Ruesink, J. L.; Griggs, C. C.; Greene, C. H. Local and geographic variation in the defensive chemistry of a West Indian gorgonian coral (*Briareum asbestinum*). *Mar. Ecol. Prog. Ser*. **1993**, *93*, 165-173.

Hay, M. E. Marine chemical ecology: what's known and what's next? *J. Exp. Mar. Biol. Ecol*. **1996**, *200*, 103-134.

Huizing, M. T.; Sparreboom, A.; Rosing, H.; van Tellingen, O.; Pinedo, H.M.; Beijnen, J. H. Quantification of paclitaxel metabolites in human plasma by high-performance liquid chromatography. *J. Chromatogr. B*. **1995**, *674*, 261-268.

Ichino, T.; Arimoto, H.; Uemura, D. Possibility of a non-amino acid pathway in the biosynthesis of marine-derived oxazole. *Chem. Commun*. **2006**, *16*, 1742-1744.

ICH (International Conference of Harmonization). *Guideline Q2(R1)-Validation of Analytical Procedures: Text and Methodology*; Geneva, 2005, 1-13.

Ishibashi, M.; Moore, R. E.; Patterson, G. M. L. Scytophycins, cytotoxic and antimycotic agents from the cyanophyte *Scytonema pseudohofmanni*. *J. Org. Chem*. **1986**, *51*, 5300-5306.

Jongrungruangchok, S.; Kittakoop, P.; Yongsmith, B.; Bavovada, R.; Tanasupawat, S.; Lartpornmatulee, N.; Thebtaranonth, Y. Azaphilone pigments from a yellow mutant of the fungus *Monascus kaoliang*. *Phytochemistry*. **2004**, *65*, 2569-2575.

Kelman, D.; Benayahu, Y.; Kashman, Y. Variation in secondary metabolite concentrations in yellow and grey morphs of the red sea soft coral *Parerythropodium fulvum fulvum*: possible ecological implications. *J. Chem. Ecol*. **2000**, *26*, 1123-1133.

Kernan, M. R.; Barrabee, E. B.; Faulkner, D. J. Variation of the metabolites of *Chromodoris Funerea*: comparison of specimens from a Palauan marine lake with those from adjacent waters. *Comp. Biochem. Physiol*. **1988a**, *89B*, 275-278.

Kernan, M. R.; Molinski, T. F.; Faulkner, D. J. Macrocyclic antifungal metabolites from the spanish dancer nudibranch *Hexabranchus sanguineus* and sponge of the genus *Halichondria*. *J. Org. Chem*. **1988b**, *53*, 5014-5020.

Kim, K. Antimicrobial activity in gorgonian corals (Coelenterata, Octocorallia). *Coral Reefs*. **1994**, *13*, 75-80.

Kim, K.; Harvell, C. D.; Kim, P. D. Smith, G. W. Merkel, S. M. Fungal disease resistance of Caribbean sea fan coral (*Gorgonia* spp.). *Mar. Biol*. **2000**, *136*, 259-267.

Klenchin, V. A.; Allingham, J. S.; King, R.; Tanaka, J.; Marriott, G.; Rayment, I. Trisoxazole macrolide toxins mimic the binding of actin-capping protein to actin. *Nat. Struct. Biol*. **2003**, *10*, 1058-1063.

Kobayashi, J.; Murata, O.; Shigemori, H. Jaspisamides A-C, new cytotoxic macrolides from the Okinawan sponge *Jaspis* sp. *J. Nat. Prod*. **1993**, *56*, 787-791.

Kobayashi, J.; Tsuda, M.; Fuse, H.; Sasaki, T.; Mikami, Y. Halishigamides A-D, new cytotoxic oxazole-containing metabolites from Okinawan sponge *Halichondria* sp. *J. Nat. Prod*. **1997**, *60*, 150-154.

Kubanek, J.; Pawlik, J. R.; Eve, T. M.; Fenical, W. Triterpene glycosides defend the Caribbean reef sponge *Erylus formosus* from predatory fishes. *Mar. Ecol. Prog. Ser*. **2000**, *207*, 69-77.

Kubanek, J.; Whalen, K. E.; Engel, S.; Kelly, S. R.; Henkel, T. P.; Fenical, W.; Pawlik, J. R. Multiple defensive roles for triterpene glycosides from two Caribbean sponges. *Oecologia*. **2002**, *131*, 125-136.

Kuroda, I.; Musman, M.; Ohtani, II.; Ichiba, T.; Tanaka, J. Pachastrissamine, a cytotoxic anhydrophytosphingosine from a marine sponge, *Pachastrissa* sp. *J. Nat. Prod*. **2002**, *65*, 1505-1506.

Leyser, O. The power of auxin in plants. *Plant Physiol*. **2010**, *154*, 501-505.

López-Legentil, S.; Bontemps-Subielos, N.; Turon, X.; Banaigs, B. Temporal variation in the production of four secondary metabolites in a colonial ascidian. *J. Chem. Ecol*. **2006**, *32*, 2079-2084.

López-Legentil, S.; Dieckmann, R.; Bontemps-Subielos, N.; Turon, X.; Banaigs, B. Qualitative variation of alkaloids in color morphs of *Cystodytes* (Ascidiacea). *Biochem. System. Ecol.* **2005**, *33*, 1107-1119.

Mahon, A. R.; Amsler, C. D.; McClintock, J. B.; Amsler, M. O.; Baker, B. J. Tissue-specific palatability and chemical defenses against macropredators and pathogens in the common articaulate branchiopod *Liothyrella uva* from the Antarctic Peninsula. *J. Exp. Mar. Biol. Ecol.* **2003**, *290*, 197-210.

Maida, M.; Carroll, A. R.; Coll, J. C. Variability of terpene content in the soft coral *Sinularia flexibilis* (Coelenterata: Octocorallia), and its ecological implications. *J. Chem. Ecol.* **1993**, *19*, 2285-2296.

Martí, R.; Fontana, A.; Uriz, A. J.; Cimino, G. Quantitative assessment of natural toxicity in sponges: toxicity bioassay versus compound quantification. *J. Chem. Ecol*. **2003**, *29*, 1307-1318.

Matsunaga, S.; Fusetani, N.; Hashimoto, K. Kabiramide C, a novel antifungal macrolide from nudibranch eggmasses. *J. Am. Chem. Soc.* **1986**, *108*, 847-849.

Matsunaga, S.; Fusetani, N.; Hashimoto, K. Further kabiramides and halichondramides, cytotoxic macrolides embracing trisoxazole, from the *Hexabranchus* egg masses. *J. Org. Chem*. **1989**, *54*, 1360-1363.

Matsunaga, S.; Nagata, Y.; Fusetani, N. Thiomycalolides: new cytotoxic trisoxazole-containing macrolides isolated from a marine sponge *Mycale* sp. *J. Nat. Prod*. **1998a**, *61*, 663-666.

Matsunaga, S.; Suguwara, T.; Fusetani, N. New macrolides from the marine sponge *Mycale magellanica* and their interconversion. *J. Nat. Prod*. **1998b**, *61*, 1164-1167.

Mayer, A. M. S.; Glaser, K. B.; Cuevas, C.; Jacobs, R.S.; Kem, W.; Little, R. D.; McIntorsh, J. M.; Newman, D. J.; Potts, B. C.; Shuster, D. E. The odyssey of marine pharmaceuticals: a current pipeline perspective. *Trends Pharmacol. Sci*. **2010**, *31*, 255-265.

Meyer, K. D.; Paul, V. J. Intraplant variation in secondary metabolite concentration in three species of *Caulerpa* (Chlorophyta: Caulerpales) and its effects on herbivorous fishes. *Mar. Ecol. Prog. Ser.* **1992**, *82*, 249-257.

McClintock, J. B.; Amsler, M. O.; Amsler, C. D.; Southworth, K. J.; Petrie, C.; Baker, B. J. Biochemical composition, energy content and chemical antifeedant and antifoulant defenses of the colonial Antarctic ascidian *Distaplia cylindrica*. *Mar. Biol*. **2004**, *145*, 885-894.

McClintock, J. B.; Baker, B. J. *Marine Chemical Ecology*, 1st ed.; CRC Press LLC: Florida, 2001; pp 325-353.

Miller, K.; Alvarez, B.; Battershill, C.; Northcote, P.; Parthasarathy, H. Genetic, morphological, and chemical divergence in the sponge genus *Lathrunculia* (Porifera: Demospongiae) from New Zealand. *Mar. Biol*. **2001**, *139*, 235-250.

Moriyasu, M.; Hashimoto, Y.; Endo, M. Kinetic stidies of fast equilibrium by means of high-performance liquid chromatography. IV. Separation of rotamers of palladium (II) dithiocarbamate. *Bull. Chem. Soc. Jpn*. **1983**, *56*, 1972-1977.

Müller, W. E. G.; Diehl-Seifert, B.; Sobel, C.; Bechtold, A.; Kljajić, Z.; Dorn, A. Sponge secondary metabolites: biochemical and ultrastructural localization of the antimitotic agent avarol in *Dysidea avara. J. Histochem. Cytochem*. **1986**, *34*, 1687-1690.

Newman, D. J.; Cragg, G. M. Natural products as sources of new drugs over the last 25 years. *J. Nat. Prod.* **2007**, *70*, 461-477.

Noyer, C.; Thomas, O. P.; Becerro, M. A. Patterns of chemical diversity in the Mediterranean sponge *Spongia lamella*. *PLoS ONE*. **2011**, *6*, 1-11.

Nuñez, C. V.; de Almeida, E. V. R.; Granato, A. C.; Marques, S. O.; Santos, K. O.; Pereira, F. R.; Macedo, M. L.; Ferreira, A. G.; Hajdu, E.; Pinheiro, U. S.; Muricy, G.; Peixinho, S.; Freeman, C. J.; Gleason, D. F.; Berlinck, R. G. S. Chemical variability within the marine sponge *Aplysina fulva*. *Biochem. Syst. Ecol.* **2008**, *36*, 283-296.

Page, M.; West, L.; Northcote, P.; Battershill, C.; Kelly, M. Spatial and temporal variability of cytotoxic metabolites in populations of the New Zealand sponge *Mycale hentscheli*. *J. Chem. Ecol*. **2005**, *31*, 1161-1174.

Paul, V. J.; Fenical, W. Chemical defense in tropical green algae, order Caulerpales. *Mar. Ecol. Prog. Ser.* **1986**, *34*, 157-169.

Paul, V.J.; Van Alstyne, K. L. Chemical defense and chemical variation in some tropical Pacific species of *Halimeda* (Halimedaceae; Chlorophyta). *Coral Reefs*. **1988**, *6*, 263-269.

Paul, V. J.; Van Alstyne, K. L. Activation of chemical defenses in the tropical green algae *Halimeda* spp. *J. Exp. Mar. Biol. Ecol*. **1992**, *160*, 191-203.

Pawlik, J. R.; Kernan, M. R.; Molinski, T. F.; Harper, M. K.; Faulkner, D. J. Defensive chemicals of the Spanisch dancer nudibranch *Hexabranchus sanguineus* and its egg ribbon: macrolides derived from a sponge diet. *J. Exp. Mar. Biol. Ecol*. **1988**, *119*, 99-109.

Petchprayoon, C.; Asato, Y.; Higa, T.; Garcia-Fernandez, L. F.; Pedpradab, S.; Marriott, G; Suwanborirux, K.; Tanaka, J. Four new kabiramides from the Thai sponge, *Pachastrissa nux*. *Heterocycles*. **2006**, *69*, 447-456.

Petchprayoon, C.; Suwanborirux, K.; Tanaka, J.; Yan, Y.; Sakata, T.; Marriott, G. Fluorescent kabiramides: new probes to quantify actin in vitro and in vivo. *Bioconjugate Chem*. **2005**, *16*, 1382-1389.

Peters, L.; Wright, A. D.; Krick, A.; König, G. M. Variation of brominated indole and terpenoid within single and different colonies of the marine bryozoans *Flustra foliacea*. *J. Chem. Ecol.* **2004**, *30*, 1165-1181.

Puglisi, M. P.; Paul, V. J.; Slattery, M. Biogeographic comparisons of chemical and structural defenses of the Pacific gorgonians *Annella mollis* and *A. reticulata*. *Mar. Ecol. Prog. Ser*. **2000**, *207*, 263-272.

Phuwapraisirisan, P.; Matsunaga, S.; van Soest, R. W. M.; Fusetani, N. Isolation of a new mycalolide from the marine sponge *Mycale izuensis*. *J. Nat. Prod*. **2002**, *65*, 942-943.

Rashid, M. A.; Gustafson, K. R.; Cardellina, J. H.; Boyd, M. R. Mycalolides D and E, new cytotoxic macrolides from a collection of the stony coral *Tubastrea faulkneri*. *J. Nat. Prod*. **1995**, *58*, 1120-1125.

Richelle-Maurer, E.; de Kluijver, M. J.; Feio, S.; Gaudêncio, S.; Gaspar H.; Gomez, R.; Tavares, R.; van de Vyver, G.; van Soest, R. W. M. Localization and ecological significance of oridin and sceptrin in the Caribbean sponge *Agelas conifer*. *Biochem. Syst. Ecol*. **2003**, *31*, 1073-1091.

Roesener, J. A.; Scheuer, P. J. Ulapaulide A and B, extraordinary antitumor macrolides from nudibranch eggmasses. *J. Am. Chem. Soc*. **1986**, *108*, 846-847.

Rohde, S.; Schupp, P. J. Allocation of chemical and structural defenses in the sponge *Melophlus sarassinorum*. *J. Exp. Mar. Biol. Ecol.* **2011**, *399*, 76-83.

Roué, M.; Domart-Coulon, I.; Ereskovsky, A.; Djediat, C.; Perez. T.; Bourguet-kondracki, M. Cellular localization of clathridimine, an antimicrobial 2-aminoimidazole alkaloid produced by the Mediterraneans calcareous sponge *Clathrina clathrus*. *J. Nat. Prod*. **2010**, *73*, 1277-1282.

Roussis, V.; Chinou, I. B.; Tsitsimpikou, C.; Vagias, C.; Petrakis, P. V. Antibacterial activity of volatile secondary metabolites from Caribbean soft corals of the genus *Gorgonia*. *Flavour Fragr. J.* **2001**, *16*, 364-366.

Sacristán-Soriano, O.; Banaigs, B.; Becerro, M. A. Relevant spatial scales of chemical variation in *Aplysina aerophoba*. *Mar. Drug*. **2011a**, *9*, 2499-2513.

Sacristán-Soriano, O.; Banaigs, B.; Casamayor, E. O.; Becerro, M. A. Exploring the links between natural products and bacterial assemblages in the sponge *Aplysina aerophoba*. *Appl. Environ. Microb*. **2011b**, *77*, 862-870.

Saito, S.; Watabe, S.; Ozaki, H.; Fusetani, N.; Karaki, H. Mycalolide B, a novel actin depolarizing agent. *J. Biol. Chem*. **1994**, *269*, 29710-29714.

Schmitz, F. J.; McDonald, F. J. Isolation and identification of cerebrosides from the marine sponge *Chondrilla nucula*. *J. Lipid Res*. **1974**, *15*, 158-164.

Schupp, P.; Eder, C.; Paul, V.; Proksch, P. Distribution of secondary metabolites in the sponge *Oceanapia* sp. and its ecological implications. *Mar. Biol*. **1999**, *135*, 573-580.

Shin. J.; Lee, H.; Kim, J.; Shin, H.; Ahn, J.; Paul, V. J. New macrolides from the sponge *Chondrosia corticata*. *J. Nat. Prod*. **2004**, *67*, 1889-1892.

Sinha, R. R.; Gehring, A. M.; Milne, J. C.; Belshaw, P. J.; Walsh, C. T. Thiazole and oxazole peptides: biosynthesis and molecular machinery. *Nat. Prod. Rep*. **1999**, *16*, 249-263.

Skehan, P.; Storeng, R.; Scudiero, D.; Monks, A.; McMahon, J.; Vistica, D., Warren, J. T.; Bokesch, H.; Kenny, S.; Boyd, M. R. New colorimetric cytotoxicity assay for anticancer-drug screening. *J. Natl. Cancer Inst*. **1990**, *82*, 1107-1112.

Slattery, M. Fungal pathogenesis of the sea fan *Gorgonia ventalina*: direct and indirect consequences. *Chemoecology*. **1999**, *9*, 97-104.

Soares, A. R.; Teixeira, V. L.; Pereira, R. C.; Villaça, R. Variation on diterpene production by the Brazillian alga *Stypopodium zonale* (Dictyotales, Phaeophyta). *Biochem. Syst. Ecol*. **2003**, *31*, 1347-1350.

Sudatti, D. B.; Rodrigue, S. V.; Pereira, R. C. Quantitative GC-ECD analysis of halogenated metabolites: determination of surface and within-thallus elatol of *Laurencia obtusa. J. Chem. Ecol.* **2006**, *32*, 835-843.

Swearingen, D. C., III.; Pawlik, J. R. Variability in the chemical defense of the sponge *Chondrilla nucula* against predatory reef fishes. *Mar. Biol*. **1998**, *131*, 619-627.

Tanaka, J.; Yan, Y.; Choi, J.; Bai, J.; Klenchin, V. A.; Rayment, I.; Marriott, G. Biomolecular mimicry in the actin cytoskeleton: machanisms underlying the toxicity of kabiramide C and related macrolides. *Proc. Natl. Acad. Sci. U. S. A.* **2003**, *100*, 13851-13856.

Thompson, J. E.; Barrow, K. D.; Faulkner, D. J. Localization of two brominated matabolites, aerothionin and homoaerothionin, in spherulous cell of the marine sponge *Aplysina fistularis* (= *Verongia thiona*). *Acta. Zoologica*. **1983**, *64*, 199-210.

Thompson, J. E.; Murphy, P. T.; Bergquist, P. R.; Evans, E. A. Environmentally induced variation in diterpene composition of the marine sponge *Rhopaloeides odorabile*. *Biochem. Syst. Ecol*. **1987**, *15*, 595-606.

Thompson, J. E.; Walker, R. P.; Wratten, S. J.; Faulkner, D. J. A chemical defense mechanism for the nudibranch *Cadlina luteomarginata*. *Tetrahedron*. **1982**, *38*, 1865-1873.

Trager, W.; Jensen, J. B. Human malaria parasites in continuous culture. *Science.* **1976**, *193*, 673-675.

Tsukamoto, S.; Koimaru, K.; Ohta, T. Secomycalolide A: a new proteasome inhibitor isolated from a marine sponge of the genus *Mycale*. *Mar. Drugs*. **2005**, *3*, 29-35.

Turon, X.; Becerro, M. A.; Uriz, M. J. Seasonal patterns of toxicity in benthic invertebrates: the encrusting sponge *Crambe crambe* (Poecilosclerida). *Oikos*. **1996**, *75*, 33-40.

Turon, X.; Becerro, M. A.; Uriz, M. J. Distribution of brominated compounds within the sponge *Aplysina aerophoba:* coupling of X-ray microanalysis with cryofixation techniques. *Cell Tissue Res.* **2000**, *301*, 311-322.

Uriz, M. J.; Becerro, M. A.; Tur, J. M.; Turon, X. Location of toxicity within the Mediterranean sponge *Crambe crambe* (Demospongiae: Poecilosclerida). *Mar. Biol.* **1996b**, *124*, 583-590.

Uriz, M. J.; Turon, X.; Galera, J.; Tur, J. M. New light on the cell location of avarol within the sponge *Dysidea avara* (Dendroceratida). *Cell Tissue Res*. **1996a**, *285*, 519-527.

U.S. FDA. U.S. Food and Drug Administration Home Page. http://www.fda.gov/NewsEvents/Newsroom/PressAnnouncements/2010/ucm233863.htm (accessed January 14, 2012).

U.S. FDA/CDER. U.S. Food and Drug Administration Home Page. http://www.accessdata.fda.gov/scripts/cder/drugsatfda/index.cfm?fuseaction=Search.DrugDetails (accessed January 14, 2012).

U.S. National Institutes of Health. ClinicalTrial.gov Home Page. http://www.clinicaltrials.gov/ct2/ results?flds=Xo&flds=a&flds=b&term=trabectedin&show_flds=Y (accessed January 14, 2012).

Van Alstyne, K. L.; Paul, V. J. The biogeography of polyphenolic compounds in marine macroalgae: temperate brown algal defenses deter feeding by tropical herbivorous fishes. *Oecologia*. **1990**, *84*, 158-163.

Yang, A.; Baker, B. J. Discorhabdin alkaloids from the antarctic sponge *Latrunculia apicalis*. *J. Nat. Prod.* **1995**, *58*, 1596-1599.

Wolfe, G. V.; Steinke, M.; Kirst, G. O. Grazing-activated chemical defence in a unicellular marine alga. *Nature*. **1997**, *387*, 894-897.

Wright, J. T.; de Nys, R.; Steinberg, P. D. Geographic variation in halogenated furanones from the red alga *Delisea pulchra* and associated herbivores and epiphytes. *Mar. Ecol. Prog. Ser*. **2000**, *207*, 227-241.

Xu, J.; Hasegawa, M.; Harada, K.; Kobayashi, H.; Nagai, H.; Namikoshi, M. Melophins P, Q, R, and S: four new tetramic acid derivatives, from two Palauan marine sponge of the genus *Melophlus*. *Chem. Pharm. Bull*. **2006**, *54*, 852-854.

Zhou, J.; Zhang, T.; Wang, Q.; Chen, J. Chromatographic fingerprint analysis of varietal differences among three species of Baishouwu and simultaneous analysis of three bioactive constituents by use of LC-DAD. *Chromatographia*. **2008**, *68*, 213-218.

APPENDIX

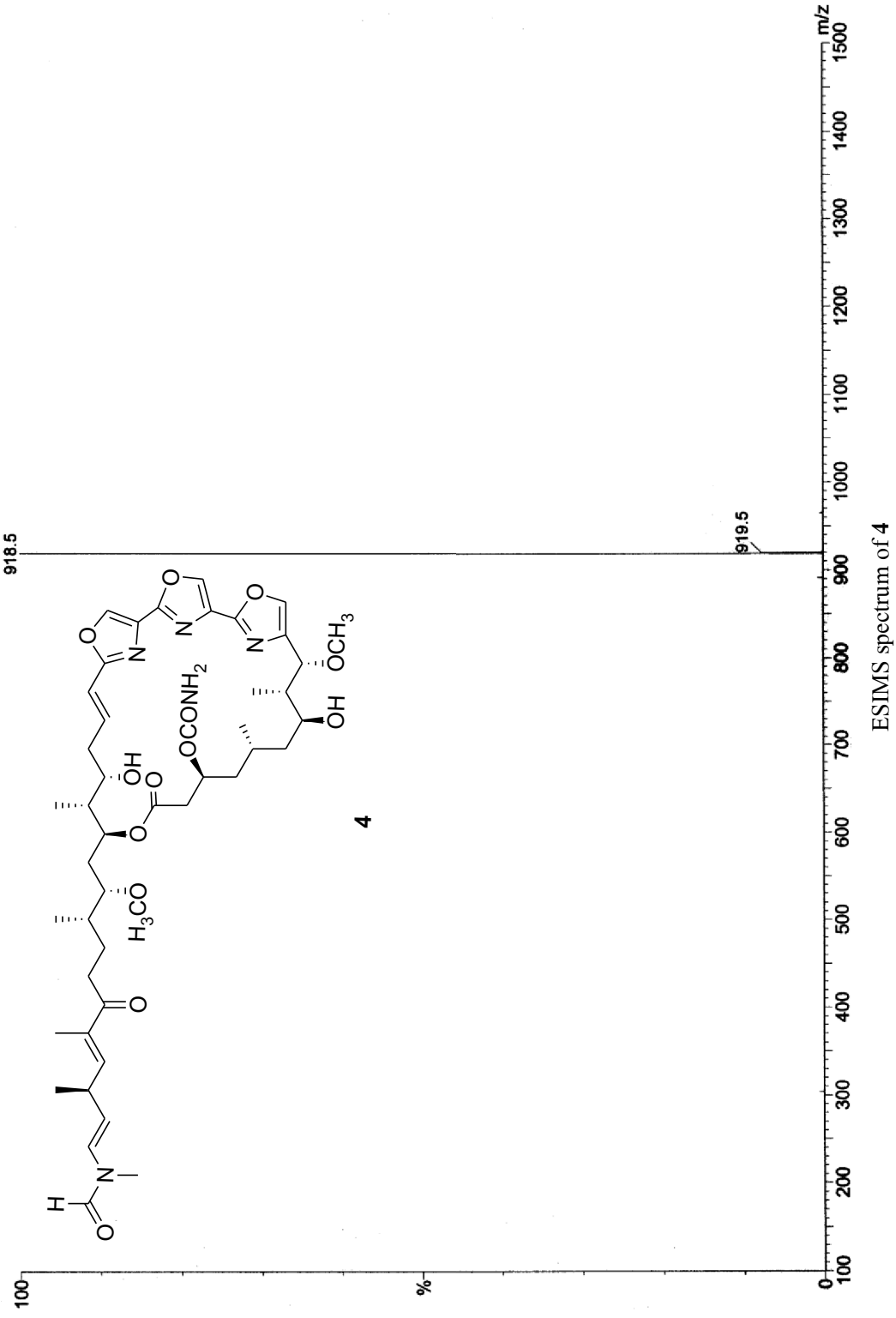

ESIMS spectrum of **4**

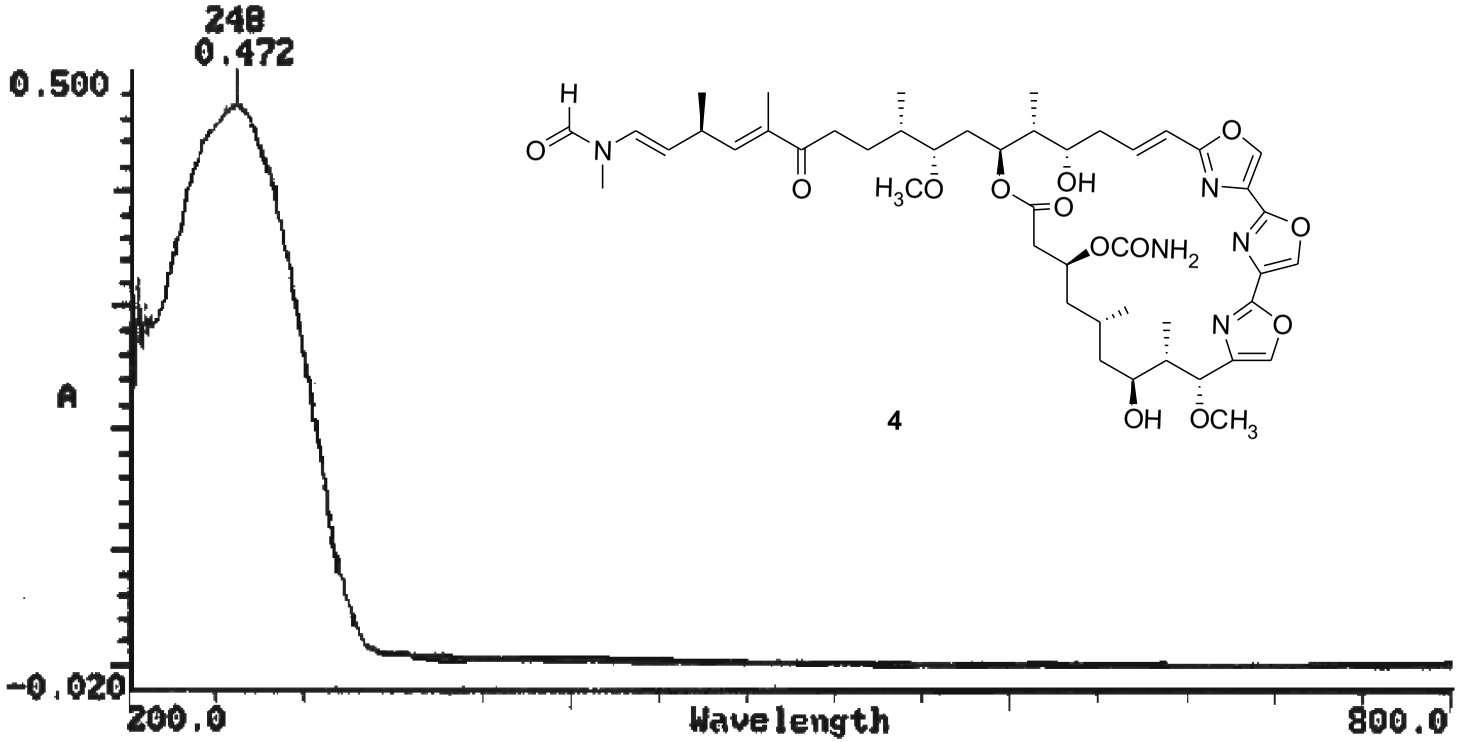

4

UV spectrum of **4** (CH_3OH)

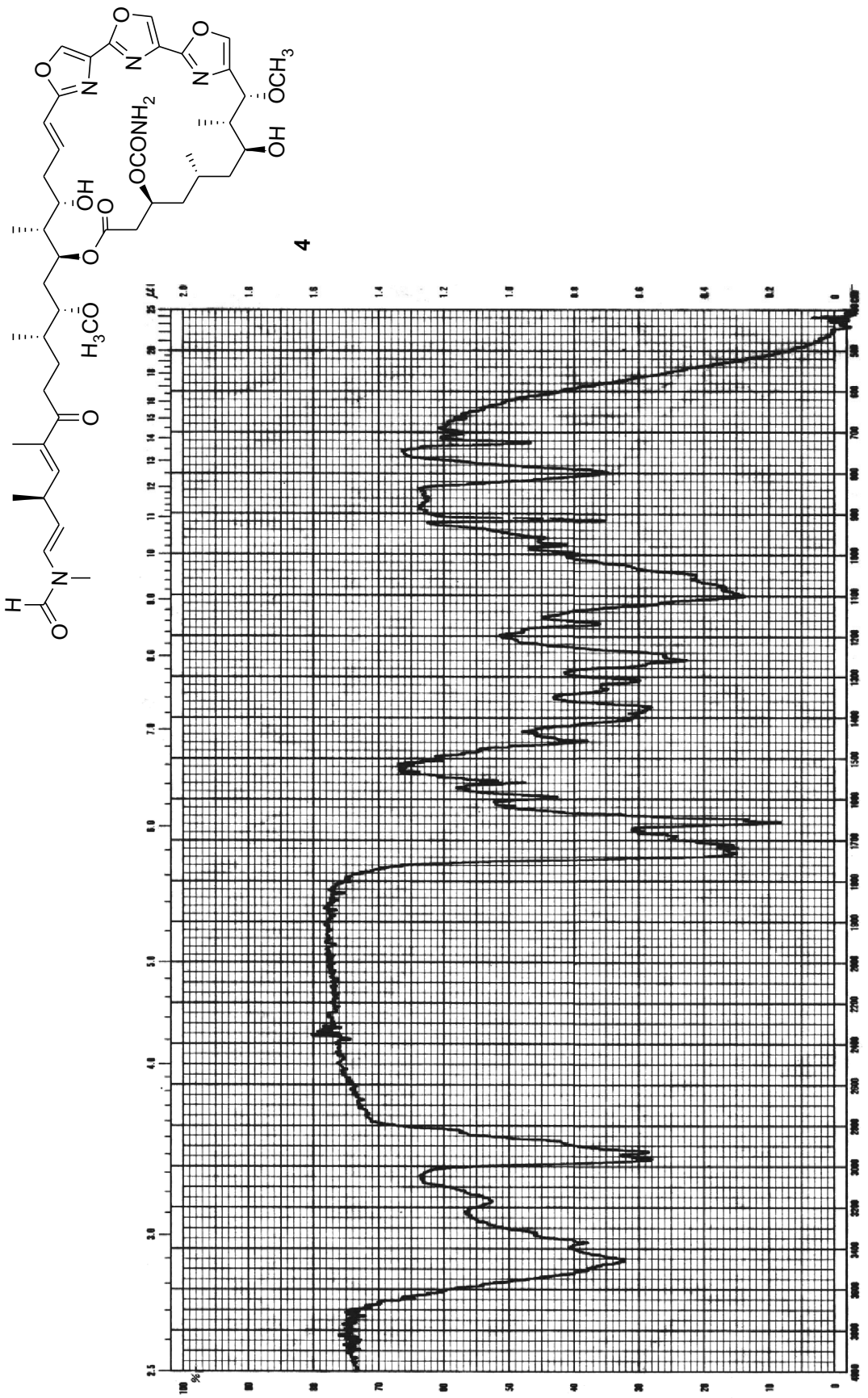

IR spectrum of **4** (neat)

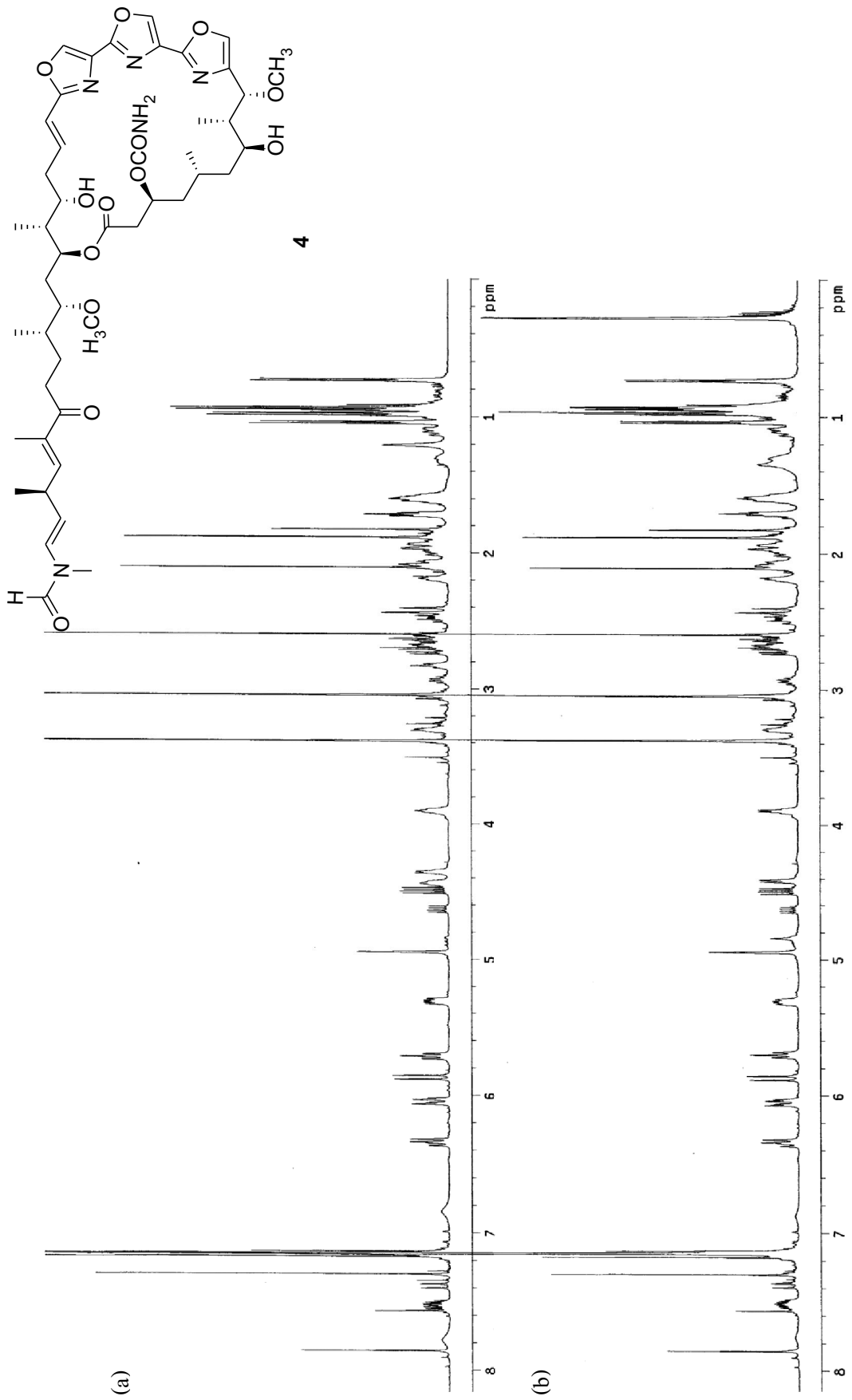

^{1}H NMR (a) and D_2O-exchange spectra (b) of **4** (500 MHz, C_6D_6)

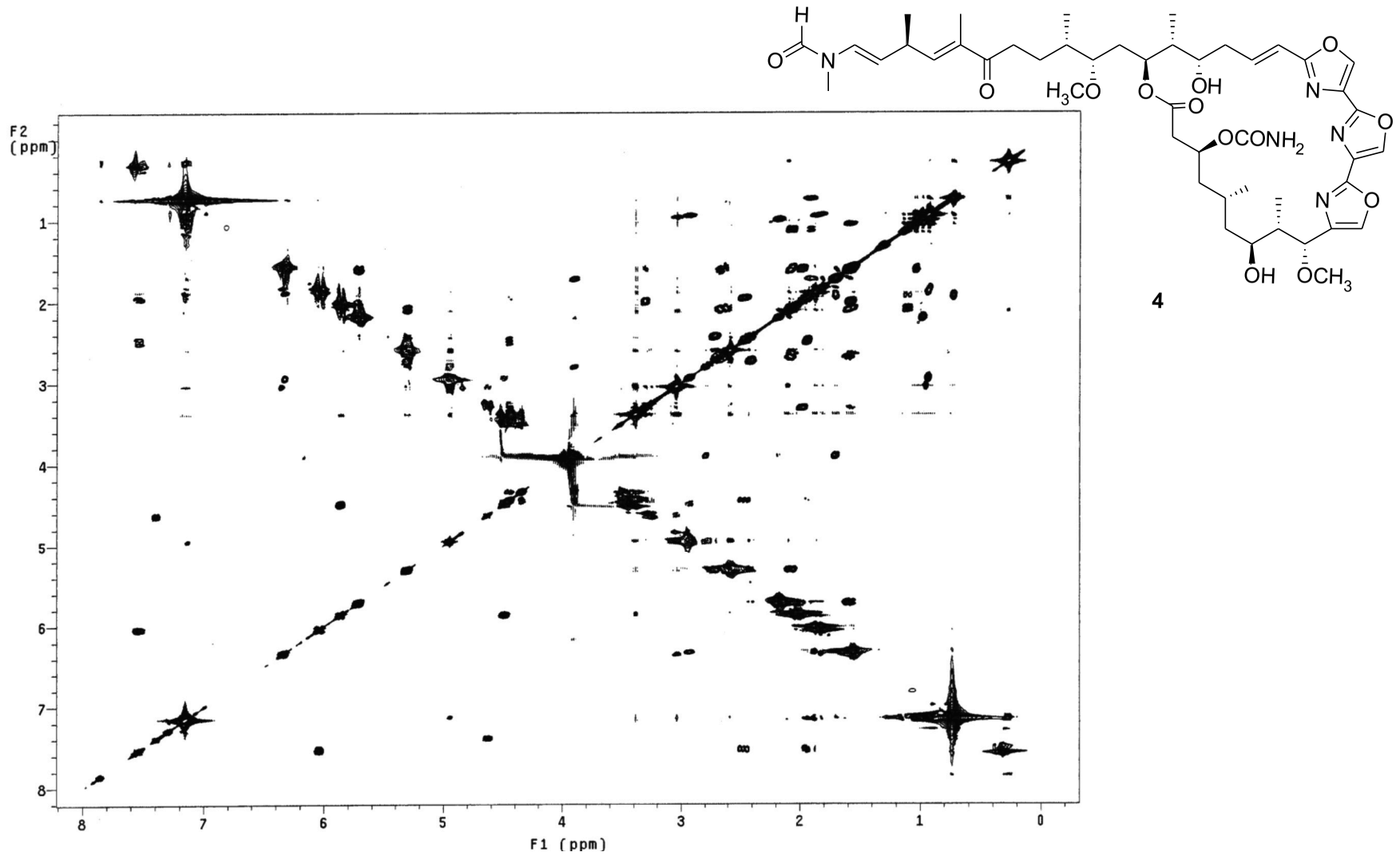

4

^{1}H-^{1}H COSY spectrum of **4** (500 MHz, C_6D_6)

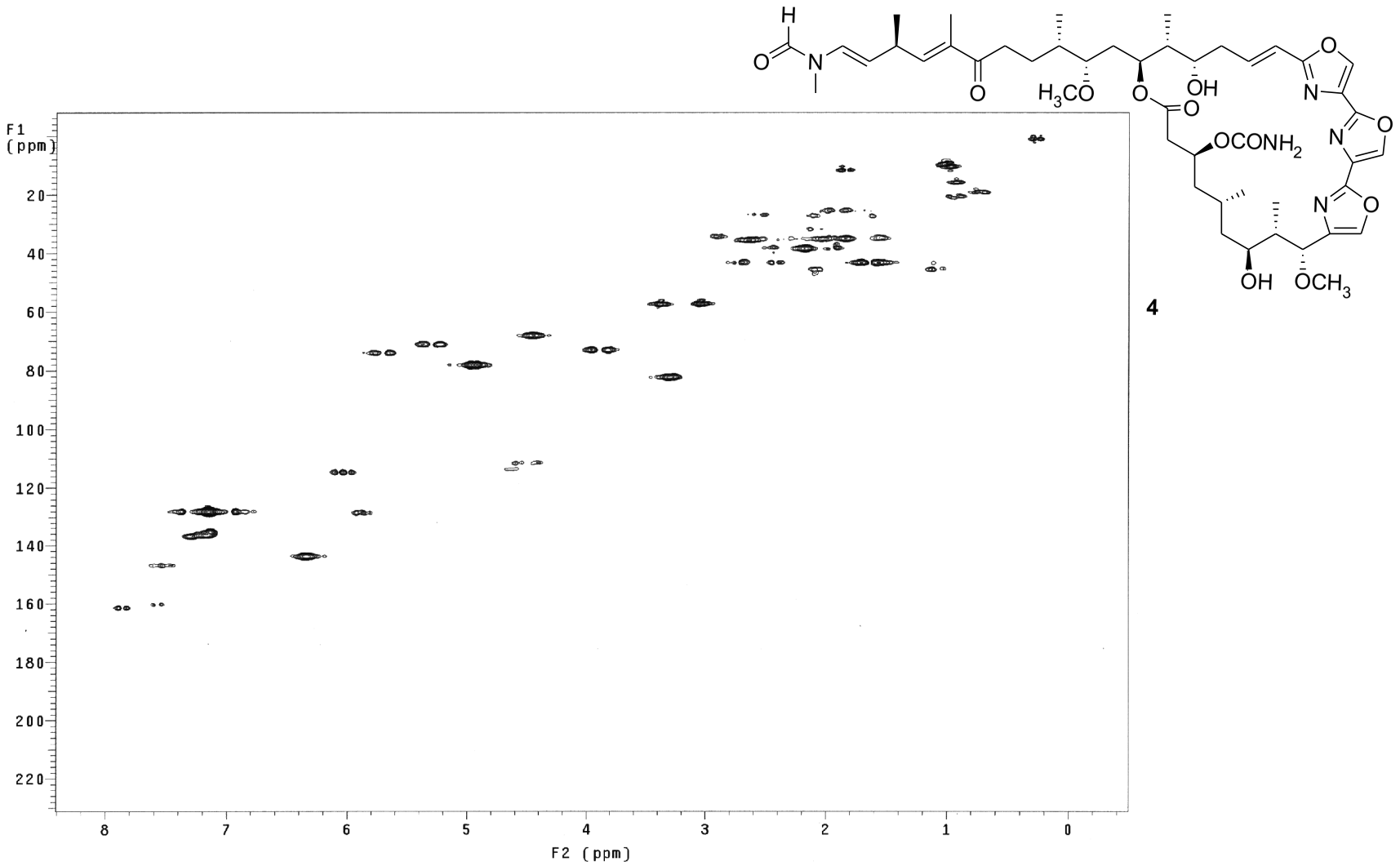

4

HMQC spectrum of **4** (500 MHz, C_6D_6)

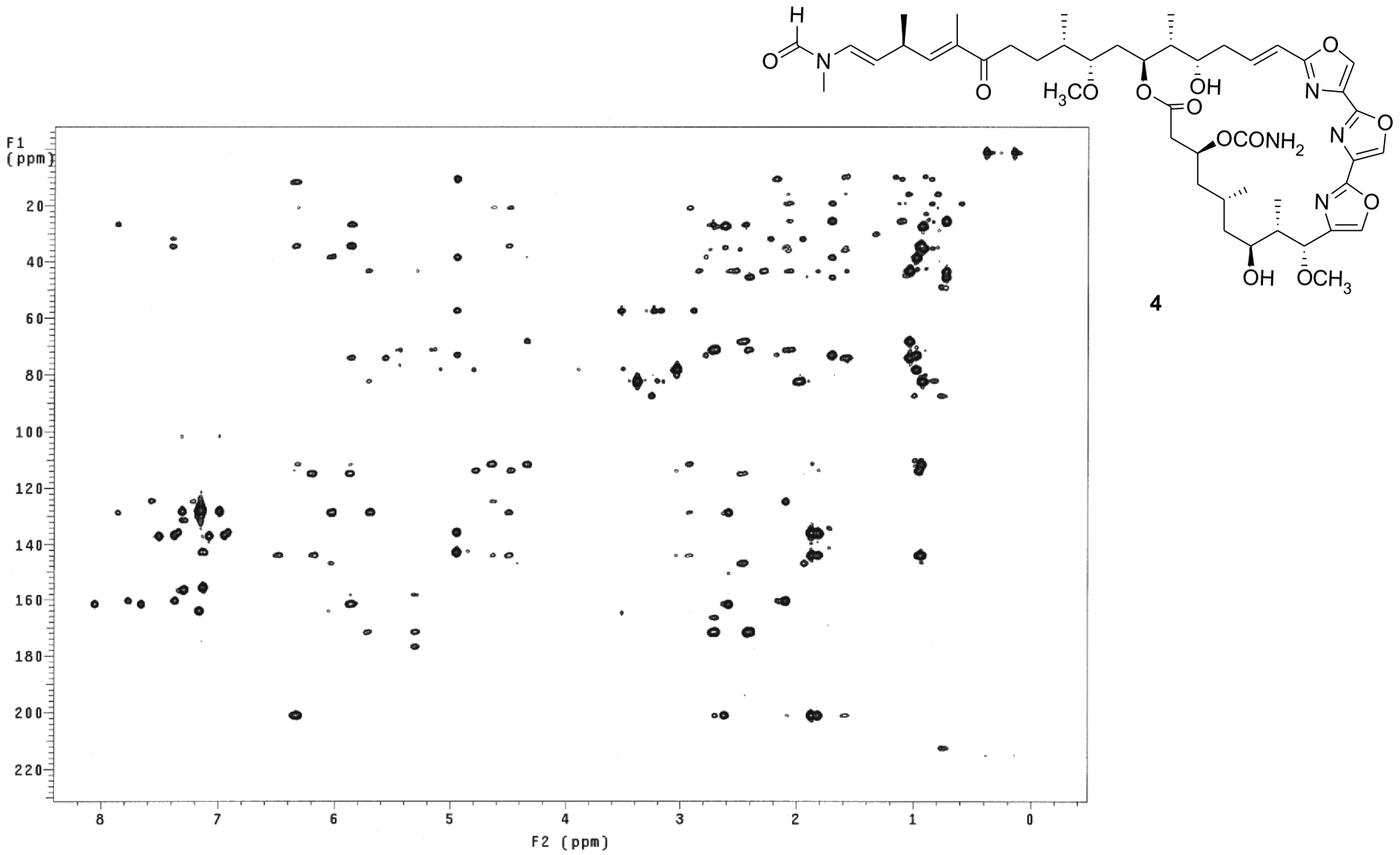

4

HMBC spectrum of **4** (500 MHz, C_6D_6)

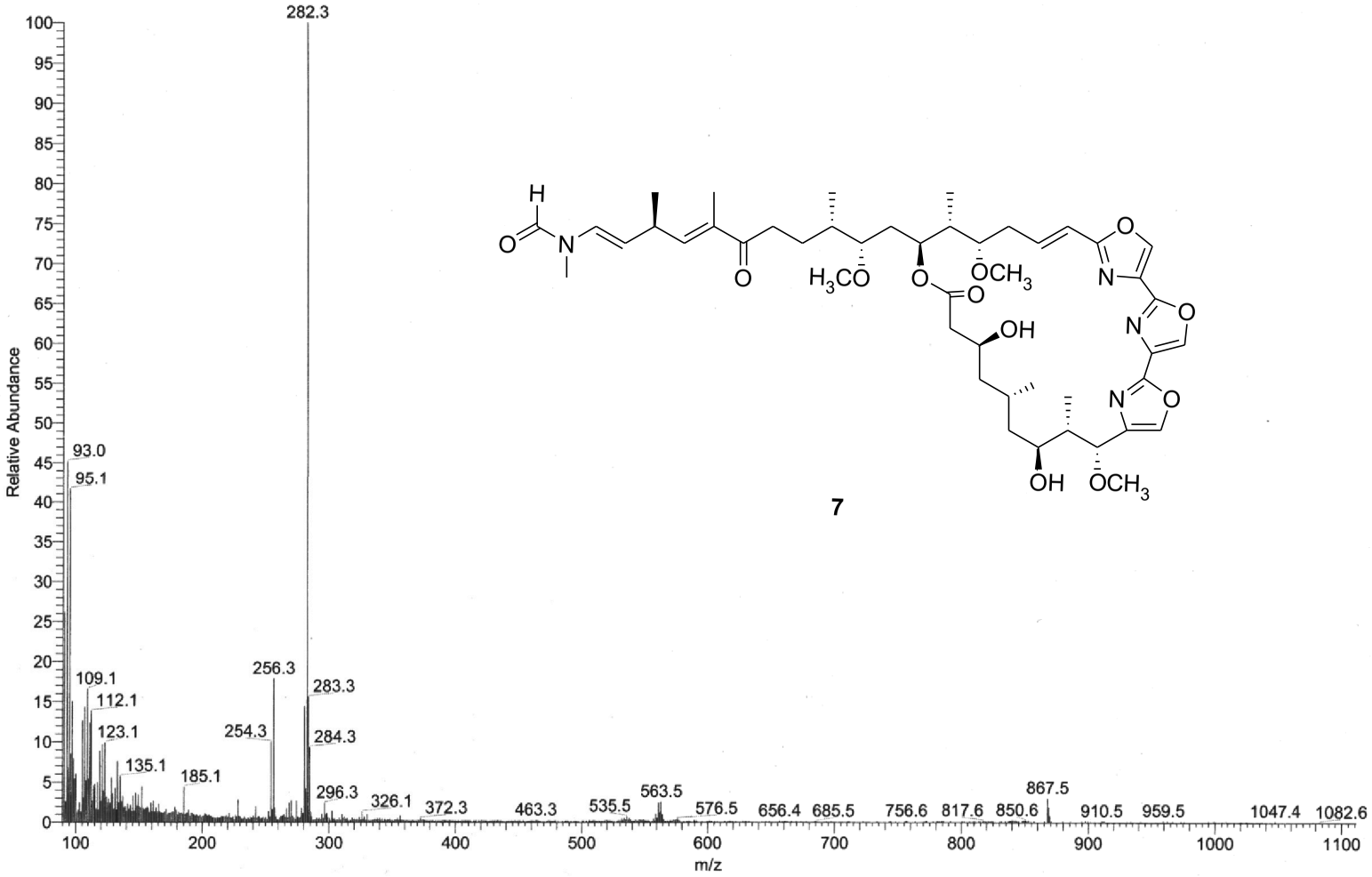

7

FABMS spectrum of **7**

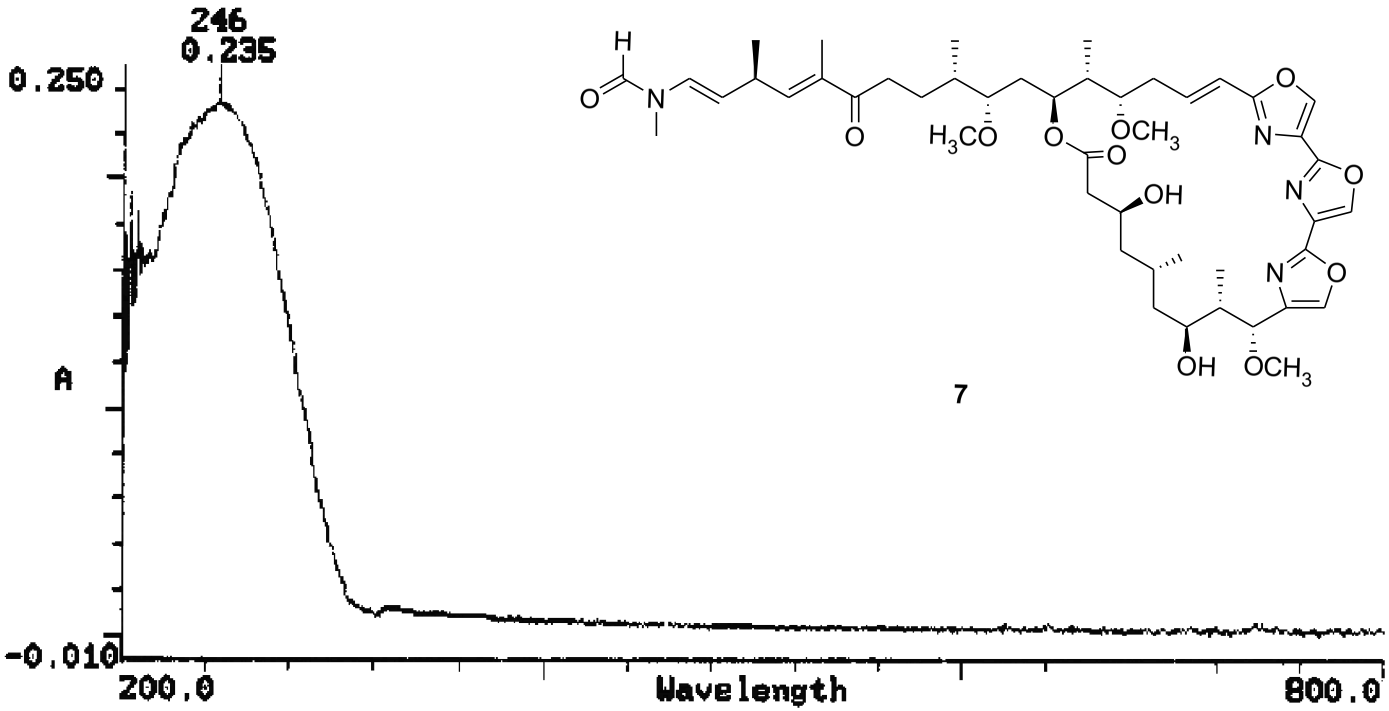

7

UV spectrum of **7** (CH_3OH)

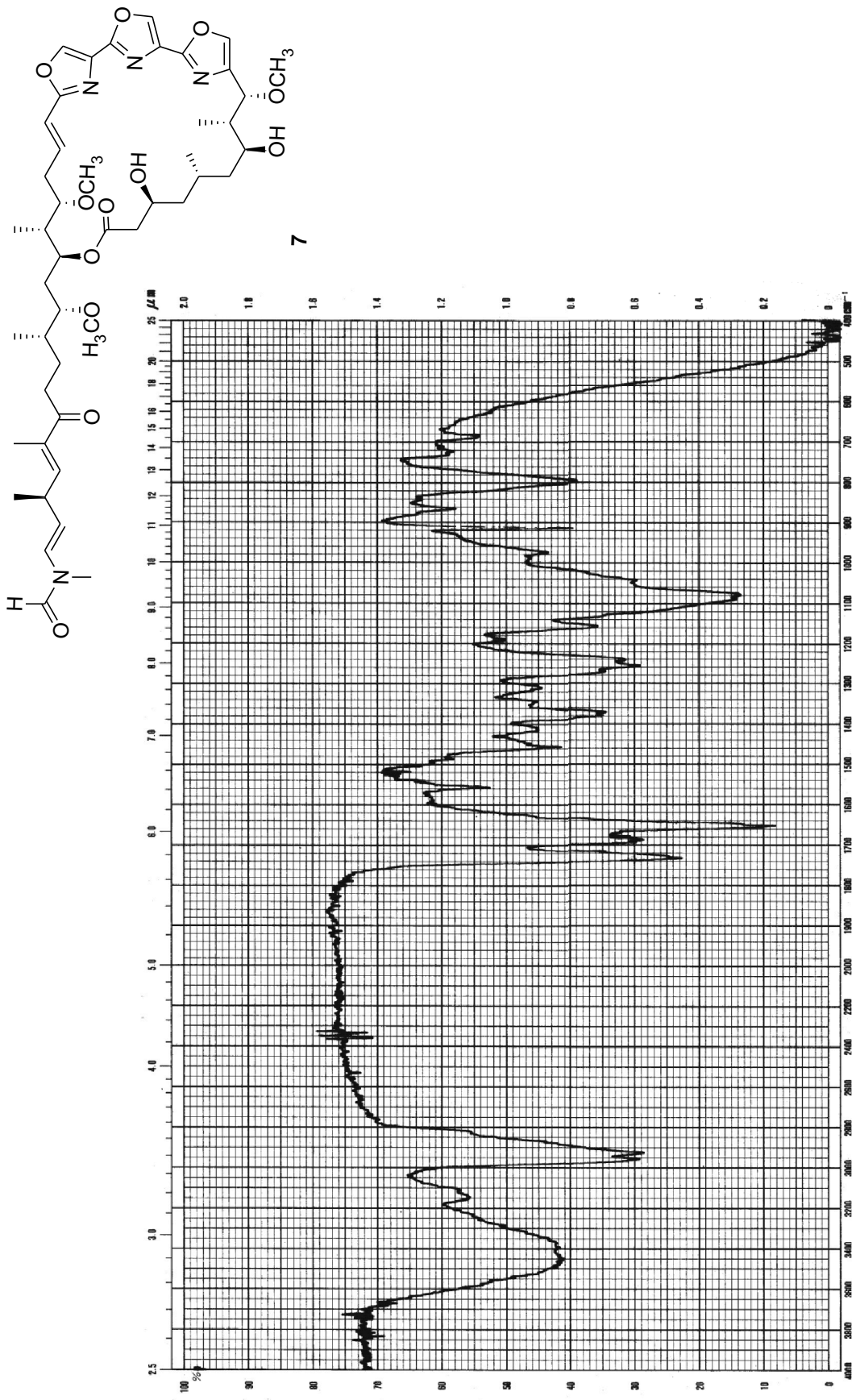

IR spectrum of **7** (neat)

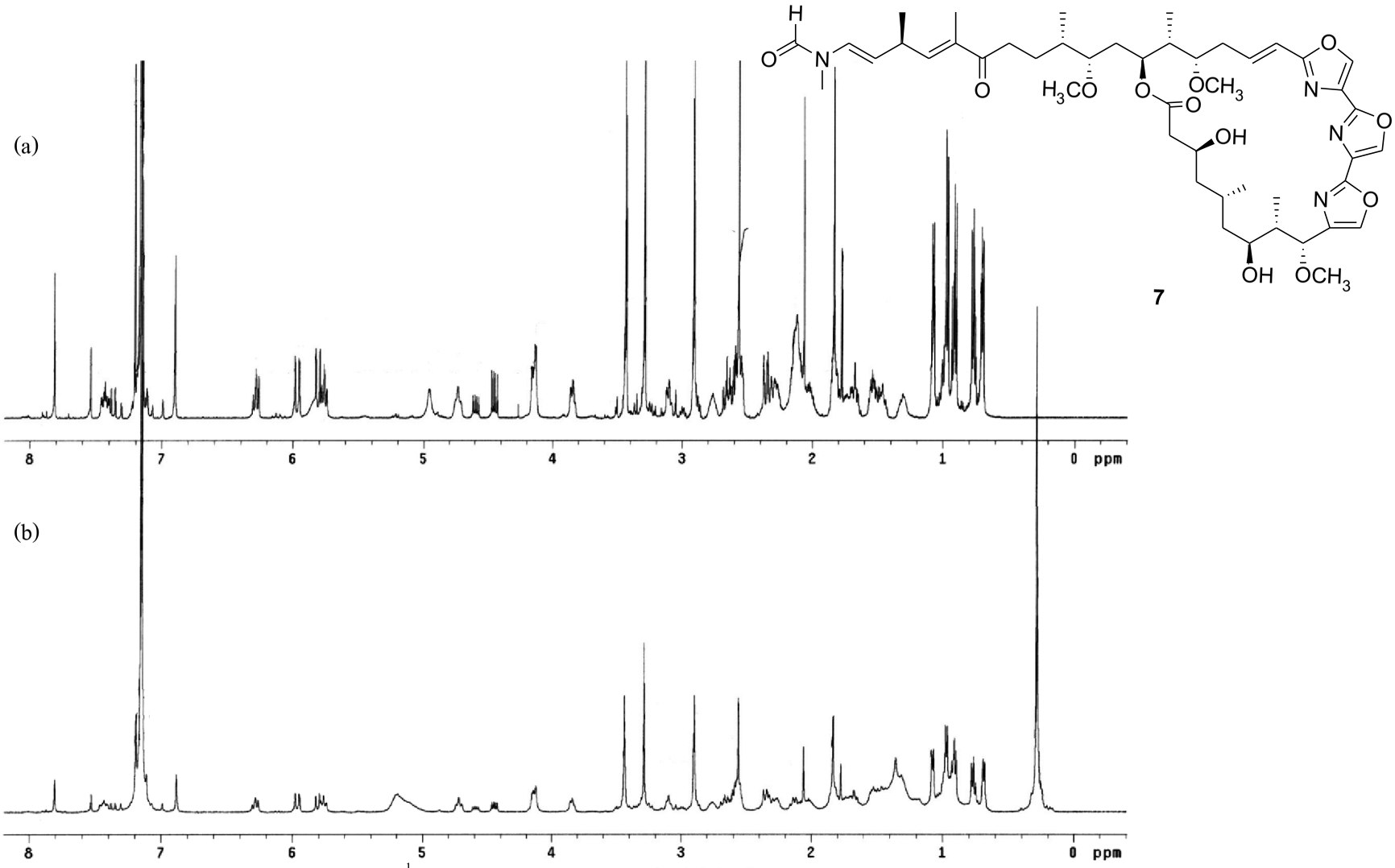

7

^{1}H NMR (a) and D_2O-exchange spectra (b) of **7** (500 MHz, C_6D_6)

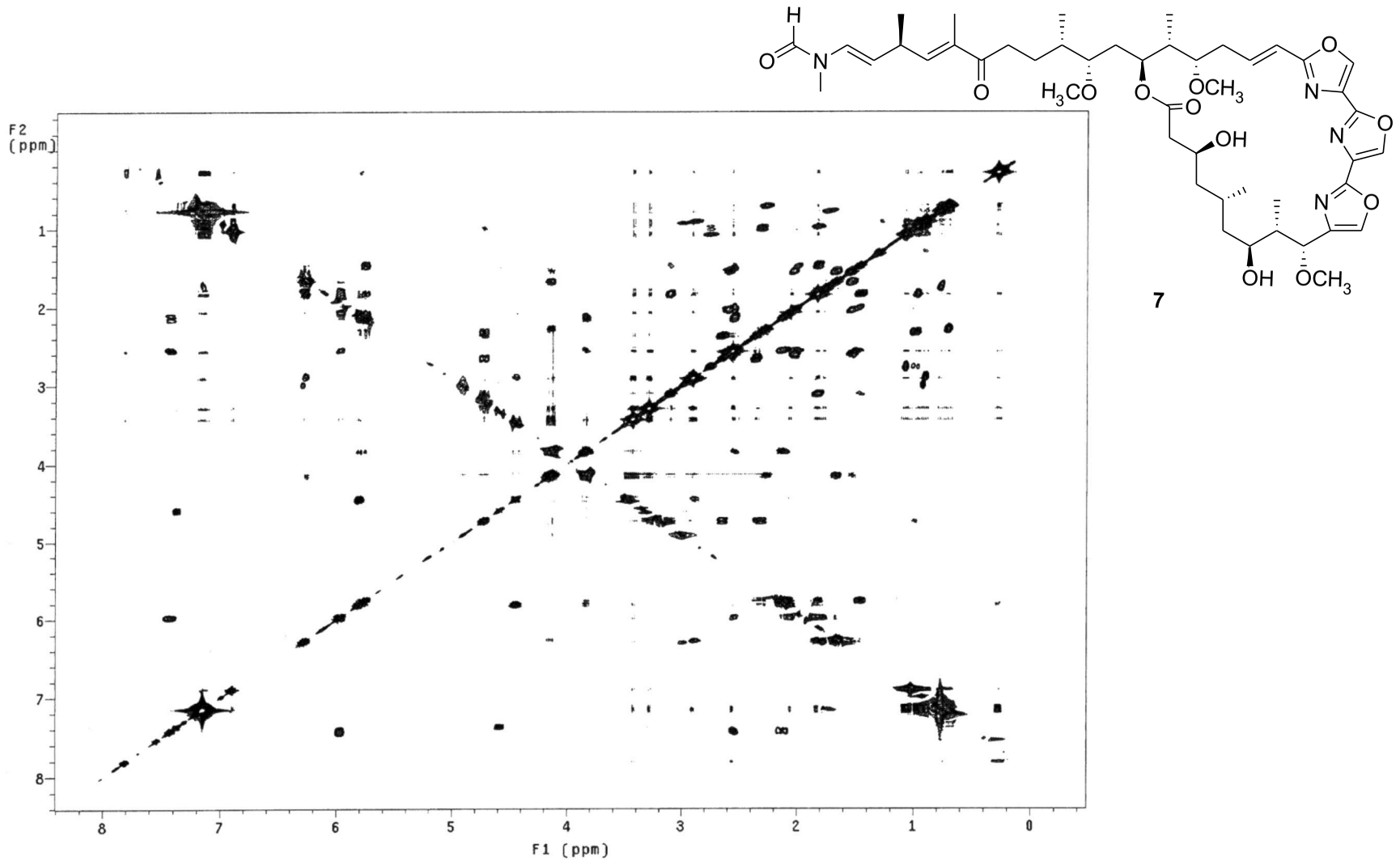

^{1}H-^{1}H COSY spectrum of **7** (500 MHz, C_6D_6)

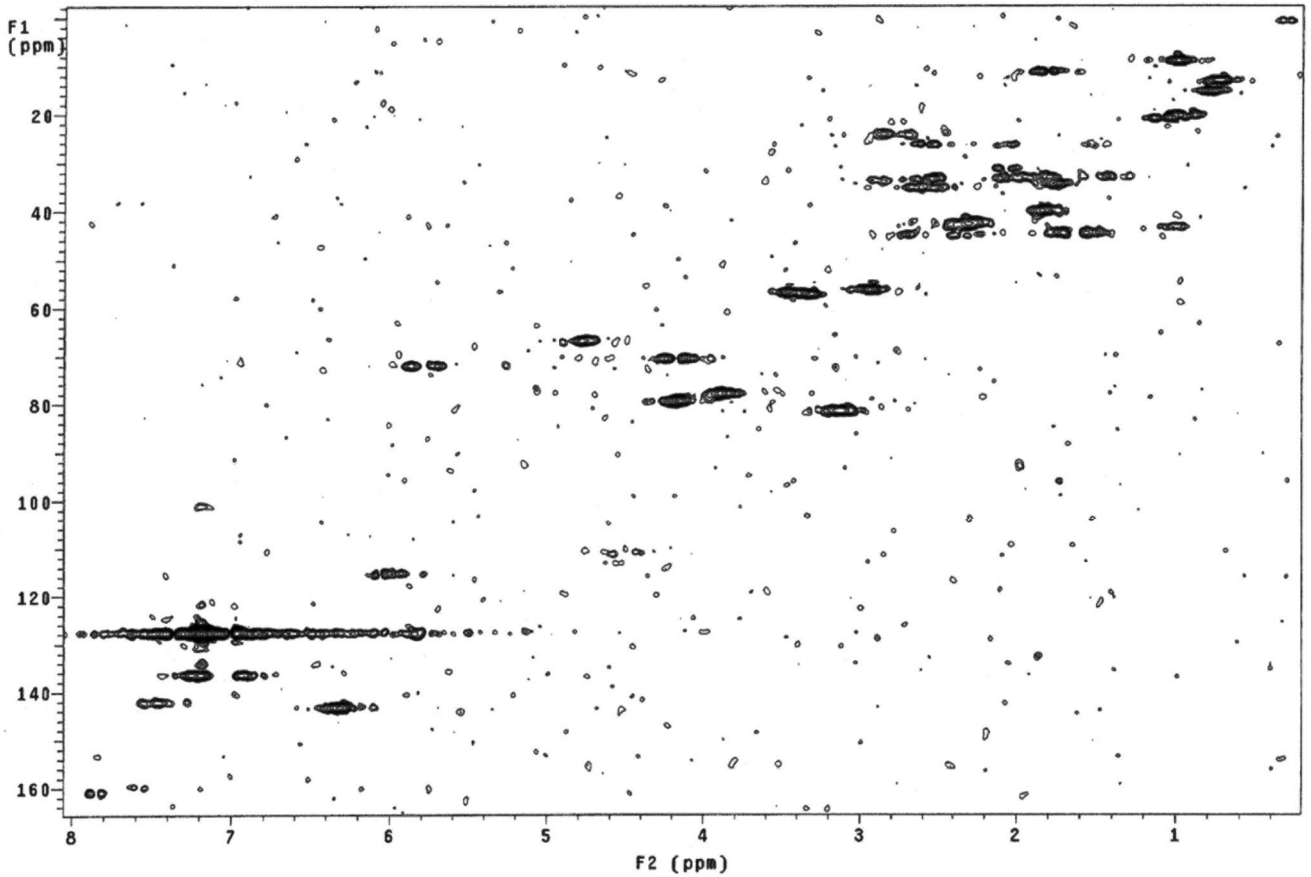

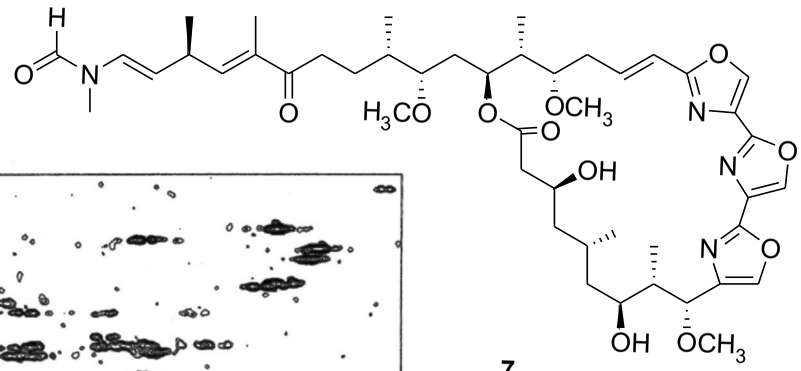

7

HMQC spectrum of **7** (500 MHz, C_6D_6)

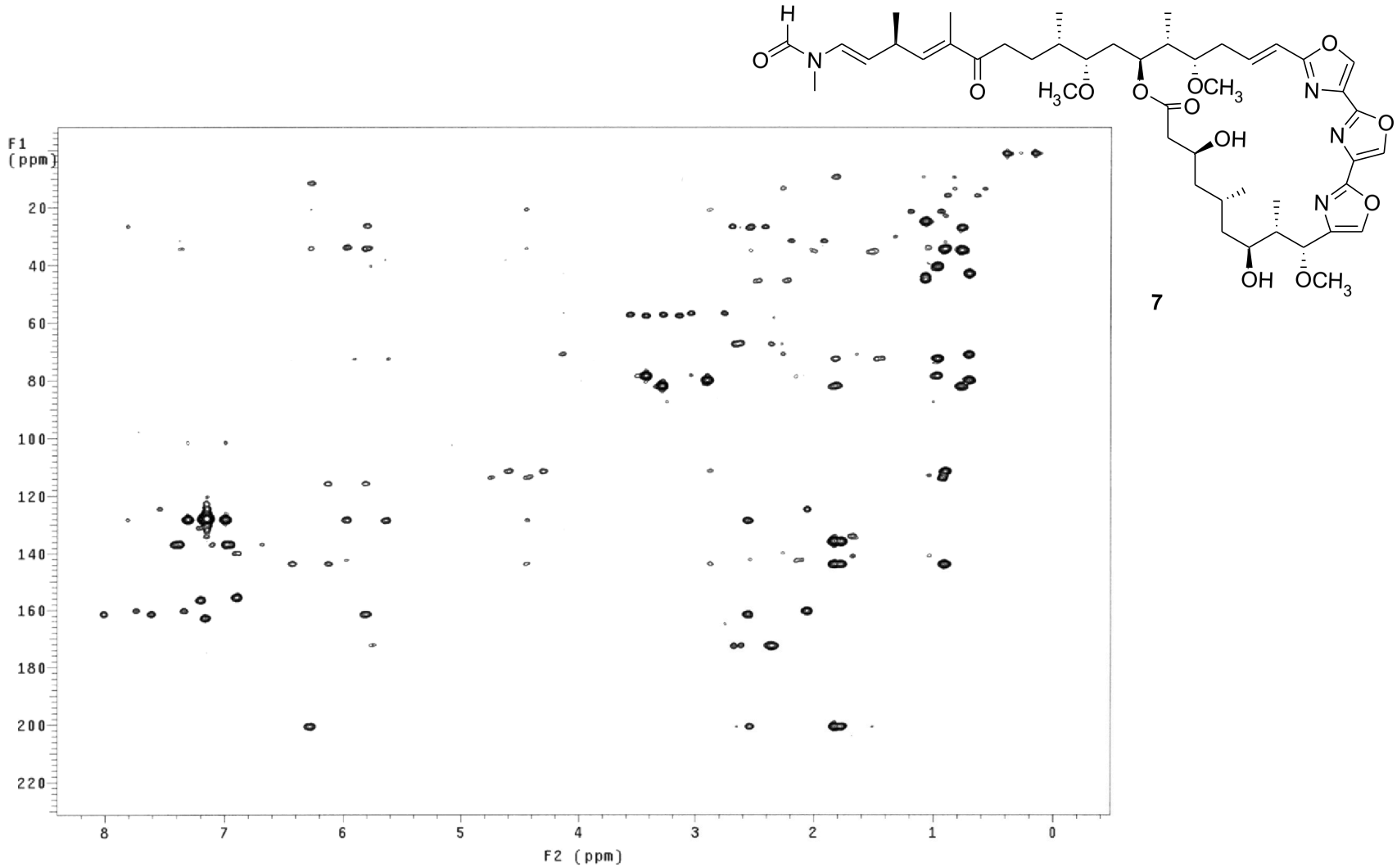

7

HMBC spectrum of **7** (500 MHz, C_6D_6)

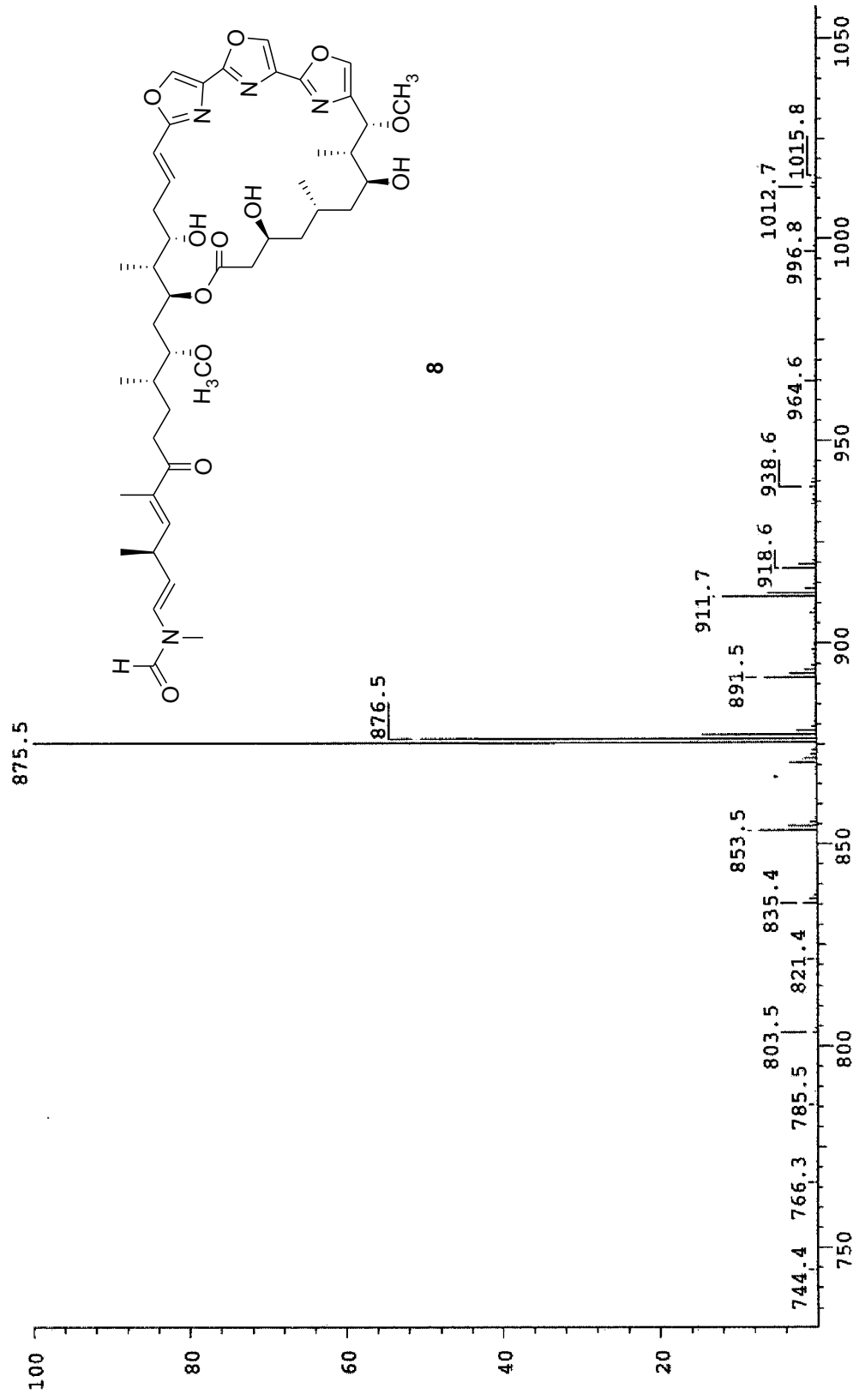

ESIMS spectrum of **8**

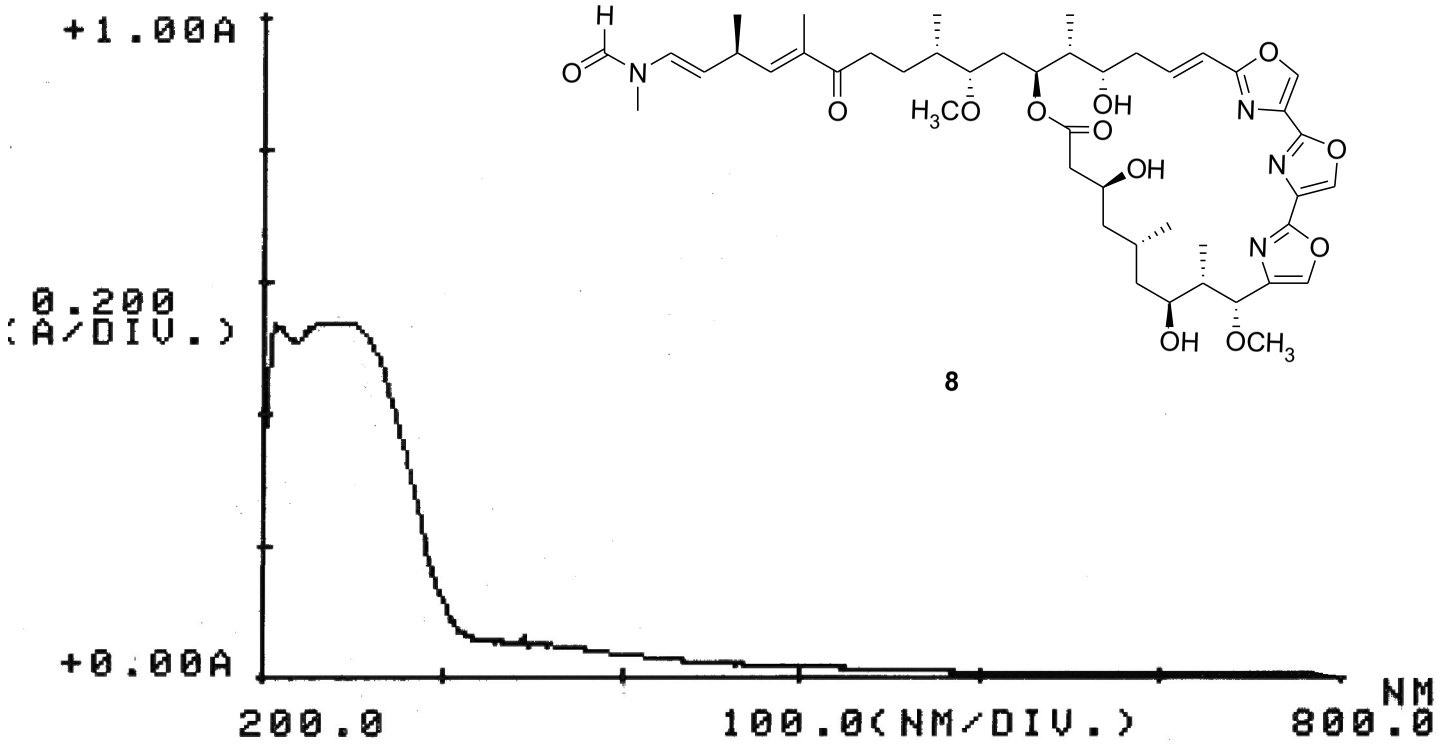

8

UV spectrum of **8** (CH_3OH)

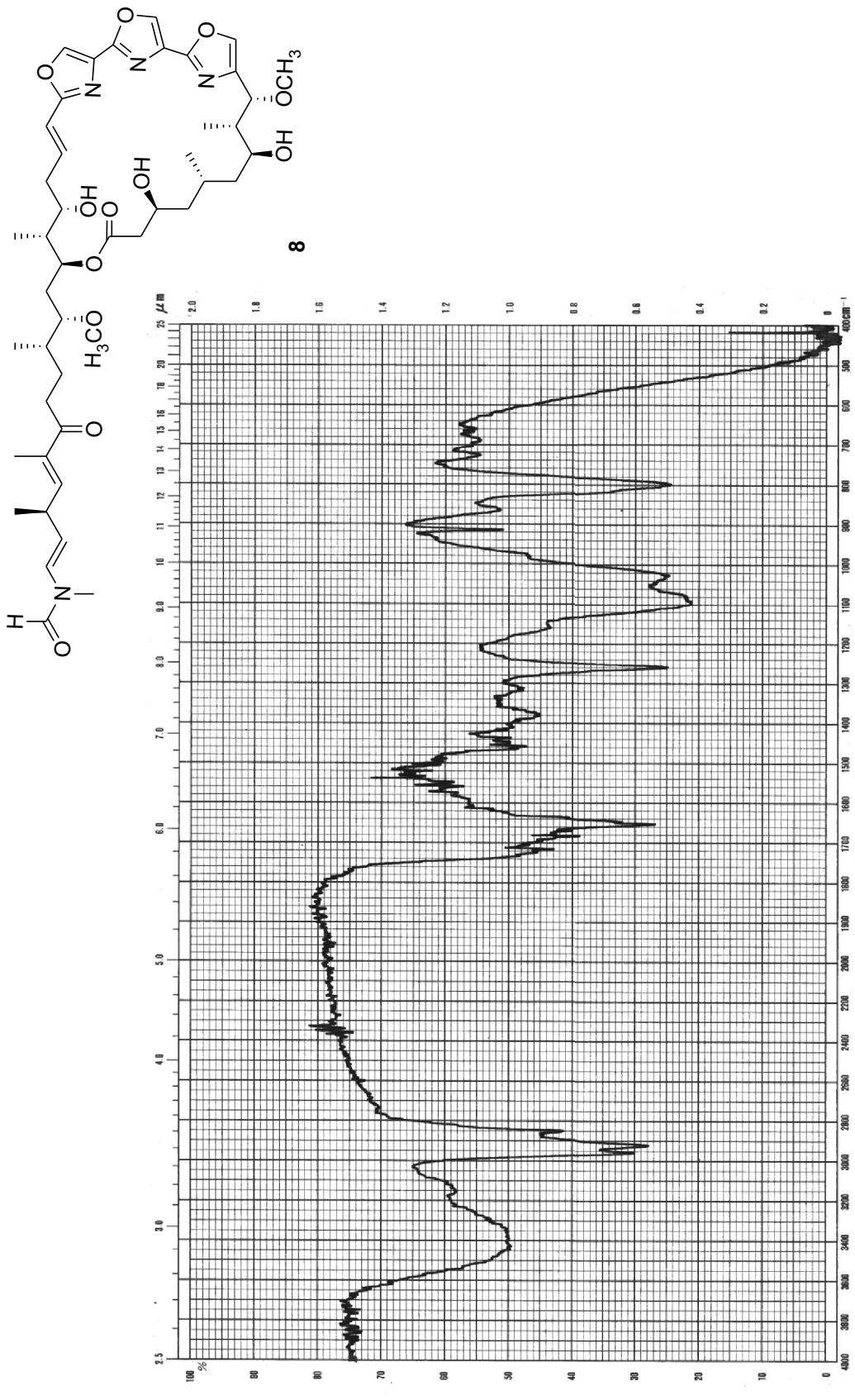

8

IR spectrum of **8** (neat)

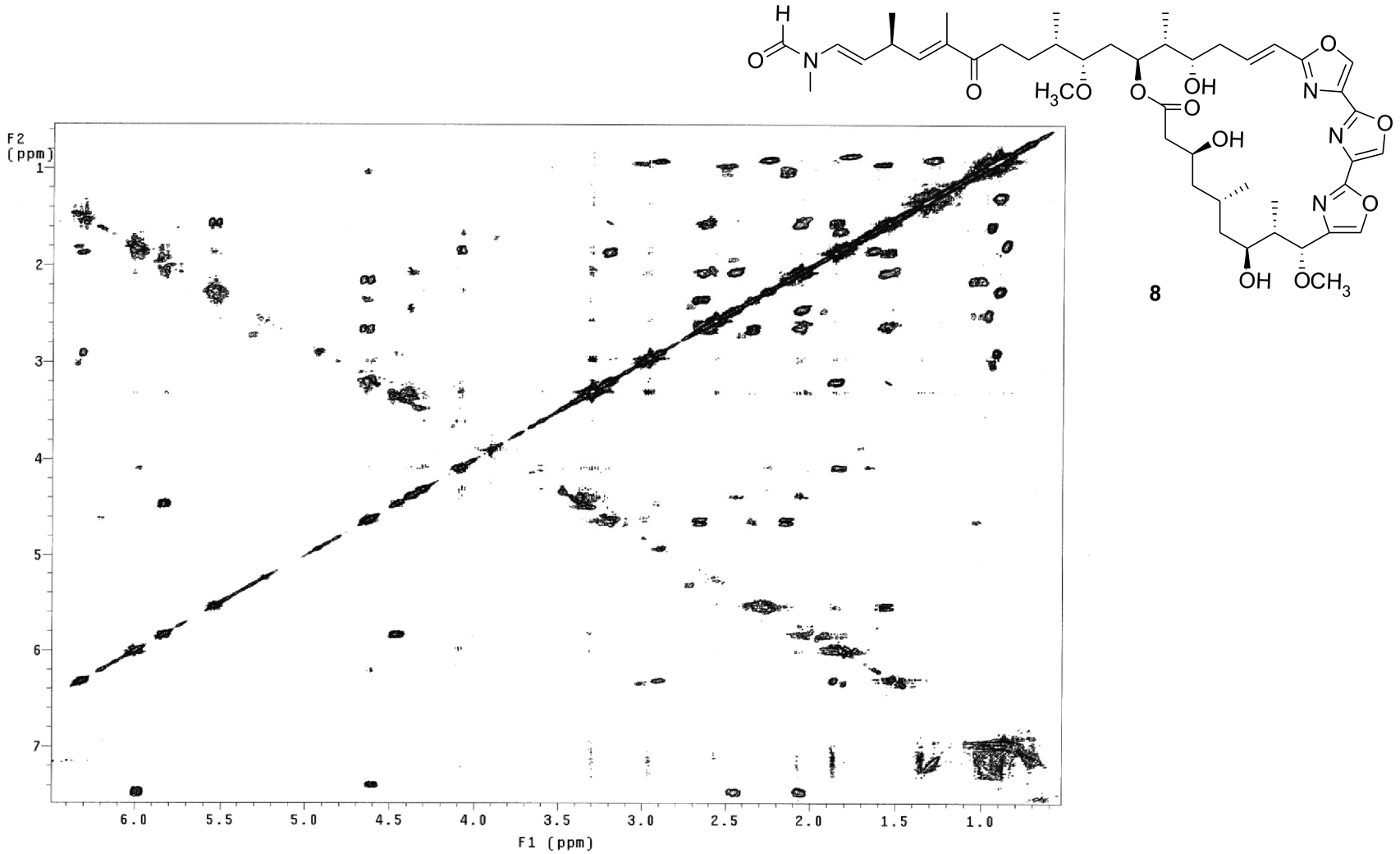

8

^{1}H-^{1}H COSY spectrum of **8** (500 MHz, C_6D_6)

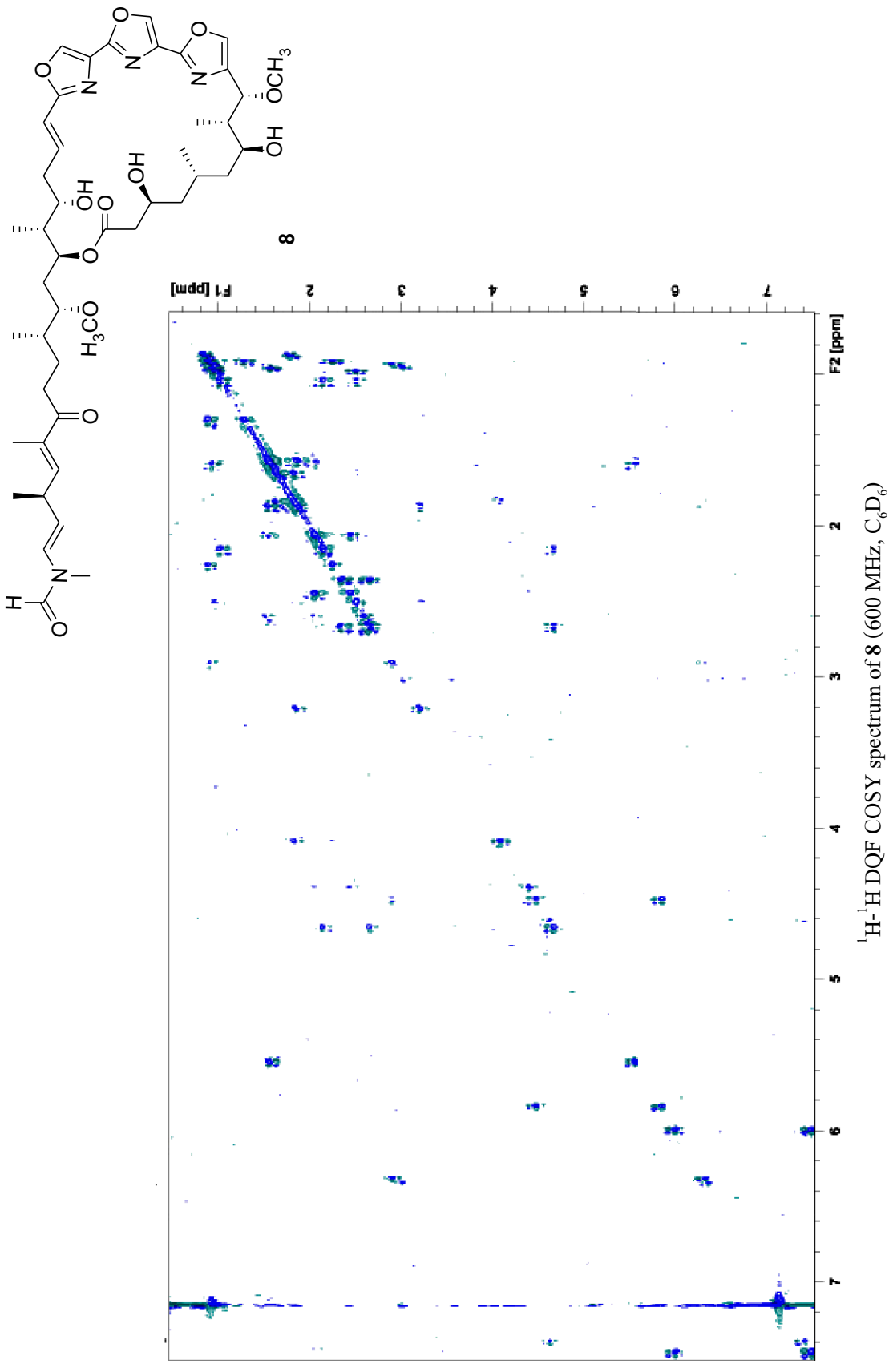

8

^{1}H-^{1}H DQF COSY spectrum of **8** (600 MHz, C_6D_6)

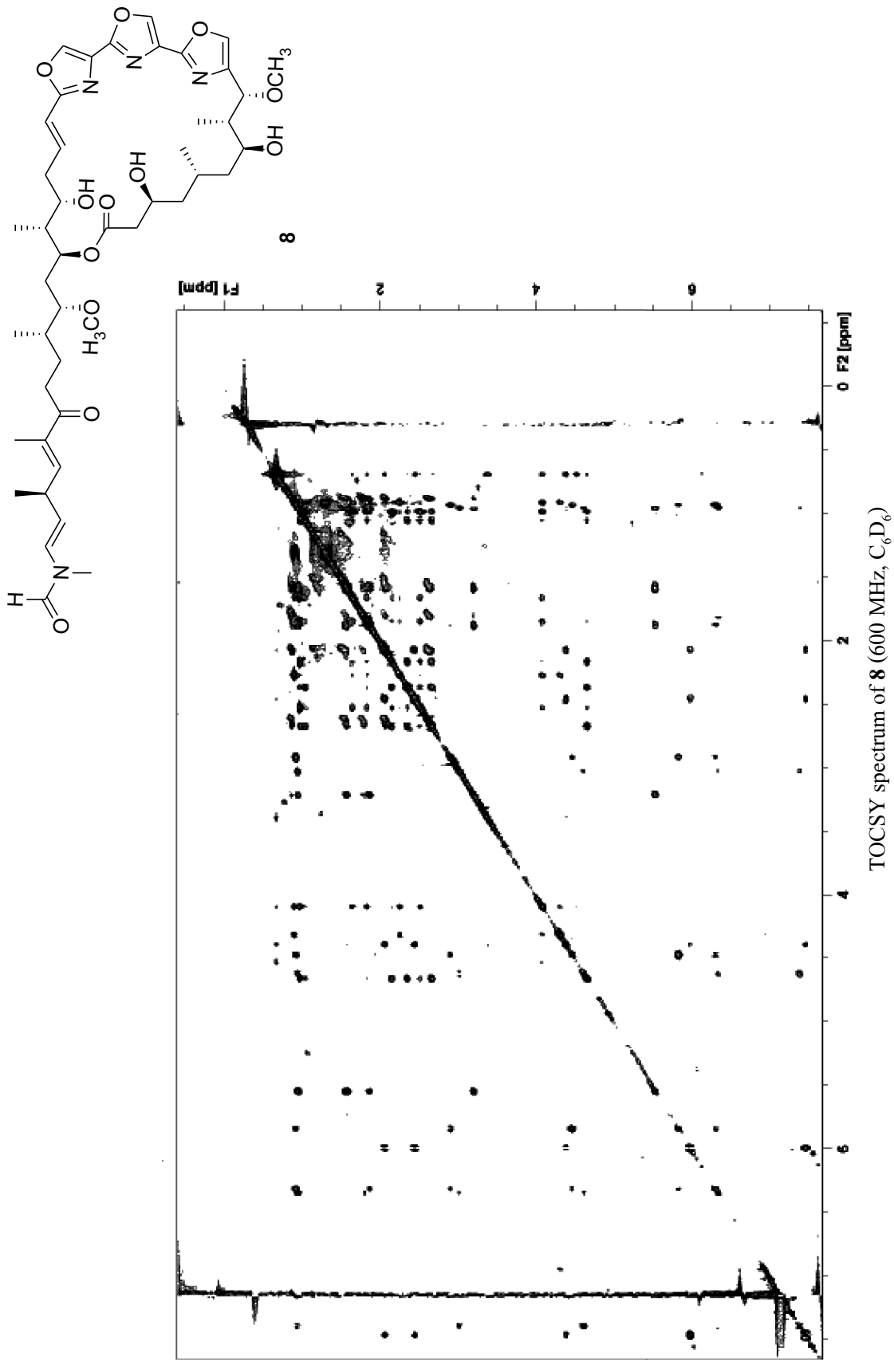

TOCSY spectrum of **8** (600 MHz, C_6D_6)

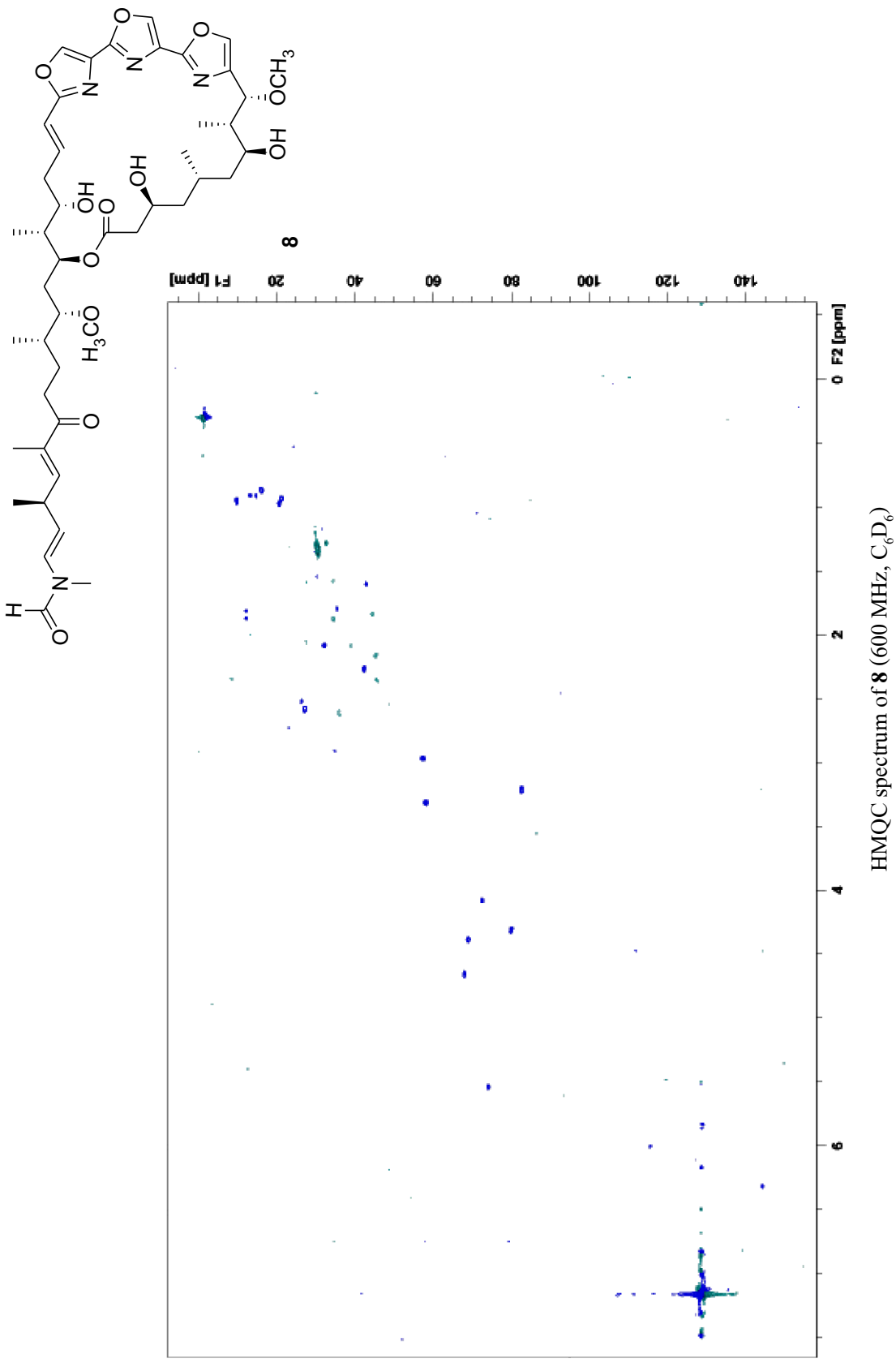

HMQC spectrum of **8** (600 MHz, C_6D_6)

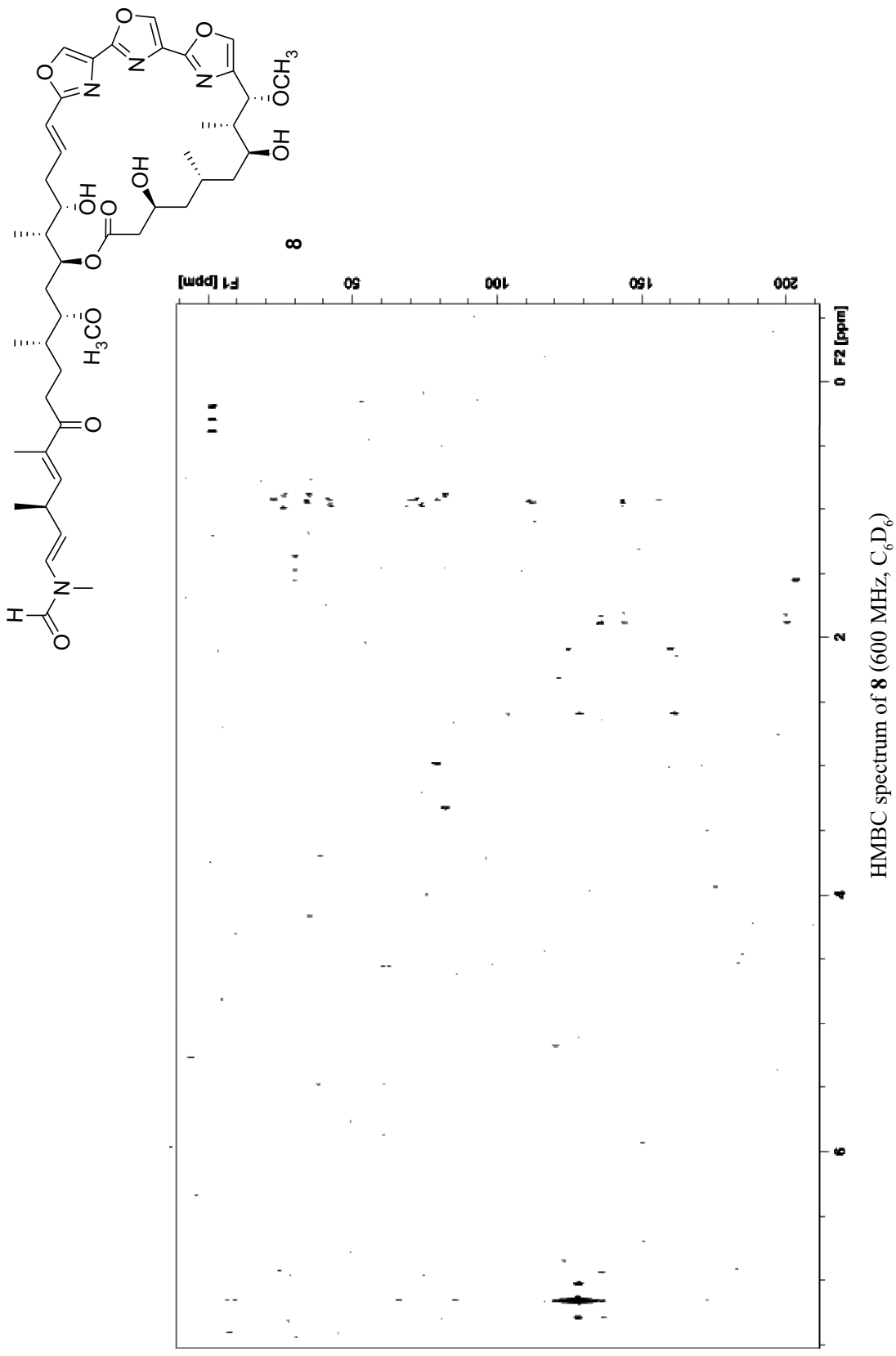

HMBC spectrum of **8** (600 MHz, C_6D_6)

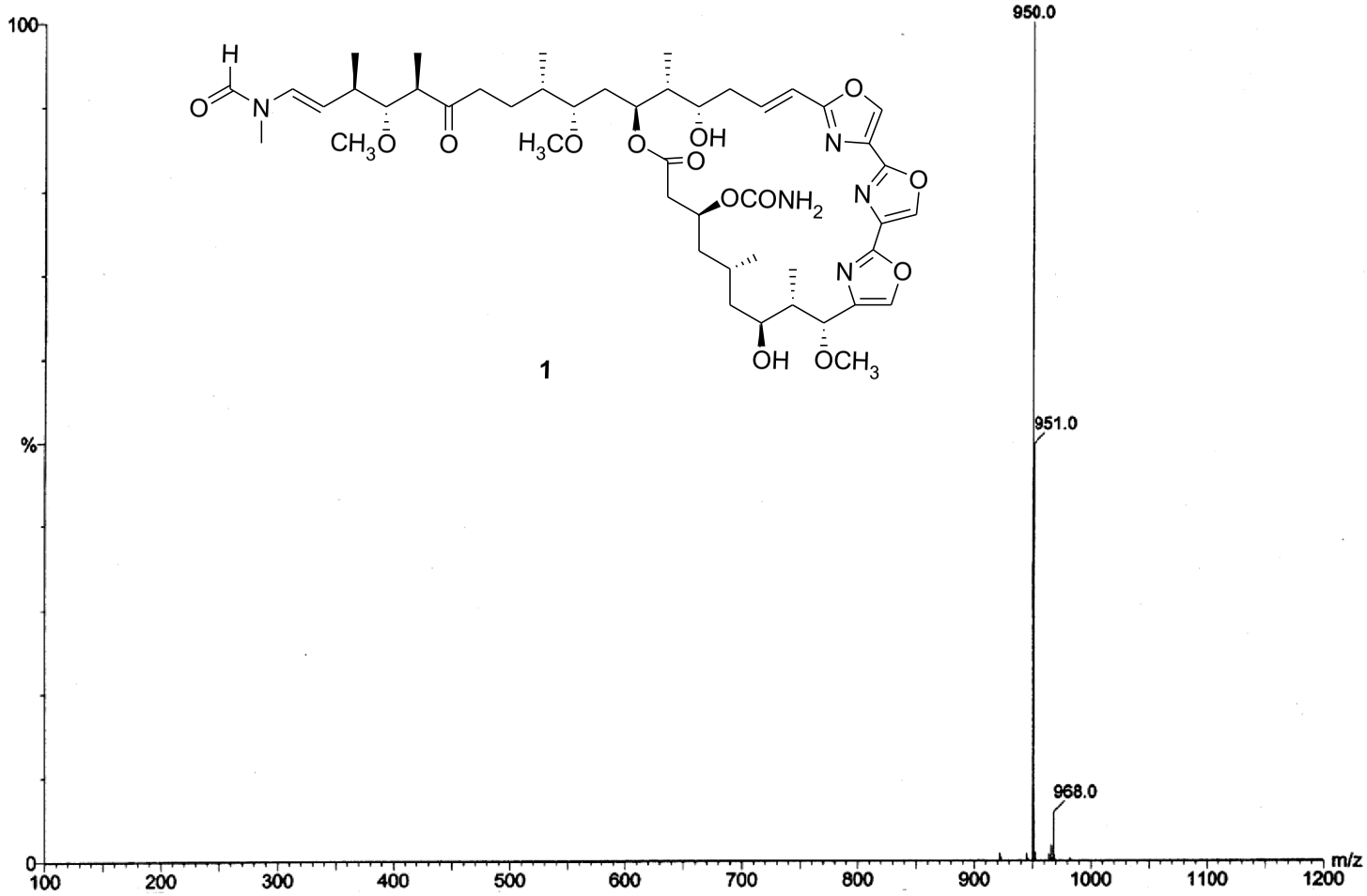

ESIMS spectrum of **1**

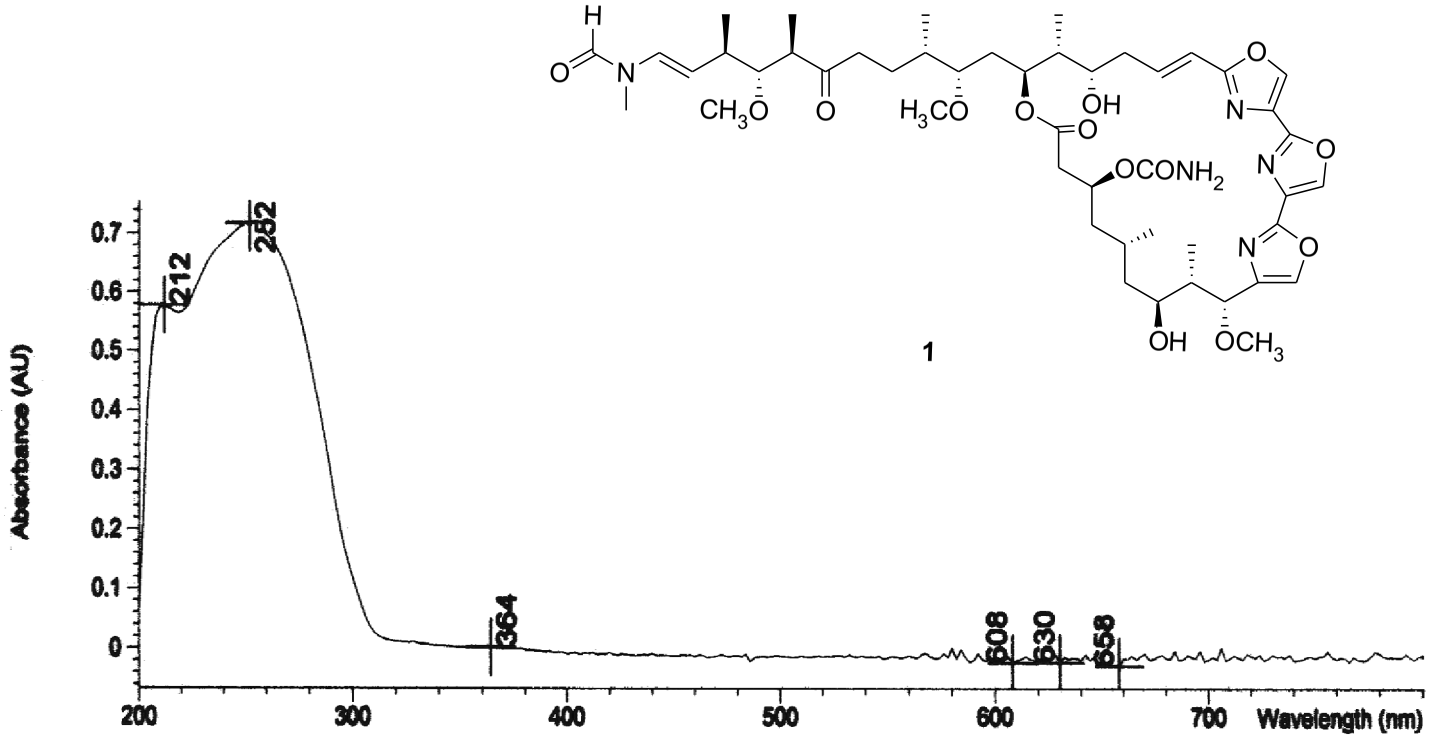

UV spectrum of **1** (CH_3OH)

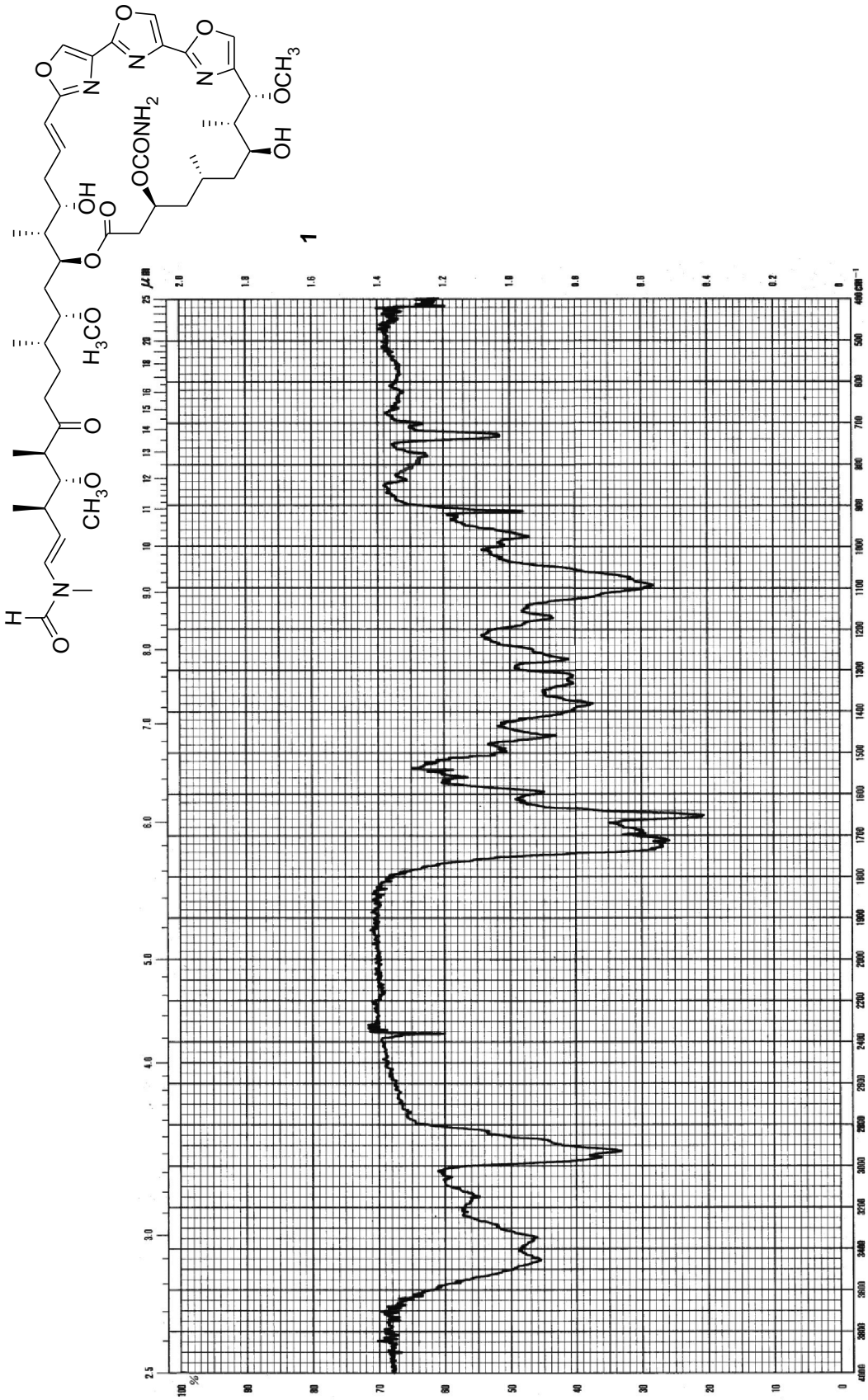

IR spectrum of **1** (neat)

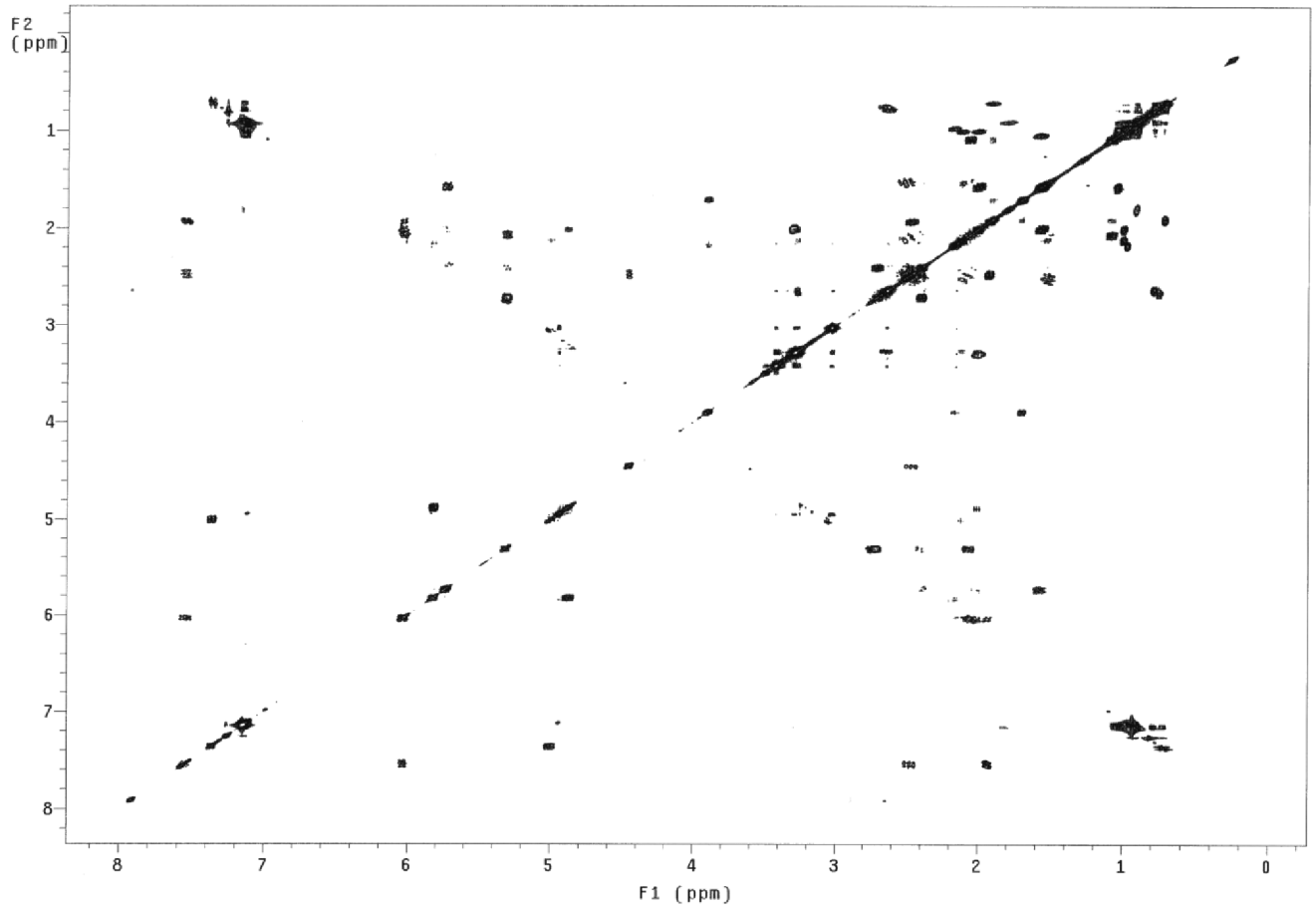

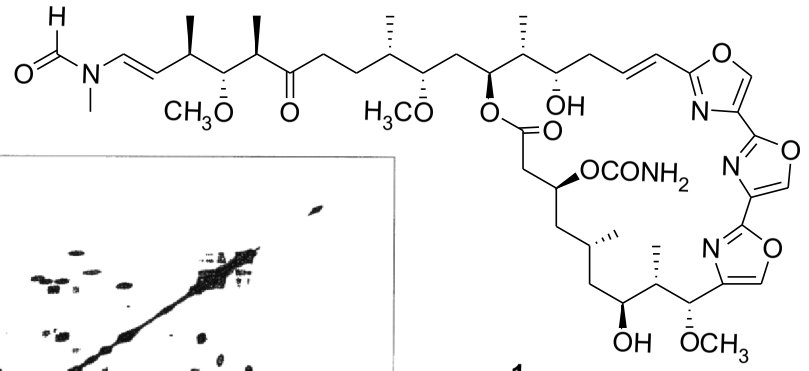

1

^{1}H-^{1}H COSY spectrum of **1** (500 MHz, C_6D_6)

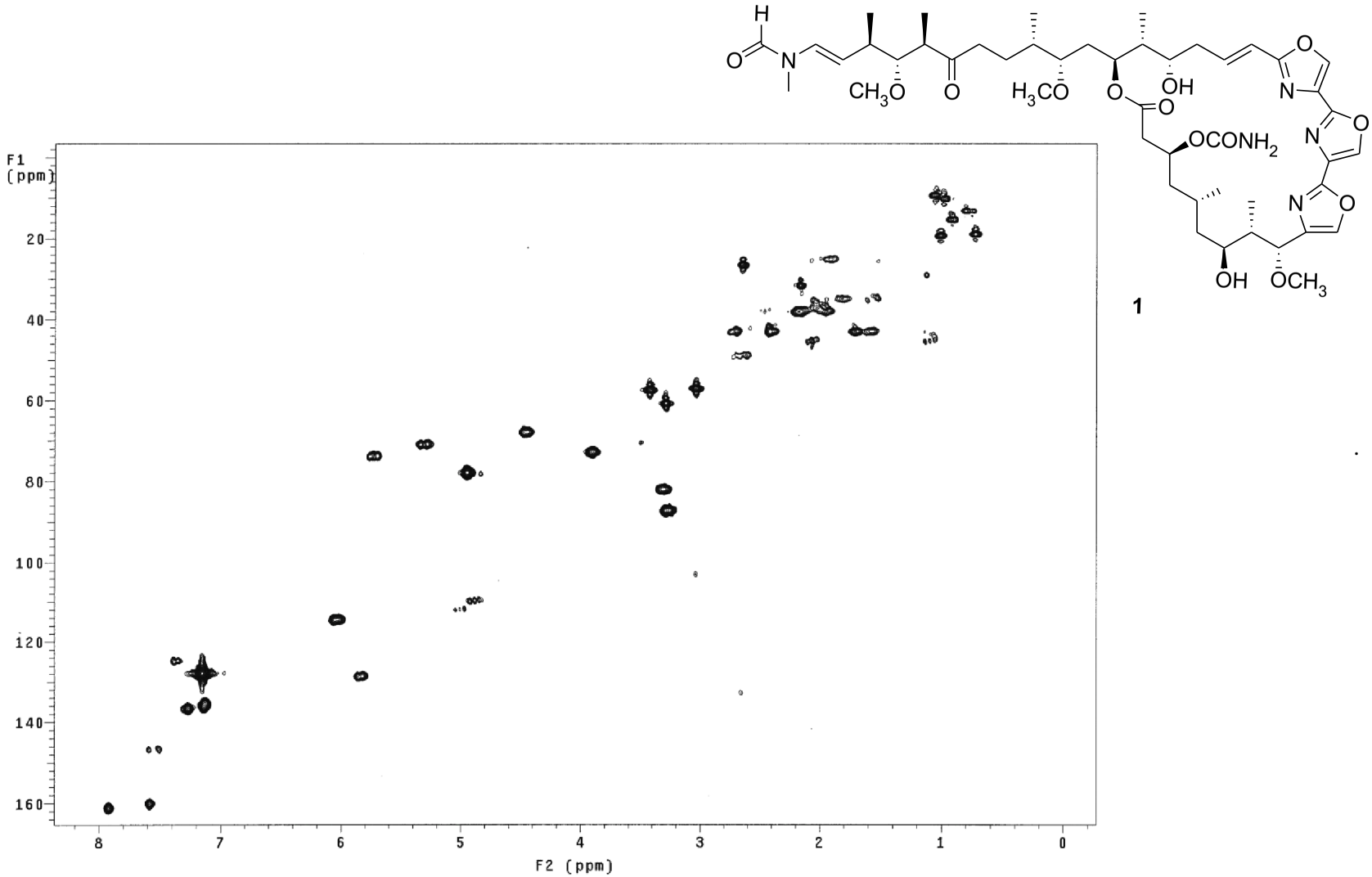

1

HMQC spectrum of **1** (500 MHz, C_6D_6)

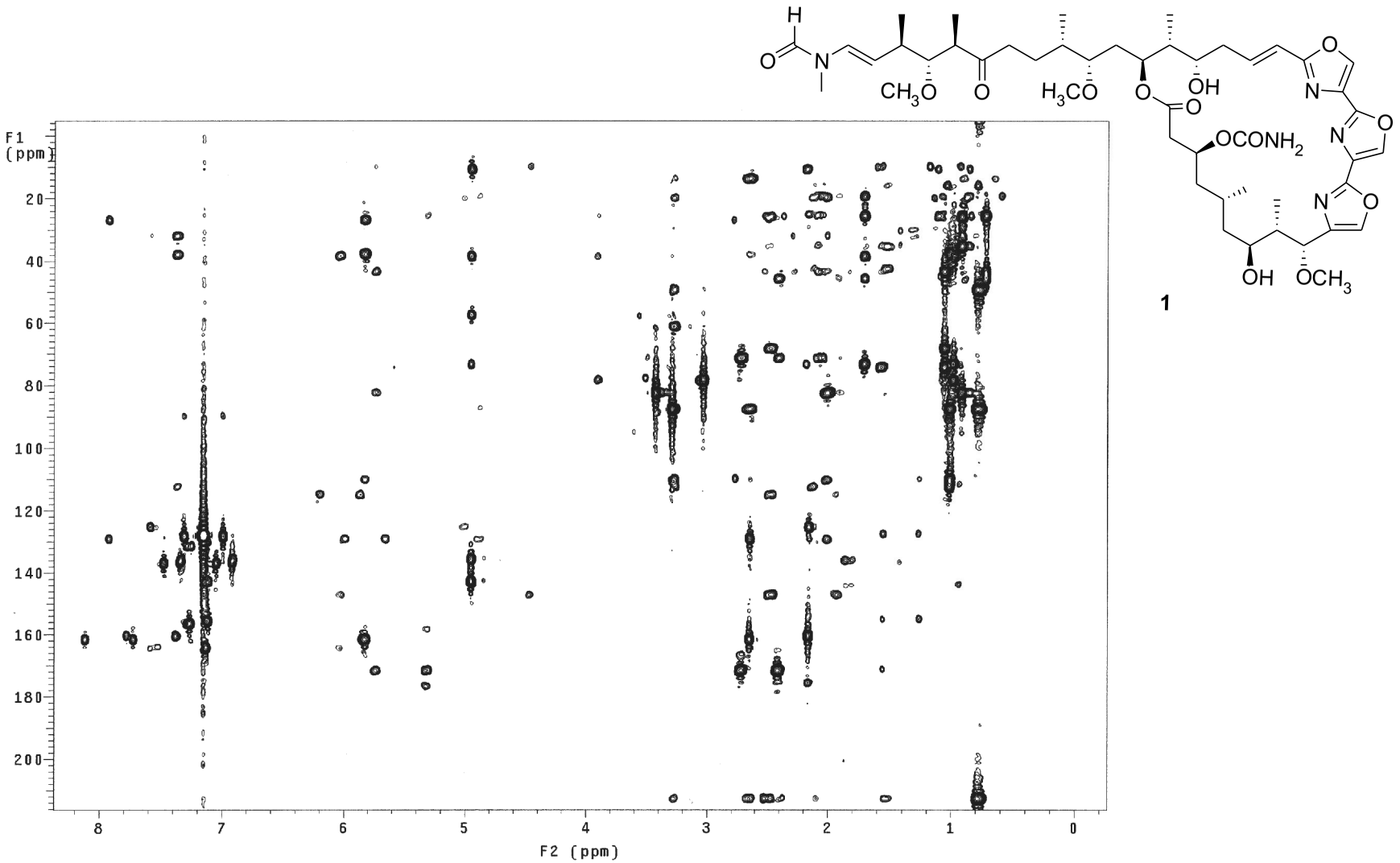

HMBC spectrum of **1** (500 MHz, C_6D_6)

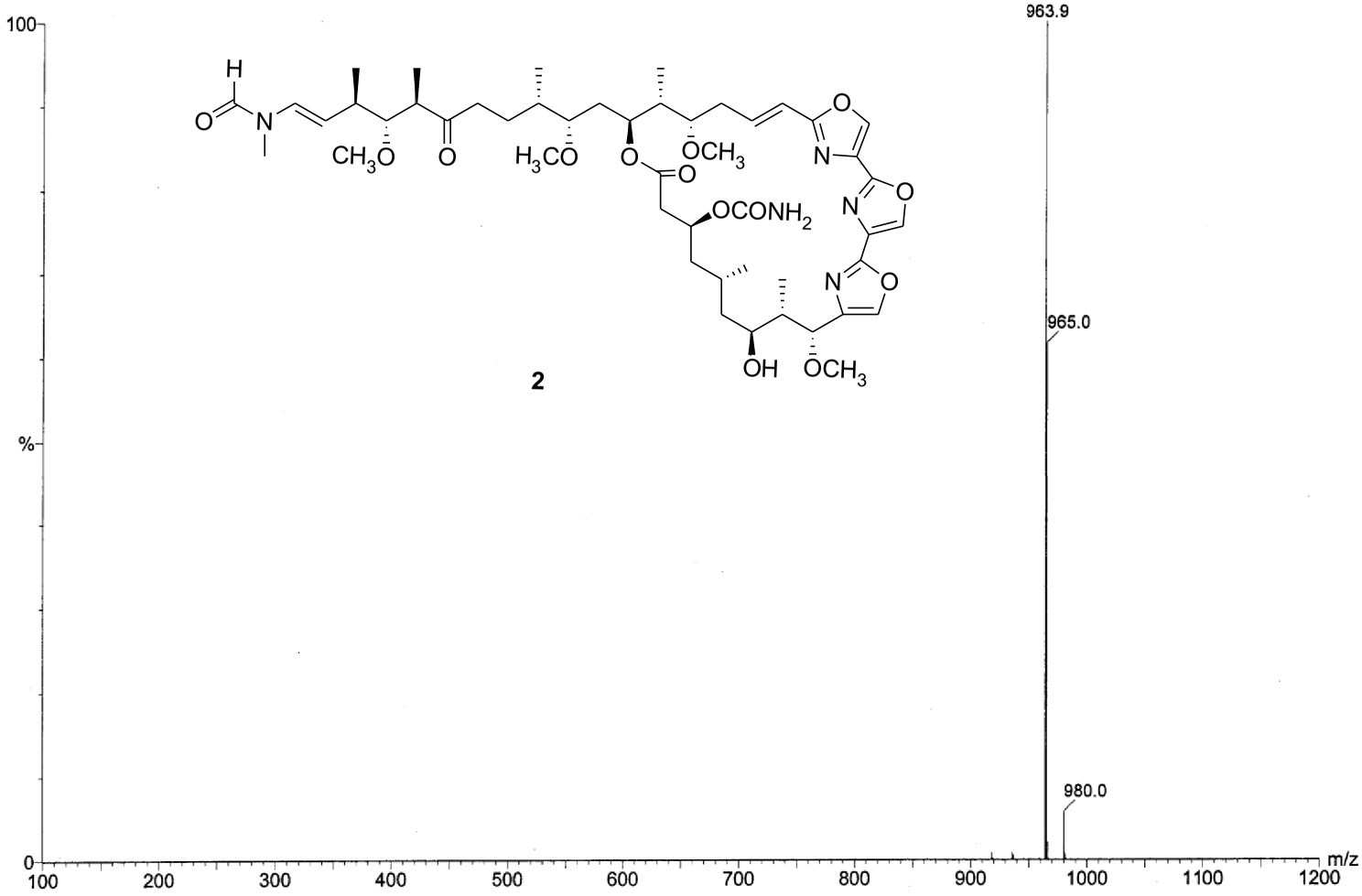

2

ESIMS spectrum of **2**

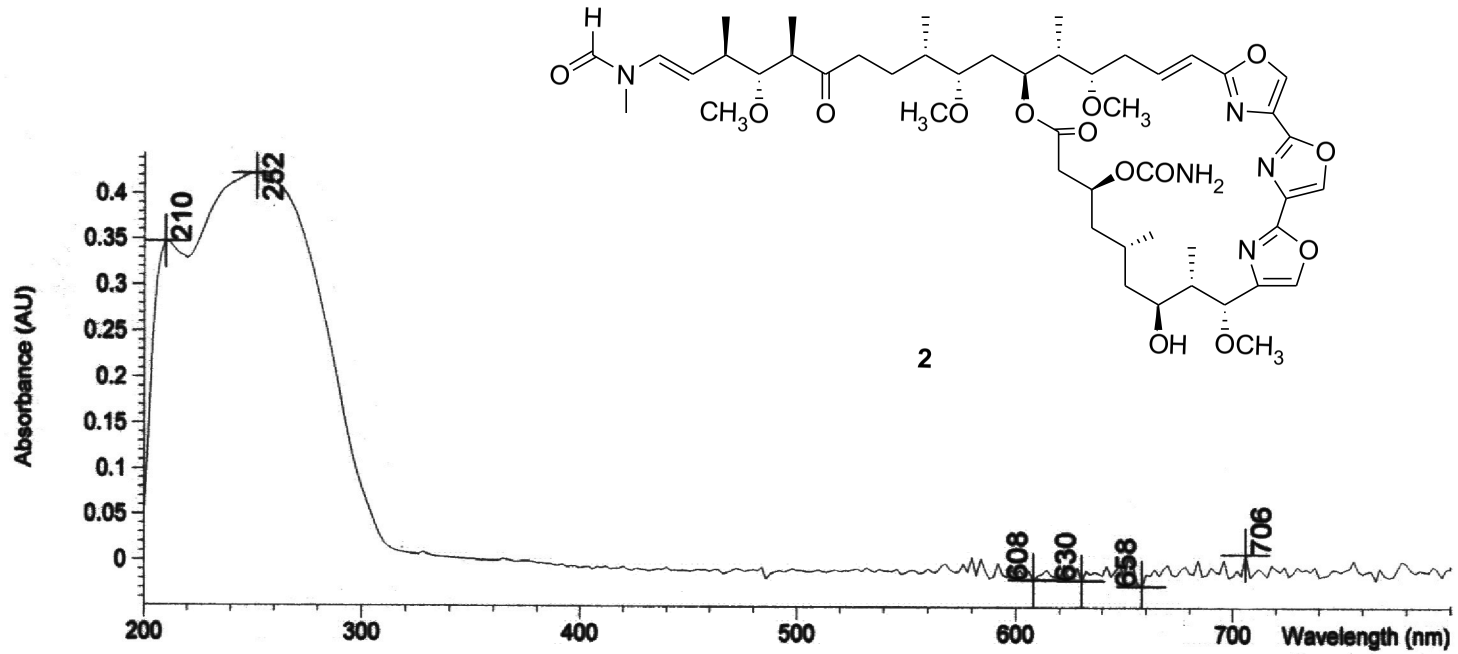

UV spectrum of **2** (CH_3OH)

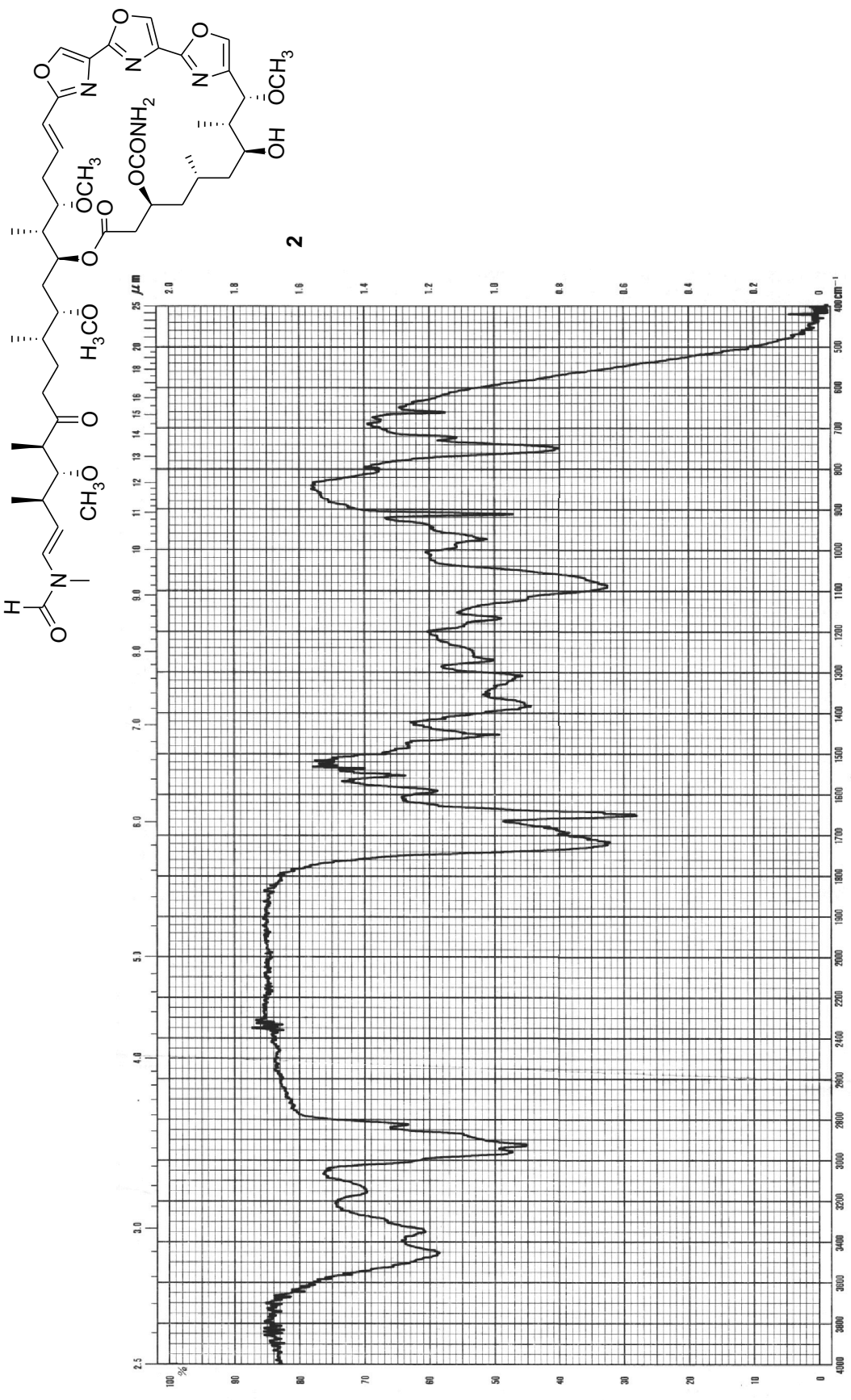

IR spectrum of **2** (neat)

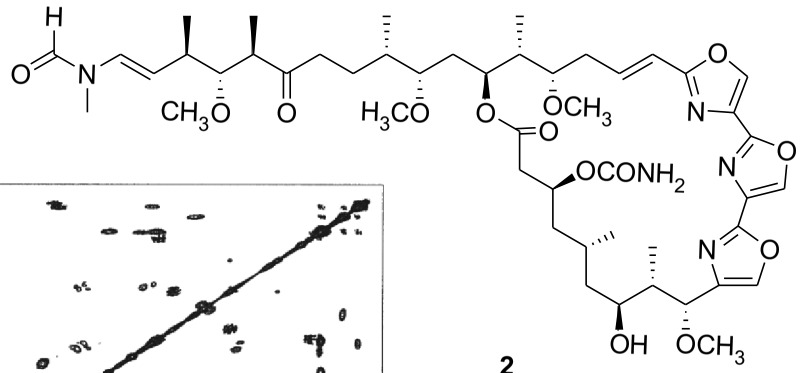

2

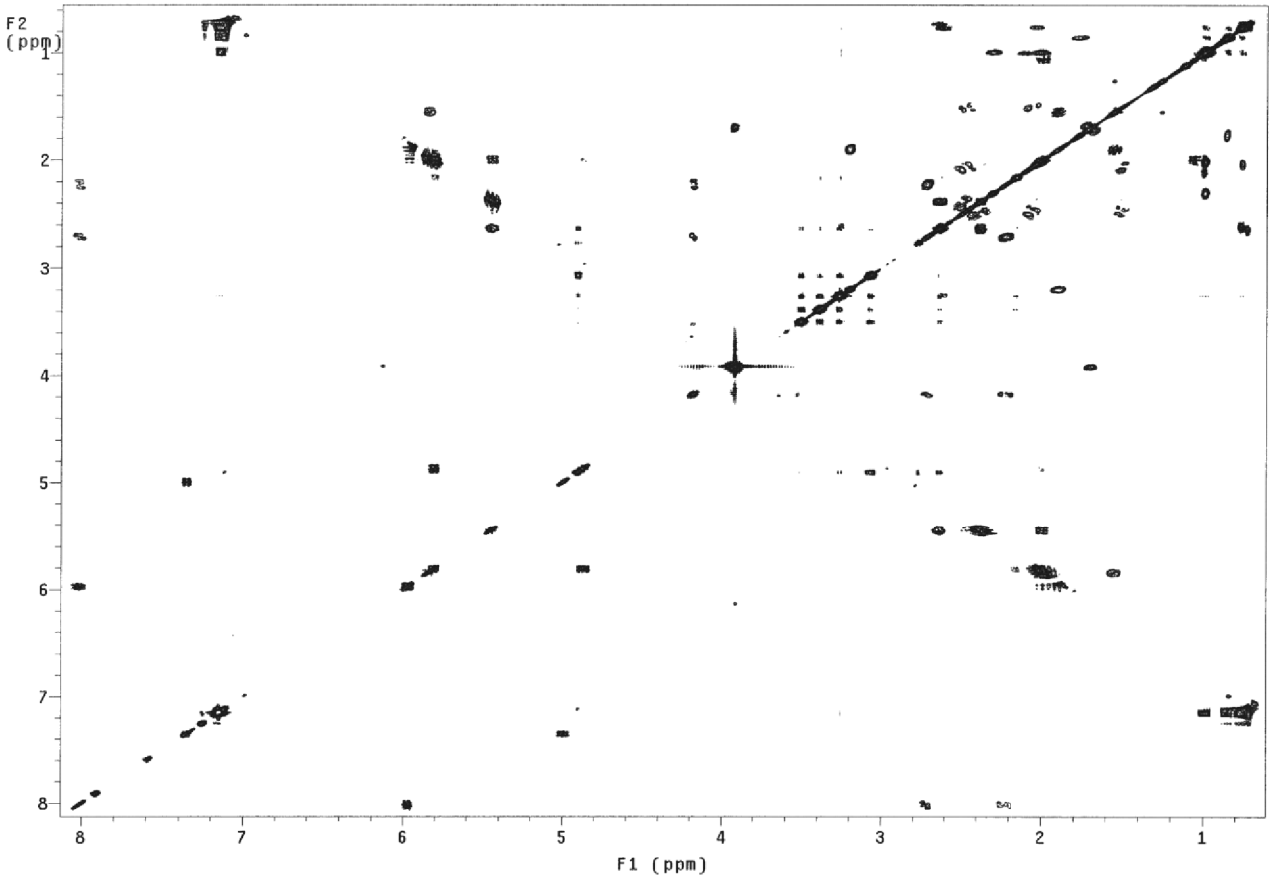

^{1}H-^{1}H COSY spectrum of **2** (500 MHz, C_6D_6)

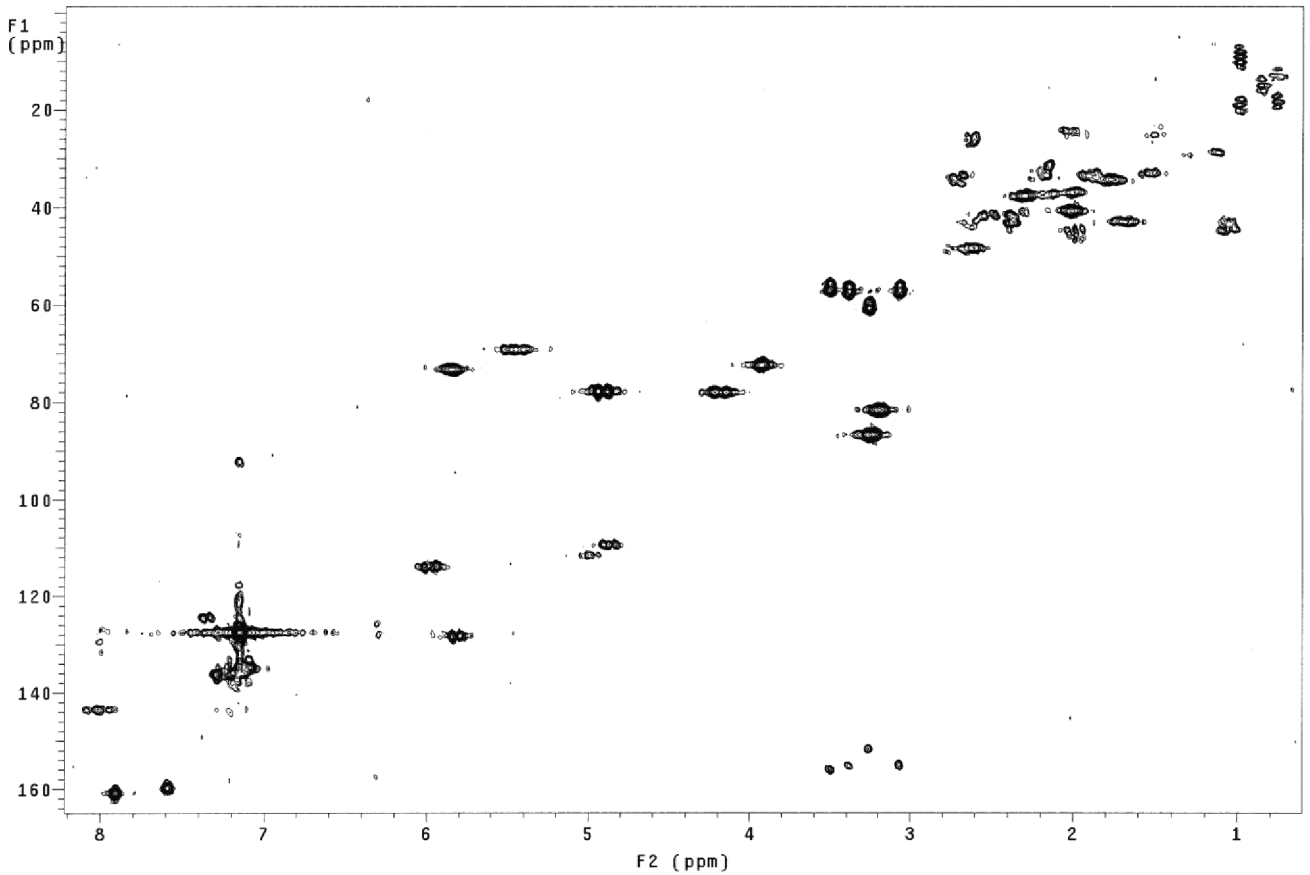

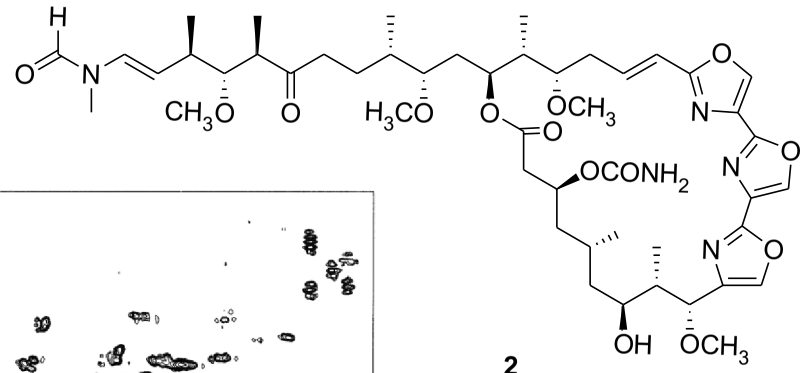

2

HMQC spectrum of **2** (500 MHz, C_6D_6)

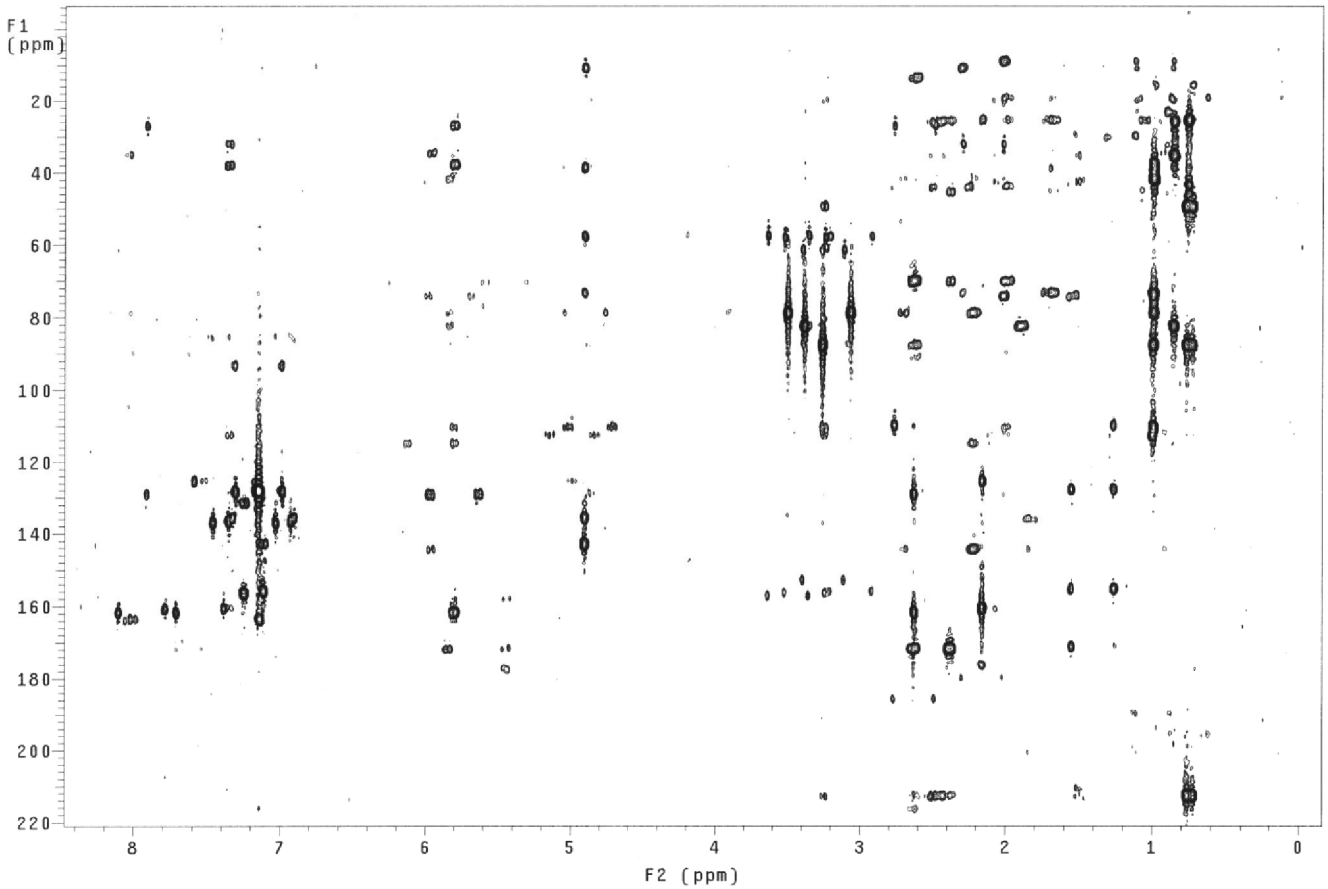

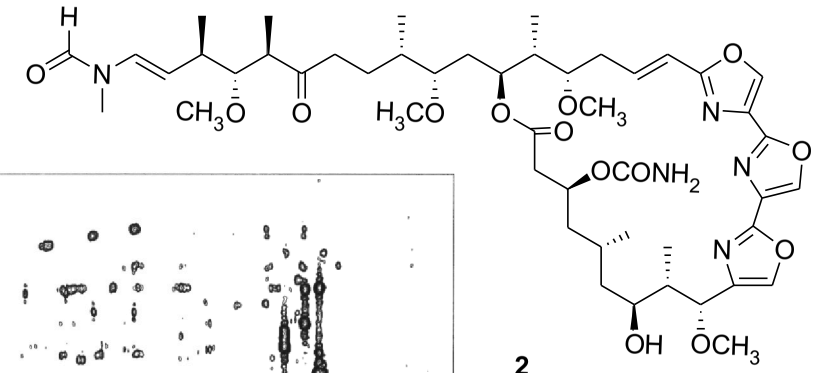

2

HMBC spectrum of **2** (500 MHz, C_6D_6)

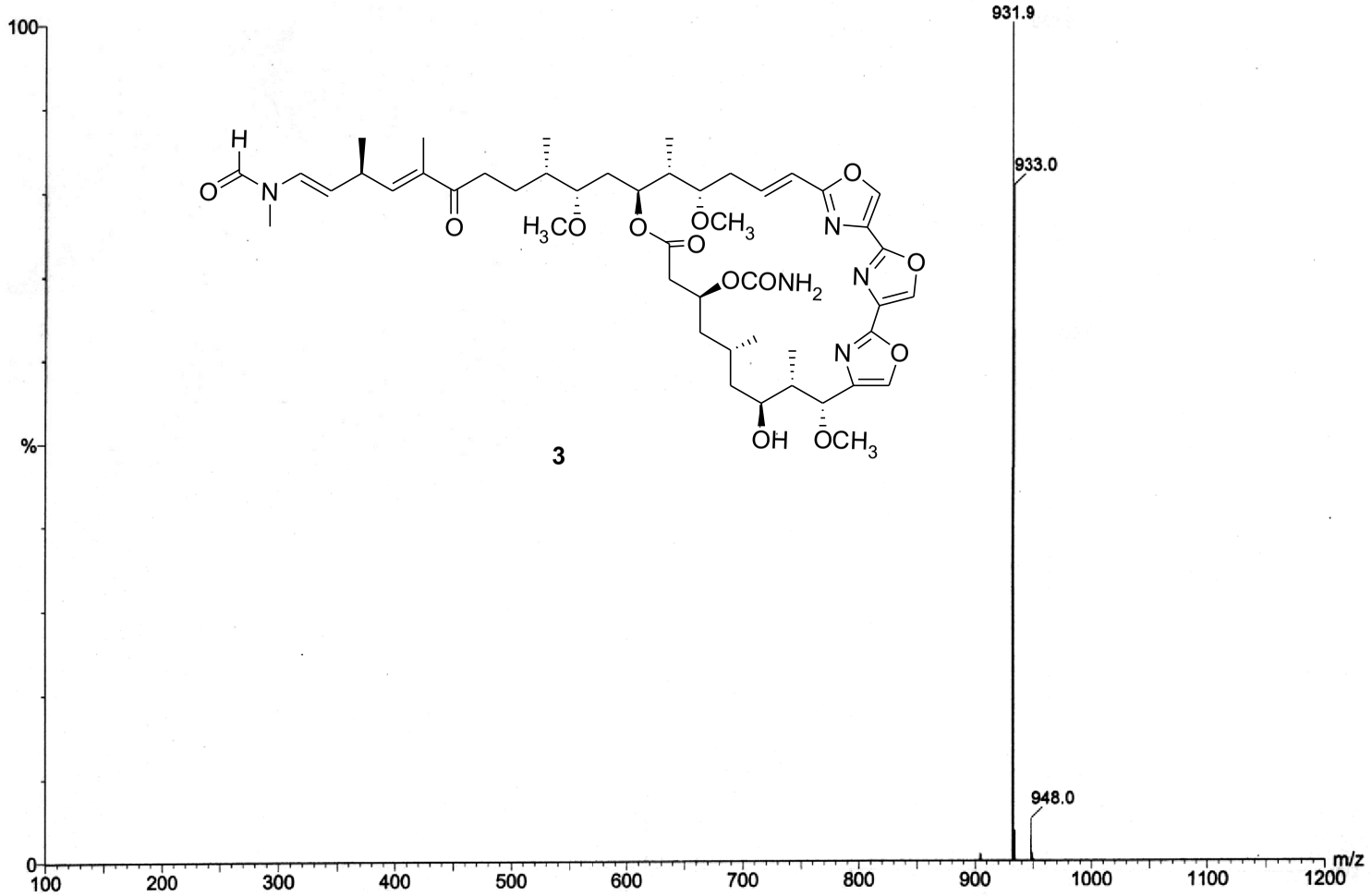

3

ESIMS spectrum of **3**

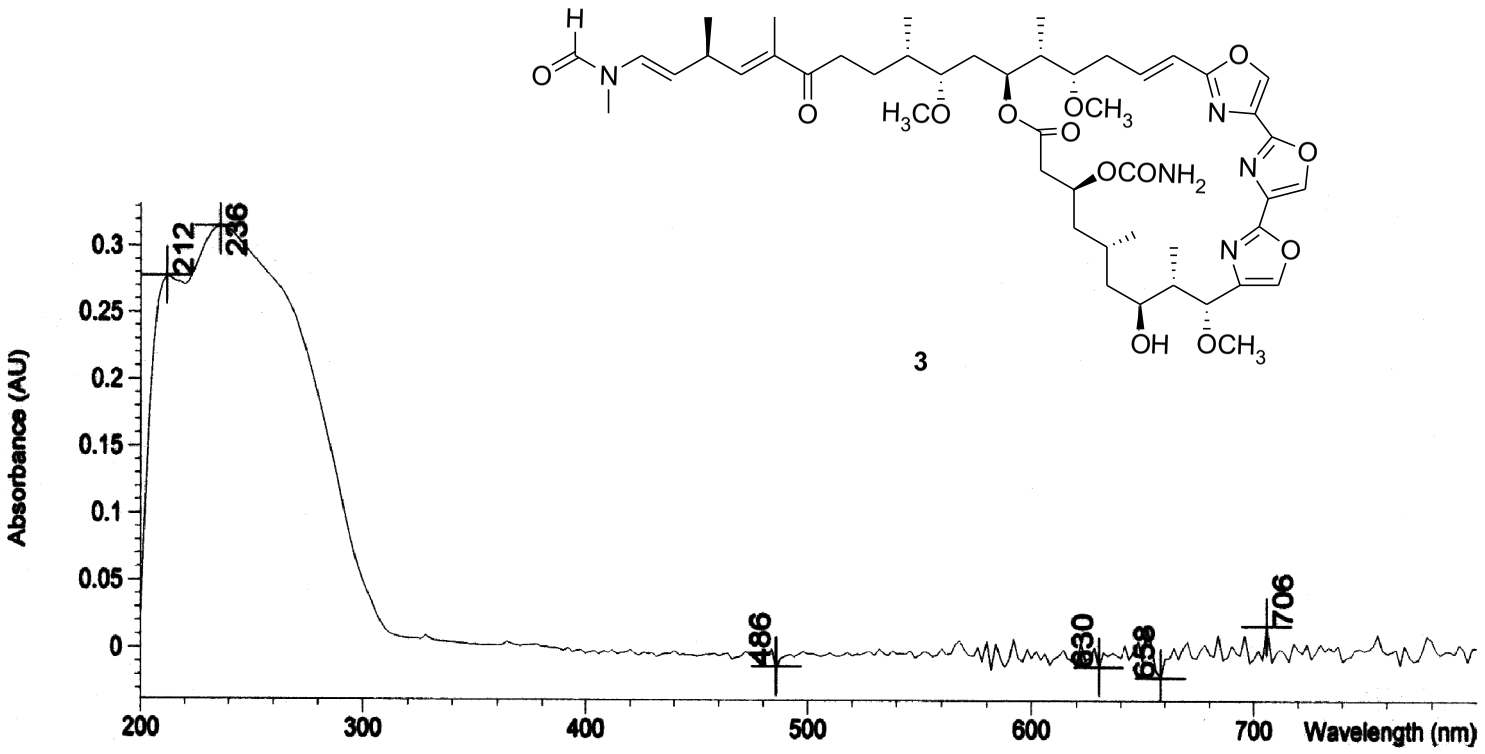

UV spectrum of **3** (CH_3OH)

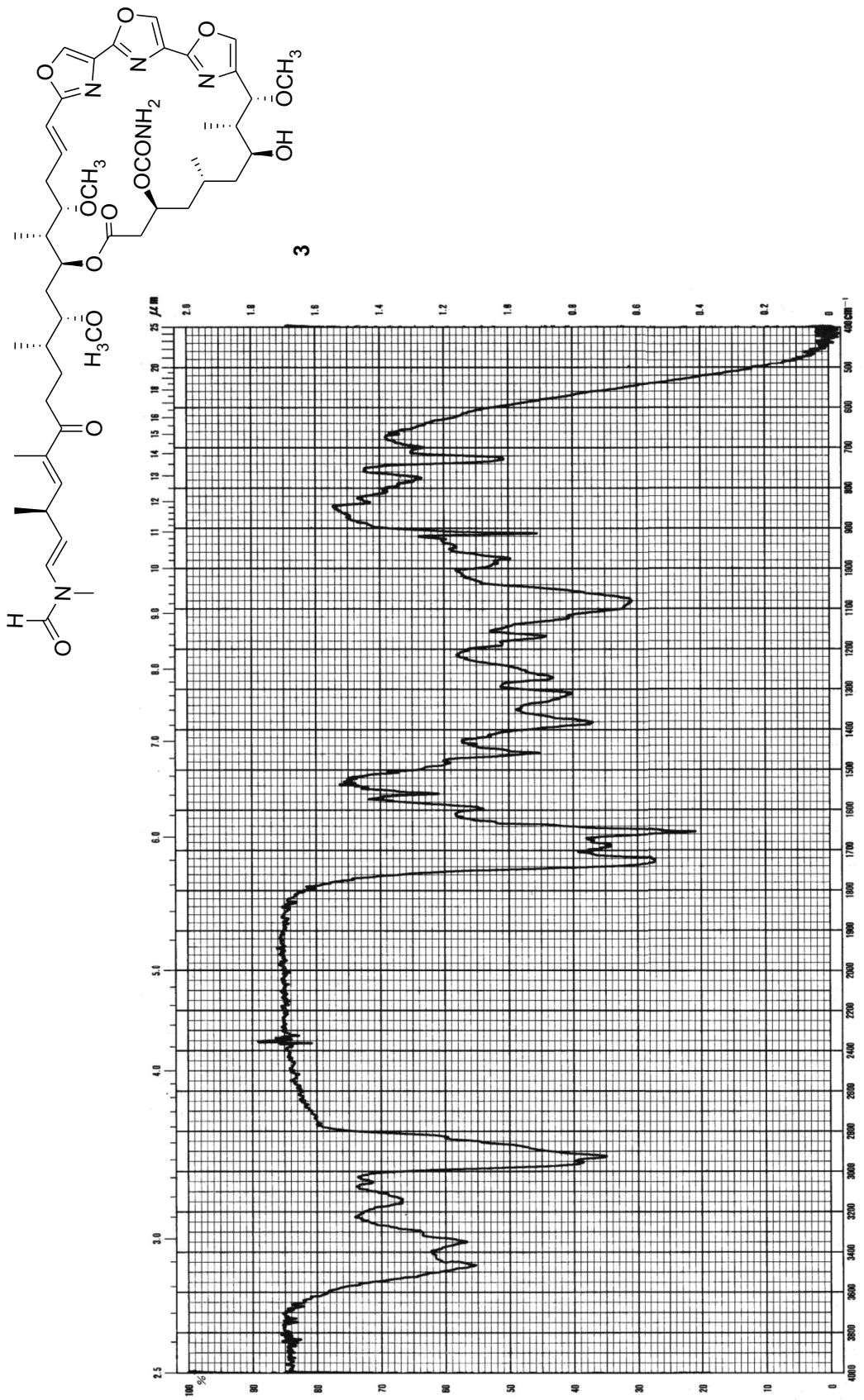

IR spectrum of **3** (neat)

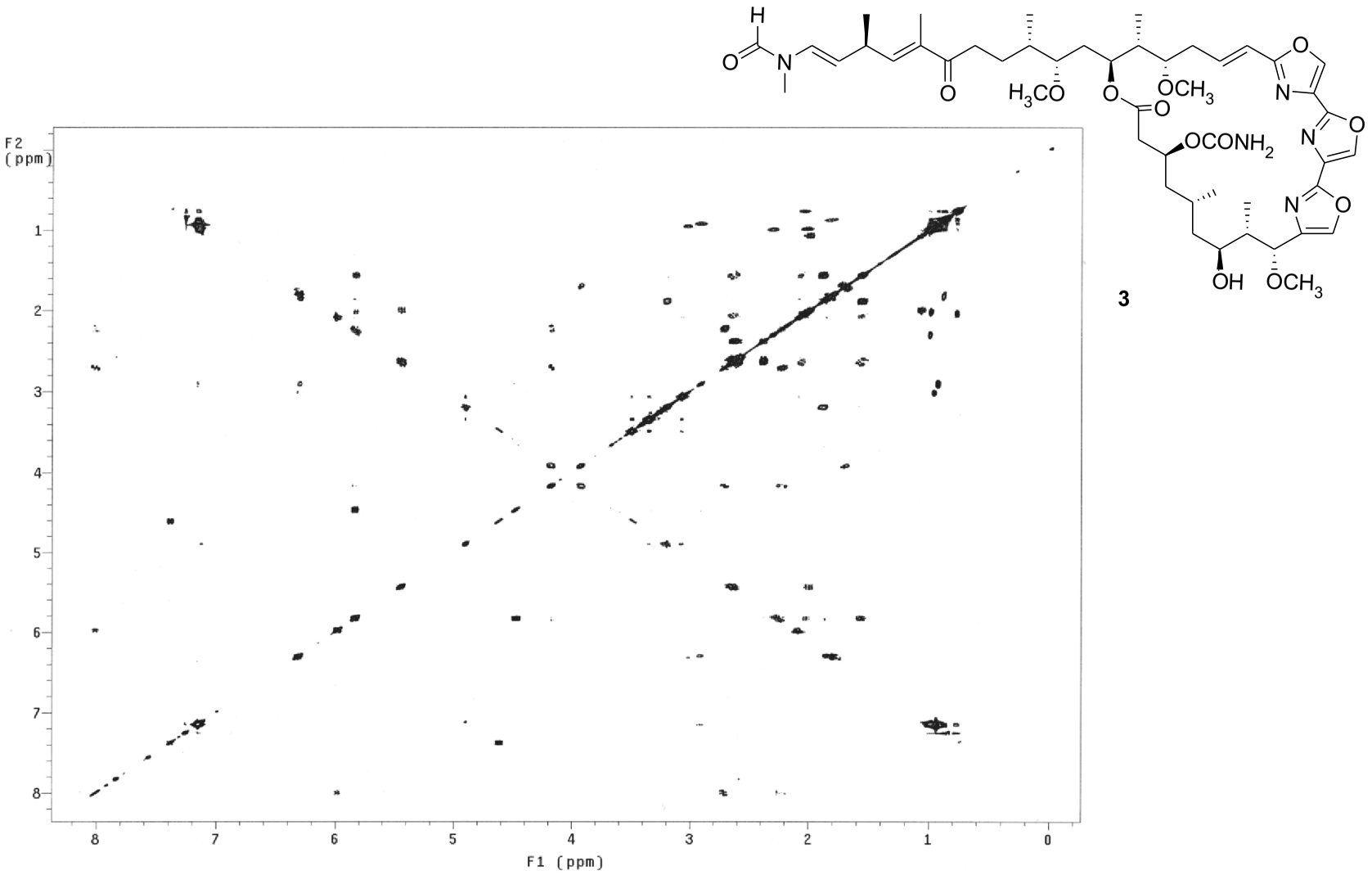

3

^{1}H-^{1}H COSY spectrum of **3** (500 MHz, C_6D_6)

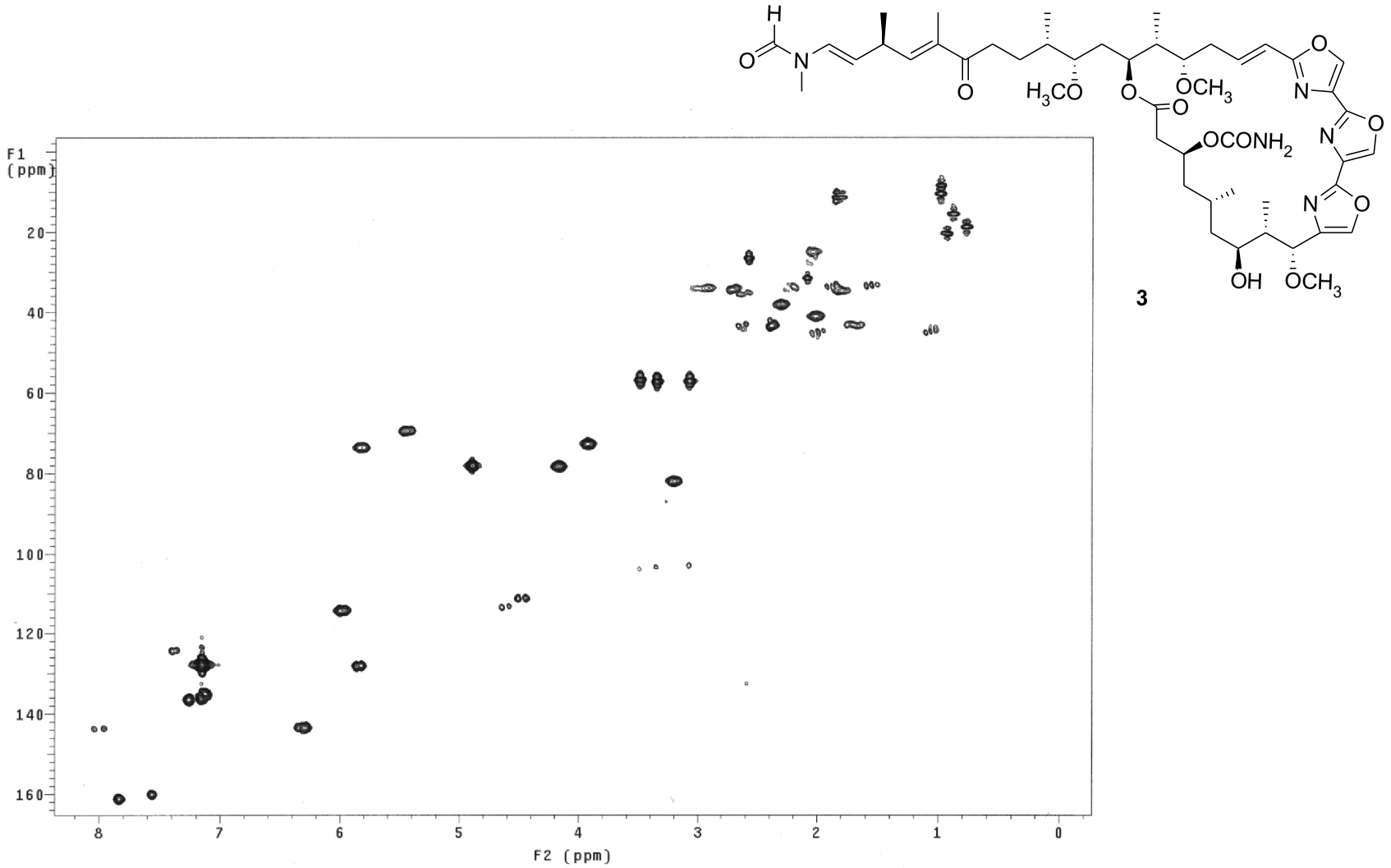

3

HMQC spectrum of **3** (500 MHz, C_6D_6)

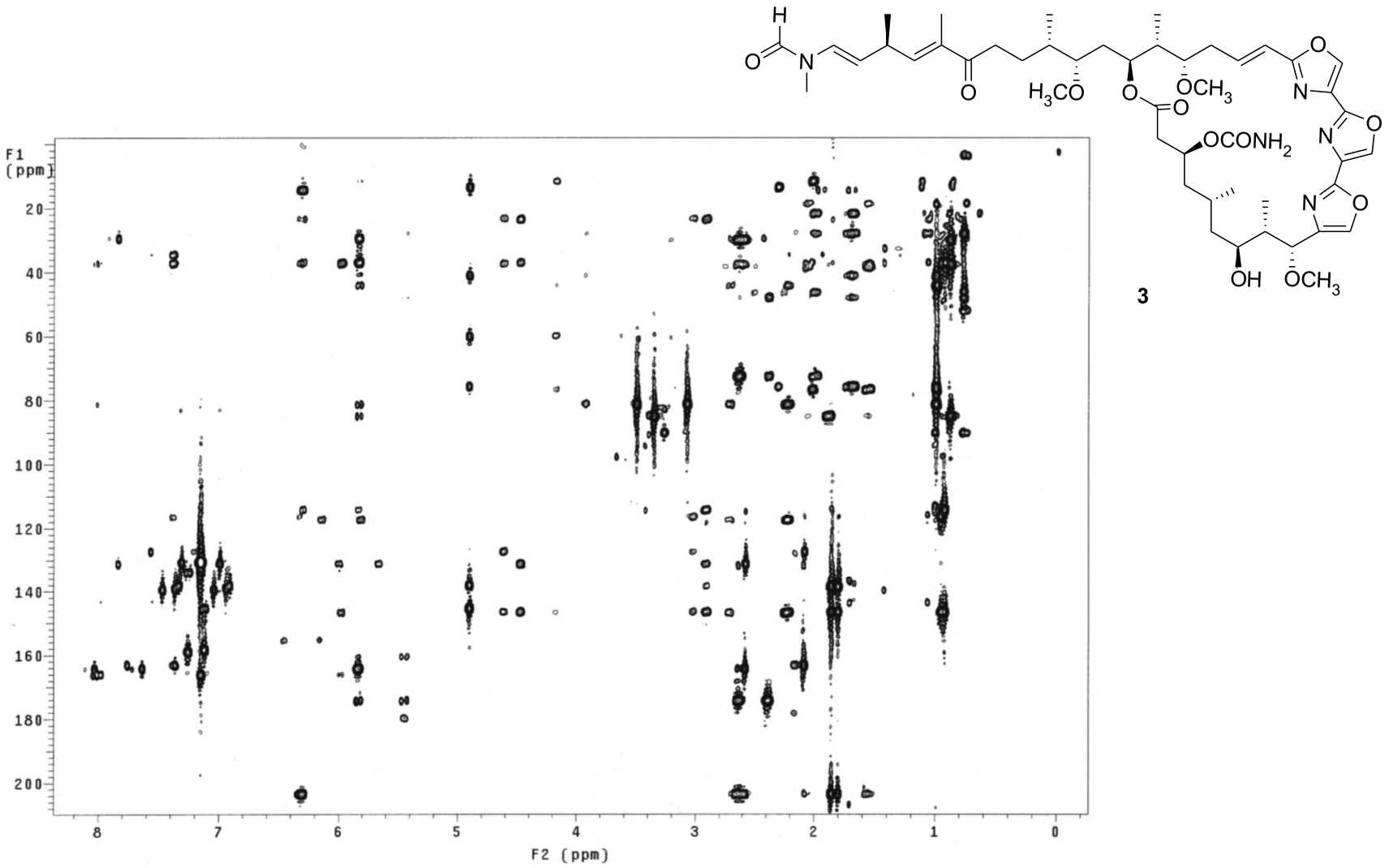

HMBC spectrum of **3** (500 MHz, C_6D_6)

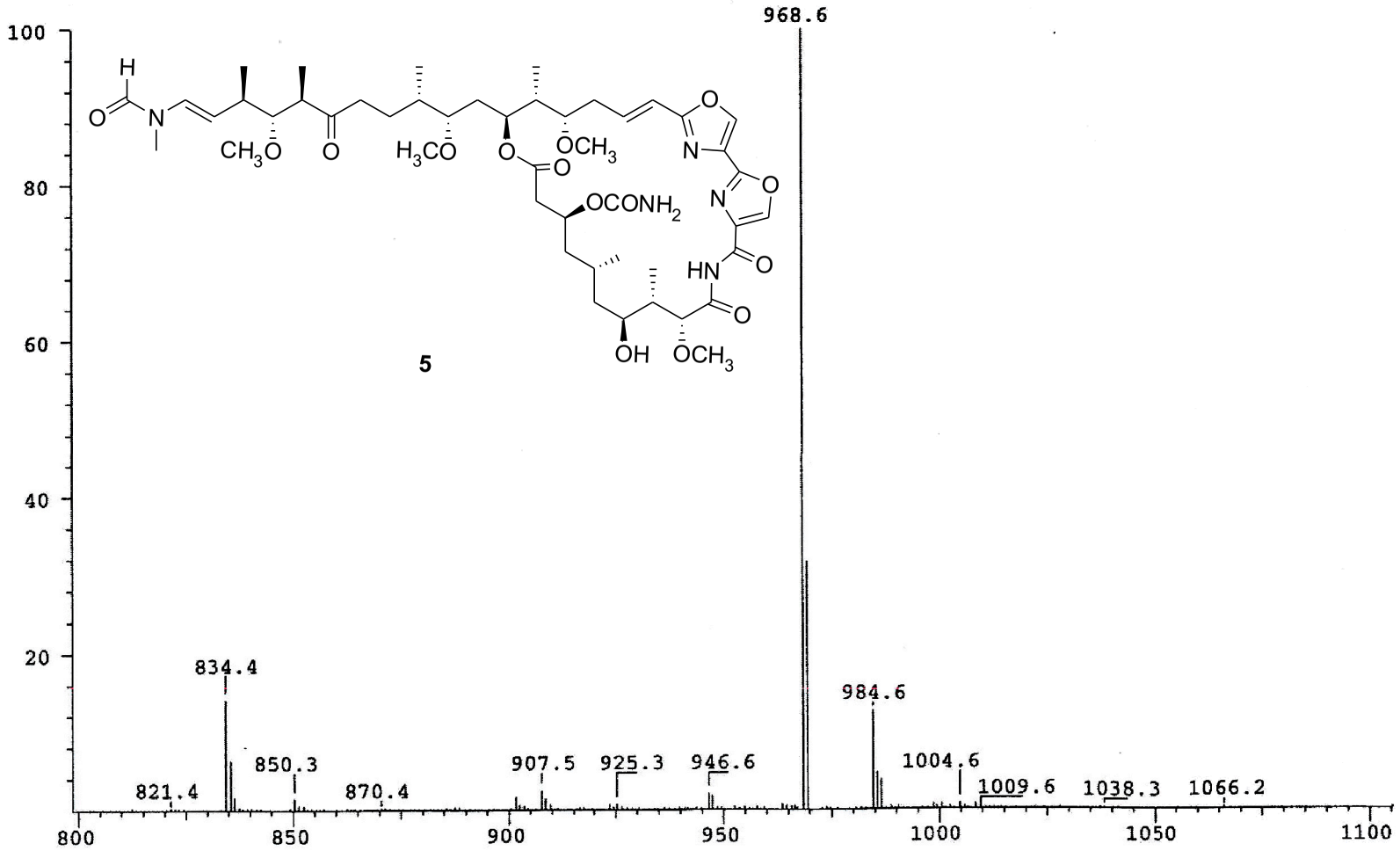

ESIMS spectrum of **5**

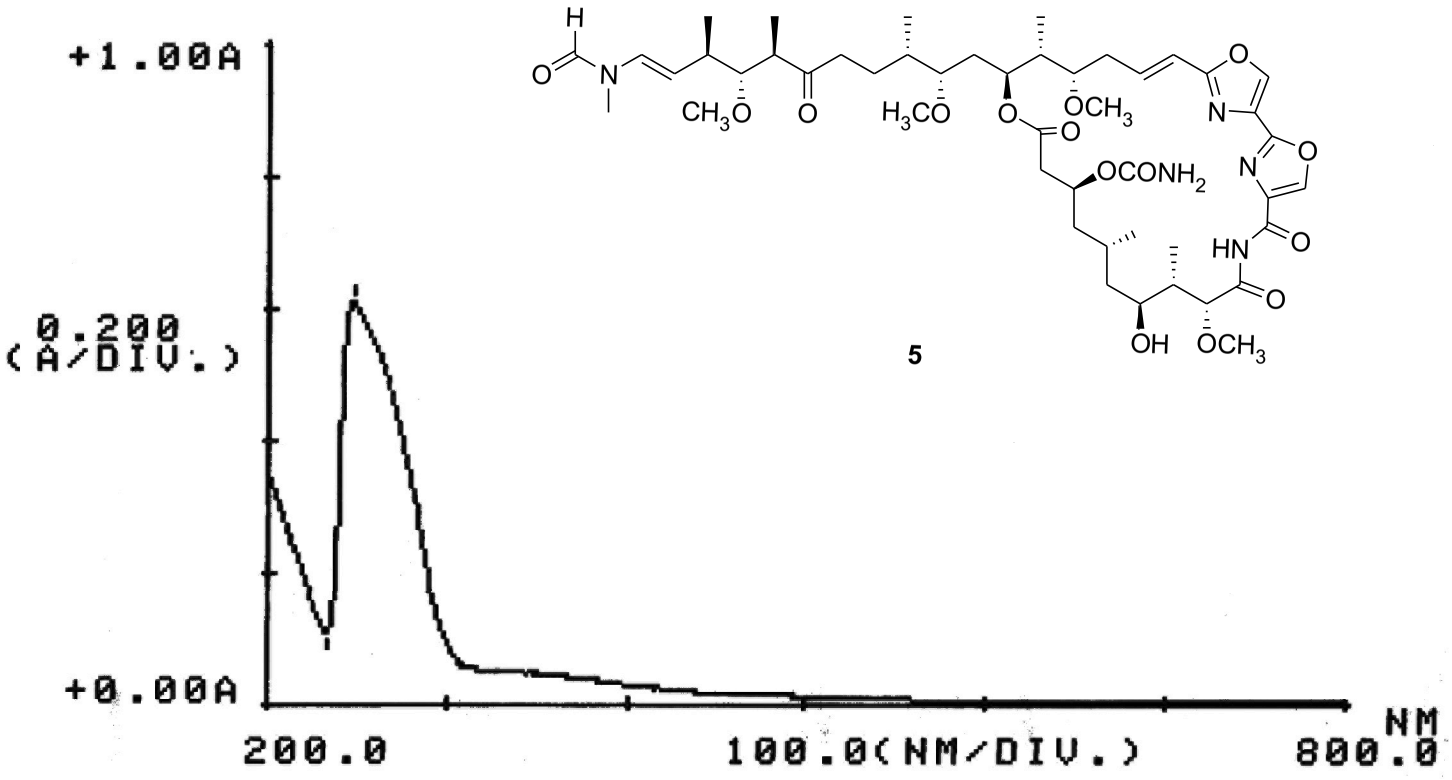

5

UV spectrum of **5** (CH_3OH)

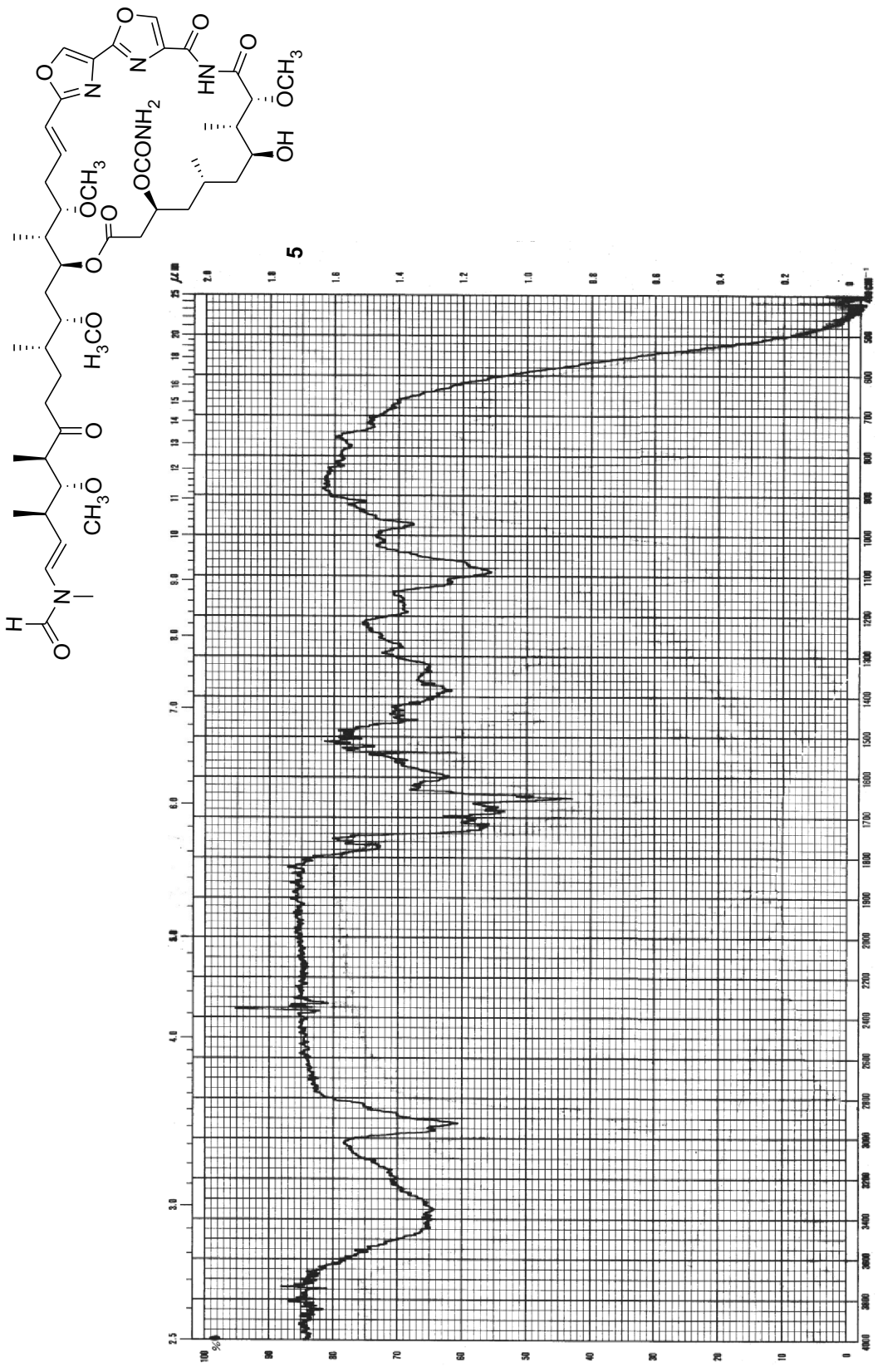

IR spectrum of **5** (neat)

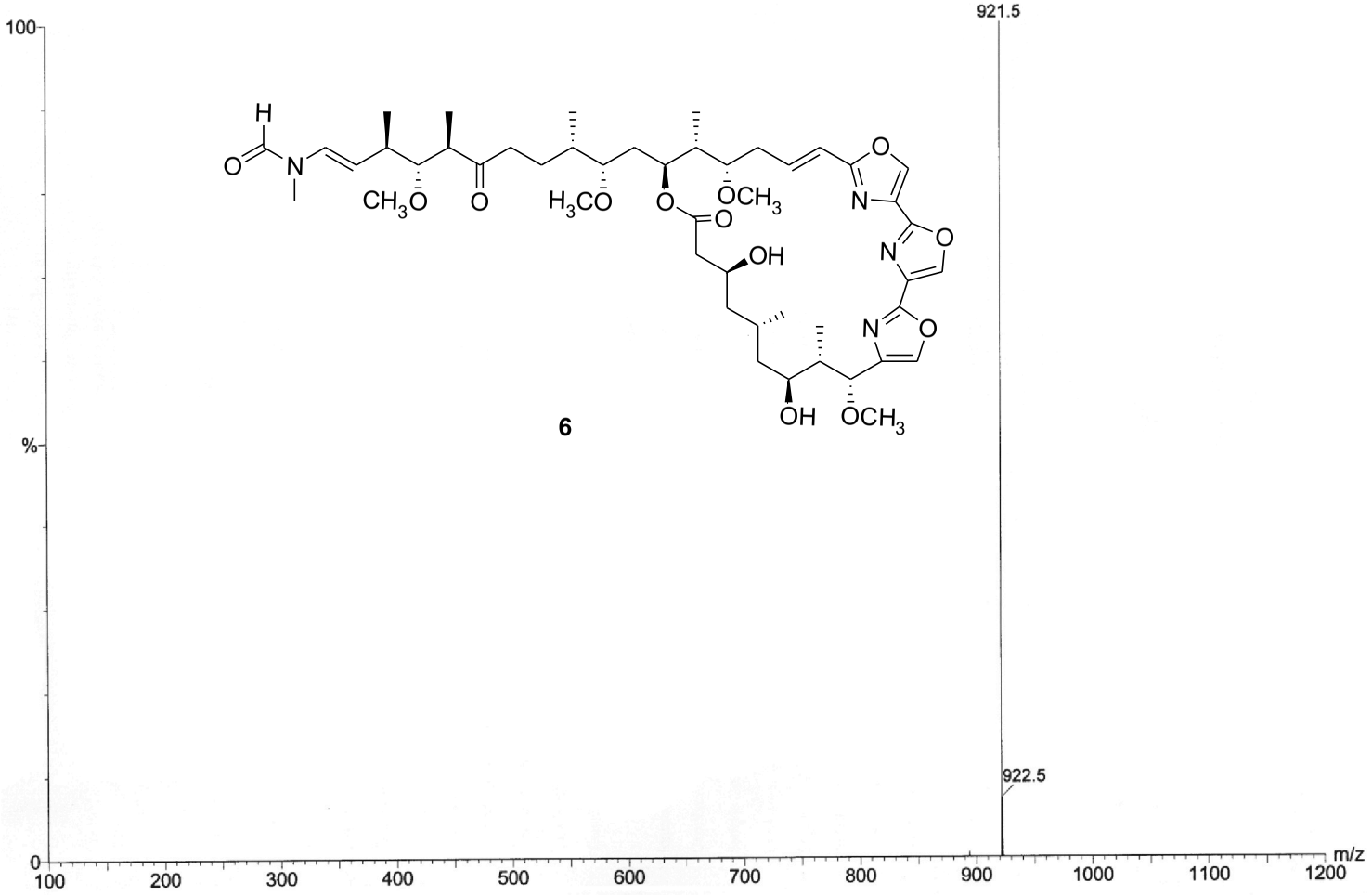

ESIMS spectrum of **6**

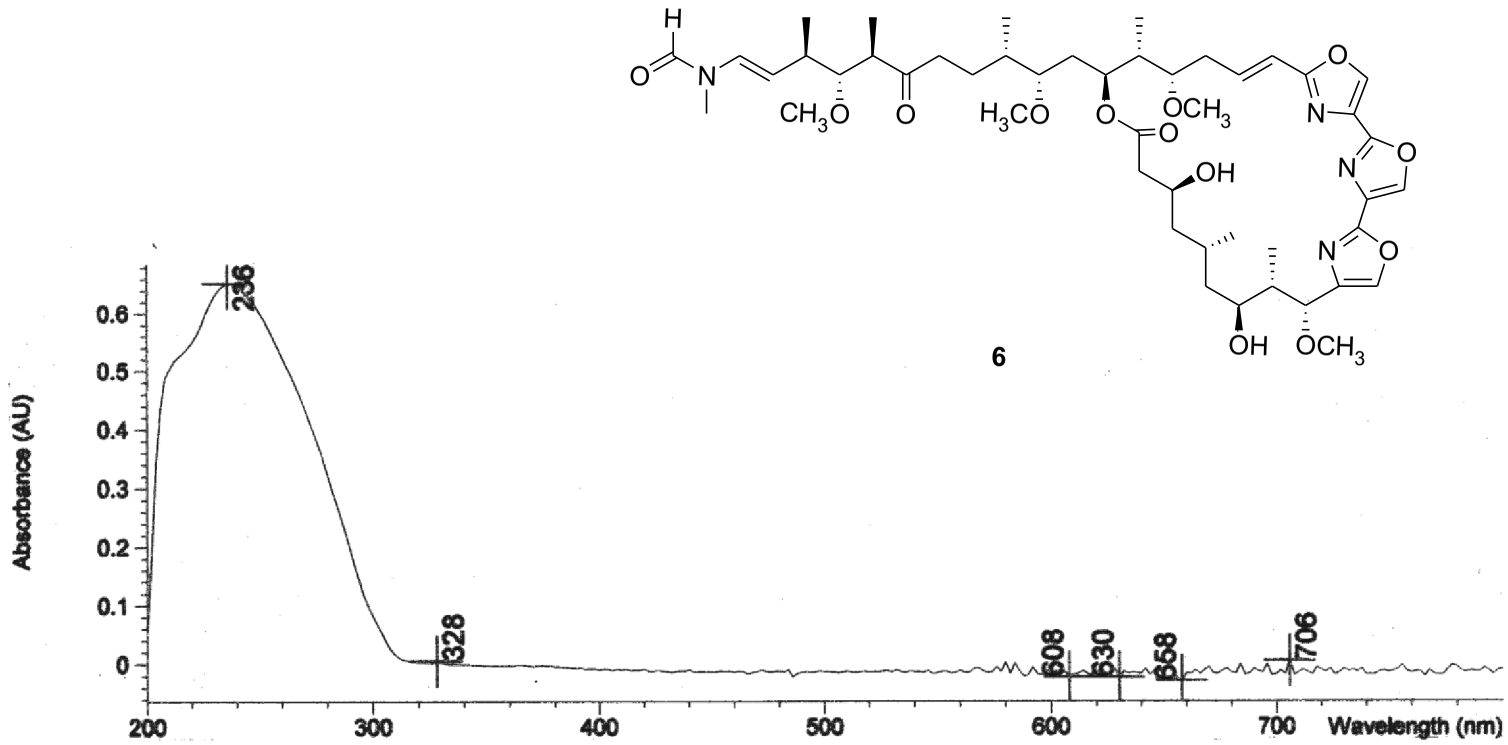

UV spectrum of **6** (CH_3OH)

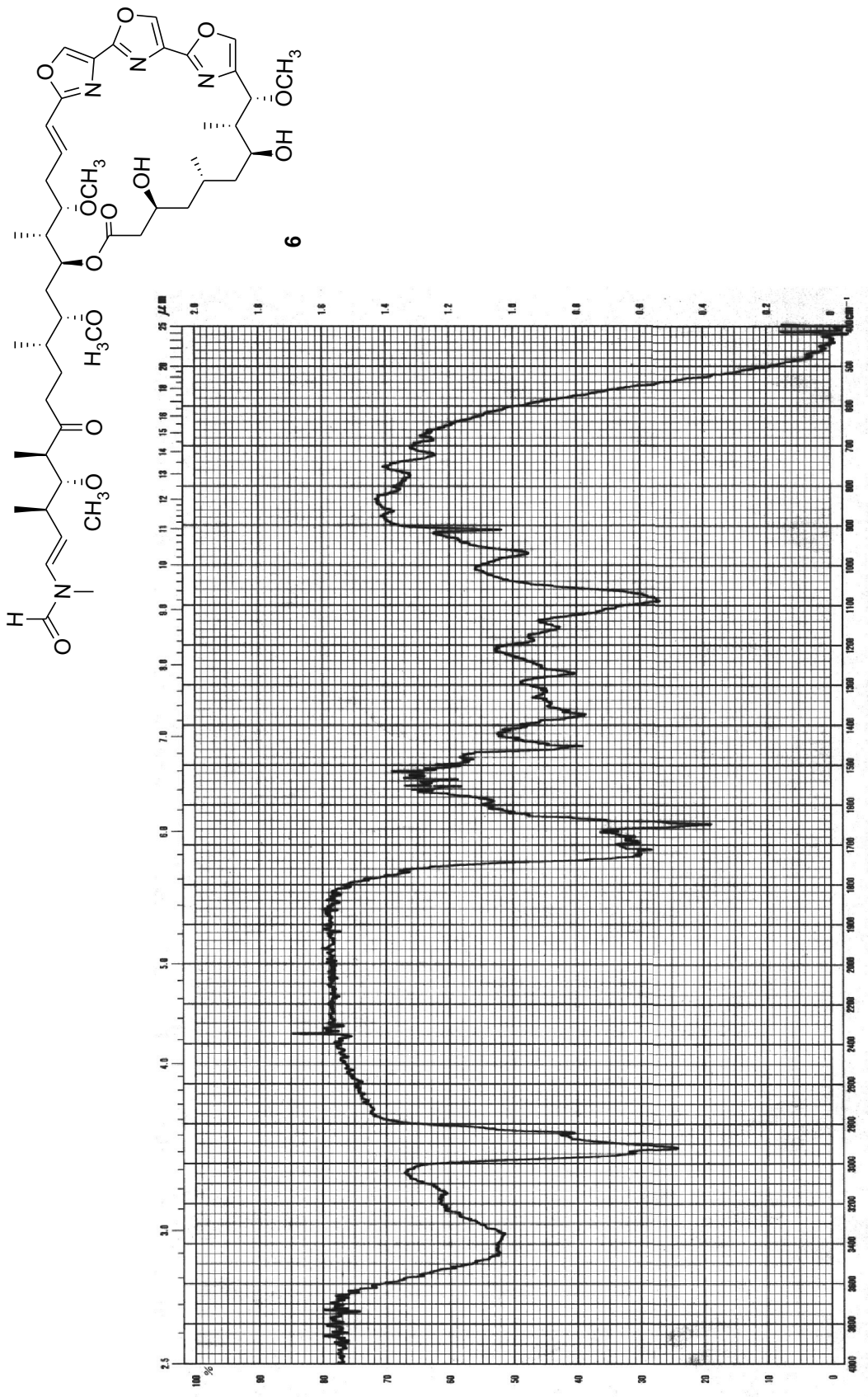

IR spectrum of **6** (neat)

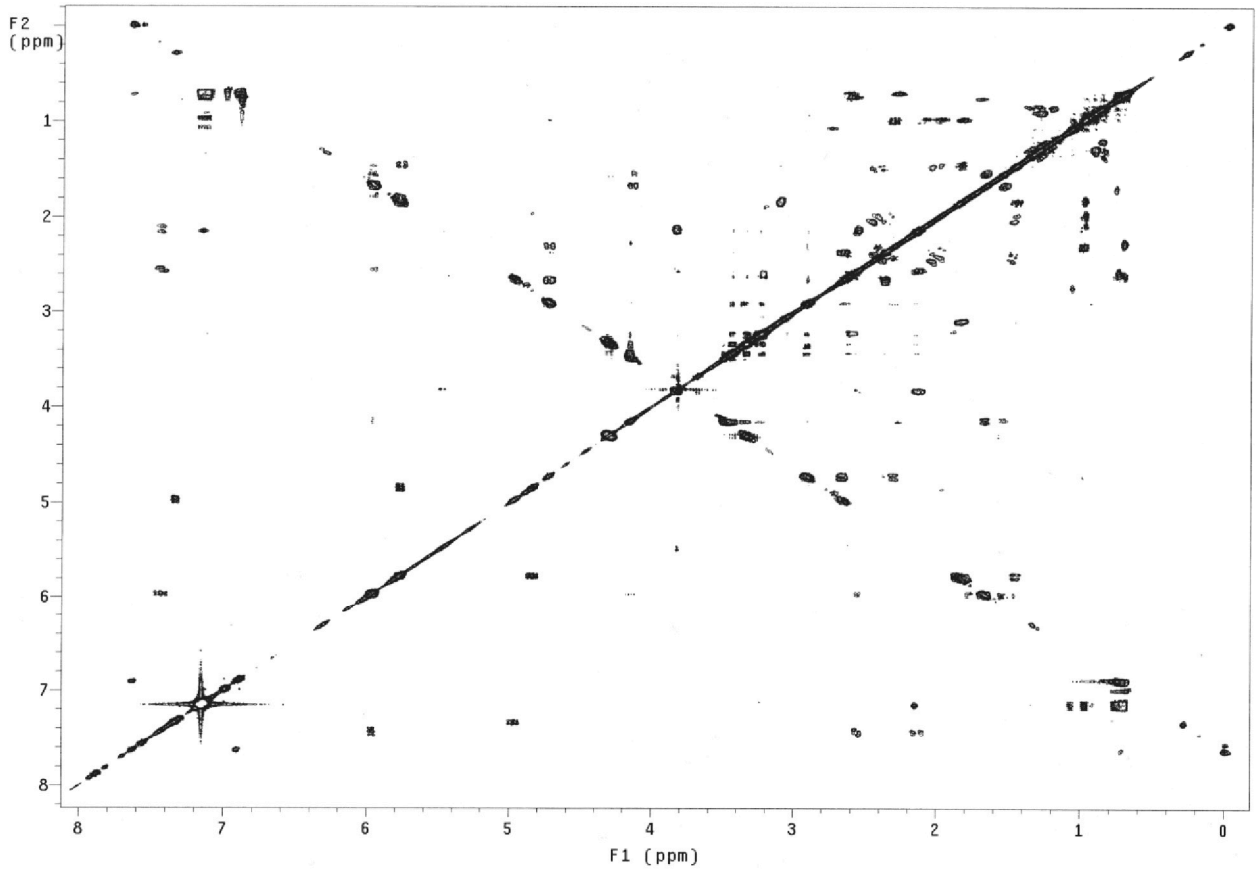

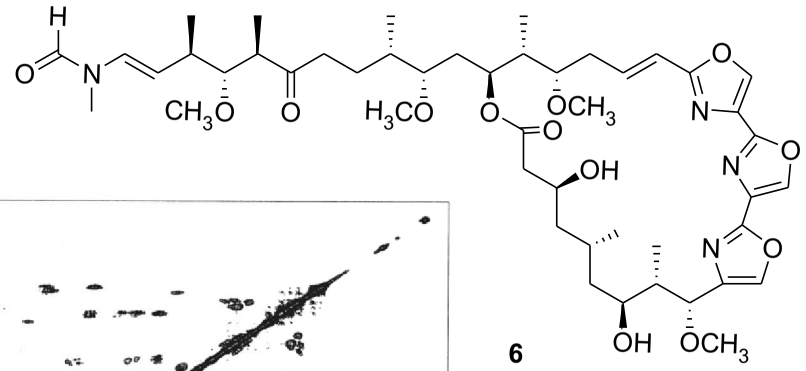

6

^{1}H-^{1}H COSY spectrum of **6** (500 MHz, C_6D_6)

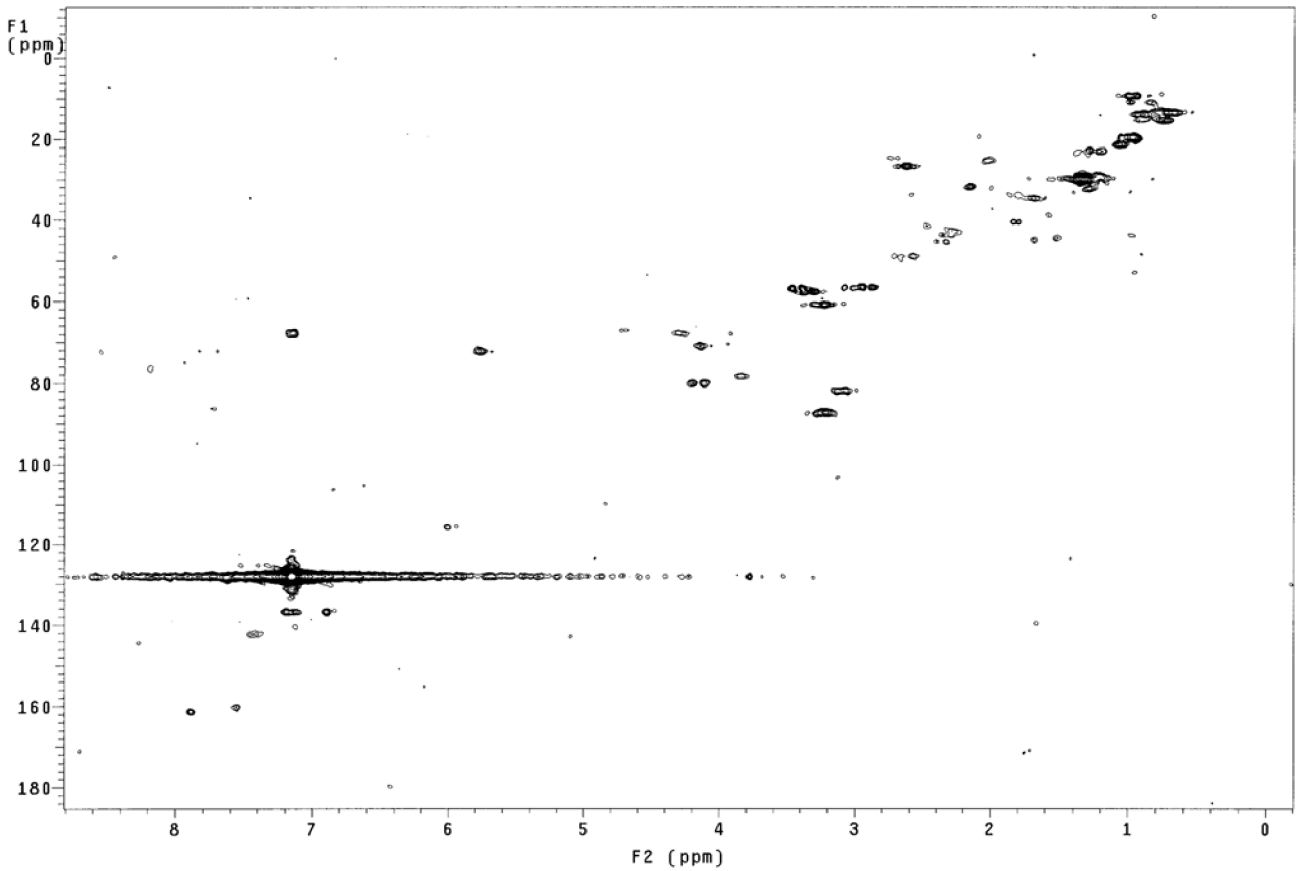

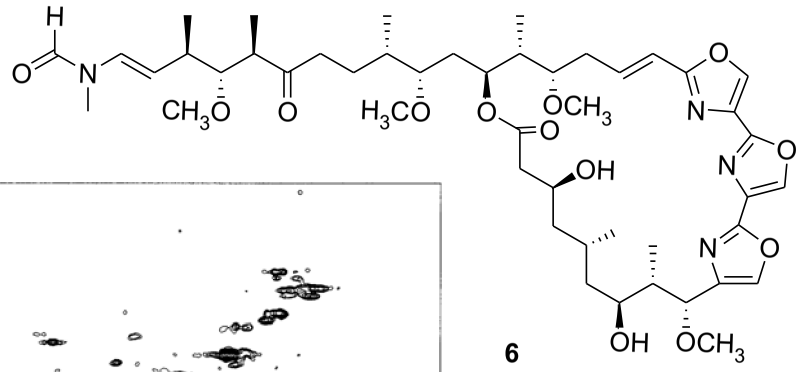

6

HMQC spectrum of **6** (500 MHz, C_6D_6)

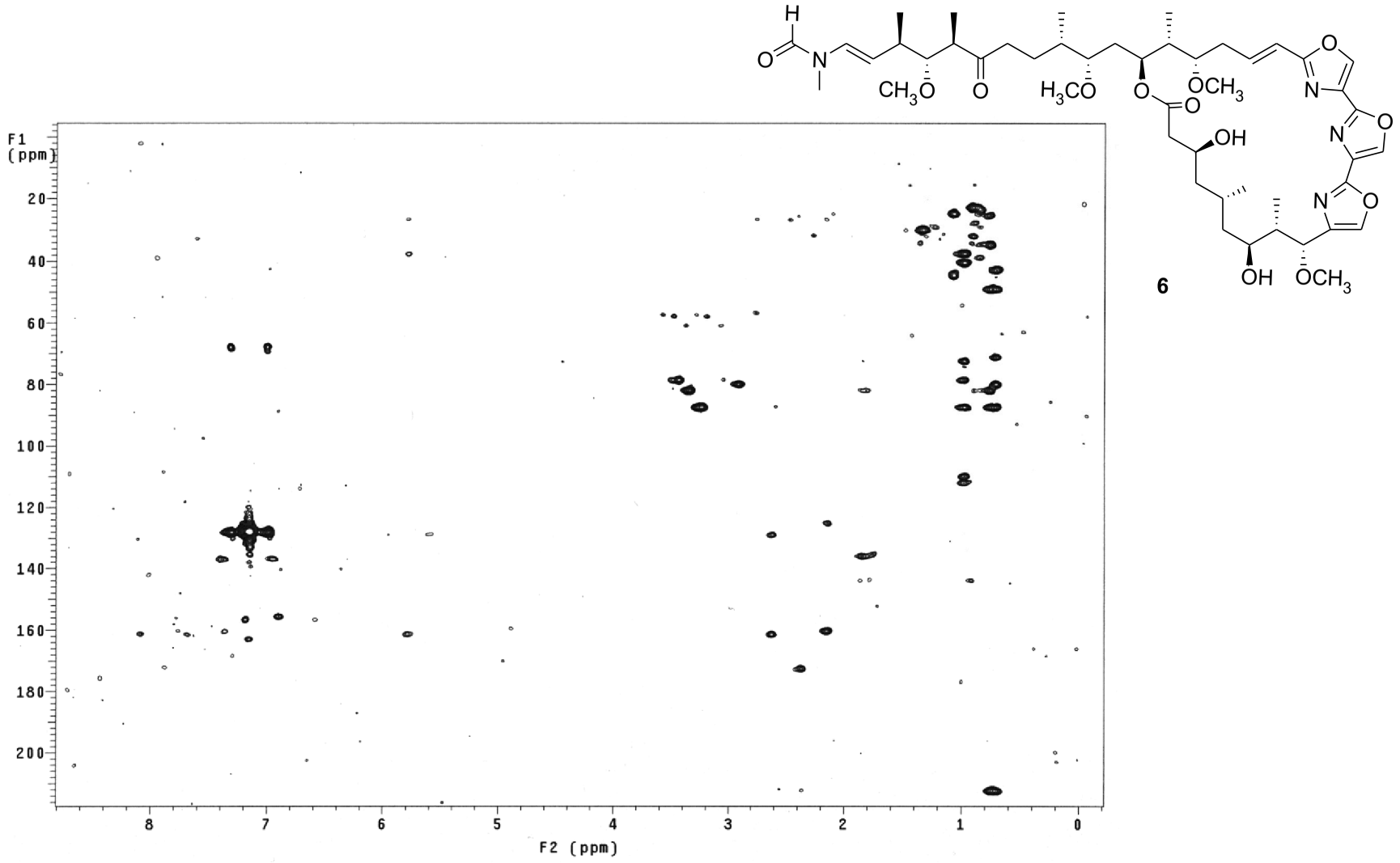

6

HMBC spectrum of **6** (500 MHz, C_6D_6)

VITAE

Name Miss Thanchanok Sirirak

Student ID 4910730001

Educational Attainment

Degree	Name of Institution	Year of Graduation
Bachelor of Pharmacy (First Class Honors)	Prince of Songkla University	2005

Scholarship Awards during Enrolment

2011 100 Young Chemist Awards, 14th Asian Chemical Congress 2011, Bangkok, Thailand.

2010 Travelling grant for PhD research, Graduate School, Prince of Songkla University.

2010-2011 TRF/BIOTEC Special Program for Biodiversity Research and Training program (BRT T653014).

2006-2011 The Academic Excellence Enhancing Program in Pharmaceutical Sciences, Prince of Songkla University.

List of Publications and Proceeding

Sirirak, T.; Intaraksa, N.; Kaewsuwan, S.; Yuenyoungsawad, S.; Suwanborirux, K.; Plubrukarn, A. Intracolonial allocation of trisoxazole macrolides in the sponge *Pachastrissa nux*. *Chem. Biodivers*. **2011**, *8*, 2238-2246.

Sirirak, T.; Kttiwisut, S.; Janma, C.; Yuenyongsawad, S.; Suwanborirux, K.; Plubrukarn, A. Kabiramides J and K, trisoxazole macrolies from the sponge *Pachastrissa nux*. *J. Nat. Prod*. **2011**, *74*, 1288-1292.

Thanchanok Sirirak, Supreeya Yuenyongsawad, Khanit Suwanborirux, and Anuchit Plubrukarn. Antimalarial and cytotoxic trisoxazole macrolides from the Thai sponge *Plakinastrella* sp. In proceeding of The Eight Joint Seminar; Innovative Research in Natural Products for Sustainable Development. Bangkok, Thailand, 3-4 December, 2008.

Sirirak, T.; Plubrukarn, A. Antimalarial trisoxazole macrolides from the Thai sponge, *Plakinastrella* sp. In proceeding of 6th Regional IMT-GT UNINET Conference 2008. Penang, Malaysia, 28-30 August, 2008.